SELF-HEALING POLYMERS MICROENCAPSULATE BIOMACROMOLECULES WITHOUT ORGANIC SOLVENTS

by

Samuel E. Reinhold III

A dissertation submitted in partial fulfillment
of the requirements for the degree of
Doctor of Philosophy
(Pharmaceutical Sciences)
in The University of Michigan
2009

Doctoral Committee:

Professor Steven P. Schwendeman, Chair
Associate Professor Zhan Chen
Associate Professor Naír Rodríguez-Hornedo
Research Professor Gregory E. Amidon

For my wife,

Gina,

with her unwavering support,

and in appreciation of my parents,

Sam and Lynn,

and my sister, Ashley

ACKNOWLEDGEMENTS

I would like to thank my advisor, Dr. Steven P. Schwendeman, for his wisdom, support, advice, and patience. Dr. Schwendeman possesses a rare combination of extraordinary intelligence, passion, and genuine thoughtfulness for others. He has been everything a research advisor should be and more, and it has been my great privilege to work for him. I am particularly grateful for his well defined taste in audio equipment, and for his assistance in bringing fine sound quality into my home for the first time.

I would also like to thank the other members of my committee. I thank Dr. Naír Rodríguez-Hornedo, who has been supportive and accessible since I first arrived at Michigan, and has really gone above and beyond that of which is expected of a committee member. I thank her immensely for her valuable input and guidance. I thank Dr. Gregory Amidon for always keeping a door open and providing a valuable fresh viewpoint. His corrections and suggestions were invaluable. I thank Dr. Zhan Chen for his valuable input and knowledge in the field of interfaces. Finally, I would like to thank the officially unofficial member of my committee Dr. Kyung-Dall Lee, who served on my committee in a somewhat unofficial capacity for most of my time here, and has provided a great deal of input and guidance in my project as well as my general education at the University of Michigan.

I need to thank those fellow students and post-doctoral researchers who have helped me along the way, both in and outside of the laboratory. These include my fellow

lab members, Kiarri Kershaw, who first taught me how to make microspheres, Dr. Li Zhang, Dr. Ying Zhang, Dr. David Gu, Andreas Sophocleous, Dr. Christian Wischke, Dr. Kashappa Goud Desai, Dr. Mangesh Deshpande, Gesine Heuck, and our scientist-in-training, Nalin Lalwani, who helped support this project directly. I'd like to thank Li, Ying, David, Christian, and Andreas specifically for their immense help and support. Additionally, many students from other labs in the College of Pharmacy have helped me in my research, including Hairat Sabit, Maria Posada, Chasity Andrews, Emily Rabinsky, and Vivien Chen, and I thank them for their assistance and friendship. Hairat was particularly gracious and supportive with his assistance over the last few years.

Numerous employees at the College of Pharmacy have helped me along the way, including Pat Greeley and L.D. Heiber, Vickie McMartin, Barbara Johnson, Dawn Coy, and Maria Herbel and I thank them all for their making life easier at the COP. Terri Azar and Jeanne Getty have been wonderful department secretaries, and I thank them both for their help. Above all, I would like to thank Lynn Alexander, who was taken from us much too early. I consider myself lucky to have known her, and I miss her laugh.

Three people need to be acknowledged for being the ones that first inspired me to attend graduate school: Dr. Shun Por-Li, Mr. Stephen Martelluci, and Dr. Der-Yang Lee. I appreciate all of their patience in initially training a pharmaceutical scientist, and their continued support of me even now, almost eight years after I first met them as an intern at McNeil Consumer and Specialty Pharmaceuticals. Thank you all for your wisdom and friendship.

I would like to thank various sources of funding, including the Fred Lyons Memorial Fellowship, the College of Pharmacy itself, the Upjohn/Vahlteich Research Grant, and the National Institutes of Health (Grant 5R01HL068345-02).

My scientific training began fairly recently, but my life training began a long time ago. Accordingly, I owe an immense debt of gratitude to my wonderful parents, Sam and Lynn Reinhold, and my sister Ashley. They have encouraged and supported me always, and have inspired me to do as much as I can with whatever skills I have. Without them, I clearly would not be where I am today.

I also would like to thank my wife's parents, Paul and Sophia Hatzivasilis. They have been extremely wonderful to me since I first met them, and have managed to look past the fact that I am partly responsible for their daughter moving over 500 miles away from them. Thank you both.

Above all, I would like to thank my wife, Gina, who inspires me in ways that she still doesn't realize. I owe this body of work to her, for without her support this research would not have been possible and I would be a much less happier man than I am today.

Table of Contents

List of Figures

Figure 3.4 Effects of theoretical $MgCO_3$ content in blank PLGA microparticle preparation on lysozyme loading (% w/w) via self-encapsulation. Four formulations were created with differing amounts of $MgCO_3$ in the organic phase. Soluble aggregation was measured through SE-HPLC and insoluble aggregation was measured through Coomassie after dissolving insoluble residual in 6M urea, 1 mM EDTA, 10 mM DTT.

Figure 3.5 Slow release of lysozyme from microparticles created by varying loading of base and constant trehalose content in the inner water phase. SM-microspheres were created using $MgCO_3$ (%, w/w) added to the organic phase: 0% (●), 1.5% (△), 4.3% (◆), and 11.0% (□).

Figure 3.6 Mass balance of lysozyme after 28 d release from microparticles created with various loading of base and constant trehalose content in inner water phase. Four SM-formulations were created using differing amounts of $MgCO_3$ (w/w): 0%, 1.5%, 4.3%, and 11.0%. Estimated amount of lysozyme recovered as aggregates (soluble and insoluble) was 9 ± 1% (0.0% $MgCO_3$), 6 ± 1% (1.5% $MgCO_3$), 5 ± 1% (4.3% $MgCO_3$), and 3 ± 1% (11% $MgCO_3$).

Figure 4.3 Appearance of unidentified peak after 28 d release of leuprolide acetate. Initial extraction of the peptide from the polymer after 28-day release (A) showed two clear peaks that moved closer 10 min after addition of 1M NaCl to the vial (B) and were completely combined 60 minutes after NaCl addition (C).

136

Figure 4.4 Morphology of leuprolide acetate microspheres, before and after encapsulation with additional loading solution to avoid microsphere congealing. PLGA (50:50, 0.57 dL/g) SM-microspheres were made using trehalose (A) or $ZnCO_3$ (B) as the porosigen. Leuprolide acetate solution (240 mg/ml) was loaded and solution dispersed at 4°C for 16 h, before additional water was needed, bringing each concentration to 120 mg/ml. Microspheres were then incubated for an additional 8 h at 4°C, and then pores were closed at 43°C for 48 h for both trehalose (C) and $ZnCO_3$ (D).

137

Figure 4.5 Cumulative leuprolide acetate release after self-healing microencapsulation. Leuprolide acetate solution (240 mg/ml) was loaded and solution dispersed at 4°C for 16 h, before additional water was needed, bringing each concentration to 120 mg/ml. Microspheres were then incubated for an additional 8 h at 4°C, and then pores were closed at 43°C for 48 h. Porosigen used for blank porous particles were either trehalose (●, 200 µl of 500 mg trehalose dihydrate in 1g PBS, pH 7.4), or $ZnCO_3$ (○, with 200 µl PBS, pH 7.4).

138

Figure 4.6 Images of leuprolide acetate microspheres, before and after encapsulation. SM-PLGA (50:50, 0.57 dL/g) microspheres were made using trehalose (A) or $ZnCO_3$ (B) as the porosigen. Particles underwent self-healing encapsulation at 4°C for 40 h and 43°C for 48 h for both trehalose (C) and $ZnCO_3$ (D).

139

Figure 4.7 Cumulative leuprolide acetate release after self-healing microencapsulation. Leuprolide acetate was loaded from 120 mg/ml peptide 4°C for 40h and 43°C for 48h. Porosigen used for SM-microparticles were either trehalose (●, 200 µl of 500 mg trehalose dihydrate in 1g PBS, pH 7.4), or $ZnCO_3$ (○, with 200 µl PBS, pH 7.4). △: 50:50 weight combination of the other two formulations.

140

Figure 4.8 30 Day release of BSA-coumarin from 0.19 dL/g microparticles. BSA-coumarin loading was 0.40% (w/w) ± 0.12% (SEM) was released over 30d. Release was in PBST (PBS + 0.02% Tween-80) and was assayed by analyzing release media for monmeric protein by SE-HPLC. N=3.

141

Figure 6.4 Hofmeister series and its effects. For over 20 years, the Hofmeister series has been thought to affect protein solubility and surface tension through its presence near, but not at, the interface. Neutral ions (middle column) have a normal amount of interaction at the interface. In solutions with chaotropic ions (right column), the oxygen at the water layer at the surface has more hydrogen bonding available to it, 'freeing up' some of its own hydrogen for solvating the solute. Kosmotropic ions (left column), 'borrow' a hydrogen bond from water molecules near the interface, thus causing the molecule at the interface to bind tighter to its hydrogen atoms, and decreasing its ability to solvate at the interface. Recent research has suggested that this model is not completely correct, however, and the ions are present on the water surface and subsequently interact with the interface themselves. (Bold ions above were used in these series of experiments.) Adapted from Collins, Zhang and Cremer, and Cacace et al.

199

Figure 6.5 Possible ion interactions at the boundary layer between two phases. An ion (dark circles) in water solutions can interact with a hydrophobic phase through A) local binding to atoms in the other phase (light circles) at certain locations along the ion impermeable phase, B) partitioning into the interfacial area, giving rise to different solvent properties of the solution, and C) uneven ion distribution due to the interfacial field. Adapted from Leontidis et al.

200

Figure 6.6 Dextran-FITC loading as a function of loading time in Hofmeister Salt Solutions. Hofmeister salt solutions (3.5M) were made with dextran-FITC (10 kDa) in solution (65 mg/ml). Shown in increasing order of availability to 'salt-in': ●:NH_4F, ★:NH_4SO_4 , ■:NH_4Cl, ▲:NH_4Br, and ◆:NH_4SCN. The open circle and square represent the control solutions (dextran-FITC only). Time 20h: incubation at 4°C; Time 0: incubation began at 42°C.

Figure 6.7 Dextran-FITC loading as a function of loading time in Hofmeister salt solutions after pre-hydration. Hofmeister salt solutions (3.5M) were made with dextran-FITC (4 kDa) in solution (35 mg/ml). Listed in increasing order of availability to 'salt-in' ammonium salts were: ★:NH_4SO_4 , ■:NH_4Cl, ⬢:NH_4I, ◆:NH_4SCN. Listed in increasing order of availability to 'salt-in' of sodium salts were: □:NH_4Cl, ◇:NH_4SCN. The open circle and x represent the control solutions (dextran-FITC only). Time -2h: incubation began at 37°C in dextran-FITC only solution; Time 0h: incubation began at 37°C in Hofmeister salt solutions.

List of Tables

ABSTRACT

SELF-HEALING POLYMERS MICROENCAPSULATE BIOMACROMOLECULES WITHOUT ORGANIC SOLVENTS

by

Samuel E. Reinhold III

Chair: Steven P. Schwendeman

Microencapsulation of medicines in modern polymeric biomaterials plays a crucial role in success of long-term injectable depots, drug-eluting stents, tissue engineering scaffolds, and blood-circulating nanoparticles. Until now, drugs are most commonly dissolved in organic solvent, which has several disadvantages. Described here is a new microencapsulation paradigm based on the polymer's own natural "self-healing" capacity to microencapsulate biomacromolecules in aqueous media without use of organic solvents. Self-healing microencapsulation (SM) was shown to reproducibly produce poly(lactic-*co*-glycolic acid) (PLGA) microparticles with high peptide and protein loadings of 1-10% (w/w), that was dependent on porous SM-microparticle excipients (e.g. $MgCO_3$ and trehalose), manufacturing parameters, protein loading solution

concentration, and overall porosity. Confocal microscopy of microspheres loaded with fluorescently-labeled BSA showed loaded protein concentrated in submicron domains throughout the microparticle. A model therapeutic peptide, leuprolide acetate, was encapsulated successfully via the self-healing microencapsulation technique. Controlled release over 30 and 60 days for both proteins and the peptide was demonstrated. Self-healing microencapsulation of a model protein lysozyme showed virtually no aggregation or enzymatic activity loss when high amounts of sucrose were loaded in conjunction with the protein, which is currently not possible with traditional encapsulation methods due to the resulting high initial burst release and low encapsulation efficiencies. Self-healing encapsulated BSA showed virtually no acid-induced aggregation (< 2%) after 30 d of release indicating the ability to successfully neutralize acid PLGA using the new encapsulation approach. The self-healing polymer process was strongly affected by different Hofmeister salts, known for their ability to influence interfacial tension. These data were consistent with the hypothesis that the polymer self-healing is driven in part by the high interfacial tension between the hydrophobic polymer and water which causes a minimization of interfacial area. Protein in microspheres loaded via self-healing microencapsulation was not exposed to the numerous destabilizing processes normally associated with protein-loaded microsphere manufacturing. Terminal sterilization of PLGA microspheres without concerns of protein stability is now theoretically possible. The new paradigm opens the door to improved compatibility with large biotechnology-derived drugs, potentially lower manufacturing cost, the ability to create new biomaterial architectures, and more practical use among other scientists and clinicians.

CHAPTER 1

Introduction

1.1 Motivation

As the libraries of pharmacologically active molecules continue to grow, delivery of these new drugs to the site of action remains one of the most challenging pharmaceutical problems. Large biomacromolecules are particularly challenging; poor bioavailability, short *in vivo* half lives, and drug instability have all been impediments in protein delivery [1]. Bioavailability concerns can be partially alleviated by delivering proteins parenterally, avoiding the challenges normally associated with oral delivery. Conjugation of polyethylene glycol (PEG) and the protein can also extend the *in vivo* half life of protein drugs. Alternatively, one delivery strategy that utilizes parenteral delivery but helps overcome proteins' short half lives is the microencapsulation of proteins in biodegradable polymers.

The use of biodegradable polymers allows for a sustained release (e.g. days to months) of the protein after intramuscular injection, reducing the number of injections required. Delivery of drugs using microparticle biodegradable polymer release systems, such as those prepared from poly(D,L-lactide-*co*-glycolide) acids (PLGA), has been

utilized for over 20 years. These delivery vehicles, aptly named microspheres, millicylinders, and nanoparticles because of their size and shape, have been considerably developed due to early promising results. While there are clear distinct advantages of such protein microencapsulation, this delivery method has yet to realize its potential because important obstacles remain: namely, the instability of the protein and high cost of manufacture. Protein instability, both during encapsulation and during its release *in vivo*, is regarded as the most challenging delivery problem facing protein biopolymer microparticle delivery [1, 2]. In addition, high manufacturing costs persist because of complex microencapsulation protocols, and the requirement of aseptic processing.

Here a new encapsulation technique, termed 'self-healing microencapsulation' is introduced. In this thesis, proof–of–principle experiments are confined to microspheres, but these data are expected to be applicable to many of the forms of protein polymer encapsulation and delivery. This new encapsulation technique circumvents many of the traditional stresses polymer-encapsulated proteins are exposed to, and offers a substantial stability advantage over them. However, in order to fully explain the uniqueness of this novel technique, traditional microsphere preparation methods and the phenomena associated with them must be introduced first.

1.2 Microsphere Preparation

One of the first steps in designing any biodegradable polymer controlled release delivery system is the choosing an appropriate polymer. Candidates include a number of biodegradable polymers such as polyesters, polyanhydrides, poly(ortho-esters), and polyiminocarbonates [3]. Of these, polyesters incorporating lactic and glycolic acids are by far the most common. One specific example of this type of polymer, poly(lactide-co-

glycolide) (PLGA), degrades via hydrolysis forming lactic and glycolic acid, which are subsequently eliminated by the body through the tricarboxylic acid cycle [4].

After the polymer is selected, selecting the form of delivery is another crucial decision. Nanoparticles circulate systemically and consequently have shorter half lives. Microparticles with encapsulated drug are injected intramuscularly or subcutaneously, whereas millicylinders require implantation. After the proper form of delivery is selected, the proper manufacturing method must be chosen as well. All manufacturing methods for all biodegradable delivery systems are outside the scope of this introduction and as such only microparticle manufacturing will be discussed here. There are a number of methods of preparing drug encapsulated polymer microparticles. The overwhelming majority of these preparation methods have been 1) spray drying, 2) phase separation (also called coacervation), 3) emulsion solvent-evaporation and solvent-extraction [5], and 4) spray freeze drying (Alkermes ProLease©). Some additional research has concentrated on novel methods, such as *in situ* forming delivery systems, and these will not be examined here as they have found little utility for protein delivery.

1.2.1 Spray Drying

In spray drying, the polymer is first dissolved in an organic phase, usually methylene chloride. The drug solution is then either dissolved directly into the organic phase [6], or it is dissolved in another solvent such as methanol [7] or water [8-10]. If the drug is dissolved in a solvent immiscible with the polymer phase, it must be dispersed into the polymer solution via ultrasonification [9] or magnetic stirring [11]. The resulting microparticles are spray dried in a spray-drier, washed and vacuum dried. This process consists of the use of organic solvents, and a myriad of interfaces to facilitate quick

solvent evaporation. Such microparticles, generally regarded as ‘microspheres,’ are often in the size range of 1-15 μm or larger, with a high drug encapsulation efficiency [5, 6]. This process has some limitations because some agglomeration of the microparticles occurs during manufacturing [12] and increased operating temperatures to remove the organic solvent is required.

1.2.2 Coacervation

Coacervation – also called phase separation – is another way to prepare drug encapsulated microspheres. The polymer is dissolved at low concentration in an organic solvent such as methylene chloride or ethyl acetate [13]. Hydrophobic drugs are dissolved directly into the polymer solution, while hydrophilic drugs are dissolved into water and dispersed into the polymer solution via ultrasonification [5]. An organic nonsolvent such as silicone oil [13, 14] or petroleum ether [15] is then slowly added to the solution while stirring, initiating phase separation of the polymer solution to a polymer poor phase and a polymer rich phase surrounding the drug. The active drug is dispersed throughout the resulting phase, in soft polymer droplets called the ‘coacervate.’ The suspension of microspheres is then added to a larger quantity of the organic nonsolvent, allowing the microspheres to harden through evaporation of the remaining polymer solvent. The microspheres are washed, collected, and vacuum dried. This preparation method has some serious drawbacks, including the high amounts of residual toxic solvents, coacervating agents, and hardening agents that remain in the microspheres even after manufacture [13].

1.2.3 Emulsions

The most common method of preparing polymer microspheres is the emulsion-solvent evaporation method. There are four types of emulsion-solvent evaporation methods: oil-in-water (O/W), water-in-oil in water (W/O/W), oil-in-oil (O/O) and solid-in-oil in water (S/O/W) [5]. These four types can subsequently be broken into two groups: single emulsion (and single suspension/emulsion) processes (O/W, O/O, and S/O/W) and double emulsion processes (W/O/W).

In the single emulsion processes, predominantly comprised of O/W and S/O/W, the polymer solution is dissolved in an organic solvent. The drug is then dissolved in the polymer phase (O/W) or dispersed into the polymer phase (S/O/W) via homogenization [16]. The polymer solution is immediately added to a large volume of water to create an emulsion. The organic solvent is removed through evaporation or extraction, leaving hardened polymer droplets. The O/W method is better suited for hydrophobic drugs because of the tendency of hydrophilic drugs to diffuse out into the larger water phase during hardening, resulting in low encapsulation efficiencies and larger burst release kinetics [5].

The other single emulsion process, O/O is sometimes used to encapsulate proteins and other hydrophilic drugs. In this process, the polymer and drug are dissolved together in a water miscible organic solvent like acetonitrile. The drug/polymer solution is then emulsified by adding it to an organic solvent such as light mineral or cottonseed oil. The solvent is removed via extraction or evaporation, and the microspheres are washed with solvents like n-hexane or petroleum ether [5, 17, 18].

The most common emulsion-based encapsulation method is the double emulsion process, W/O/W, which is very suitable for water soluble proteins and peptides. In this method, the drug is dissolved in an aqueous solution while the polymer is dissolved in an organic solution such as methylene chloride. The two solutions are then combined and stirred vigorously, creating the first microfine emulsion. This emulsion solution is added to a larger volume of aqueous solution that contains an emulsifier such as polyvinyl alcohol (PVA). The suspension is then stirred and the organic solvent removed via evaporation or extraction. The microspheres are then washed, collected and dried.

1.2.4 Traditional Preparation Limitations

All current microsphere formulation methods have weaknesses, particularly for encapsulating and delivering proteins. Chief among these limitations is the instability of the encapsulated protein during microsphere manufacture, lyophilization, storage, and release. Additional drawbacks include the inability to terminally sterilize microspheres after preparation and the variability within and across different formulations. The latter short coming contributes to the high cost normally associated with aseptic microsphere production.

1.3 Stability Concerns

Microspheres can be used to deliver both small molecule drugs and larger biological molecules such as peptides and proteins. Whereas small molecule active drugs typically only suffer from chemical modes of instability, proteins and large peptides can become biologically inactive due to numerous physical instability pathways, such as protein unfolding or loss in tertiary structure [19]. Due to their higher rate of incidence,

physical stability concerns sometimes overwhelm any chemical stability concerns in polymeric protein delivery. Such physical instability mechanisms include aggregation, denaturation, and precipitation. Most of the focus of biopolymer delivery is consequently aimed at increasing physical stability, a characteristic unique to proteins and large peptides.

1.3.1 Protein Instability during Encapsulation

During polymeric microparticle encapsulation, a protein is exposed to a number of conditions that can negatively influence its physical stability. These factors include the existence of an organic/aqueous interface [20], shear, the air-liquid interface [21], and higher temperatures. Protein instability during encapsulation is regarded as one of the two most significant obstacles of controlled-release injectable delivery vehicles [2] (the other being instability during *in vivo* release).

Without any additional mechanical forces, organic solvents such as DMSO and methylene chloride have been shown to cause extensive denaturation of proteins if they dissolve the protein [22, 23]. However, encapsulation of proteins in microspheres often requires the addition of an aqueous solution. With this additional phase, an organic/aqueous interface is produced. Because proteins contain both hydrophilic and hydrophobic parts, they are considered surface active, and adsorb at the organic/aqueous interface. At this interface, proteins can irreversibly aggregate [20] to form dimers and polymers through disulfide bond reshuffling [24] and hydrophobic interactions [25]. Thus, while the organic solvent itself is detrimental for many proteins, this organic/aqueous interface may be more detrimental to proteins as observed with α-

chymotrypsin [26], ribonuclease A [20], tetanus toxoid [27], ovalbumin [24] and lysozyme [28].

Shear with mixing and the air-liquid interface also have an impact on protein denaturation and aggregation. During the homogenization process of drug microencapsulation, the protein is exposed to both high levels of shear as well as an extensive air-liquid interface. While shear and shear rate alone were observed not to have a large effect on aggregation [29], shear in conjunction with the air-liquid interface is very detrimental to proteins [21]. It is generally believed that the protein adsorbs to the air-liquid interface and then unfolds, initiating aggregation of the hydrophobic chains [30]. During microsphere preparation, shear may play its destructive role primarily through increasing the air-liquid interface renewal rate [21].

In some microencapsulation methods, it is necessary to disperse the aqueous protein into the organic polymer phase via ultrasonication. However, this introduces energy into the emulsion. Protein stability may be affected by the local temperature extremes and/or formation of free radicals generated through such processes [31].

1.3.2 Protein Instability during Storage

Prior to use, microspheres are often freeze dried so that they can be stored until they are to be used. By removing the water and any residual organic solvent, degradation should occur at a slower rate. However, during the freezing process such proteins are exposed to extremes of concentrations and pH, which can also harm the protein. Thus, it is necessary to quickly freeze the protein to help reduce some of those freezing stresses. While the frozen solution sublimes, any salts present will greatly increase in concentration, which has been found to be deleterious to protein stability. Studies have

indeed indicated that dehydration of proteins can cause significant irreversible conformational changes without the presence of certain stabilizers [32].

Additional concerns exist when the protein is lyophilized with a hydrophobic polymer. First, the existence of such a hydrophobic interface provides another surface for protein denaturation to take place. Additionally, during lyophilization the temperature can rise, melting ice into the liquid phase again. If this residual water is left in the microspheres, premature degradation of the polymer and protein can occur. As the polymer degrades, it generates acidic groups, lowering the pH and potentially degrading the protein [33]. Moisture can also cause aggregation by providing a medium for thiol-disulfide exchange [34] or cross-linking by formaldehyde-mediated processes for formaldehyde-treated protein antigens [35].

1.3.3 Protein Instability during Release

When microspheres are placed into the *in vitro* or *in vivo* aqueous release environment, the microspheres become hydrated. The amount and speed of water uptake is dependent upon the properties of the polymer and microsphere, such as polymer molecular weight, composition, excipient identity, and structure. Generally, the amount of water uptake of the entire microsphere is in the range of 20% to 100% of the polymer dry weight [1].

Naturally, as the polymer becomes hydrated the protein is exposed to water as well. Rehydration of a solid protein has been shown to destabilize proteins [36]. Additionally, at increasing water content, the protein molecule is more flexible and reactive, [37, 38] providing the opportunity for destabilization. The moisture level affects the amount of aggregation. At low and high moisture rates, the amount of

aggregation is minimal, while a maximum aggregation amount is seen an intermediate moisture rates [34]. This increased aggregation at intermediate moisture amounts is dependent on the protein as well as the pH [1].

The aqueous pores of PLGA microspheres are often referred to as 'microclimates,' since each may possess a unique environment depending on the amount of water penetration, the extent of polymer degradation, and the number of water-soluble acids. As the polyester polymer degrades through hydrolysis, acid is produced, subsequently lowering the pH. Within a single formulation, these microclimates are at least slightly different from one another with respect to pH. Across different formulations, the microclimate pH differs markedly. In some formulations the pH in these aqueous pores are neutral (pH 6 to 7) [39], however in many formulations they are reported as acidic (pH 2 to 6) [40-42]. This difference is dependent on the presence of any encapsulated buffering species, as well as the type of polymer, specifically its rate of degradation and permeability in transporting acid byproducts [1].

A low microclimate pH can be severely detrimental to the protein species present. When a protein is at a pH far lower than its isoelectric point, it loses any negative charges and contains only positive charges. These positive charges will repel each other and may lead to protein denaturation [43]. In some instances, denaturation may be great enough that irreversible aggregation results. Any acid labile peptide bonds will undergo rapid hydrolysis at low pH [44]. Simulations of a bovine serum albumin (BSA) in a very acidic microclimate pH (pH < 2) showed denaturing, peptide bond hydrolysis, and noncovalent aggregation [45]. The addition of a base such as $Mg(OH)_2$, $MgCO_3$, $ZnCO_3$

and $Ca(OH)_2$, to the polymer has been shown to diminish some of these effects by increasing the pH [45, 46].

An additional mechanism that can destabilize the protein involves the polymer surface. It is known that the proteins can adsorb to polymers such as PLGA [47]. This adsorption stems from the interaction between the hydrophobic protein interior and the hydrophobic polymer chain, and can instigate irreversible conformational changes [48]. The addition of a surfactant such as sodium dodecyl sulfate (SDS) has been shown to increase the release of BSA at later stages of release [49], although it is not clear whether this increased release is due to BSA being released from the surface of the polymer [49] or due to dissolving noncovalent aggregates [1, 45] . Though the extent of this polymer surface/protein interaction is unknown, it is believed that no more than 10% of the original amount of loaded protein is adsorbed [1].

Additional causes of protein instability during release include the presence of water-soluble oligomers, chemical reactivity between protein and polymer [3], and chemical changes such as deamidation and oxidation [50]. These factors are generally thought to have only a small role in the destabilizing process and as such they will not be discussed here.

1.3.4 Stability during Sterilization

In parenteral applications, especially ocular delivery, the delivery systems are required to be unconditionally free of microorganisms [51]. Thus, the removal or destruction of all living cells, bacterial spores, and viruses is of critical importance in controlled-release biodegradable polymer delivery. However, sterilization of protein-

encapsulated microspheres is not trivial, especially considering its antithetic objective: destroy all living things, but leave the biological drug molecules undamaged.

Common methods of sterilization include heat, filtration, radiation, and chemical sterilization [52]. Some of these processes have clear limitations when applied to microsphere sterilization. For instance, heat can melt the polymer and damage the protein. Filtration is not likely to be successful, since any microorganisms can be entrapped inside the microsphere matrix. There are also no chemical treatments that are suitable for microsphere applications. Ethylene oxide, commonly used to sterilize disposable laboratory supplies, increases polymer degradation, disrupts the polymer matrix, and is highly toxic [53]. Ethanol has been used only as a chemical disinfectant for polyester scaffolds because it lacks the ability to destroy hydrophilic viruses and bacterial spores [54], but can not fully penetrate a microsphere for sterilization and also can swell the polymer, altering the polymer matrix.

Consequently, radiation has been the focal point of microsphere sterilization. However this sterilization method has serious drawbacks as well. One type of radiation generally used for sterilization purposes, γ-irradiation, has been shown to initiate degradation of the polymer, dependent on the dosage of radiation [54, 55]. A recent experiment revealed that γ-irradiation of recombinant human insulin-like growth factor-I encapsulated PLGA microspheres caused aggregation of the protein as well as differences in the formulation release rate [56]. Even more alarming, γ-irradiation of drug encapsulated microspheres was shown to cause the formation of free radicals in clonazepam, an antiepileptic small molecule drug [57], as well as in the protein

ovalbumin [58]. The amount and persistence of free radicals generated was large enough to be able to be used as irradiation markers [57].

Clearly, there are problems with producing a microparticle delivery system devoid of any microorganisms while maintaining protein integrity. Thus, it is currently necessary to produce protein-encapsulated microsphere in expensive aseptic facilities.

1.4 Formulation Variability

Across a series of research groups, a particular microparticle formulation can vary considerably in drug content and release profile. Each group has its own equipment for homogenizing, stirring, and measuring. For instance, it is known that the microsphere pore structure is dependent on the organic solvent removal profile, which is in turn dependent on stirring rate during hardening as well as temperature [59]. These factors can vary between different equipment, interpretation of measurement, and location, among other factors.

Even more variability is observed across different formulations. The release profile of an encapsulated protein with a loading of 10% (w/w) will not be exactly the same as another protein, even at the same loading. The amount of water phase used to dissolve the drug in an w/o/w itself will have an influence on microsphere morphology [60]. Furthermore, the makeup of the polymer, including variation across molecular weights, manufacturer, and different lots from the same manufacturer, has an obvious impact on the morphology and release rate of the microsphere.

The consequence of this variability is that every time a new drug is used in microparticle delivery, a new formulation must be prepared. Various factors need to be manipulated in order to produce a formulation with an acceptable amount of encapsulated

drug as well as an acceptable release profile. These factors include but are not limited to: polymer type, amount of encapsulated drug, identity of organic solvent, polymer concentration in the organic phase, identity and amount of excipients, stirring rate during hardening, temperature during preparation, speed of homogenization, organic/aqueous phase ratios, continuous phase amount, and identity and amount of stabilizers. The formulation must undergo a series of extensive tests to find the optimal parameters and release characteristics, as well as to evaluate its effectiveness.

1.5 Pores

1.5.1 Porosity

Another critical artifact of manufacturing, particularly visible in the emulsion based preparation, is porosity. After microsphere preparation, the morphology of the microspheres can be investigated through electron microscopy. The microspheres will sometimes be honeycomb or sponge like, with pores visible on the surface. Channels connecting these internal pores are often visible. In combination, the pores, which percolate throughout the polymer with interconnecting channels, are referred to as a *pore network*. These porous spaces are locations where water or organic solvent were present before lyophilization, preventing hydrophobic polymer occupation. These pores can range in size from 10 nm to 2000 nm [61]. This is larger than the diameter of a large protein, bovine serum albumin, reported to be around 7-9 nm [62]. The extent and development of this pore network is dependent on the particular formulation. The *porosity* , a measure of the total amount of empty space, is important because it has been shown to correlate with the amount of drug release during the initial release [63, 64].

Some researchers have attempted to increase this initial burst by increasing the porosity, with the ultimate goal of getting a more immediate pharmacological response due to the higher initial drug concentration [65].

The extent of pore formation in w/o/w emulsion microspheres has been found to be dependent on a number of processing parameters. The composition and size of the inner aqueous phase was found to play a role in porosity. For instance, a higher amount of water in the first emulsion was found to increase porosity [60] and substituting methanol for water also increased the porosity [66]. The type of emulsifier may also have an effect on porosity [67, 68]. Additionally, the osmotic pressure difference between the dispersed phase and the continuous phase during hardening was found to play a large role. The addition of salt to the continuous phase to raise the osmotic pressure of that phase succeeding in creating denser particles with a lower initial burs t[69, 70]. Similarly, adding substances to increase the osmotic pressure of the dispersed phase was found to substantially increase porosity as well [65]. Perhaps the largest determinant of porosity is the rate of evaporation of the organic solvent from the microspheres. High evaporation rates have generally produced much more porous spheres [71-73] with larger pore size[59]. This evaporation rate can be augmented by increasing the amount of water in the second emulsion [59, 74], increasing the temperature [72], and increasing the temperature ramp [71, 74], among other parameters.

1.5.2 Pore Closing / Opening

Previous work has examined the mechanisms surrounding the porosity during release. During incubation at typical biological temperature, i.e. 37°C, the polymer spontaneously rearranges. After beginning irregularly shaped, the pores become slightly

smaller and circular in shape after a short incubation period of somewhere on the order of 24 – 48 hours. Eventually the pores previously visible on the surface are closed. After about 5 hours of incubation, a thin layer of film or 'skin' formed around each microsphere. These morphological changes were observed via SEM, and their termination correlated to the cessation of the initial burst release. This polymer rearrangement was observed to occur from the inside out, and stopped after 1 day of incubation [61]. The authors theorize that this polymer rearrangement and subsequent closing of the pores is at least partially responsible for the appearance of the initial drug burst and its subsequent termination. Additionally, this pore closing phenomenon was observed to occur faster at pH 4 than pH 7 [75], though the effects of acetate as a plasticizer in that study should not be ignored.

This work presented another interesting phenomenon. The microsphere pore closing that correlated with the initial burst and also corresponded to a decrease in permeability of the microspheres to dextran tetramethylrhodamine (TMR), a fluorescent dye with an approximate molecular weight of 3000. Microspheres were incubated in release media at 37°C for either 0, 5, or 24 hours and then treated for 30 minutes with a solution of dextran TMR. A stark difference in the degree of penetration of dextran TMR was seen. Treatment with dextran TMR before any incubation showed considerable penetration into the microsphere. However, after 24 hours of incubation, little penetration by dextran TMR into the microsphere was observed [75]. Later work repeated this using a dextran bodipy conjugate with a molecular weight of approximately 10,000 [76]. This work corroborated the existence of an extensive pore network throughout the microsphere, since deep penetration of the dextran dye was seen even with minimal pores

visible on the surface. After incubation of blank microspheres at 4°C in dextran dye solution for 12 hours, and then placing them in a blank release medium at the same temperature, a great deal of dextran remained inside. The authors suggested that this was evidence that some of the inner pore network closes even at this low temperature [76].

1.6 Self-Healing of Polymers

1.6.1 Background

As evidenced by the pore closing phenomenon, polymers in solution can be very mobile. In fact, a number of materials, including metals, ceramics, and polymers, are capable of undergoing processes to repair internal damages such as fracture or indentation. This process of intrinsic repair is called 'self-healing'. Due to their wide range of properties and types, including their potential for biocompatibility, such self-healing in polymers has been the focus of much recent research work.

One type of healing in polymer systems is observed through the use of healing agents. Systems that require such additional agents are called 'irreversible systems,' [77] and while they are self-healing, these agents must be dispersed throughout the system and it consequently has a finite number of possible repairs. For example, there have been reports of encapsulated fibers or microcapsules with a reactive healing fluid that when ruptured and exposed to the matrix can polymerize, healing any defects [78-80]. Yet perhaps the term 'self-healing polymers' is a misnomer; these polymers require isolated liquid capsules capable of rupturing and subsequently filling to counteract any inflicted damage. Consequently, the systems may be 'self-healing,' but the polymers phase itself is not.

Alternatively, polymers exist that are homogenous in their makeup and are capable of self-healing without the incorporation of healing agents. These polymeric systems, capable of undergoing repair repeatedly, are referred to as reversible systems. After damage is inflicted, the polymers can 'repolymerize,' joining two sections of damaged polymer. This reattachment of two sections of material can be through covalent bonding, e.g. Diels-Alder, thiol, or N-O bonding, or through non-covalent interactions, where the polymerization or cross-linking depends on intermolecular interactions of the monomer units and side-chains [77], such as hydrogen or ionic bonding or even chain entanglement [81]. It has been observed however, that healing without chemical reactions leads to a healing strength comparatively less than covalent bonding [82].

1.6.2 Self-healing Steps

Once a dent appears in a polymer surface, the most important driving force behind healing of the polymer is surface tension, in an attempt to keep the polymer surface as small as possible [83]. The time scale of such rearrangement depends ultimately on the mobility of the polymer chains, i.e. the glass transition temperature of the polymer [83]. For such processes, heat/energy is required [84], and more specifically the temperature needs to be above the polymer glass transition temperature, in order to give mobility to the chains. Furthermore, these dents have been shown to either a) grow, eventually leading to complete rupture or b) heal, giving rise to a repaired polymer surface [85, 86]. The determination for this direction is the amount of excess surface energy introduced to the surface of the polymer film. Excess surface energy above a critical value $\Delta F_{\gamma,crit}$ indicates the indentation will grow, and an excess surface energy below $\Delta F_{\gamma,crit}$ means the

indentation will heal. It should be noted that a small region exists surrounding $\Delta F_{\gamma,crit}$ where either path may be taken [87].

However, if a crack appears as opposed to just a dent, for healing to occur it is necessary that the two interfaces are held close enough to each other and held in a relatively fixed position during the healing step [84]. As with healing of indentations, the temperature needs to be above the glass transition temperature to impart mobility to the polymer. Such is the case with shape memory polymers, which utilize a annealing stage of 3h at 100°C after damage [88]. Alternatively, healing in poly(methyl methacrylate) was observed using methanol and ethanol as co-solvents [89], subsequently reducing the surface T_g and initiating interdiffusion of the interface polymer chains.

While polymer 'joining' or 'self-healing' can occur after damage to the polymer, it also can be observed if two separate, undamaged polymer interfaces are brought in close contact with one another. For either mechanism, a mechanism has been proposed by Wool and O'Connor [90, 91] discussing the steps for polymer healing. These five stages are 1) *surface rearrangement*, including post-crack chain-end distribution changes at the surface and surface chemical reactions, 2) *surface approach*, or the time, space, and force required to bring the two surfaces in contact with each another, 3) *wetting*, specifically the initial formation of an interface between the two surfaces, 4) *diffusion*, the migration and diffusion of the polymer chains with one another, and 5) *randomization*, the further random crossing of the interface, forming new polymer entanglements [92-94]. These last two steps, diffusion and randomization of the polymer chain segments, are what gives the healed polymer segment its strength.

Self-healing has also been observed via the spontaneous formation of latex films from a spread of latex particles, in a dry open air state above the T_g of the polymer [95, 96]. The activation energy for this agglomeration of particles was not dependent on polymer molecular weight [95]. Furthermore, this film formation was divided into two steps: *void closure* and *interdiffusion*, the latter of which corresponds to Wool and O'Connor's aforementioned diffusion and randomization steps. Void closure is seen in the beginning step of the annealing process, as the particles have increasing surface energy to flow and spread [97]. Brownian motion is believed to be responsible for this chain interdiffusion across the polymer gap [97]. The healing of this gap is only possible once the polymer coils from each side are at least capable of spanning half the distance during their random motion, meeting one another in the middle [97]. The strength increases with time and temperature and follows a $t^{1/4}$ law using the reptation model of confining polymer chains to 'tubes' [98].

1.6.3 Surface versus Bulk

While healing is possible between two polymer surfaces above the glass transition temperature, it is important to note that in polymer films the T_g at or very near the surface of the polymer can differ markedly from the T_g of the bulk polymer, as seen in polystyrene [99-104] and poly(methyl methacrylate) [102]. This reduced T_g of the polymer is typically seen at thicknesses less than 50 – 100 nm from the surface, with increasing T_g as the distance into the bulk increases [105-107]. The reduced glass transition values at the surface have been explained by an increase of free volume from the chain end groups at the surface and reduced cooperativity of intermolecular coupling between motions of different chains because of the existence of the polymer surface

[101]. Thus, the polymer near the surface has a higher amount of inherent mobility than the bulk polymer [108]. In fact, with polystyrene films less than 100 nm thick, the polymer film had so much mobility that annealing above the T_g ruptured the polymer film, where upon the polystyrene formed polymer droplets. The authors point out that this coalescing into droplets minimizes the film/substrate interface [109], and subsequently the interfacial energy. Thus, these polymers had so much mobility that droplet formation, presumably due to the driving force of interfacial tension minimization, overpowered the cohesive forces of the polymer film. The observed reduced surface glass transition temperature prompted Keddie et al [106] to prophetically state over 15 years ago that this potential decrease in glass transition temperature at the surface and subsequent more mobile surface layer may allow for "the autoadhesion of glassy polymers" in the future . Indeed, polystyrene has been observed to heal at a temperature significantly below (23-43°C below) its bulk T_g [110]. This ultimate threshold temperature, at which healing is possible, appears to be dependent on the molecular weight of the polymer, which corresponds to the amount of polymer mobility [111].

Such features are apparent in the biodegradable polymers utilized in this research. For instance, polymer rearrangement (e.g. visible changes in a smooth surface and spherical shape) of polymeric poly(D,L-lactic acid) (PLA) microspheres was only seen in lower molecular weight PLA, specifically when the now revised polymer T_g (due to degradation and decreasing oligomer MW) passed below the incubation temperature [112, 113], showing the importance of surpassing T_g for polymer mobility. Additional surface mobility has been reported in PLA and PLGA films, as the methyl side chains in the lactic acid units were discovered to exist preferentially at the polymer/air surface and

are more free to vibrate, especially in films over 1 μm in thickness [114]. Such films go through reformation as their surface is wetted with water, with the methyl side chains units reorientation believed to be the major movement responsible for rearrangement [114].

1.7 Conclusion

Clearly, much of the future focus for polymer protein delivery must be on maintaining stability of the encapsulated molecule. Numerous ways of improving stability during encapsulation have been reported, but all still expose the protein to non-biological solvents, and none completely alleviate the stability problem. Furthermore, during release, these controlled release systems are subjected to additional stresses, including an increasingly acidic pH. Separately, during release the pores in these controlled release systems are observed to rearrange, sealing off their internal network from the outside environment. This polymer rearrangement appears to be related to an intrinsic ability of the polymer to 'self-heal.' Self-healing has been studied in many other polymers, although questions about its mechanism still remain.

An earlier set of experiments utilized penetration of a fluorescently labeled sugar molecule to visualize a phenomenon similar to self-healing, the pore closing phenomenon in PLGA microspheres. These experiments succeeded in using this procedure to visualize the pore network, but also created microspheres with a polysaccharide encapsulated inside. Thus, perhaps this pore closing, 'self-healing' phenomenon could be used to encapsulate proteins in a novel way, where the encapsulated molecules are not subjected to the stability perils usually associated with protein encapsulated microsphere manufacture. The aim of this research project is to exploit pore closing to create

microparticles with encapsulated protein that is more stable, as well as presumably displaying different release characteristics. This new method of drug encapsulation is called ‘self-healing microencapsulation’ since it is the polymer and its environment, not external forces or chemicals, that drives the encapsulation.

1.8 References

1. Schwendeman, S. P., Recent advances in the stabilization of proteins encapsulated in injectable PLGA delivery systems. *Critical Reviews in Therapeutic Drug Carrier Systems* **2002,** 19, (1), 73-98.
2. Fu, K.; Klibanov, A. M.; Langer, R., Protein stability in controlled-release systems. *Nature Biotechnology* **2000,** 18, (1), 24-25.
3. Schwendeman, S. P.; Costantino, H. R.; Gupta, R. K.; Langer, R., Peptide, Protein, and Vaccine Delivery from Implantable Polymeric Systems. In *Controlled Drug Delivery - Challenges and Strategies*, Park, K., Ed. American Chemical Society: Washington, D.C., 1997; pp 229-267.
4. Athanasiou, K. A.; Niederauer, G. G.; Agrawal, C. M., Sterilization, toxicity, biocompatibility and clinical applications of polylactic acid/ polyglycolic acid copolymers. *Biomaterials* **1996,** 17, (2), 93-102.
5. Jain, R. A., The manufacturing techniques of various drug loaded biodegradable poly(lactide-co-glycolide) (PLGA) devices. *Biomaterials* **2000,** 21, (23), 2475-2490.
6. Wagenaar, B. W.; Muller, B. W., Piroxicam Release from Spray-Dried Biodegradable Microspheres. *Biomaterials* **1994,** 15, (1), 49-54.
7. Witschi, C.; Doelker, E., Influence of the microencapsulation method and peptide loading on poly(lactic acid) and poly(lactic-co-glycolic acid) degradation during in vitro testing. *Journal of Controlled Release* **1998,** 51, (2-3), 327-341.
8. Walter, E.; Moelling, K.; Pavlovic, J.; Merkle, H. P., Microencapsulation of DNA using poly(DL-lactide-co-glycolide): stability issues and release characteristics. *Journal of Controlled Release* **1999,** 61, (3), 361-374.
9. Thomasin, C.; Corradin, G.; Men, Y.; Merkle, H. P.; Gander, B., Tetanus toxoid and synthetic malaria antigen containing poly(lactide)/poly(lactide-co-glycolide) microspheres: Importance of polymer degradation and antigen release for immune response. *Journal of Controlled Release* **1996,** 41, (1-2), 131-145.
10. Prior, S.; Gamazo, C.; Irache, J. M.; Merkle, H. P.; Gander, B., Gentamicin encapsulation in PLA/PLGA microspheres in view of treating Brucella infections. *International Journal of Pharmaceutics* **2000,** 196, (1), 115-125.
11. Blanco-Prieto, M. J.; Besseghir, K.; Zerbe, O.; Andris, D.; Orsolini, P.; Heimgartner, F.; Merkle, H. P.; Gander, B., In vitro and in vivo evaluation of a somatostatin analogue released from PLGA microspheres. *Journal of Controlled Release* **2000,** 67, (1), 19-28.
12. Shigeyuki, T.; Yoshiaki, U.; Hajime, T.; Yasuaki, O., Preparation and characterization of copoly(dl-lactic/glycolic acid) microparticles for sustained release of thyrotropin releasing hormone by double nozzle spray drying method. *Journal of Controlled Release* **1994,** 32, (1), 79-85.
13. Thomasin, C.; Ho, N. T.; Merkle, H. P.; Gander, B., Drug microencapsulation by PLA/PLGA coacervation in the light of thermodynamics. 1. Overview and theoretical considerations. *Journal of Pharmaceutical Sciences* **1998,** 87, (3), 259-268.

14. Thomasin, C.; Johansen, P.; Alder, R.; Bemsel, R.; Hottinger, G.; Altorfer, H.; Wright, A. D.; Wehrli, G.; Merkle, H. P.; Gander, B., A contribution to overcoming the problem of residual solvents in biodegradable microspheres prepared by coacervation. *European Journal of Pharmaceutics and Biopharmaceutics* **1996,** 42, (1), 16-24.
15. Zhang, J. X.; Zhu, K. J.; Chen, D., Preparation of bovine serum albumin loaded poly (D, L-lactic-co-glycolic acid) microspheres by a modified phase separation technique. *Journal of Microencapsulation* **2005,** 22, (2), 117-126.
16. Takada, S.; Yamagata, Y.; Misaki, M.; Taira, K.; Kurokawa, T., Sustained release of human growth hormone from microcapsules prepared by a solvent evaporation technique. *Journal of Controlled Release* **2003,** 88, (2), 229-242.
17. Jiang, W. L.; Schwendeman, S. P., Stabilization of a model formalinized protein antigen encapsulated in poly(lactide-co-glycolide)-based microspheres. *Journal of Pharmaceutical Sciences* **2001,** 90, (10), 1558-1569.
18. Murty, S. B.; Wei, Q.; Thanoo, B. C.; DeLuca, P. P., In vivo release kinetics of octreotide acetate from experimental polymeric microsphere formulations using oil/water and oil/oil processes. *Aaps Pharmscitech* **2004,** 5, (3).
19. Costantino, H. R.; Langer, R.; Klibanov, A. M., Solid-Phase Aggregation of Proteins under Pharmaceutically Relevant Conditions. *Journal of Pharmaceutical Sciences* **1994,** 83, (12), 1662-1669.
20. Sah, H., Protein behavior at the water/methylene chloride interface. *Journal of Pharmaceutical Sciences* **1999,** 88, (12), 1320-1325.
21. Maa, Y. F.; Hsu, C. C., Protein denaturation by combined effect of shear and air-liquid interface. *Biotechnology and Bioengineering* **1997,** 54, (6), 503-512.
22. Desai, U. R.; Klibanov, A. M., Assessing the Structural Integrity of a Lyophilized Protein in Organic-Solvents. *Journal of the American Chemical Society* **1995,** 117, (14), 3940-3945.
23. Castellanos, I. J.; Griebenow, K., Improved α-Chymotrypsin Stability Upon Encapsulation in PLGA Microspheres by Solvent Replacement. *Pharmaceutical Research* **2003,** 20, (11), 1873-1880.
24. Sah, H., Stabilization of proteins against methylene chloride water interface-induced denaturation and aggregation. *Journal of Controlled Release* **1999,** 58, (2), 143-151.
25. Sah, H.; Bahl, Y., Effects of aqueous phase composition upon protein destabilization at water/organic solvent interface. *Journal of Controlled Release* **2005,** 106, (1-2), 51-61.
26. Perez-Rodriguez, C.; Montano, N.; Gonzalez, K.; Griebenow, K., Stabilization of alpha-chymotrypsin at the CH2Cl2/water interface and upon water-in-oil-in-water encapsulation in PLGA microspheres. *Journal of Controlled Release* **2003,** 89, (1), 71-85.
27. Alonso, M. J.; Gupta, R. K.; Min, C.; Siber, G. R.; Langer, R., Biodegradable Microspheres as Controlled-Release Tetanus Toxoid Delivery Systems. *Vaccine* **1994,** 12, (4), 299-306.
28. van de Weert, M.; Hoechstetter, J.; Hennink, W. E.; Crommelin, D. J. A., The effect of a water/organic solvent interface on the structural stability of lysozyme. *Journal of Controlled Release* **2000,** 68, (3), 351-359.

29. Maa, Y. F.; Hsu, C. C., Effect of high shear on proteins. *Biotechnology and Bioengineering* **1996,** 51, (4), 458-465.
30. Oliva, A.; Santovena, A.; Farina, J.; Llabres, M., Effect of high shear rate on stability of proteins: kinetic study. *Journal of Pharmaceutical and Biomedical Analysis* **2003,** 33, (2), 145-155.
31. Wang, J. J.; Chua, K. M.; Wang, C. H., Stabilization and encapsulation of human immunoglobulin G into biodegradable microspheres. *Journal of Colloid and Interface Science* **2004,** 271, (1), 92-101.
32. Prestrelski, S. J.; Tedeschi, N.; Arakawa, T.; Carpenter, J. F., Dehydration-Induced Conformational Transitions in Proteins and Their Inhibition by Stabilizers. *Biophysical Journal* **1993,** 65, (2), 661-671.
33. van de Weert, M.; Hennink, W. E.; Jiskoot, W., Protein instability in poly(lactic-co-glycolic acid) microparticles. *Pharmaceutical Research* **2000,** 17, (10), 1159-1167.
34. Liu, W. R.; Langer, R.; Klibanov, A. M., Moisture-Induced Aggregation of Lyophilized Proteins in the Solid-State. *Biotechnology and Bioengineering* **1991,** 37, (2), 177-184.
35. Schwendeman, S. P.; Costantino, H. R.; Gupta, R. K.; Siber, G. R.; Klibanov, A. M.; Langer, R., Stabilization of Tetanus and Diphtheria Toxoids against Moisture-Induced Aggregation. *Proceedings of the National Academy of Sciences of the United States of America* **1995,** 92, (24), 11234-11238.
36. Carpenter, J. F.; Pikal, M. J.; Chang, B. S.; Randolph, T. W., Rational design of stable lyophilized protein formulations: Some practical advice. *Pharmaceutical Research* **1997,** 14, (8), 969-975.
37. Ahlneck, C.; Zografi, G., The Molecular-Basis of Moisture Effects on the Physical and Chemical-Stability of Drugs in the Solid-State. *International Journal of Pharmaceutics* **1990,** 62, (2-3), 87-95.
38. Putney, S. D.; Burke, P. A., Improving protein therapeutics with sustained-release formulations. *Nature Biotechnology* **1998,** 16, (2), 153-157.
39. Cleland, J. L.; Duenas, E. T.; Park, A.; Daugherty, A.; Kahn, J.; Kowalski, J.; Cuthbertson, A., Development of poly-(D,L-lactide-coglycolide) microsphere formulations containing recombinant human vascular endothelial growth factor to promote local angiogenesis. *Journal of Controlled Release* **2001,** 72, (1-3), 13-24.
40. Mader, K.; Gallez, B.; Liu, K. J.; Swartz, H. M., Non-invasive in vivo characterization of release processes in biodegradable polymers by low-frequency electron paramagnetic resonance spectroscopy. *Biomaterials* **1996,** 17, (4), 457-461.
41. Mader, K.; Bittner, B.; Li, Y. X.; Wohlauf, W.; Kissel, T., Monitoring microviscosity and microacidity of the albumin microenvironment inside degrading microparticles from poly(lactide-co-glycolide) (PLG) or ABA-triblock polymers containing hydrophobic poly(lactide-co-glycolide) A blocks and hydrophilic poly(ethyleneoxide) B blocks. *Pharmaceutical Research* **1998,** 15, (5), 787-793.
42. Shenderova, A.; Burke, T. G.; Schwendeman, S. P., The acidic microclimate in poly(lactide-co-glycolide) microspheres stabilizes camptothecins. *Pharmaceutical Research* **1999,** 16, (2), 241-248.
43. Peters, T., Serum-Albumin. *Advances in Protein Chemistry* **1985,** 37, 161-245.

44. Manning, M. C.; Patel, K.; Borchardt, R. T., Stability of Protein Pharmaceuticals. *Pharmaceutical Research* **1989,** 6, (11), 903-918.
45. Zhu, G. Z.; Mallery, S. R.; Schwendeman, S. P., Stabilization of proteins encapsulated in injectable poly (lactide-co-glycolide). *Nature Biotechnology* **2000,** 18, (1), 52-57.
46. Zhu, G. Z.; Schwendeman, S. P., Stabilization of proteins encapsulated in cylindrical poly(lactide-co-glycolide) implants: Mechanism of stabilization by basic additives. *Pharmaceutical Research* **2000,** 17, (3), 351-357.
47. Butler, S. M.; Tracy, M. A.; Tilton, R. D., Adsorption of serum albumin to thin films of poly(lactide-co-glycolide). *Journal of Controlled Release* **1999,** 58, (3), 335-347.
48. Van Tassel, P. R.; Guemouri, L.; Ramsden, J. J.; Tarjus, G.; Viot, P.; Talbot, J., A particle-level model of irreversible protein adsorption with a postadsorption transition. *Journal of Colloid and Interface Science* **1998,** 207, (2), 317-323.
49. Crotts, G.; Park, T. G., Stability and release of bovine serum albumin encapsulated within poly(D,L-lactide-co-glycolide) microparticles. *Journal of Controlled Release* **1997,** 44, (2-3), 123-134.
50. Cleland, J. L.; Mac, A.; Boyd, B.; Yang, J.; Duenas, E. T.; Yeung, D.; Brooks, D.; Hsu, C.; Chu, H.; Mukku, V.; Jones, A. J. S., The stability of recombinant human growth hormone in poly(lactic-co-glycolic acid) (PLGA) microspheres. *Pharmaceutical Research* **1997,** 14, (4), 420-425.
51. Herrero-Vanrell, R.; Ramirez, L.; Fernandez-Carballido, A.; Refojo, M. F., Biodegradable PLGA microspheres loaded with ganciclovir for intraocular administration. Encapsulation technique, in vitro release profiles, and sterilization process. *Pharmaceutical Research* **2000,** 17, (10), 1323-1328.
52. Kelly-Wintenberg, K.; Hodge, A.; Montie, T. C.; Deleanu, L.; Sherman, D.; Roth, J. R.; Tsai, P.; Wadsworth, L., Use of a one atmosphere uniform glow discharge plasma to kill a broad spectrum of microorganisms. *Journal of Vacuum Science & Technology a-Vacuum Surfaces and Films* **1999,** 17, (4), 1539-1544.
53. Volland, C.; Wolff, M.; Kissel, T., The Influence of Terminal Gamma-Sterilization on Captopril Containing Poly(D,L-Lactide-Co-Glycolide) Microspheres. *Journal of Controlled Release* **1994,** 31, (3), 293-305.
54. Holy, C. E.; Cheng, C.; Davies, J. E.; Shoichet, M. S., Optimizing the sterilization of PLGA scaffolds for use in tissue engineering. *Biomaterials* **2001,** 22, (1), 25-31.
55. Gilding, D. K.; Reed, A. M., Biodegradable Polymers for Use in Surgery - Polyglycolic-Poly(Actic Acid) Homopolymers and Copolymers .1. *Polymer* **1979,** 20, (12), 1459-1464.
56. Carrascosa, C.; Espejo, L.; Torrado, S.; Torrado, J. J., Effect of gamma-sterilization process on PLGA microspheres loaded with insulin-like growth factor-I (IGF-I). *Journal of Biomaterials Applications* **2003,** 18, (2), 95-108.
57. Montanari, L.; Cilurzo, F.; Valvo, L.; Faucitano, A.; Buttafava, A.; Groppo, A.; Genta, I.; Conti, B., Gamma irradiation effects on stability of poly(lactide-co-glycolide) microspheres containing clonazepam. *Journal of Controlled Release* **2001,** 75, (3), 317-330.

58. Dorati, R.; Genta, I.; Montanari, L.; Cilurzo, F.; Buttafava, A.; Faucitano, A.; Conti, B., The effect of gamma-irradiation on PLGA/PEG microspheres containing ovalbumin. *Journal of Controlled Release* **2005,** 107, (1), 78-90.
59. Li, W. I.; Anderson, K. W.; Mehta, R. C.; DeLuca, P. P., Prediction of solvent removal profile and effect on properties for peptide-loaded PLGA microspheres prepared by solvent extraction/evaporation method. *Journal of Controlled Release* **1995,** 37, (3), 199-214.
60. Crotts, G.; Park, T. G., Preparation of Porous and Nonporous Biodegradable Polymeric Hollow Microspheres. *Journal of Controlled Release* **1995,** 35, (2-3), 91-105.
61. Wang, J. Characterization of Microsphere Drug Delivery Systems During Encapsulation and Initial Drug Release. The Ohio State University Columbus, 2000.
62. Han, A. P.; Schurmann, G.; Mondin, G.; Bitterli, R. A.; Hegelbach, N. G.; de Rooij, N. F.; Staufer, U., Sensing protein molecules using nanofabricated poresn. *Applied Physics Letters* **2006,** 88, (9).
63. Sah, H. K.; Toddywala, R.; Chien, Y. W., The Influence of Biodegradable Microcapsule Formulations on the Controlled-Release of a Protein. *Journal of Controlled Release* **1994,** 30, (3), 201-211.
64. Yang, Y. Y.; Chung, T. S.; Bai, X. L.; Chan, W. K., Effect of preparation conditions on morphology and release profiles of biodegradable polymeric microspheres containing protein fabricated by double-emulsion method. *Chemical Engineering Science* **2000,** 55, (12), 2223-2236.
65. Ravivarapu, H. B.; Lee, H.; DeLuca, P. P., Enhancing initial release of peptide from poly(d,l-lactide-co-glycolide) (PLGA) microspheres by addition of a porosigen and increasing drug load. *Pharmaceutical Development and Technology* **2000,** 5, (2), 287-296.
66. Tuncay, M.; Calis, S.; Kas, H. S.; Ercan, M. T.; Peksoy, I.; Hincal, A. A., Diclofenac sodium incorporated PLGA (50 : 50) microspheres: formulation considerations and in vitro/in vivo evaluation. *International Journal of Pharmaceutics* **2000,** 195, (1-2), 179-188.
67. Zhang, J. X.; Zhu, K. J., An improvement of double emulsion technique for preparing bovine serum albumin-loaded PLGA microspheres. *Journal of Microencapsulation* **2004,** 21, (7), 775-785.
68. Zhang, J. X.; Chen, D.; Wang, S. J.; Zhu, K. J., Optimizing double emulsion process to decrease the burst release of protein from biodegradable polymer microspheres. *Journal of Microencapsulation* **2005,** 22, (4), 413-422.
69. Jiang, G.; Thanoo, B. C.; DeLuca, P. P., Effect of osmotic pressure in the solvent extraction phase on BSA release profile from PLGA microspheres. *Pharmaceutical Development and Technology* **2002,** 7, (4), 391-399.
70. Luan, X.; Skupin, M.; Siepmann, J.; Bodmeier, R., Key parameters affecting the initial release (burst) and encapsulation efficiency of peptide-containing poly(lactide-co-glycolide) microparticles. *International Journal of Pharmaceutics* **2006,** 324, (2), 168-175.
71. Freiberg, S.; Zhu, X., Polymer microspheres for controlled drug release. *International Journal of Pharmaceutics* **2004,** 282, (1-2), 1-18.

72. Izumikawa, S.; Yoshioka, S.; Aso, Y.; Takeda, Y., Preparation of Poly(L-Lactide) Microspheres of Different Crystalline Morphology and Effect of Crystalline Morphology on Drug Release Rate. *Journal of Controlled Release* **1991,** 15, (2), 133-140.
73. Chung, T. W.; Huang, Y. Y.; Liu, Y. Z., Effects of the rate of solvent evaporation on the characteristics of drug loaded PLLA and PDLLA microspheres. *International Journal of Pharmaceutics* **2001,** 212, (2), 161-169.
74. Jeyanthi, R.; Thanoo, B. C.; Metha, R. C.; DeLuca, P. P., Effect of solvent removal technique on the matrix characteristics of polylactide/glycolide microspheres for peptide delivery. *Journal of Controlled Release* **1996,** 38, (2-3), 235-244.
75. Wang, J.; Wang, B. A.; Schwendeman, S. P., Characterization of the initial burst release of a model peptide from poly(D,L-lactide-co-glycolide) microspheres. *Journal of Controlled Release* **2002,** 82, (2-3), 289-307.
76. Kang, J.; Schwendeman, S. P., Dynamic Transition between Open Pores and Isolated Pores in Biodegradable Polymers and the Implication on the Controlled Release of Protein Drugs. **2004**.
77. Bergman, S. D.; Wudl, F., Mendable polymers. *Journal of Materials Chemistry* **2008,** 18, (1), 41-62.
78. White, S. R.; Sottos, N. R.; Geubelle, P. H.; Moore, J. S.; Kessler, M. R.; Sriram, S. R.; Brown, E. N.; Viswanathan, S., Autonomic healing of polymer composites. *Nature* **2001,** 409, (6822), 794-797.
79. Dry, C.; Sottos, N. In *Smart Structures and Materials 1993: Smart Materials*, SPIE, Bellingham, WA, 1993; Varadan, V. K., Ed. SPIE: Bellingham, WA, 1993; p 438.
80. Suryanarayana, C.; Rao, K. C.; Kumar, D., Preparation and characterization of microcapsules containing linseed oil and its use in self-healing coatings. *Progress in Organic Coatings* **2008,** 63, (1), 72-78.
81. Wu, D. Y.; Meure, S.; Solomon, D., Self-healing polymeric materials: A review of recent developments. *Progress in Polymer Science* **2008,** 33, (5), 479-522.
82. Avramova, N., Study of the healing process of polymers with different chemical structure and chain mobility. *Polymer* **1993,** 34, (9), 1904-1907.
83. Benthem, R.; Ming, W.; With, G., Self Healing Polymer Coatings. In *Self Healing Materials*, 2007; pp 139-159.
84. Zwaag, S., An Introduction to Material Design Principles: Damage Prevention versus Damage Management. In *Self Healing Materials*, 2007; pp 1-18.
85. Karapanagiotis, I.; Gerberich, W. W.; Evans, D. F., Early dewetting stages of thin polymer films initiated by nanoindentation. *Langmuir* **2001,** 17, (8), 2375-2379.
86. Karapanagiotis, I.; Gerberich, W. W., A criterion for dewetting initiation from surface disturbances on ultrathin polymer films. *Langmuir* **2005,** 21, (20), 9194-9198.
87. Karapanagiotis, L., An energetic criterion to compare the evolution of thermally-excited surface disturbances and nanoindentation-induced defects on thin polymer films. *Surface Science* **2007,** 601, (16), 3426-3430.
88. Li, G. Q.; John, M., A self-healing smart syntactic foam under multiple impacts. *Composites Science and Technology* **2008,** 68, (15-16), 3337-3343.
89. Hsieh, H. C.; Yang, T. J.; Lee, S., Crack healing in poly(methyl methacrylate) induced by co-solvent of methanol and ethanol. *Polymer* **2001,** 42, (3), 1227-1241.

90. Wool, R. P.; Oconnor, K. M., A Theory of Crack Healing in Polymers. *Journal of Applied Physics* **1981,** 52, (10), 5953-5963.
91. Wool, R. P., Self-healing materials: a review. *Soft Matter* **2008,** 4, (3), 400-418.
92. Zeinolebadi, A.; Mohammadi, N.; Sangari, H. H., The Role of Polymer/Polymer Miscibility in Interfacial Healing Kinetics and Equilibrium Adhesion Energy: A Universal Approach. *Journal of Adhesion Science and Technology* **2008,** 22, (12), 1301-1311.
93. Farinha, J. P. S.; Wu, J.; Winnik, M. A.; Farwaha, R.; Rademacher, J., Polymer diffusion in gel-containing poly(vinyl acetate-co-dibutyl maleate) latex films. *Macromolecules* **2005,** 38, (10), 4393-4402.
94. Arda, E.; Pekcan, O., Time and temperature dependence of void closure, healing and interdiffusion during latex film formation. *Polymer* **2001,** 42, (17), 7419-7428.
95. Ertan Arda, S. K. Ö. P., A photon transmission study for film formation from poly(vinyl acetate) latex particles with different molecular weights. *Journal of Polymer Science Part B: Polymer Physics* **2007,** 45, (20), 2918-2925.
96. Canpolat, M.; Pekcan, Ö., Healing and interdiffusion processes at particle--particle junction during film formation from high-T latex particles. *Polymer* **1995,** 36, (10), 2025-2031.
97. Kara, S.; Pekcan, O.; Sarac, A.; Arda, E., Film formation stages for poly(vinyl acetate) latex particles: a photon transmission study. *Colloid and Polymer Science* **2006,** 284, (10), 1097-1105.
98. Shim, M.-J.; Kim, S.-W., Characteristics of polymer welding by healing process. *Materials Chemistry and Physics* **1997,** 48, (1), 90-93.
99. Meyers, G. F.; DeKoven, B. M.; Seitz, J. T., Is the molecular surface of polystyrene really glassy? *Langmuir* **1992,** 8, (9), 2330-2335.
100. Satomi, N.; Takahara, A.; Kajiyama, T., Determination of Surface Glass Transition Temperature of Monodisperse Polystyrene Based on Temperature-Dependent Scanning Viscoelasticity Microscopy. *Macromolecules* **1999,** 32, (13), 4474-4476.
101. Tanaka, K.; Takahara, A.; Kajiyama, T., Rheological Analysis of Surface Relaxation Process of Monodisperse Polystyrene Films. *Macromolecules* **2000,** 33, (20), 7588-7593.
102. Fryer, D. S.; Nealey, P. F.; de Pablo, J. J., Thermal Probe Measurements of the Glass Transition Temperature for Ultrathin Polymer Films as a Function of Thickness. *Macromolecules* **2000,** 33, (17), 6439-6447.
103. Forrest, J. A.; Dalnoki-Veress, K.; Stevens, J. R.; Dutcher, J. R., Effect of Free Surfaces on the Glass Transition Temperature of Thin Polymer Films. *Physical Review Letters* **1996,** 77, (10), 2002.
104. DeMaggio, G. B.; Frieze, W. E.; Gidley, D. W.; Zhu, M.; Hristov, H. A.; Yee, A. F., Interface and Surface Effects on the Glass Transition in Thin Polystyrene Films. *Physical Review Letters* **1997,** 78, (8), 1524.
105. Hsu, D. T.; Shi, F. G.; Zhao, B.; Brongo, M. In *Theory for the thickness dependent glass transition temperature of amorphous polymer thin films*, 4th International Symposium on Low and High Dielectric Constant Materials/2nd International Symposium on Thin Film Materials for Advanced Packaging Technologies, Seattle, Wa, May 02-07, 1999; Singh, R.; Rathore, H. S.; Thakur, R. P. S.; Ang,

S. S.; Laboda, M. J.; Ulrich, R. K., Eds. Electrochemical Society Inc: Seattle, Wa, 1999; pp 53-61.

106. Keddie, J. L.; Jones, R. A. L.; Cory, R. A., Size-Dependent Depression of the Glass-Transition Temperature in Polymer-Films. *Europhysics Letters* **1994,** 27, (1), 59-64.
107. Mayes, A. M., Glass Transition of Amorphous Polymer Surfaces. *Macromolecules* **1994,** 27, (11), 3114-3115.
108. Kawaguchi, D.; Tanaka, K.; Takahara, A.; Kajiyama, T., Surface mobile layer of polystyrene film below bulk glass transition temperature. *Macromolecules* **2001,** 34, (18), 6164-6166.
109. Karapanagiotis, I.; Gerberich, W. W., Polymer film rupturing in comparison with leveling and dewetting. *Surface Science* **2005,** 594, (1-3), 192-202.
110. Boiko, Y. M.; Bach, A.; Lyngaae-Jorgensen, J., Self-bonding in an amorphous polymer below the glass transition: A T-peel test investigation. *Journal of Polymer Science Part B-Polymer Physics* **2004,** 42, (10), 1861-1867.
111. Zhang, X. M.; Tasaka, S.; Inagaki, N., Surface mechanical properties of low-molecular-weight polystyrene below its class-transition temperatures. *Journal of Polymer Science Part B-Polymer Physics* **2000,** 38, (5), 654-658.
112. Viswanathan, N. B.; Patil, S. S.; Pandit, J. K.; Lele, A. K.; Kulkarni, M. G.; Mashelkar, R. A., Morphological changes in degrading PLGA and P(DL)LA microspheres: implications for the design of controlled release systems. *Journal of Microencapsulation* **2001,** 18, (6), 783-800.
113. Park, T. G., Degradation of Poly(D,L-Lactic Acid) Microsphers - Effect of Molecular Weight. *Journal of Controlled Release* **1994,** 30, (2), 161-173.
114. Paragkumar N, T.; Edith, D.; Six, J.-L., Surface characteristics of PLA and PLGA films. *Applied Surface Science* **2006,** 253, (5), 2758-2764.

CHAPTER 2

Proof of Principle and Formulation

2.1 Abstract

Microencapsulation of medicines in modern polymeric biomaterials plays a crucial role in success of long-term injectable depots, drug-eluting stents, tissue engineering scaffolds, and blood-circulating nanoparticles. Until now, drugs are most commonly dissolved in organic solvent, which has several disadvantages. Described here is a new microencapsulation paradigm based on the polymer's own natural "self-healing" capacity in aqueous media without use of organic solvents. For initial evaluation of the feasibility of this method, porous microspheres were dispersed in concentrated solutions of protein (BSA and lysozyme) (45-330 mg/mL), with or without 150 mg/mL sucrose as a protein stabilizer, at 4°C, $T < T_g$ of the polymer, and then the pores were closed by raising the temperature to 37 – 42 °C, $T > T_g$, before washing and lyophilization, microencapsulating the protein inside. Drug loading and release kinetics in PBS + 0.02% Tween 80 at 37°C were determined. Microsphere size and morphology were determined by SEM. Protein was quantified by SE-HPLC and Coomassie Plus protein assay. By using high aqueous sugar solution concentrations in the inner water phase, or suspending low concentrations of $MgCO_3$ in the organic phase, 20-90 μm microspheres were

reproducibly loaded with 1-6% w/w protein or peptide after self-encapsulation and exhibited controlled release over 30 or 60 days. Confocal micrographs of FITC-BSA loaded and coumarin-BSA loaded microspheres localized the loaded molecules in a pore network throughout the microspheres. This loading amount was found to be strongly dependent on blank particle manufacturing excipients and the loading solution protein concentration. The new paradigm opens the door to improved compatibility with large biotechnology derived drugs, potentially lower manufacturing cost, the ability to create new biomaterial architectures, and more practical use among non-formulation scientists and clinicians.

2.2 Introduction

Polymeric biomaterials are widely used for the *in vivo* sustained release of drugs over a period of days or even years [1]. Such polymers can be utilized in numerous biomedical and pharmaceutical forms (spheres, rods, coatings, porous matrices) including micro- to millimeter scale injectable depots [2, 3], drug-eluting stents [4], scaffolds for engineering tissues [5], and blood-circulating nanoparticles [6] and can be made biodegradable or nondegradable. Up to this point however, drugs, particularly peptides and proteins, are most commonly microencapsulated after mixing with a polymer/organic solvent solution [7]. Before or after this combination the drug is either micronized (e.g., by homogenization, sonication, or grinding) or molecularly dissolved in the solvent, and later becomes dispersed throughout the final polymer matrix [7]. Both steps can compromise protein stability [8, 9], due to the manufacturing stresses proteins are exposed to, including increased temperatures, water/organic interfaces, air/liquid interfaces, and shear forces. Before use, the organic solvent is removed to clinically

acceptable levels and the polymer/drug matrix is dried. Additionally, because the biomacromolecule is often subject to destabilization through sterilization processes (e.g. γ-irradiation), the entire encapsulation process has to be conducted under aseptic conditions.

Presented here is a new microencapsulation paradigm based on the polymer's own natural "self-healing" capacity in aqueous media [10, 11], possible through polymer surface self-association. This new encapsulation technique is thus called 'self-healing microencapsulation.' The key steps to this new encapsulation technique are: 1) using porosigens to create a blank porous particle through a traditional w/o/w encapsulation technique, absent of drug; 2) loading of the drug through the polymer network by simple mixing at a temperature less than the T_g of the polymer (e.g., like mixing naked DNA to lipofectin gene delivery vector [12]); and 3) self-healing of the particle and the pores, through incubation at a temperature above the T_g of the polymer. This paradigm allows the biomacromolecule to be encapsulated without being exposed to the stresses during particle manufacturing, including the aforementioned interfaces, shear forces, and increased temperatures. Furthermore, this process also provides the ability for the manufactured microsphere to be terminally sterilized, since the protein/peptide that could be harmed by the irradiation is not encapsulated until sometime after microparticle manufacture. Additionally, since previous research has correlated surface pore closing with the cessation of initial burst from the microparticles [11], this new method of microencapsulation may provide a new way to reduce or eliminate the initial burst release as the pores are closed during the encapsulation process and before *in vivo* delivery.

A summary of the differences between the traditional method of encapsulation and this new method is shown in Figure 2.1. As shown in the figure, self-healing microencapsulation can be used after manufacture with many different biomacromolecular drugs and may not require extensive variation in blank particle formulation for each. One possible scenario for application of this new encapsulation method is a point-of care encapsulation (Figure 2.2). Other examples of point-of care encapsulation have already been discussed in the literature [13], but this appears to be the only one that completely avoids toxic substances at the time of injection.

In order to determine the feasibility of this new self-healing microencapsulation, the goal of this study was to perform a series of experiments exploring the optimal conditions for encapsulation, loading, and release to demonstrate for the first time this new principle.

2.3 Materials and Methods

2.3.1 Materials

Several PLGAs were used. PLGA with an i.v. = 0.19 dL/g (50:50, PLGA DL 2M, methyl ester end group, Alkermes Lot No. 1158-515, 19 kD MW) was purchased from Lakeshore Biomaterials (Birmingham, AL), formerly Alkermes; PLGA with an i.v. = 0.20 dL/g (50:50, Part #B6017-1G, Lot #A07-044) was from Lactel Absorbable Polymers from DURECT Corporation (Cupertino, CA), formerly Birmingham Polymers; PLGA with an i.v. = 0.57 dL/g (50:50, PLGA DL LOW IV, Lot No. W3066-603, lauryl ester end group, 51 kD) was purchased from Lakeshore Biomaterials (Birmingham, AL), formerly Alkermes; PLGA with an i.v. = 0.20 dL/g (50:50, PLGA Resomer RG 502H,

free acid end group, Lot. No. 1029124) was purchased from Boehringer Ingelheim (Germany). PLGA-Glu, a copolymer of PLGA and glucose (50:50, MW of 50 kDa), was a generous gift from Novartis Pharm AG (Basle, Switzerland). α,α-Trehalose dihydrate was purchased from Pfanstiehl (Waukegon, IL), zinc carbonate ($ZnCO_3$) was purchased from ICN Biomedicals Inc. (Aurora, OH), polyethylene glycol (PEG), MW 17,500, was purchased from Fluka (Steinheim, Germany), poly(vinyl alcohol) or PVA (25 kDa, 88% mol hydrolyzed) was purchased from Polysciences, Inc. (Warrington, PA), and Poly(vinyl alcohol) (9-10 kDa, 80% mol hydrolyzed) was purchased from Sigma Aldrich (St. Louis, MO). Magnesium carbonate ($MgCO_3$), Bovine serum albumin (BSA), fraction V, and lysozyme (from chicken egg white) was purchased from Sigma Aldrich (St. Louis, MO). α-Chymotrypsin, from bovine pancreas, Type II was obtained from Sigma Aldrich (St. Louis, MO). Phthaldialdehyde reagent, P0532, containing 1 mg σ-phthaldialdehyde (P 0657) per mL solution with 2-mercaptoethanol as the sulfhydryl moiety, was obtained from Sigma Aldrich (St. Louis, MO). Leuprorelin acetate (Lot No. 071002) was purchased from Shanghai Shnjn Modern Pharmaceutical Technology Co. (Shanghai, China). 7-methoxycoumarin-3-carbonyl azide was purchased from Molecular Probes (Eugene, OR), now Invitrogen (Carlsbad, CA). All other common salts, reagents, and solvents were purchased from Sigma Aldrich (St. Louis, MO).

HPLC columns used included an SE-HPLC column from Tosoh Biosciences (TSK gel G3000SWxl column or TSK gel G2000SWxl column), an SE guard column (Shodex, Protein KW-G), C18 column (4 μm Nova-Pak, 3.9 x 150 mm, Waters, Part #WAT086344, Serial #112837351338), and a C18 guard column (Bonda-Pak, C18 Guard-Pak, Waters, 4 μm).

2.3.2 Methods

2.3.2.1 Conjugating BSA to a pH-Insensitive Fluorescent Coumarin

1.2 g of BSA was dissolved in 40 ml of 0.2 M sodium bicarbonate pH 4.5 and to this was added 2 ml of 10 mg/ml 7-methoxycoumarin-3-carbonyl azide in DMSO while stirring. The solution was stirring continuously at room temperature in darkness for 90 min. To quench the reaction, 4 ml of 1.5 M hydroxylamine hydrochloride was added and then the solution was extensively dialyzed using a 25,000 MWCO membrane against dd H_2O at 4°C.

2.3.2.2 Preparation and Loading of PLGA-Glu Microparticles

150 µl of H_2O was added to 2 ml of 300 mg PLGA-Glu in 1 ml CH_2Cl_2 and homogenized at 10,000 rpm for 1 min in an ice water bath. 2 ml 5% PVA (9-10k, 80% hydrolyzed) added to tube and the solution was vortexed for 15 seconds, then immediately poured into 100 ml of 0.5% PVA and stirred for 3h. Microspheres were sieved, washed with dd H_2O, and separated into 20-90 µm, 90-120 µm, and > 120 µm fractions, then lyophilized.

PLGA-Glu microspheres were dispersed in either 32.5 mg/ml BSA-FITC or 152 mg/ml BSA at 4°C for 36 hours and then at either a) 4°C for an additional 24 hours or b) 37°C for 24 hours. For BSA loading, particles exposed to 37°C were washed 10 times in a 1X PBS buffer, with the particles collected via centrifugation at 2,000 rpm for 60 seconds, while particles exposed only to 4°C were washed using 4°C 1X PBST. For BSA-FITC washing, those particles exposed only to 4°C were washed once with 4°C 1X PBST, and then immediately observed via confocal microscopy.

2.3.2.3 Preparation of Blank PLGA (i.v. = 0.19 dL/g) Microparticles with Porosigen

Inner water phases with or without a solution of a porosigen (e.g., 150 µl of 300 mg/ml BSA, 300 mg/ml gum Arabic, 270 mg/ml dextran, 55 mg/ml dextran, etc.) in 1X PBS (pH 7.4) was added to 1 ml of 700 mg PLGA in 1 ml CH_2Cl_2 and immediately homogenized at 10,000 rpm for 1.0 min. 2 ml of 5% PVA (9-10 kDa, 80% hydrolyzed) was added and the mixture vortexed for 15 seconds at a high setting, and the mixture was then poured into 100 ml of 0.5% PVA (9-10 kDa, 80% hydrolyzed) solution under continuous stirring. Microspheres were stirred for 3 h at room temperature for in-water drying, and collected and washed with dd H_2O through sieves, separated by size into 20-45 µm or 20-63 µm, 45-90 µm or 63-90 µm, 90-120 µm, and 120+ µm fractions.

2.3.2.4 Preparation of Blank PLGA (i.v. = 0.57 dL/g) Microparticles with Porosigen

An inner water phase of 100-200 µl in PBS (normally 500 mg trehalose dehydrate in 1g 1X PBS) was added to 1 ml of 50:50 (i.v. = 0.57 dL/g) PLGA/CH_2Cl_2 solution and immediately homogenized in an ice water bath at 10,000 rpm for 1.0 minutes creating the first emulsion. 2 ml of 5% PVA (9-10 kDa, 80% hydrolyzed) was added and the mixture vortexed for 15 s, and the resulting emulsion was poured into 100 ml of 0.5% PVA (9-10 kDa, 80% hydrolyzed) solution under continuous stirring. Microspheres were stirred for 3 h at room temperature for in-liquid drying, and collected and washed with dd H_2O through sieves, separated by size into 20-45 µm, 45-90 µm, 90-120 µm, and 120+ µm fractions or 20-63 µm, 63-90 µm, 90-120 µm, and 120+ µm fractions.

2.3.2.5 Preparation of Blank PLGA (Resomer 502H) Microparticles with Porosigen

An inner water phase of 500 mg trehalose dehydrate in 1g 1X PBS pH 7.4 (150 or 300 µl) was added to 1 g 502H PLGA in 1 ml CH_2Cl_2 and homogenized at 17,000 rpm for 1.5 minutes in a syringe. 3 ml 3% PVA (25k, 88% hydrolyzed) was immediately added to a syringe and the mixture was homogenized at speed of 6,000 rpm for 30 seconds, and then injected into 100 ml of 0.5% PVA (25kD, 88% hydrolyzed) under continuous stirring. Microspheres were stirred for 3 h at room temperature, collected and washed with dd H_2O through sieves, separated into 20-63 µm and 63-90 µm fractions.

2.3.2.6 Loading of Microparticles

Dry microspheres were dispersed in concentrated protein solutions (43-325 mg/ml) at 4°C for 24-48 h on a rocking platform, then the pores were closed on a rotary shaker at 37°C for 20-24 h (PLGA i.v. = 0.19 dL/g) or at 42.5°C for 44-48 h (PLGA i.v. = 0.57 dL/g). After loading, microspheres were washed with distilled, deionized (dd) H_2O, collected by centrifugation at 3200 rpm for 5 min, and the supernatant removed. This washing step was repeated 10-fold, and the microspheres were then freeze dried.

2.3.2.7 Evaluation of Loading and Release of Microparticles

For determination of soluble lysozyme, BSA, and BSA-Coumarin, particles were dissolved in acetone and dispersed for 1 hour, centrifuged at 13,000 rpm for 10 minutes and the supernatant removed. Centrifugation/supernatant removal was repeated three times, and the residual solvent was removed via concentrator. The remaining protein was

then dissolved in 10 mM potassium phosphate buffer, pH 7.0 (lysozyme) or 1X PBS, pH 7.4 (BSA).

To quantify the protein, an SE column (Tosoh Biosciences TSKgel G3000SWxl) with a guard column (Shodex Protein KW-G) was used. The mobile phase for lysozyme was 0.05 M potassium phosphate, 0.2M NaCl, pH 7.0 at a flow rate of 0.9 ml/min, and for BSA and BSA-Coumarin, 1X PBS, pH 7.4. UV detection at 215 and 280 nm and fluorescence detection with excitation and emission wavelengths of 278 nm and 350 nm for BSA and lysozyme, and 384 nm and 480 nm for BSA-Coumarin were used.

For the release study, 0.5 – 1.0 ml of PBST (0.02% Tween 80), pH 7.4 was added to approximately 4-10 mg of microspheres and release was conducted at 37°C under agitation. Release medium was removed and replace with fresh buffer at specified time intervals. For determination of soluble protein monomer remaining in the particle, the release media sample was run according to the procedure used to analyze the loading of the microparticles.

2.4 Results and Discussion

2.4.1 Initial Feasibility of Self-healing Microencapsulation and Visualization of Loaded Molecule

In order to confirm the feasibility of loading large biomacromolecules through the pore network, BSA-FITC, a commercially available 51 kDa fluorescently-labeled protein, was selected for loading observation. After blank PLGA-Glu microparticles were created, they were incubated in a dilute solution of BSA-FITC in H_2O at 4°C, a temperature well below the T_g of the hydrated PLGA. The particles were incubated at

4°C for 36 hours, and then split into two groups: 4°C for an additional 24 hours or 37°C for 24 hours.

Both particle groups showed large pockets of encapsulated BSA-FITC throughout the particles, even in the center of the spheres (Figure 2.3), showing that deep penetration of BSA-FITC through the pore network was possible. The internal pore structure appeared to contain large pores and was unevenly distributed in size between particles. However, the amount of loaded BSA was similar, at 0.26% ± 0.03 (SEM) for the 4°C incubated particles versus 0.31% (± 0.18 SEM) for the 37°C incubated particles. Furthermore, after setting up a short in vitro release, those particles exposed to 37°C still had a small detectable amount (5-10%) of BSA remaining inside after 5 days of release whereas no BSA was detected in the particles incubated only at 4°C.

In another feasibility test, coumarin, an amine reactive pH insensitive fluorescent probe, was conjugated to BSA to create a model protein. Because of its pH insensitivity, BSA-coumarin is not subject to changes in fluorescent intensity due to the pH heterogeneity found throughout the microparticle. The effective conjugation of BSA-coumarin was confirmed by SE-HPLC of the BSA-coumarin detected at 280 nm and by fluorescence (ex. 350 nm, em. 415 nm) (Table 2.1).

BSA-coumarin was loaded into blank PLGA (i.v. = 0.19 dL/g) microparticles that had been prepared using either 300 mg/ml BSA in 1X PBS, pH 7.4 or only 1X PBS, pH 7.4 as the inner water phase. The BSA-coumarin was loaded using a protein solution concentration of 111 mg/ml in H_2O. After incubation at 4°C for 24 hours, followed by a pore closing period at 42°C for 18 hours, loading was determined via SE-HPLC to be 0.19% (w/w) ± 0.01% (SEM) and 0.40% (w/w) ± 0.12% (SEM) for the PBS and PBS

with BSA microparticles, respectively. Imaging of the dye through confocal microscopy using a Coherent UV laser in the higher loaded particles indicates the dye was throughout the particle in pore 'pockets' (Figure 2.4). These pore pockets appeared to be smaller and more homogeneously dispersed than the PLGA-Glu microparticles investigated previously. Furthermore, BSA-coumarin continued to be released from the particles through 30 days (Figure 2.5), suggesting the pore network had rearranged, closing some of the internal pore structure from the outside environment, and a sustained, long-term release of the encapsulated molecule was possible.

In a third feasibility test, self-healing encapsulation was observed using particles prepared with a higher MW PLGA (i.v. = 0.57 dL/g) with α,α-trehalose dihydrate used in the inner water phase to improve percolation of the pore network. After sugar leaching, pores on the scale of 250 to 2500 nm were easily viewed by electron microscopy (Figure 2.6). The dry microspheres were incubated at 4°C (<< hydrated T_g ~ 30 °C) in concentrated lysozyme solution (230 mg/ml) for 48 h to allow the protein to enter the open pores. Self-healing of the pores was initiated without organic solvent by raising the temperature (> T_g) to 42.5°C for 44 h, resulting in lysozyme-encapsulated microspheres with a high mass fraction protein (3.84 ± 0.09% loading, SEM, N=5) and a nonporous polymer surface (Figure 2.6).

2.4.2 Effect of Loading Solution Concentration on Loading

To investigate the effect the loading solution concentration has on overall loading, four different concentrations of BSA-Coumarin (43, 79, 115, and 157 mg/ml) were loaded into the same formulation of 0.19 dL/g microspheres that were prepared using unlabeled BSA as the inner water (i.w.) phase porosigen. It was discovered that the

loading was strongly correlated with the loading solution concentration (Figure 2.7), and of the 5 concentrations tested, no maximum loading was achieved. This loading correlation with solution concentration suggests that the loading of the protein was not taking place by a simple adsorption to the surface of the microparticle, and instead the protein was equilibrating in the pores available before being encapsulated. Thus, the loading through self-encapsulation can be altered by changing the drug concentration in the loading solution. Furthermore, the loaded microspheres showed similar burst release, as is evidenced by their 3 day release curves (Figure 2.8).

2.4.3 Internal Pore Structure Changing

During these experiments, it became evident that during the pore closing step, the internal pore network was changing as well as the surface pore structure. While thorough washing of the porous microspheres before pore closing would remove virtually all the protein residing inside the microsphere pore network, during release the protein never underwent a rapid release, even after the degradation phase had begun. This lack of a 'burst' phase at any time during release suggests that the protein was isolated in pockets after pore closing, and exposure of one pore channel to the outside environment did not result in exposure of the entire internal network to the outside environment. Indeed, even in instances where the surface pore structure did not completely close and additional surface pores were visible on the surface, a significant amount of protein remained inside the microsphere. Later mechanistic experiments also will show that protein or dextran loading will take place even before the surface pore structure appears to close.

Thus, it is hypothesized that the internal pore structure is changing even before the surface pores visually close. It is expected that the mechanism of this internal

polymer rearrangement is the same as the external pore rearrangement. Confocal images of loaded protein in the microspheres localizes the protein in small, spherical internal pores, indicating that this internal rearrangement ultimately results in spherical pores isolated from each other.

2.4.4 Particle Formulation Parameters Effect on Loading and Release

2.4.4.1 Effect of Different i.w. Phase Excipients on Loading in Low MW PLGA

The effect of different excipients on the loading was also investigated. Nine different inner water phases were used in otherwise identical formulations utilizing 50:50 PLGA (i.v. = 0.19 dL/g). The 45-90 μm fraction of each formulation was subsequently loaded with BSA-coumarin solution (205 mg/ml) in 1X PBS. Loading varied greatly with the type and amount of inner water phase excipients used as the porosigen (Figure 2.9). Some formulations, particularly those with high concentrations of sugar or protein porosigens, loaded high levels of protein (approximately 2% w/w) while others, especially those with extremely low porosigen concentrations, loaded almost no protein. All formulations had a similar burst release of 8 to 20% release in first 48 hours of release (*data not shown*).

After a short 7 day release, the remaining BSA-coumarin was recovered and analyzed. Of the formulations with higher protein loading, only that which used BSA as a porosigen had near complete recovery of the loaded BSA-coumarin (Figure 2.10). This suggests that the BSA may have helped to stabilize the BSA-Coumarin, as has been reported previously for molecules competing for the interface [14]. In addition, protein

itself can help buffer acidic solution pH Several excipients were then used to create blank particles in PLGA (i.v. = 0.19 dL/g and 0.57 dL/g) and excipient type had a profound affect on both the loading and release (Figure 2.11). Further analysis suggests that higher concentrations of substances in the inner water phase tend to lead towards higher loading (Figure 2.12), presumably due to known effects that osmotic pressure differences have on creating pores [15] and thus a more comprehensive pore network.

SEM images of two formulations show the surface morphology of particles before, during, and after loading (Figure 2.13). After manufacture, the surface of the particle is porous, and pores are still visible after incubation at 4°C, while after incubation at 37°C nearly all the surface pores are gone. The pores close only after the T_g of the hydrated PLGA is passed. Additionally, a formulation using a low concentration of PEG, which had an extremely low loading, had almost no visible surface pores after manufacture, further supporting the conclusion that loading occurs through the porous network and stressing the importance of excipient type and concentration.

2.4.4.2 Effect of Polymer Concentration on Loading

In early experiments, it was observed that when the polymer concentration in microparticles using the low MW PLGA (i.v. = 0.19 dL/g) was changed from 700 mg PLGA to 650 mg PLGA in 1 ml CH_2Cl_2, porous microparticles were unable to close. Subsequently, 6 formulations of microparticles of varying polymer concentration were created, this time a higher MW PLGA (i.v. = 0.57 dL/g). These six formulations were identical except for the amount of polymer (200, 240, 280, 320, 360, or 400 mg) in 1 ml of CH_2Cl_2. All formulations had a loading above 2% w/w (Figure 2.14), and only the lowest concentration (200 mg PLGA) had a significant burst in the first 48h of release (>

50% w/w). Polymer concentration does appear to have an effect on microsphere loading via self-healing microencapsulation, as lower loadings were seen at both lower and higher concentrations. This may partially be explained by previous research suggesting a less interconnecting pore network when lower polymer concentrations are used [16] as well as decreased porosity at higher concentrations [17, 18].

2.4.4.3 Effect of Incubation Temperature on Pore Closing

Two formulations were prepared using different concentrations of PLGA (i.v. = 0.57 dL/g) in CH_2Cl_2 (280 mg and 320 mg PLGA in 1 ml CH_2Cl_2). These particles were incubated in a 240 mg/ml BSA solution for 48h at 4°C and 24h at 37°C, followed by incubation in for an additional 24h at either 37°C or 42°C. When the particles were loaded at the higher incubation temperature, the amount of protein loaded strongly increased, while the burst release similarly decreased (Table 2.2). Evidently with the higher MW PLGA, a loading temperature of 42°C was critical for pore closing to take place within 48 h.

2.4.4.4 502H Resomer Pore Closing

To confirm pore closing is universal to PLGA, and not an artifact of one particular manufacturer or lot number, microspheres were prepared with using another commonly used PLGA, Boeringher Ingelheim's 502H Resomer. Indeed, pore closing with 502H Resomer was achieved (Figure 2.15). Both preparations were incubated at 42°C in dd H_2O as well as low and high concentrations of octreotide, a eight amino acid peptide, and pore closing in all cases were complete before 76 h of incubation.

2.5 Conclusion

Initial evaluation of self-healing microencapsulation indicated a deep penetration of the loaded molecule into the microsphere, visible through confocal microscopy. This loading was only possible after a self-healing step of incubation at a temperature above the T_g of the hydrated polymer was introduced. The loading was observed to depend on a number of blank particle formulation parameters, including polymer and excipient type and concentration. The temperature used during the self-healing step was also deemed to be important, as well as the loading solution concentration. Overall, the feasibility of loading through self-healing has been confirmed, and the loading and release are greatly affected by manufacturing parameters.

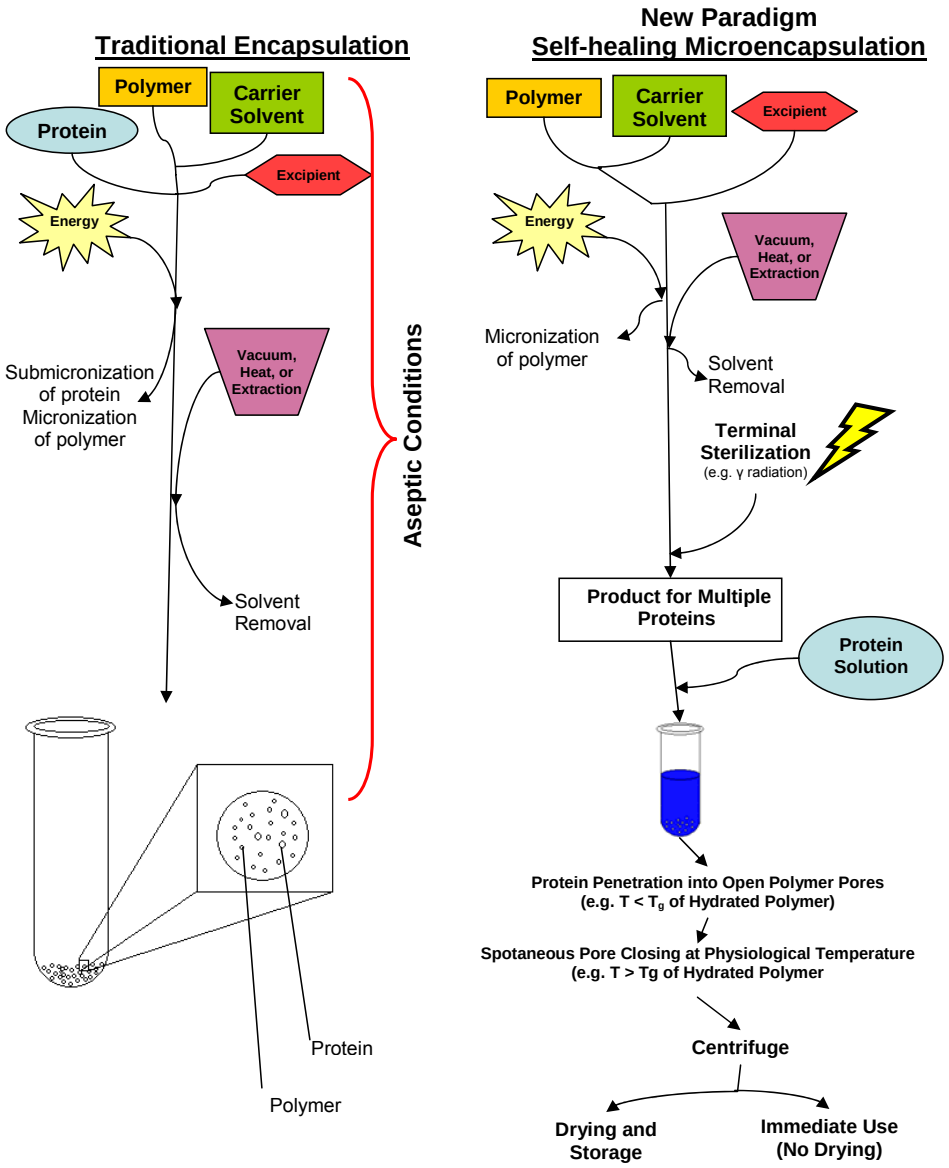

Figure 2.1 Traditional and New Self-healing Microencapsulation Microsphere Encapsulation Methods. Self-healing microencapsulation provides a means to pre-sterilize the delivery device, whereas traditional methods do not.

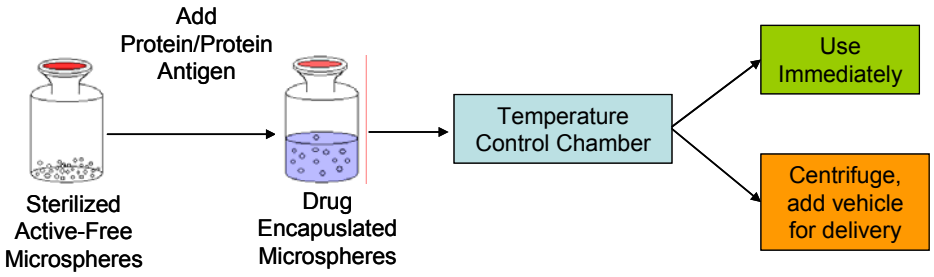

Figure 2.2 Scenarios for Self-healing Microencapsulation Use. Point-of-care encapsulation is one scenario where self-healing microencapsulation could be utilized.

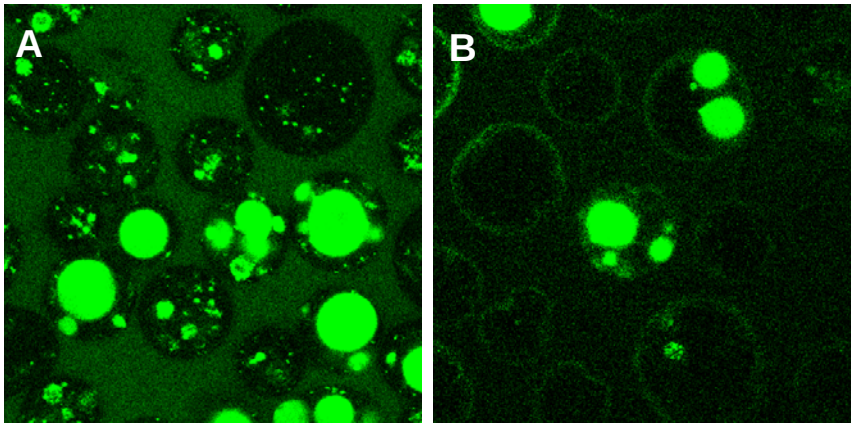

Figure 2.3 Observing BSA-FITC distribution in microsphere through confocal microscopy. Microspheres were incubated in BSA-FITC solution for either A) 60h at 4°C or B) 36h at 4°C and 24h at 37°C.

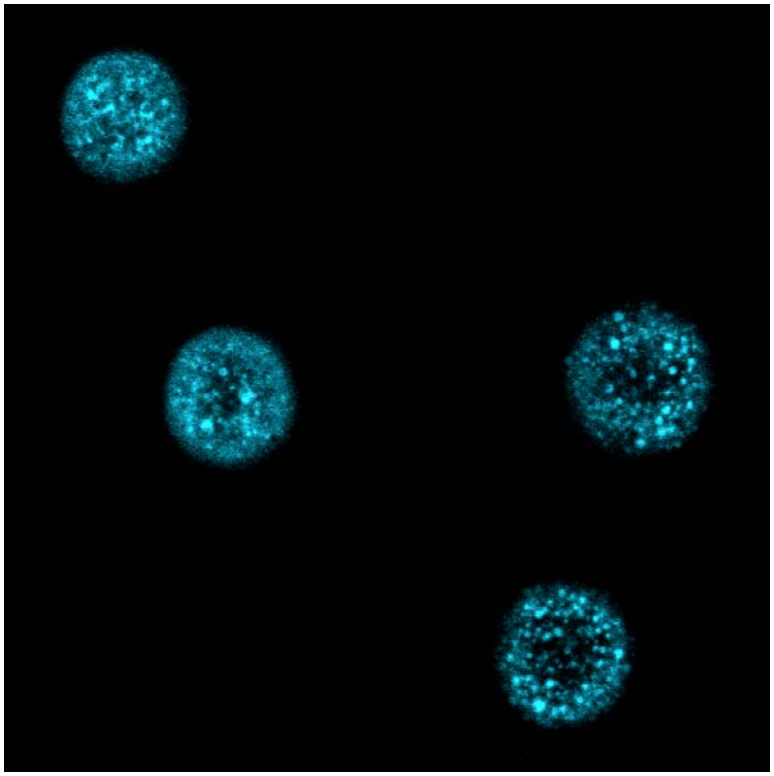

Figure 2.4 Visualization of BSA-Coumarin in 0.19 dL/g Microparticles. Loading was 0.40% (w/w) ± 0.12% (SEM).

	UV (280 nm)	Fluorescence (360 nm ex., 415 nm em.)
BSA (0.02 mg/ml)	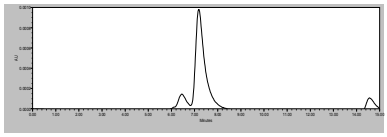	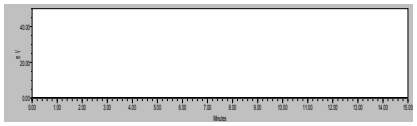
BSA-Coumarin (0.013 mg/ml)	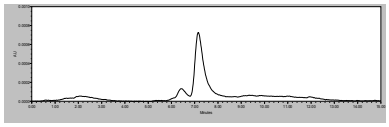	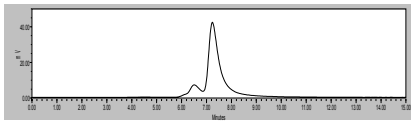

Table 2.1 Fluorescently Labeled BSA and Unlabeled BSA. BSA and BSA-Coumarin conjugate solutions of similar concentration injected into HPLC with a size exclusion column, mobile phase of 1X PBS (1 ml/min).

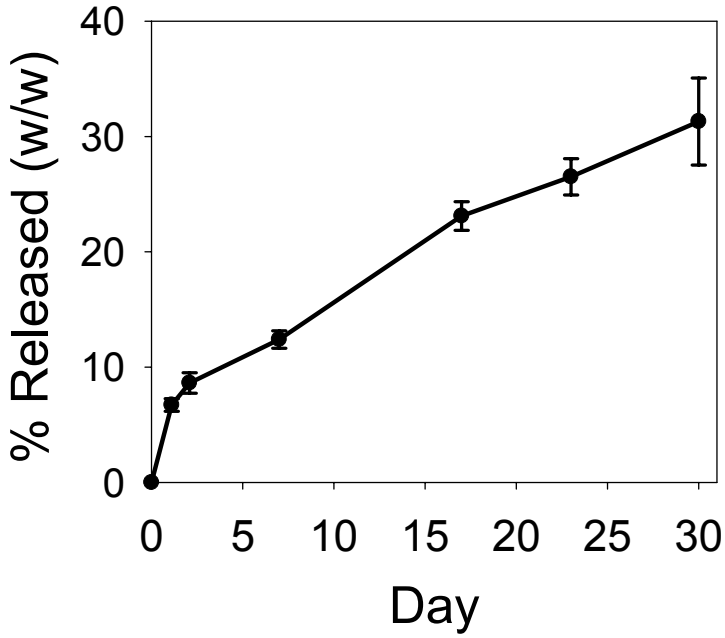

Figure 2.5 30 Day release of BSA-coumarin from 0.19 dL/g microparticles. BSA-Coumarin, loading at 0.40% (w/w) ± 0.12% (SEM) was released over 30d. Release of monomeric protein was in PBST (0.02% Tween-80) and assayed by SE-HPLC of the release media through SE-HPLC. N=3.

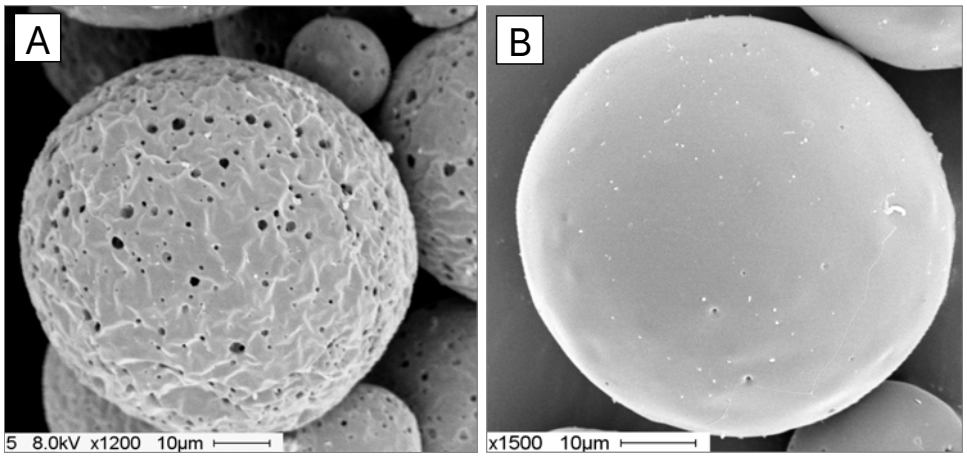

Figure 2.6 Surface morphology before and after self-healing microencapsulation. $MgCO_3$ was incorporated in PLGA 50/50 (i.v. = 0.57 dL/g) microspheres by double emulsion method (dd H_2O i.w. phase). Dried pre-loaded microspheres were incubated with 230 mg/ml Lysozyme at 4°C to load protein in porous microspheres while pores were open for 48h (A) and then pores were closed at 42°C for 44 h (B). Microspheres were sieved between 45 and 90 µm.

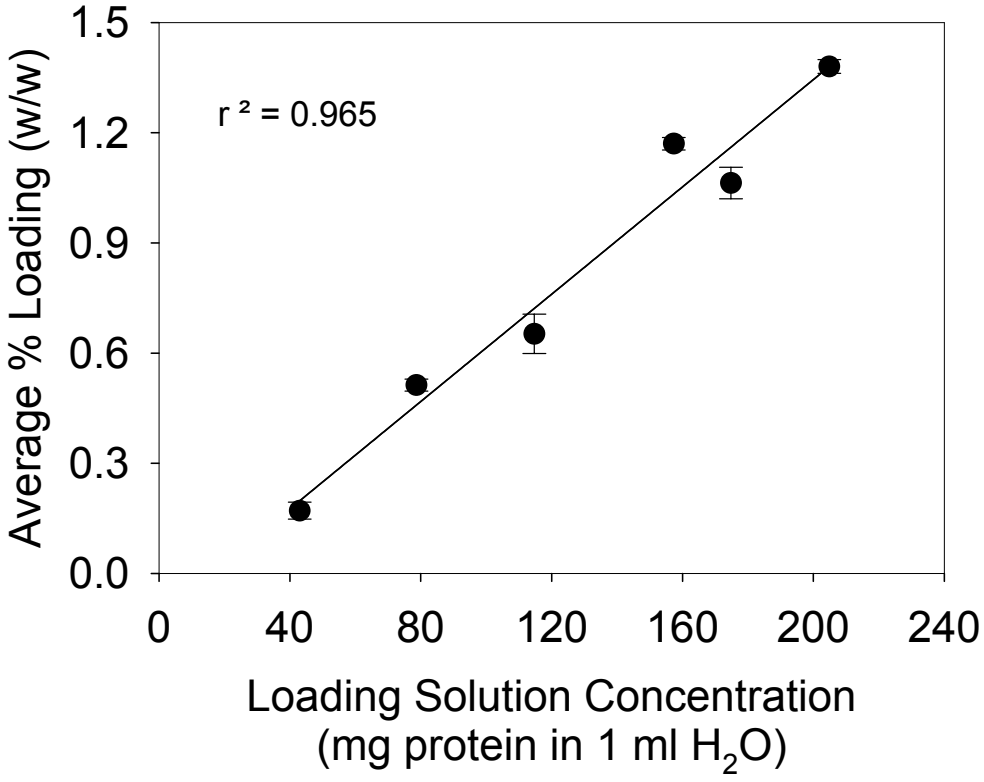

Figure 2.7 Average % loading vs. loading solution concentration. 6 different loading solution concentrations (43, 79, 115, 157, 175, and 204 mg/ml) were loaded in the same formulation (150 µl 300 mg/ml BSA in PBS as i.w. phase, 700 mg PLGA (i.v. = 0.19 dL/g) in 1 ml CH_2Cl_2, 20 to 90 µm size). N=5.

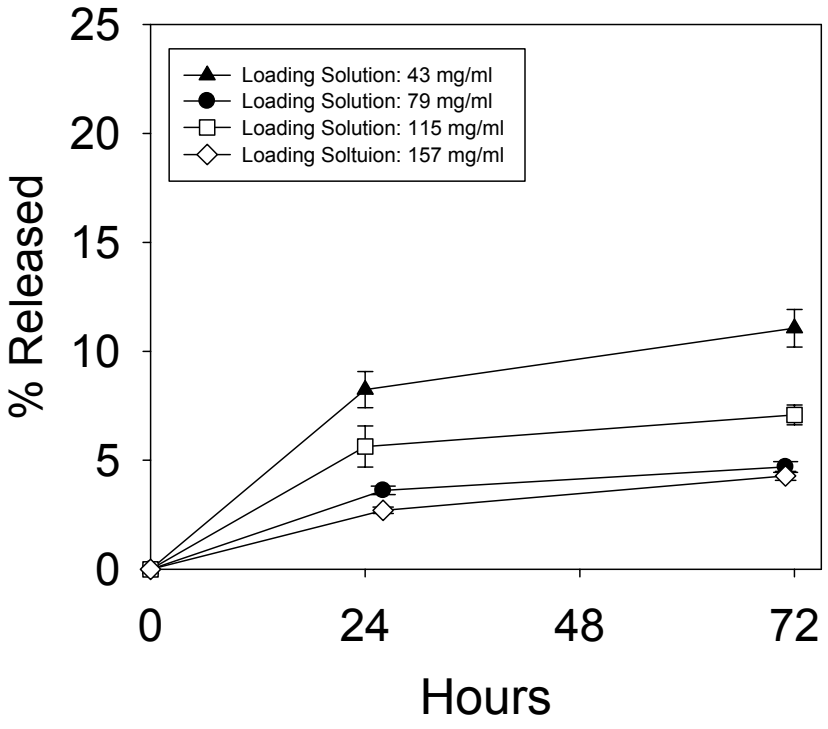

Figure 2.8 Similar release curves of microspheres loaded by different concentrations of protein solution. Formulation loadings are in Figure 2.7. N=3.

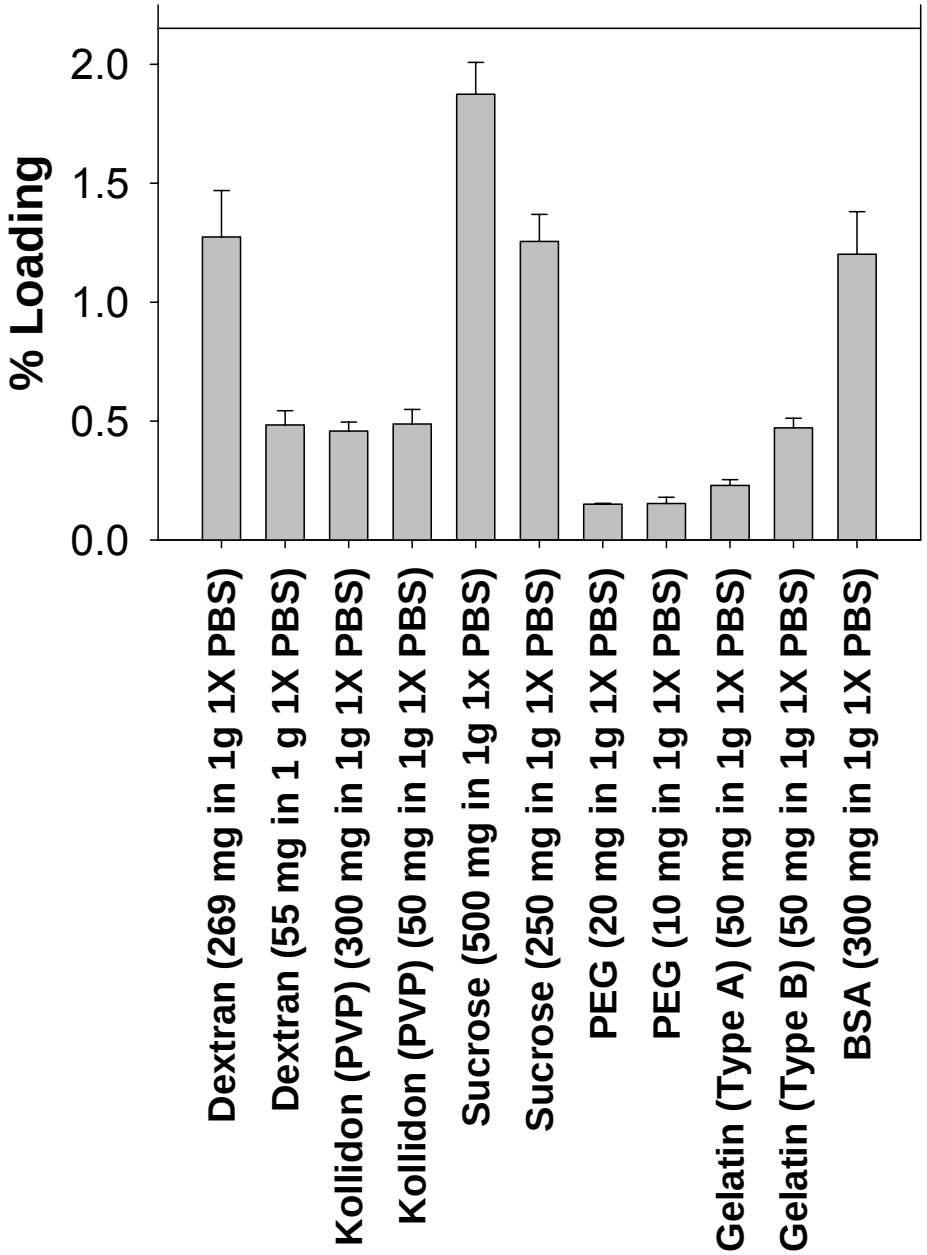

Figure 2.9 Effect of i.w. phase porosigen type and concentration on loading of BSA-coumarin via self-healing microencapsulation in blank PLGA microparticles. Particles were prepared using 150 µl of i.w. phase (above) in 1 g PLGA (50:50, i.v. = 0.19 dL/g) in 1 ml CH_2Cl_2, with all particles between 20 and 90 µm. N=5.

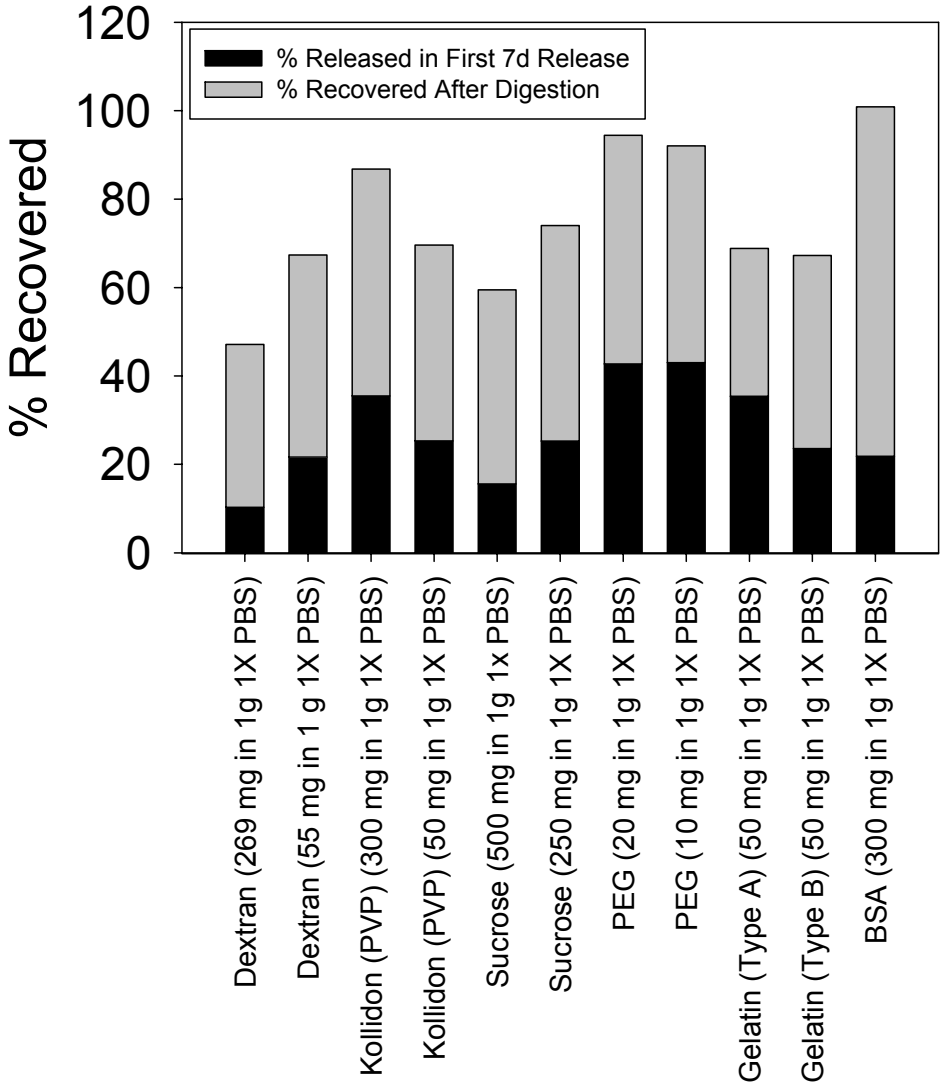

Figure 2.10 Recovered BSA-coumarin after loading and subsequent 7d release. Dark bars represent the % released in the first 7d of release, while the grey bars represent the amount recovered after digestion of the remaining particles. Blank particles were prepared using 150 µl of i.w. phase (above) in 1 g PLGA (50:50, i.v. = 0.19 dL/g) in 1 ml CH_2Cl_2, with all particles between 20 and 90 µm. N=3.

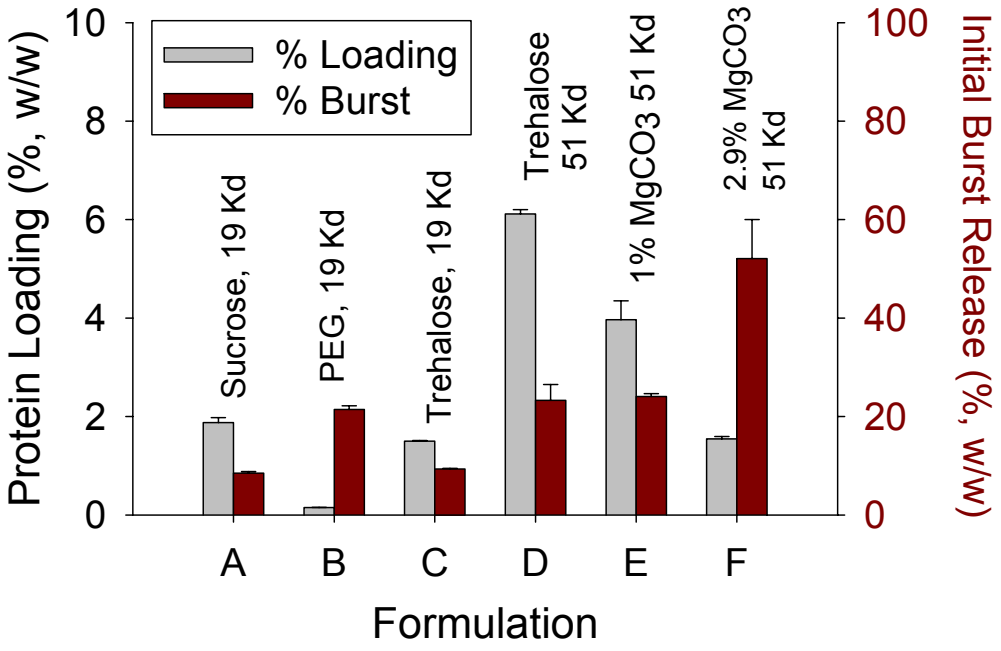

Figure 2.11 Loading and Burst Release for Microspheres Prepared with Different Excipients. Blank particles were prepared with different excipients in 1X PBS using 50:50 PLGA (19 kD or 51 kD MW), and subsequently loaded with 250 mg/ml BSA.

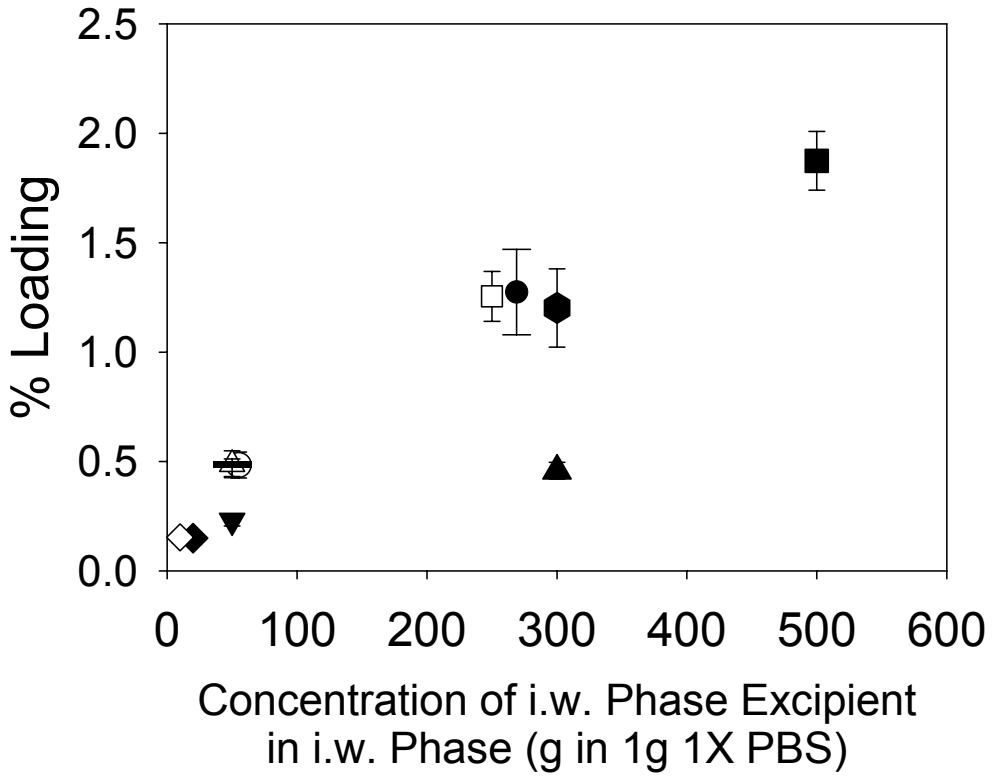

Figure 2.12 The effect of the concentration of the i.w. phase porosigen on % loading. All formulation parameters were identical except for the identity and concentration of the i.w. phase porosigen in 1 g 1X PBS, pH 7.4, which was either 270 mg dextran (●), 55 mg dextran (○), 300 mg Kollidon (PVP)(▲), 50 mg Kollidon (PVP) (Δ), 500 mg sucrose (■), 250 mg sucrose (□), 20 mg PEG (◆), 10 mg PEG (◇), 50 mg gelatin type A (▼), 50 mg gelatin type B (─), and 300 mg BSA (⬢).

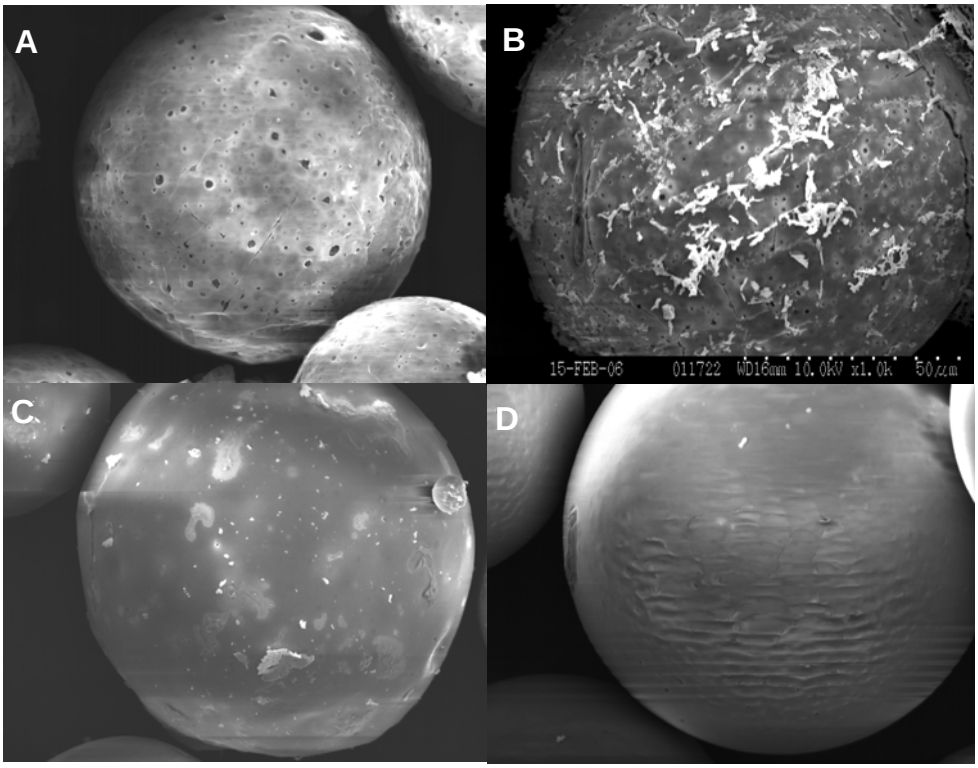

Figure 2.13 SEMs of microspheres before and after loading. Two formulations of i.v. = 0.19 dL/g microparticles were manufactured and freeze dried, and then incubated to close the pores. A) Manufactured particles using sucrose as the i.w. phase, B) Microparticle surface after incubating in BSA-Coumarin solution at 4°C for 48h and C) Surface morphology after incubating in BSA-Coumarin at 4°C for 48h followed by 37°C for 20h. D) Image of a separate formulation, a microparticles using low concentration of PEG as the i.w. phase, directly after manufacture and before any incubation.

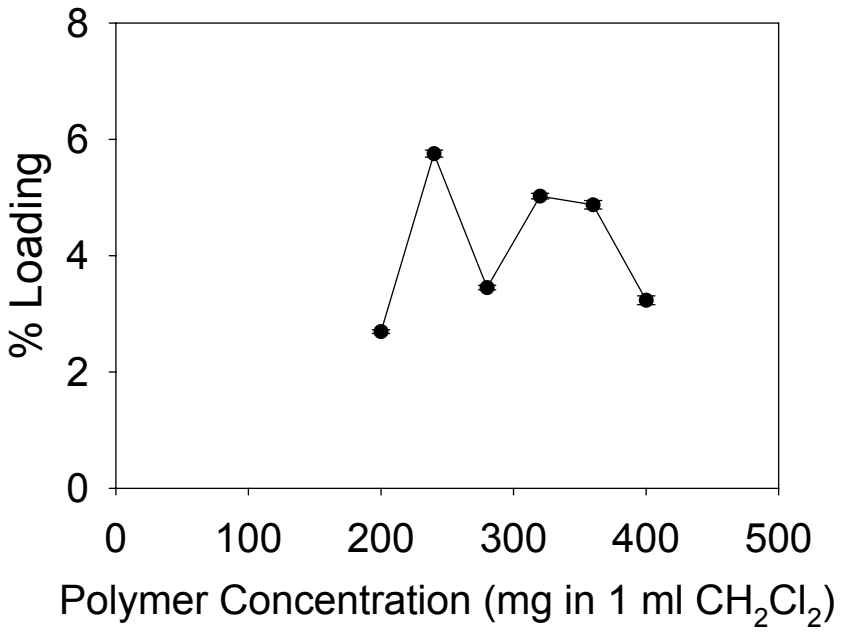

Figure 2.14 Dependence of loading on initial polymer concentration. Microparticles were prepared using 50:50 PLGA (i.v. = 0.57 dL/g), N=5.

	Formulation A		Formulation B	
	% Loading (w/w)	% Burst Release	% Loading (w/w)	% Burst Release
37°C Pore Closing	**1.24** (± 0.01)	**50.91** (± 1.52)	**1.87** (± 0.03)	**41.39** (± 0.99)
42°C Pore Closing	**5.12** (± 0.04)	**17.64** (± 1.71)	**6.04** (± 0.15)	**16.97** (± 1.44)

Table 2.2 Effect of pore closing temperature on loading and burst release for two formulations. Loading increases and burst release (BSA released in the first 48 hours) decreases when the pore closing temperature for the last 24h of loading is changed from 37°C to 42°C for both formulation A (280 mg/ml PLGA concentration) and formulation B (320 mg/ml PLGA concentration). Calculated error is standard error of the mean, N=3.

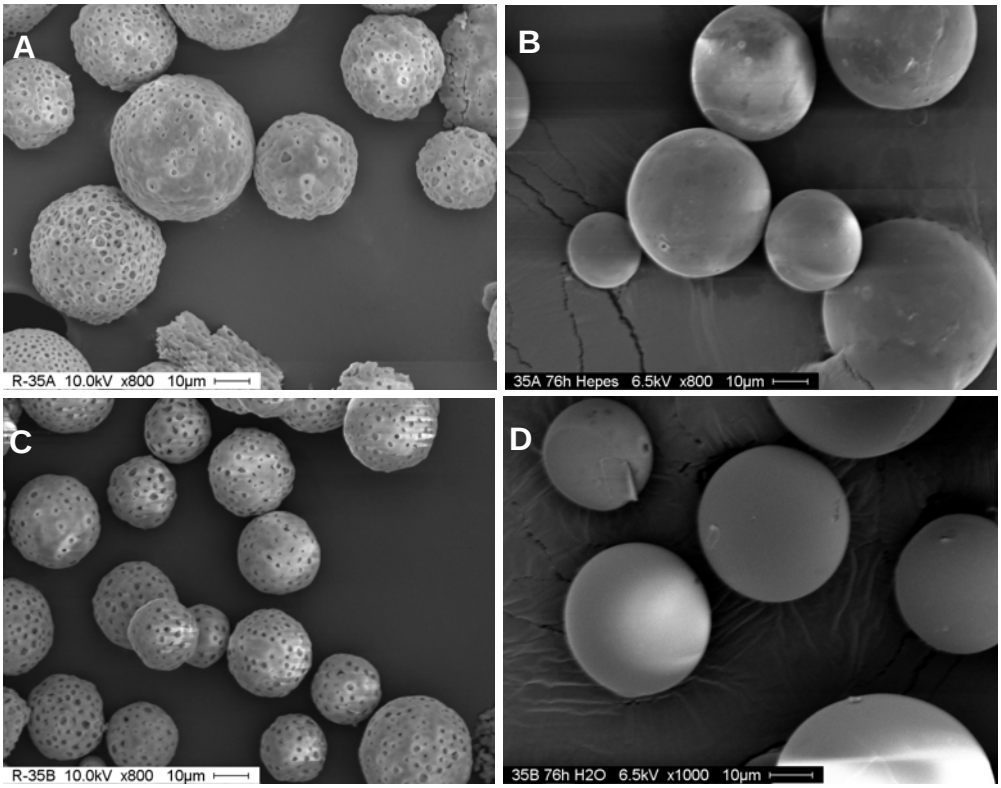

Figure 2.15 Pore closing of Resomer 502H. Microparticles were prepared using trehalose in PBS as the inner water phase in either 300 µl (A&B) or 150 µl (C&D). Pores were closed by incubating in H_2O for 76h at 42°C.

2.6 References

1. Langer, R., New Methods of Drug Delivery. *Science* **1990,** 249, (4976), 1527-1533.
2. Furr, B. J. A.; Hutchinson, F. G. In *A Biodegradable Delivery System for Peptides - Preclinical Experience with the Gonadotropin-Releasing Hormone Agonist Zoladex*, 3rd International Symp on Disposition and Delivery of Peptide Drugs, Leiden, Netherlands, Jul 05-07, 1991; Elsevier Science Bv: Leiden, Netherlands, 1991; pp 117-127.
3. Okada, H., One- and three-month release injectable microspheres of the LH-RH superagonist leuprorelin acetate. *Advanced Drug Delivery Reviews* **1997,** 28, (1), 43-70.
4. Stone, G. W.; Moses, J. W.; Ellis, S. G.; Schofer, J.; Dawkins, K. D.; Morice, M.; Colombo, A.; Schampaert, E.; Grube, E.; Kirtane, A. J.; Cutlip, D. E.; Fahy, M.; Pocock, S. J.; Mehran, R.; Leon, M. B., Safety and efficacy of sirolimus- and paclitaxel-eluting coronary stents. *New England Journal of Medicine* **2007,** 356, (10), 998-1008.
5. Langer, R.; Vacanti, J. P., Tissue Engineering. *Science* **1993,** 260, (5110), 920-926.
6. Gref, R.; Minamitake, Y.; Peracchia, M. T.; Trubetskoy, V.; Torchilin, V.; Langer, R., Biodegradable Long-Circulating Polymeric Nanospheres. *Science* **1994,** 263, (5153), 1600-1603.
7. Donbrow, M., *Microcapsules and Nanoparticles in Medicine and Pharmacy*. CRC Press: Boca Raton, FL, Ann Arbor, London, 1991.
8. Schwendeman, S. P.; Cardamone, M.; Brandon, M. R.; Klibanov, A.; Langer, R., *Stability of proteins and their delivery from biodegradable polymer microspheres. in: Microparticulate Systems for the Delivery of Proteins and Vaccines*. Marcel Dekker: New York, 1996.
9. Putney, S. D.; Burke, P. A., Improving protein therapeutics with sustained-release formulations. *Nature Biotechnology* **1998,** 16, (2), 153-157.
10. Wool, R. P., Self-healing materials: a review. *Soft Matter* **2008,** 4, (3), 400-418.
11. Wang, J.; Wang, B. A.; Schwendeman, S. P., Characterization of the initial burst release of a model peptide from poly(D,L-lactide-co-glycolide) microspheres. *Journal of Controlled Release* **2002,** 82, (2-3), 289-307.
12. Felgner, P. L.; Gadek, T. R.; Holm, M.; Roman, R.; Chan, H. W.; Wenz, M.; Northrop, J. P.; Ringold, G. M.; Danielsen, M., Lipofection - A Highly Efficient, Lipid-mediated DNA-Transfection Procedure. *Proceedings of the National Academy of Sciences of the United States of America* **1987,** 84, (21), 7413-7417.
13. Jain, R. A.; Rhodes, C. T.; Railkar, A. M.; Malick, A. W.; Shah, N. H., Controlled delivery of drugs from a novel injectable in situ formed biodegradable PLGA microsphere system. *Journal of Microencapsulation* **2000,** 17, (3), 343-362.
14. van de Weert, M.; Hoechstetter, J.; Hennink, W. E.; Crommelin, D. J. A., The effect of a water/organic solvent interface on the structural stability of lysozyme. *Journal of Controlled Release* **2000,** 68, (3), 351-359.
15. Herrmann, J.; Bodmeier, R. In *The Effect of Particle Microstructure on the Somatostatin Release from Poly(Lactide) Microspheres Prepared by a W/O/W*

Solvent Evaporation Method, 3rd European Symposium on Controlled Drug Delivery, Noordwijk, Netherlands, Apr 04-06, 1994; Elsevier Science Bv: Noordwijk, Netherlands, 1994; pp 63-71.

16. Yang, Y. Y.; Chung, T. S.; Ng, N. P., Morphology, drug distribution, and in vitro release profiles of biodegradable polymeric microspheres containing protein fabricated by double-emulsion solvent extraction/evaporation method. *Biomaterials* **2001,** 22, (3), 231-241.
17. Li, W. I.; Anderson, K. W.; Mehta, R. C.; DeLuca, P. P., Prediction of solvent removal profile and effect on properties for peptide-loaded PLGA microspheres prepared by solvent extraction/evaporation method. *Journal of Controlled Release* **1995,** 37, (3), 199-214.
18. Schlicher, E.; Postma, N. S.; Zuidema, J.; Talsma, H.; Hennink, W. E., Preparation and characterisation of poly(D,L-lactic-co-glycolic acid) microspheres containing desferrioxamine. *International Journal of Pharmaceutics* **1997,** 153, (2), 235-245.

CHAPTER 3

Effects of Porosity on Self-Encapsulation

3.1 Abstract

The purpose of this study was to elucidate the effects of porosity on self-microencapsulating (SM) poly(lactic-co-glycolic acid) (PLGA) microparticles on the microencapsulation of proteins. SM-microparticles were prepared by standard solvent evaporation methods without loaded protein. Porosity was controlled by adjusting three parameters: the amount of inner water phase, the amount of acid-neutralizing and pore forming $MgCO_3$, and the concentration of polymer in the oil phase. SM-microspheres were loaded with lysozyme via self-encapsulation and porosity and size distribution measurements were detected by mercury porosimetry. Protein loading and aggregation were quantified through Coomasie Plus protein assay and SE-HPLC. Specific activity of encapsulated lysozyme was determined through established methods. Microspheres prepared with varying inner water phase and base content had observable increases in porosity concurrent with increasing excipient content, with a slight decrease in porosity with those formulations with the most excipients. Overall, the calculated porosity ranged from ~ 50% to 70% of total microparticle volume. More importantly, the porosity in formulations with varying inner water phase and base content had a striking linear correlation with the loading (r^2 = 0.949). The release of those microspheres prepared

with varying base content had increasing amounts of burst and subsequent total release over 28 days, with release [% w/w ± SEM] of 30.4 ± 0.7% (0% $MgCO_3$), 41.3 ± 0.5% (1.5% $MgCO_3$), 51 ± 4% (4.3% $MgCO_3$), and 57 ± 4% (11.0% $MgCO_3$) for loaded lysozyme. The amount of aggregation decreased as base content increased, with aggregation determined to be [% w/w ± SEM] 8.7 ± 0.6% (0.0% $MgCO_3$), 6.0 ± 0.2% (1.5% $MgCO_3$), 4.7 ± 0.2% (4.3% $MgCO_3$), and 3.4 ± 0.1% (11% $MgCO_3$) of total loading. Overall, increases in porosity of the SM-microparticles increased the loading via self-encapsulation. These porosity changes also affected the release rates of the microparticles over a 28 day release. The addition of acid-neutralizing base was found to help stabilize the encapsulated lysozyme over this release, reducing aggregation and increasing enzymatic activity.

3.2 Introduction

In the solvent evaporation preparation technique of preparing polymeric microparticles, a number of processing parameters have been found to influence the encapsulation efficiency, microsphere morphology, and subsequent release of the encapsulated molecule. These processing parameters include polymer molecular weight [1], preparation atmospheric pressure [2], and the dispersed phase/continuous phase ratio [3] along with many others. All of these parameters affect the rate of exchange of organic solvent and drug inside the microemulsion with the continuous phase. Ultimately they affect drug loading and release by altering the properties of the resulting microspheres, including size, composition, and notably, the pore network.

It has been shown that the amount of excipients or drug inside the microparticle affects encapsulation efficiency and pore structure. Addition of these excipients affect

the osmotic pressure gradient between the inner microsphere and the continuous network [4], increasing the uptake of water, and increasing the porosity of the particles as well as subsequently decreasing the encapsulation efficiency [5]. This has been seen for numerous substances, including antacids [6, 7], Pluronic F-58 [8], PEGs [8, 9], and various salts and sugars [10, 11], all of which generally increased the porosity and release rate. After a loaded microsphere is first subjected to aqueous release conditions, a common observation is a quick release of hydrophilic biomacromolecular drugs into the surrounding environment, a phenomenon known as the 'initial burst.' Previous work has shown that the initial burst release ceases once the surface pores are closed [12], thus linking porosity with release rate.

Because of these artifacts due to porosity – reduced encapsulation efficiency and rapid drug release – much of the research surrounding microsphere porosity has been in an attempt to retard its formation or eliminate its surface presence through coating the particle after manufacture [13]. One approach to reduce said porosity is to minimize the aforementioned osmotic pressure difference during manufacture. Thus, the addition of salt and other additives into the continuous phase has been shown to help minimize this net uptake of water in the microemulsion, leading to a lower internal porosity, a higher encapsulation efficiency and a denser internal structure [14-16].

Therefore, the amount of excipients in microspheres, including base for acid neutralization [6], can affect the pore structure and porosity. Likewise, it has been established that increasing the inner water phase volume increases the porosity of the particles [17-20]. However, the effect of polymer concentration on porosity is not as well understood. The rate of solvent removal has a clear impact on microsphere morphology

[21] though not always predictable. The concentration of polymer directly influences how fast the microparticles harden, and in turn how developed the pore network becomes. Higher initial PLGA concentrations will allow polymer to precipitate quickly in the periphery preventing internal solvent from migrating to the continuous phase, and potentially allowing higher residual organic solvent in the microparticle [3]. Higher initial polymer concentrations are generally believed to cause a decrease in porosity [3, 17, 22] and have been shown to cause a decrease in the release rate of the encapsulated drug [20]. However, low initial polymer concentrations can cause a less torturous porous network, and consequently can result in higher porosity, but less interconnecting of these pores [23].

In self-encapsulation however, early research has demonstrated that a large and well developed pore network is crucial; a rich pore network in self-microencapsulating (SM) microparticles allows extensive and deep penetration of the loaded drug throughout the microsphere, increasing loading and decreasing the initial burst. Thus, studying parameters that can increase not only the pore volume, but also the pore network percolation, are critical. Here, we sought to control microsphere porosity in an attempt to improve the pore network and subsequent loading and release after self-encapsulation by adjusting three different formulation variables: 1) the amount of excipients used, e.g., a pore-forming base, $MgCO_3$; 2) the amount of inner water phase and excipients therein; and 3) the initial concentration of polymer solution. By altering these three parameters, their effect on porosity and on self-encapsulation was investigated. Additionally, the relationship between porosity and loading, release, and stability of the encapsulated protein, in this case lysozyme, was explored.

3.3 Materials and Methods

3.3.1 Materials

PLGA with an i.v. = 0.57 dL/g (50:50, PLGA DL LOW IV, Lot No. W3066-603, lauryl ester end group, 51 kD) was purchased from Lakeshore Biomaterials (Birmingham, AL), formerly Alkermes. α,α-Trehalose dihydrate was purchased from Pfanstiehl (Waukegon, IL) and poly(vinyl alcohol) (9-10 kDa, 80% mol hydrolyzed) was purchased from Sigma Aldrich (St. Louis, MO). Magnesium carbonate ($MgCO_3$), Bovine serum albumin (BSA), fraction V, and lysozyme (from chicken egg white) were purchased from Sigma Aldrich (St. Louis, MO). Coomassie Plus Protein Reagent was purchased from Pierce (Thermo Fisher Scientific, Rockford, IL). All other common salts, reagents, and solvents were purchased from Sigma Aldrich (St. Louis, MO).

HPLC columns used included an SE-HPLC column from Tosoh Biosciences (TSK gel G3000SWxl column or TSK gel G2000SWxl column), an SE guard column (Shodex, Protein KW-G), C18 column (4 μm Nova-Pak, 3.9 x 150 mm, Waters, Part #WAT086344, Serial #112837351338), and a C18 guard column (Bonda-Pak, C18 Guard-Pak, Waters, 4 μm).

3.3.2 Methods

3.3.2.1 Preparing SM-Microencapsulating Particles with Varying $MgCO_3$ Content

Two hundred µl trehalose dehydrate solution (500 mg in 1g 1X PBS, pH 7.4) was added to 320 mg PLGA (50:50, 0.57 dL/g) with or without $MgCO_3$ (0, 4.8, 14.4, or 39.5 mg), in 1 ml of CH_2Cl_2 in a 5 ml syringe and immediately homogenized in an ice water bath at 17,000 rpm for 1.0 minutes creating the first emulsion. 2 ml of 5% PVA (9-10kDa, 80% hydrolyzed) was added and the mixture homogenized at 6,000 rpm for 25 seconds, creating the second emulsion and the resulting solution was injected into 100 ml of 0.5% PVA (9-10kDa, 80% hydrolyzed) solution under continuous stirring. Microspheres were stirred 3h at room temperature, and collected with sieves to separate by size and washed thoroughly with dd H_2O to remove residual PVA, sugar, salt, and solvent. The particles were immediately freeze dried after collecting 20-63 µm and 63-90 µm fractions.

3.3.2.2 Preparing SM-Microencapsulating Particles with Varying Polymer Concentration

Two hundred µl trehalose dehydrate solution (500 mg in 1g 1X PBS, pH 7.4) was added to 200, 260, 320, or 400 mg PLGA (50:50, 0.57 dL/g) with 4.8 mg $MgCO_3$, in 1 ml of CH_2Cl_2 in a 6 ml syringe and immediately homogenized in an ice water bath at 17,000 rpm for 1.0 min to create the first emulsion. Two ml of 5% PVA was added and the mixture homogenized at 6,000 rpm for 20 s to create the second emulsion and the resulting solution was injected into 100 ml of 0.5% PVA solution under continuous

stirring. Microspheres were stirred 3h at room temperature, and collected with sieves to separate by size and washed thoroughly with dd H_2O to remove residual PVA, sugar, salt, and solvent. The particles were immediately freeze dried. The sizes collected were 20-63 μm and 63-90 μm fractions.

3.3.2.3 Preparing SM-Microencapsulating Particles with Varying Inner Water Phase Volume

25, 100, 200, or 350 μl trehalose dehydrate solution (500 mg in 1g 1X PBS, pH 7.4) was added to 320 mg PLGA (50:50, 0.57 dL/g) in 1 ml of CH_2Cl_2 in a 6 ml syringe and immediately homogenized in an ice water bath at 17,000 rpm for 1.0 minutes creating the first emulsion. 2 ml of 5% PVA (9-10kDa, 80% hydrolyzed) was added and the mixture homogenized at 6,000 rpm for 20 seconds, creating the second emulsion and the resulting solution was injected into 100 ml of 0.5% PVA (9-10kDa, 80% hydrolyzed) solution under continuous stirring. Microspheres were stirred 3h at room temperature, and collected with sieves to separate by size and washed thoroughly with dd H_2O to remove residual PVA, sugar, salt, and solvent. The particles were immediately freeze dried. The sizes collected were 20-63 μm and 63-90 μm fractions.

3.3.2.4 Loading SM-Microencapsulating Particles

Approximately 1 ml of 250 mg/ml 4°C lysozyme solution was added to approximately 80 mg of 20-63 μm blank particles and the microsphere/protein solutions were incubated at 4°C for 3 d on a rocking platform, and then transferred to a 43°C incubator on a rotary shaker for 46 h. Microspheres were removed and washed

thoroughly with dd H_2O, centrifuging at 3,800 rpm for 5 min to collect the microspheres after each of 10 washes, and then freeze dried.

3.3.2.5 Microsphere Loading and Release

For loading analysis, approximately 4 mg of microspheres were dissolved in approximately 1.5 ml of acetone, and the protein was concentrated by centrifugation at 13,200 rpm for 15 min, and the supernatant removed. This was repeated three times, and the residual acetone was removed via evaporation.

For the release study, 1.0 ml of PBST (0.02% Tween 80), pH 7.4 was added to approximately 7-10 mg of microspheres and incubated at 37°C. Release medium was removed and assayed for protein content at each time point and replaced by fresh media.

For determination of soluble lysozyme monomer in the release media and in the loading assays, a Coomassie protein assay was run, using Coomassie Plus Protein Reagent and measuring the protein solution absorbance at 595 nm. For determination of soluble lysozyme monomer remaining in the particle, the sample was run using SE-HPLC (Tosoh Biosciences TSKgel G3000SWxl) using a guard column (Shodex Protein KW-G), with a mobile phase of 0.05 M potassium phosphate, 0.2M NaCl, pH 7.0 at an isocratic flow rate of 0.9 ml/min. The absorbance at 215 and 280 nm were measured.

Insoluble lysozyme was determined after removing all soluble lysozyme in 6 M urea, 1 mM EDTA, 10 mM DL-dithiothreitol (Cleland's Reagent) (DTT), and after brief vortexing and assaying the protein using Coomassie Plus Protein Reagent as above. Standards were analyzed in the same denaturing and reducing solution.

3.3.2.6 Determination of SM-Microencapsulating Particle Porosity

Porosity measurements on blank particles were made by Porous Materials, Inc. (Ithaca, NY) using an AMP-60K-A-1 mercury porosimeter, generating pore volume versus pressure data. The pore volume was reported as amount of volume per gram (cc/g). Total microparticle volume was calculated as the sum of the pore volume and the polymer volume, where the polymer density (1.25 g/cc, provided by manufacturer) and sample weight of the porosimetry sample were used to calculate the pore volume. Porosity was calculated as the quotient of pore volume to total microparticle volume. Pressure associated with microsphere packing and surface wetting, before mercury intrusion into the pores had taken place, was not calculated into the final pore volume (Figure 3.1), as has been reported previously [24].

3.3.2.7 Activity of Lysozyme

The activity of the loaded soluble lysozyme was determined according to established methods [25, 26]. Briefly, lysozyme was extracted from the microspheres and dissolved in PBST (0.02% Tween), pH 7.4, of approximately 8.5 (± 1) μg/ml. Standard solutions were dissolved in the same buffer at the same approximate concentration at the same time. For analysis, 0.15 ml of soluble protein solution was combined with 0.15 ml of 1.5 mg/ml *Micrococcus lysodeikticus* in 1X PBS, pH 7.4 and the absorbance at 450 nm was monitored every 30 s for a period of 5 min. The activity was calculated using the decrease in absorbance for the linear portion (between 0.5 and 3.0 min) assuming one unit of enzyme activity will reduce the $\triangle A_{450nm}$ by 0.001/min. Specific activity is defined in units of activity per mg of protein and is given as % of the specific activity of

the native, standard lysozyme. The actual amount of soluble monomer lysozyme in the solution was determined via SE-HPLC and was used for the specific activity calculations.

3.3.2.8 Scanning Electron Microscopy

Surface images of microspheres were taken after a brief gold coating (60s) using a Hitachi S3200N Scanning Electron Microscope at voltages ranging from 5 to 10 kV.

3.4 Results and Discussion

3.4.1 Effect of Base on Self-Encapsulation

3.4.1.1 Loading and Release

All four blank formulations that incorporated differing amounts of pore-forming $MgCO_3$ (0, 1.5, 4.3, 11.0% w/w) had a surprisingly similar surface morphology (Figure 3.2), although the amount of surface pores appeared to increase with the amount of base encapsulated and also those surface pores visibly decreased slightly in size with increasing base content. After the pore closing/encapsulation step, all microspheres had very similar morphologies, with the highest base content (11% w/w) having a slightly rougher surface (Figure 3.3). Thus, any differences in loading would be expected to result from differences in porosity, and not because of incomplete pore closing.

The loading of lysozyme in the particles increased with increasing $MgCO_3$ content, suggesting higher porosity with increasing base amount, except there was a slight decrease with the highest $MgCO_3$ added (Figure 3.4). Enzyme loading was (% w/w ± SEM) 4.5 ± 0.2% (0% $MgCO_3$), 6.4 ± 0.1% (1.5% $MgCO_3$), 9.8 ± 0.3% (4.3% $MgCO_3$), and 8.7 ± 0.4% (11.0% $MgCO_3$). This drop in loading due to the highest base

content may be attributed to insufficient internal pore closing due to the very porous internal structure.

The release rate of the particles directly correlated with the amount of base used to create the blank particles (Figure 3.5). The amount released from the microspheres after 28 days was (% ± SEM) 30 ± 1% (0% $MgCO_3$), 41 ± 1% (1.5% $MgCO_3$), 51 ± 4% (4.3% $MgCO_3$), and 57 ± 4% (11.0% $MgCO_3$). Increases in base content resulted in increased burst release after 4 days, whereas all formulations displayed a similar lag period, with virtually no protein release, from day 7 to day 28.

3.4.1.2 Recovery and Activity

The amount of protein remaining in the microspheres after 28 days of release, including soluble monomer, soluble aggregates, and insoluble aggregates, was quantified. Nearly 100% mass balance was achieved for all formulations (Figure 3.6). Total amount recovered was (% ± SEM) 92 ± 2% (0.0% $MgCO_3$), 91 ± 1% (1.5% $MgCO_3$), 99 ± 4% (4.3% $MgCO_3$), and 110 ± 4% (11% $MgCO_3$). The total amount of soluble protein, both released over 28 days and recovered as residual soluble monomer was (% ± SEM) 83.1 ± 1.6% (0.0% $MgCO_3$), 85.0 ± 0.5% (1.5% $MgCO_3$), 94.5 ± 3.6% (4.3% $MgCO_3$), and 107.0 ± 3.3% (11% $MgCO_3$).

The amount of aggregation was observed to decrease with increasing base content (Figure 3.6), as has been reported previously [7, 27, 28] and therefore was expected. The percent of loaded protein that had aggregated in the recovered enzyme from the particles after 28 days of release was 8.7 ± 0.6% (0.0% $MgCO_3$), 6.0 ± 0.2% (1.5% $MgCO_3$), 4.7 ± 0.2% (4.3% $MgCO_3$), and 3.4 ± 0.1% (11% $MgCO_3$). Thus, it is presumed that the addition of base as a porosigen in the blank particles helped neutralize acid microclimates

during degradation of the PLGA microparticles and/or facilitated subsequent release of acidic monomers, minimizing acid-induced aggregation.

The specific activity of the residual lysozyme remaining in the particles after 28 days of release was analyzed. The specific activity was calculated based upon the total amount of soluble protein analyzed, both monomer and aggregated. The specific activity, given as the percentage of the specific activity of the native, standard lysozyme was 102 ± 6% (0.0% $MgCO_3$), 116 ± 19% (1.5% $MgCO_3$), 100 ± 5% (4.3% $MgCO_3$), and 97 ± 5% (11% $MgCO_3$). Thus, the soluble lysozyme retained in the microparticles after 28d of release was still completely active within experimental error for all formulations.

3.4.1.3 Porosity Measurements

The blank particle porosity was calculated from mercury porosimetry. The intrusion volume per gram showed a similar trend as the loading: generally increasing with increasing base content, although a slight decrease was seen with the highest base content. This intrusion volume per gram was 1.20 (0.0% $MgCO_3$), 1.44 (1.5% $MgCO_3$), 1.76 (4.3% $MgCO_3$), and 1.57 cc/g (11% $MgCO_3$). Samples were consumed with the testing, and thus only one test was run and there is no statistical variance. Porosity was calculated as the percentage of volume of pores in the microspheres over the entire volume of the microspheres. These measurements were 60.0% (0.0% $MgCO_3$), 64.3% (1.5% $MgCO_3$), 68.8% (4.3% $MgCO_3$), and 66.2% (11% $MgCO_3$).

A graph of the loading versus the porosity shows the strong linear correlation between the loading and the porosity, with an r-squared value of 0.96 (Figure 3.8). Additionally, the amount of pore volume utilized for loading increased with base amount, but appeared to level off at around 24% of the total pore volume (Figure 3.9).

3.4.2 Effect of Inner Water Phase Volume on Self-Encapsulation

3.4.2.1 Loading and Release

The surface morphology of four blank formulations prepared with differing amounts of inner water phase (25, 100, 200, and 350 µl of 500 mg trehalose dehydrate in 1 g PBS, pH 7.4) had a similar appearance to one another (Figure 3.10) except for the formulation prepared with the lowest i.w. phase (25 µl), which appeared less porous. After the pore closing/encapsulation step (self-healing), all had indistinguishable morphologies. Thus again, any differences in loading would be expected to result from differences in porosity, and not because of incomplete pore closing (Figure 3.11).

The loading of lysozyme in the particles increased with increasing i.w. phase volume, suggesting a higher porosity with increasing i.w. phase volumes, although there was a slight decrease with the highest i.w. phase volume (Figure 3.12). Loading was (% w/w ± SEM) 1.15 ± 0.05% (25 µl), 5.7 ± 0.2% (100 µl), 7.5 ± 0.3% (200 µl), and 5.3 ± 0.2% (350 µl).

The 28-d release of these formulations showed no distinct trend based upon i.w. phase volume and all released between 24 and 34% of lysozyme by Day 28 (Figure 3.13). The amount released from the microspheres after 28 days was (% ± SEM) 29.7 ± 0.3% (25 µl), 25.9 ± 0.3% (100 µl), 33 ± 2% (200 µl), and 24.5 ± 0.6% (350 µl).

3.4.2.2 Recovery and Activity

The amount of total remaining protein in the microspheres after 28 days of release was quantified. Nearly 100% mass balance was achieved for 3 formulations (Figure 3.14). Total amount recovered was 117 ± 5% (25 µl), 96 ± 3% (100 µl), 100 ± 3% (200

µl), and 85 ± 1% (350 µl). The lack of 100% mass balance for the 350 µl formulation may be in part attributed to the existence of some of the lysozyme as soluble aggregates and fragments not quantified by SE-HPLC. In fact, when Coomassie was run on the soluble protein remaining, a mass balance of 4% greater was achieved (88.6 ± 0.6%). The total amount of soluble protein, both released over 28 days and recovered as residual soluble monomer was 84 ± 4% (25 µl), 86 ± 3% (100 µl), 92 ± 3% (200 µl), and 75.4 ± 0.8% (350 µl).

The amount of aggregates, both soluble and insoluble, was calculated as well (Figure 3.15). The percent of loaded protein that was aggregated that was recovered in the microspheres after 28 days of release was (% ± SEM) 33.2 ± 2.0% (25 µl), 9.5 ± 0.3% (100 µl), 7.9 ± 0.4% (200 µl), and 9.2 ± 0.2% (350 µl). The lowest i.w. phase had a significant amount of aggregation, but this may be an artifact of either the low loading of lysozyme or the low porosity. The low porosity microspheres may sequester higher levels of acidic degradation products, whereas the higher porosity particles are expected to more rapidly release hydrolysis products into the release media. Additionally, it has been shown that the presence of bulk protein can stabilize other proteins [29], so in the higher loadings much of the polymer/water interfaces may have become saturated, and much of the encapsulated protein is not at the interface, whereas at lower loadings, much of the loaded lysozyme may be exposed to acidic interfaces, leading to a higher percentage of unstable protein.

The specific activity of the residual lysozyme remaining inside the microspheres after 28 days of release was (% ± SEM) 28.0 ± 5.5% (25 µl), 84.9 ± 0.6% (100 µl), 86 ± 6% (200 µl), and 85.0 ± 0.8% (350 µl) (Figure 3.16). Thus, except for the lowest i.w.

phase volume formulation, the soluble lysozyme that was retained in the microparticles after 28 d of release was still mostly enzymatically active.

3.4.2.3 Porosity Measurements

The blank particle porosity was calculated by mercury porosimetry. The intrusion volume per gram displayed a similar trend as the loading: generally increasing with increasing inner water phase volume, though a slight decrease was seen with the highest base content. This intrusion volume per gram was 0.78 (25 µl), 1.23 (100 µl), 1.43 (200 µl), and 1.18 cc/g (350 µl), corresponding to the following porosity values: 49.5% (25 µl), 60.6% (100 µl), 64.0% (200 µl), and 59.7% (350 µl).

A graph of the loading versus the porosity showed a very strong linear correlation between the loading and the porosity, with an r-squared value of 0.997 (Figure 3.17). Additionally, the amount of pore volume utilized for loading increased with base amount, but appeared to level off at around 20-25% of the total pore volume (Figure 3.18).

It is clear that the porosity decreased once the inner water phase volume was increased from 200 µl to 350 µl. One possible explanation for this is the 350 µl formulation may have been a more porous particle immediately after creation but part of what had made it so porous – the large amount of inner water volume – allowed the porosigen to be released out of the microparticle quicker than other formulations. Thus, by the end of the hardening phase, this particle may have seen less water uptake due to a lower osmotic gradient, generating a particle that was less porous. Similarly, a higher inner water phase volume and more extensive channels initially provides a greater surface area for the methylene chloride pockets to migrate to, increasing the rate of phase

separation and hardening. As discussed previously, increased hardening rate decreases the porosity of microparticles prepared via the solvent evaporation method.

3.4.3 Effect of Polymer Concentration on Self-Encapsulation

3.4.3.1 Loading and Release

The four blank formulations that were created using differing concentrations of PLGA in the organic phase (200, 260, 320, and 400 mg PLGA in 1 ml CH_2Cl_2) had similar surface morphologies, although the pore size did appear to decrease with increasing polymer concentration (Figure 3.19). After the pore closing/encapsulation step, the number of visible pores on the surface appeared to increase with polymer concentration as well, suggesting that there was incomplete pore closing with ahigh polymer concentration (400 mg in 1 ml CH_2Cl_2) formulation (Figure 3.20).

The loading of lysozyme in the particles was roughly constant followed by an increase at the highest polymer concentration formulation (Figure 3.21). Loading was (% w/w ± SEM) 6.7 ± 0.3% (200 mg), 6.4 ± 0.2% (260 mg), 7.4 ± 0.2% (320 mg), and 9.9 ± 0.4% (400 mg).

The 28-d release of these formulations show no distinct trend, although the differences between the formulations was larger than that seen for previous formulations. The highest release rate was the 400 mg PLGA formulation, while the slowest and least released over 28d was the 260 mg PLGA formulation. By day 28, 21 to 57% of lysozyme was released in all formulations (Figure 3.22). The amount released from the microspheres after 28 days was (% ± SEM) 34.4 ± 0.3% (200 mg), 20.6 ± 0.9% (260 mg), 46.6 ± 0.5% (320 mg), and 57 ± 2% (400 mg).

3.4.3.2 Recovery and Activity

Nearly 100% mass balance was achieved for 3 formulations after 28 days of release (Figure 3.23). The total amount recovered was (% ± SEM) 93 ± 2% (200 mg), 100 ± 2% (260 mg), 95 ± 3% (320 mg), and 89 ± 2% (400 mg), i.e. slightly higher than the total amount of soluble protein, both released over 28 days and recovered as residual soluble monomer, at 86 ± 2% (200 mg), 90 ± 2% (260 mg), 86 ± 2% (320 mg), and 84 ± 2% (400 mg).

The amount of aggregates, both soluble and insoluble, was calculated as well (Figure 3.24). The percent of loaded protein, recovered in the particles after 28 days of release which had aggregated, was 7.7 ± 0.5% (200 mg), 9.6 ± 0.4% (260 mg), 9 ± 3% (320 mg), and 5.2 ± 0.3% (400 mg). The formulation that utilized 400 mg PLGA in 1 ml CH_2Cl_2 clearly had less aggregation, but also had the highest amount of unrecovered lysozyme (over 10%), so it is unlikely the lysozyme in that formulation was the most stable of the group.

The specific activity of the residual lysozyme left inside the particles after 28 days of release was analyzed. The specific activity was calculated based upon the total amount of soluble protein analyzed, both monomer and aggregated. The specific activity, relative to native lysozyme was 89 ± 1% (200 mg), 97 ± 5% (260 mg), 108 ± 4% (320 mg), and 91 ± 3% (400 mg). Here again, the soluble lysozyme retained in the microparticles after 28 d of release was still mostly enzymatically active (Figure 3.25), although surprisingly the formulation with a polymer concentration of 320 mg in 1 ml CH_2Cl_2 conferred higher enzyme stability relative to the other formulations.

3.4.3.3 Porosity Measurements

The blank particle porosity was calculated through mercury porosimetry. The intrusion volume per gram showed no distinct trend. The intrusion volumes were 1.50 (200 mg), 1.25 (260 mg), 2.13 (320 mg), and 1.46 cc/g (400 mg), corresponding to porosities of 65.2% (200 mg), 61.0% (260 mg), 72.7% (320 mg), and 64.6% (400 mg).

A graph of the loading versus the porosity shows no visible correlation between the loading and the porosity (Figure 3.26). Additionally, the amount of pore volume utilized for loading does not show a strong correlation with increasing polymer concentration, but the highest polymer concentration did utilize the higher percentage of pores, using over 30% of the total pore volume (Figure 3.27).

The trend of increasing loading with increasing porosity is seen for these varying polymer concentrations, although the 400 mg in 1 ml CH_2Cl_2 is not consistent with this trend. Previous work has indicated that with a PLGA of a similar MW (53,600), a significant increase in residual methylene chloride content was observed with a similar polymer concentration [30], where 200, 300, and 400 mg/ml solutions of PLGA were used to create microparticles and the residual solvent in the microparticles was 0.01 ± 0.01%, 0.60 ± 0.07%, and 1.62 ± 0.07%, respectively.

It is clear that highest polymer concentration had the highest loading although with just moderate porosity. There are a few possible explanations for this apparent discrepency. First, the transfer of methylene chloride to the continuous phase assumingly approached a slow, minimal rate much more quickly in the 400 mg/ml formulation than the 300 mg/ml formulation. This has been predicted theoretically before [3]. This can be attributed to the formation of a polymer buildup on the periphery, a ‘skin’ that prevents

migration of the CH_2Cl_2 to the continuous phase. These results suggest that a high polymer concentration may create a formulation with less pores, but with increased residual solvent and subsequent more polymer chain mobility during encapsulation, and higher loading associated with those formulations.

Secondly, the quicker hardening of the higher concentration formulation could have meant that much of the porosigen was still trapped inside during freeze drying. Once the particles were incubated at a temperature above their T_g during the self-healing microencapsulation step, freedom of mobility would have been given to the polymer chains, perhaps creating even more pores due to the osmotic pressure differences. Thus, the actual measurement of the porosity of the dry particles may not be an exact representation of the entire porosity during encapsulation.

Thirdly, although its porosity is relatively modest, the percolation and interconnecting network of this formulation may be higher relatively than the other formulations. Perhaps the interconnectiveness of the pore network decreases during the hardening process, presumably from further phase separation. Consequently, it may be possible to increase loading via self-encapsulation by shortening the hardening process by increasing polymer concentration or the amount of continuous phase.

3.5 Conclusions

By adjusting various formulation parameters during microsphere manufacture, microsphere porosity can be controlled over a broad range. Loading via self-encapsulation is strongly dependent on this porosity. Here we have demonstrated that increasing amounts of excipient, in this case a base, $MgCO_3$, causes increases in porosity and subsequent loading. Likewise, an increase in the inner water phase also increases the

porosity of microspheres. The effects of increasing polymer concentration on porosity are not clearly defined, but the potential for high loading of drug via self-encapsulation can be seen when high concentrations of polymer are employed for blank particle manufacture. The results demonstrate that self-healing microencapsulation loading correlates strongly with porosity created by excipients. Nearly a 100% mass balance after 28 day release was achieved for most formulations, allowing aggregation and release to be accurately measured. The inclusion of acid-neutralizing base has again been demonstrated to minimize the amount of protein aggregation and increase enzymatic activity during release. Results also show that no more than 30% of the available pores were utilized during loading. Thus, clearly there is room for increased loading via self-encapsulation, perhaps allowing sufficient loading to take place even at low protein loading solution concentration.

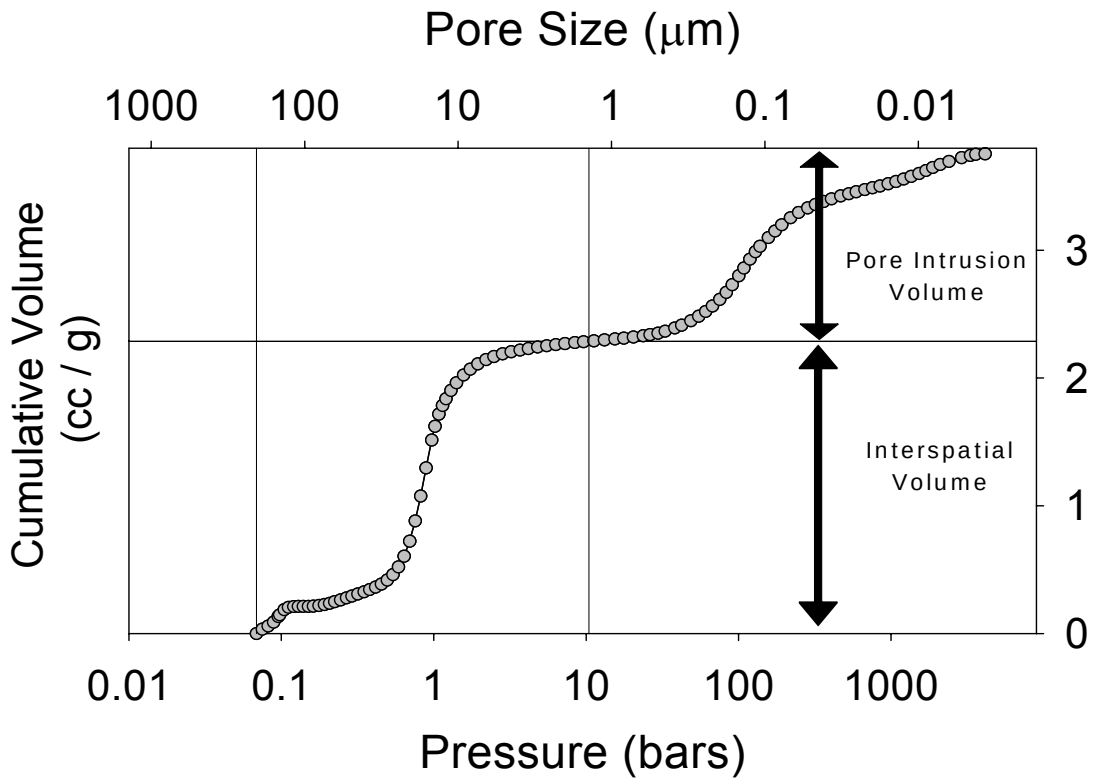

Figure 3.1 Representative pore volume data obtained by mercury porosimetry. Pressure was required to spread and wet the microspheres before penetration into pore network. Here, a pressure of 10.4 bars (1.4 μm) was required for wetting and spreading. Therefore the size of pores measured was 1.4 μm or smaller.

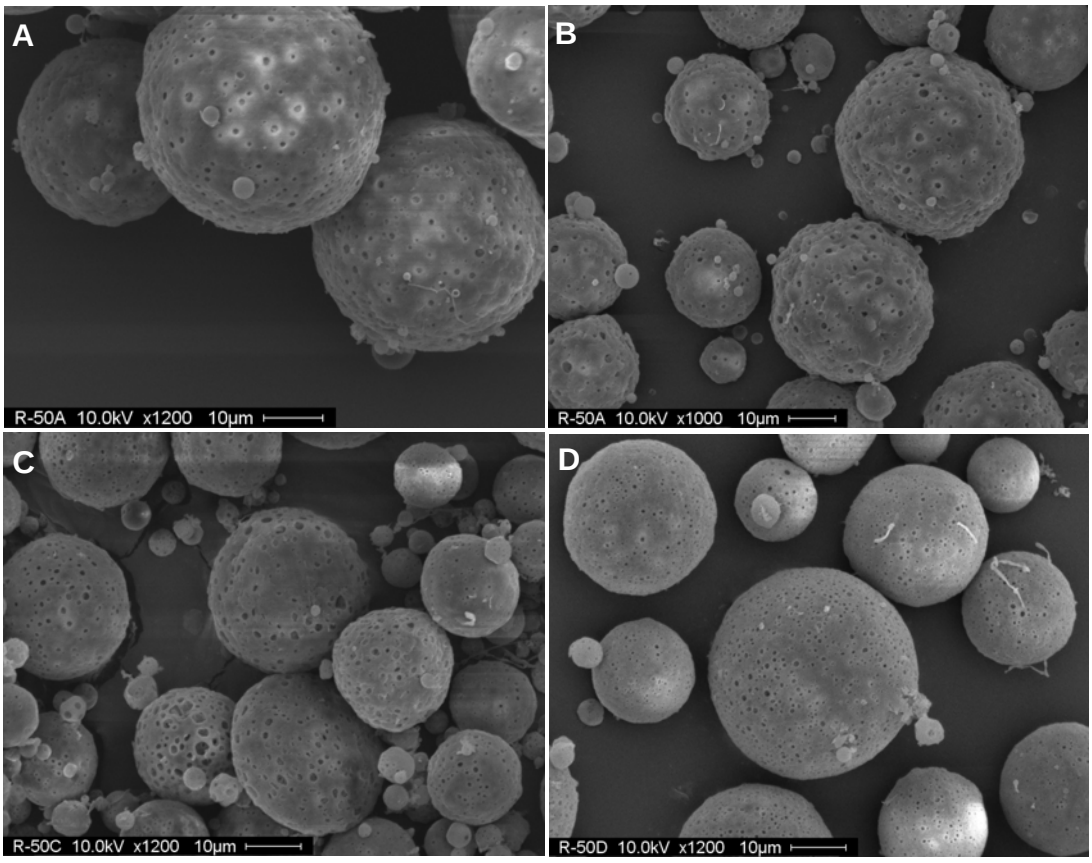

Figure 3.2 Effect of base on blank particle morphology by SEM. Four formulations were created using PLGA and trehalose in PBS in the inner water phase with varying amounts of theoretical loading of $MgCO_3$ (w/w): A) 0%, B) 1.5%, C) 4.3%, and D) 11.0%.

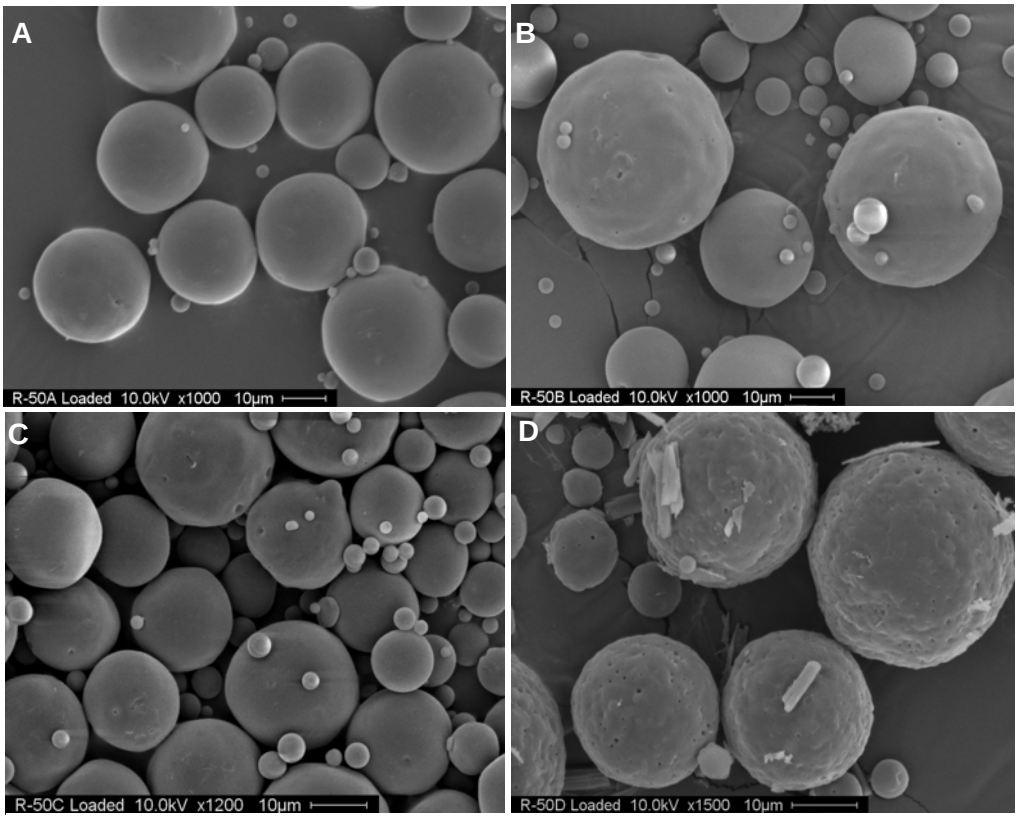

Figure 3.3 Effect of base on lysozyme loaded particle morphology by SEM. Four formulations were created using trehalose in PBS in the inner water phase with varying amounts of theoretical loading of $MgCO_3$ (w/w): A) 0%, B) 1.5%, C) 4.3%, and D) 11.0%. Loading/pore closing in lysozyme solution was conducted at 4°C for 72h and 42°C for 46h.

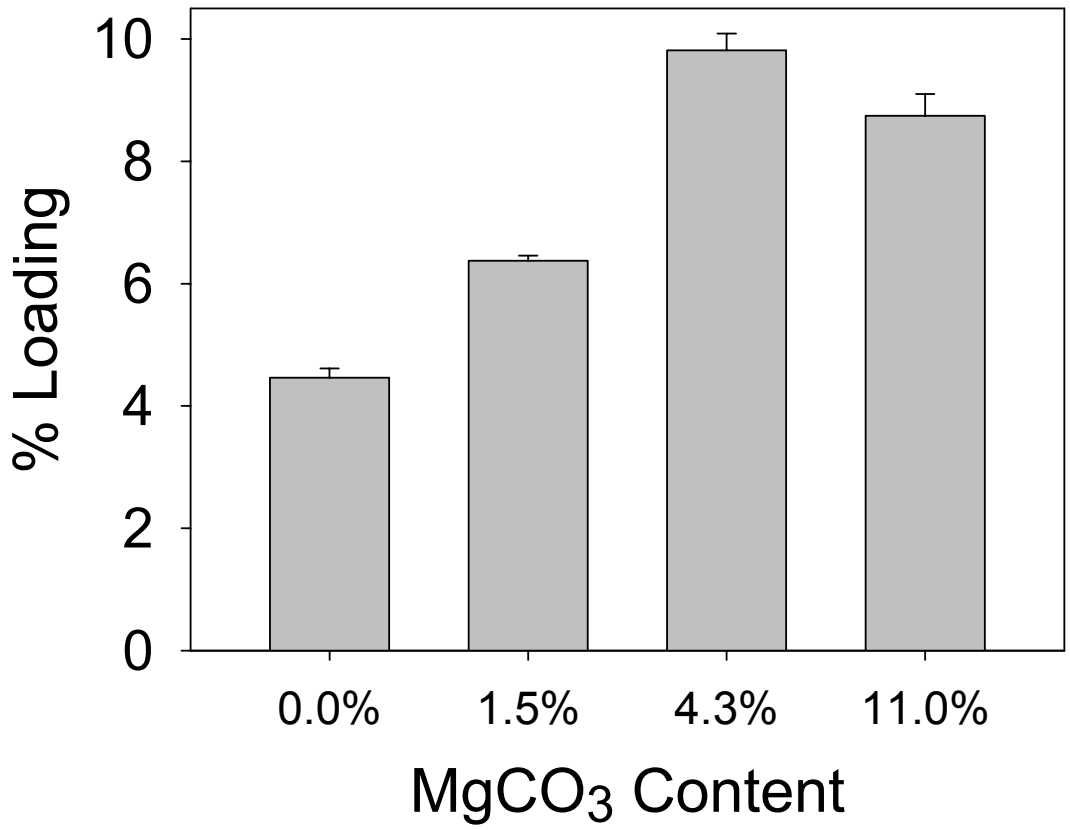

Figure 3.4 Effects of theoretical $MgCO_3$ content in blank PLGA microparticle preparation on lysozyme loading (% w/w) via self-encapsulation. Four formulations were created with differing amounts of $MgCO_3$ in the organic phase. Soluble aggregation was measured through SE-HPLC and insoluble aggregation was measured through Coomassie after dissolving insoluble residual in 6M urea, 1 mM EDTA, 10 mM DTT.

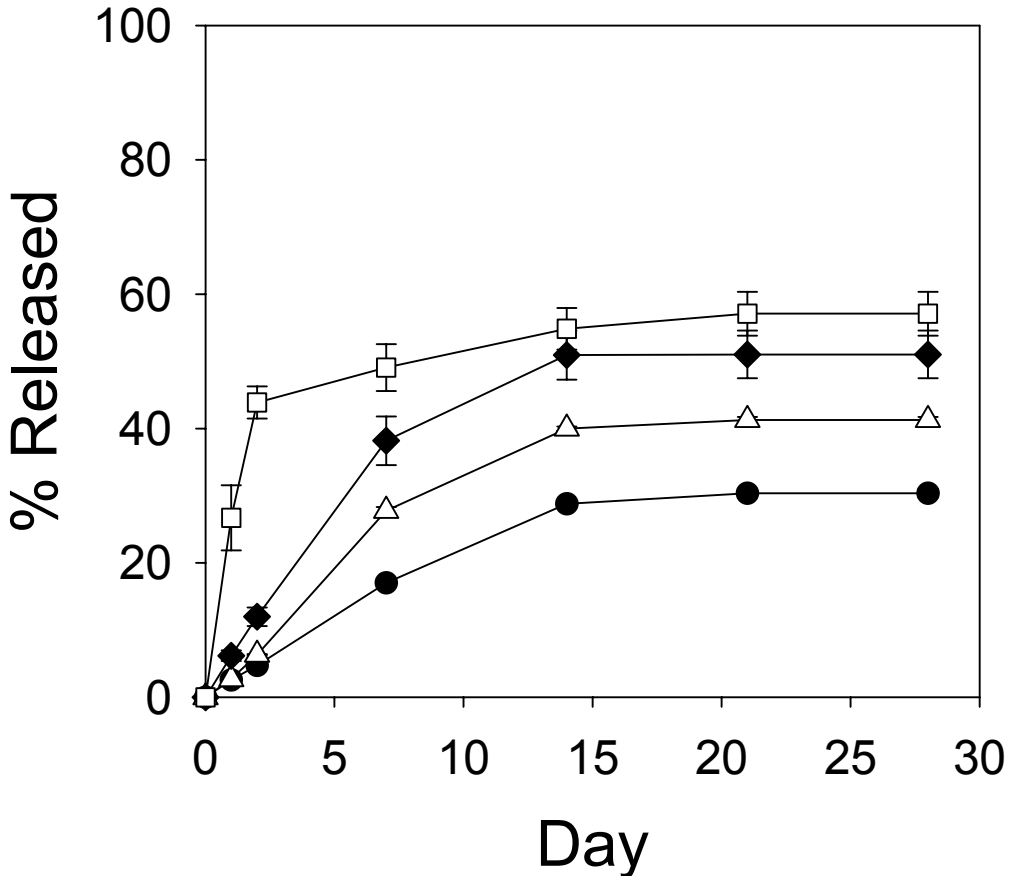

Figure 3.5 Slow release of lysozyme from microparticles created by varying loading of base and constant trehalose content in the inner water phase. SM-microspheres were created using $MgCO_3$ (%, w/w) added to the organic phase: 0% (●), 1.5% (△), 4.3% (◆), and 11.0% (□).

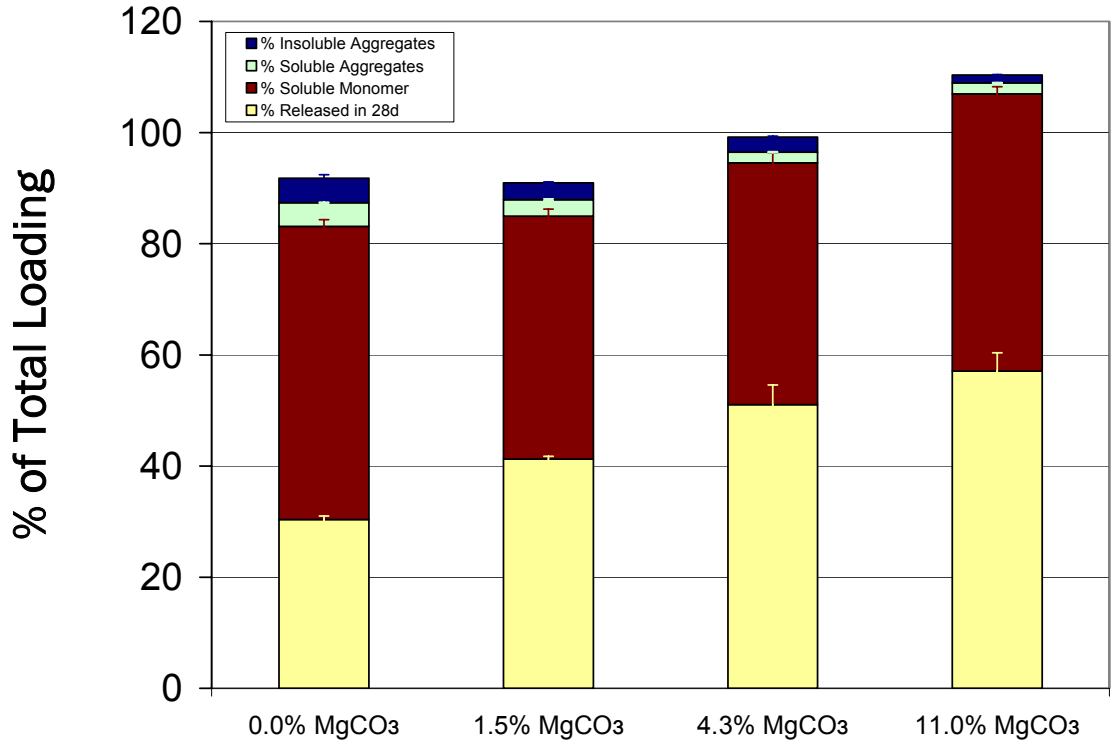

Figure 3.6 Mass balance of lysozyme after 28 d release from microparticles created with various loading of base and constant trehalose content in inner water phase. Four SM-formulations were created using differing amounts of $MgCO_3$ (w/w): 0%, 1.5%, 4.3%, and 11.0%. Estimated amount of lysozyme recovered as aggregates (soluble and insoluble) was 9 ± 1% (0.0% $MgCO_3$), 6 ± 1% (1.5% $MgCO_3$), 5 ± 1% (4.3% $MgCO_3$), and 3 ± 1% (11% $MgCO_3$).

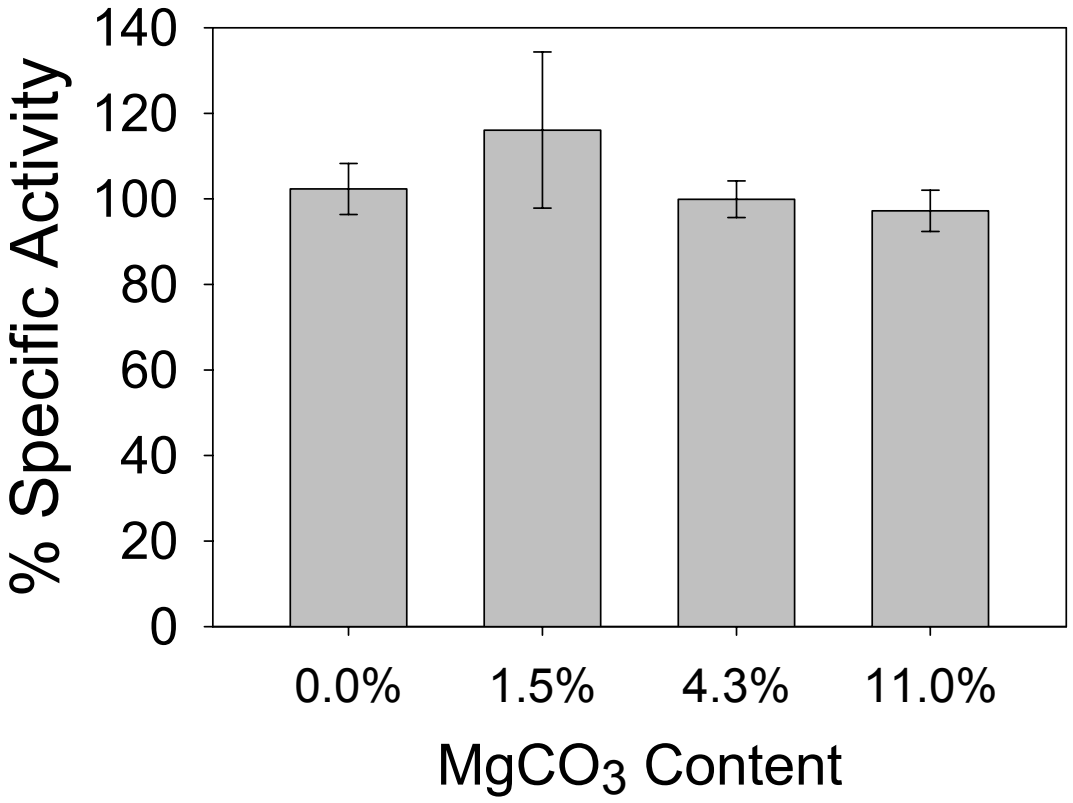

Figure 3.7 Specific activity of lysozyme remaining in microspheres after 28 d release. Four SM-formulations were created using differing amounts of $MgCO_3$ (w/w): 0%, 1.5%, 4.3%, and 11.0%. [% Specific activity was calculated as a percentage of the specific activity of fresh, unencapsulated lysozyme.]

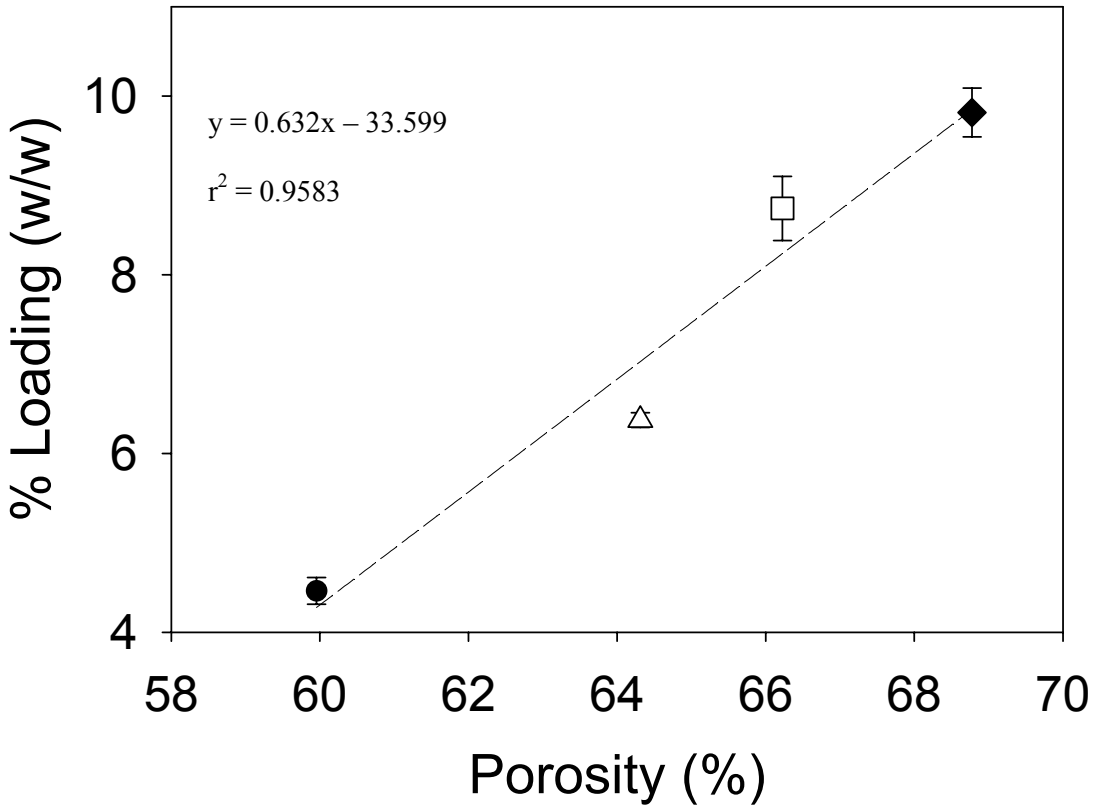

Figure 3.8 Lysozyme loading as a function of porosity from microspheres created with varying amounts of base and constant trehalose content in inner water phase. Four SM-formulations were created using trehalose in PBS as the inner water phase and differing amounts of $MgCO_3$ (w/w): 0% (●), 1.5% (△), 4.3% (◆), and 11.0% (□).

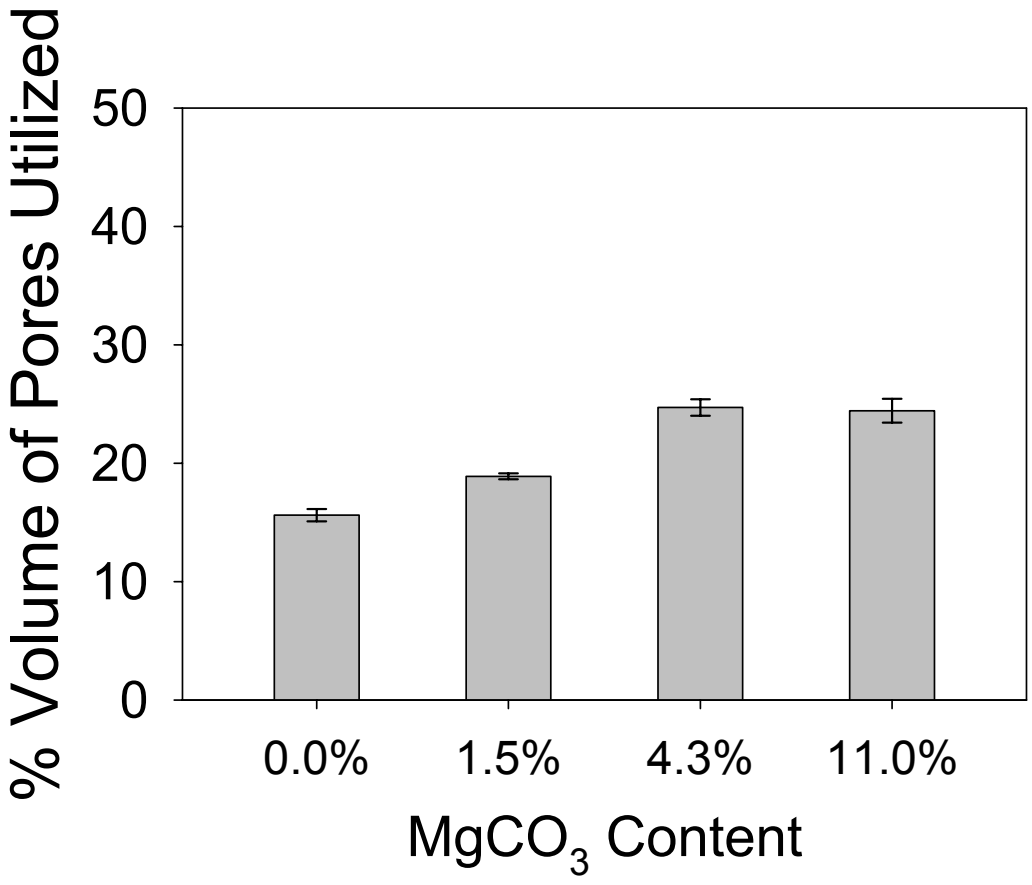

Figure 3.9 Estimate of percentage of pore volume utilized for lysozyme loading in microspheres created with varying amounts of base. SM-formulations were created with differing amounts of $MgCO_3$ (%, w/w) in the organic phase. Fraction of pore volume utilized for self-encapsulation was estimated by the SM-microsphere porosity measured by mercury porosimetry and assuming concentration of lysozyme in pores for encapsulation equaled external solution concentration.

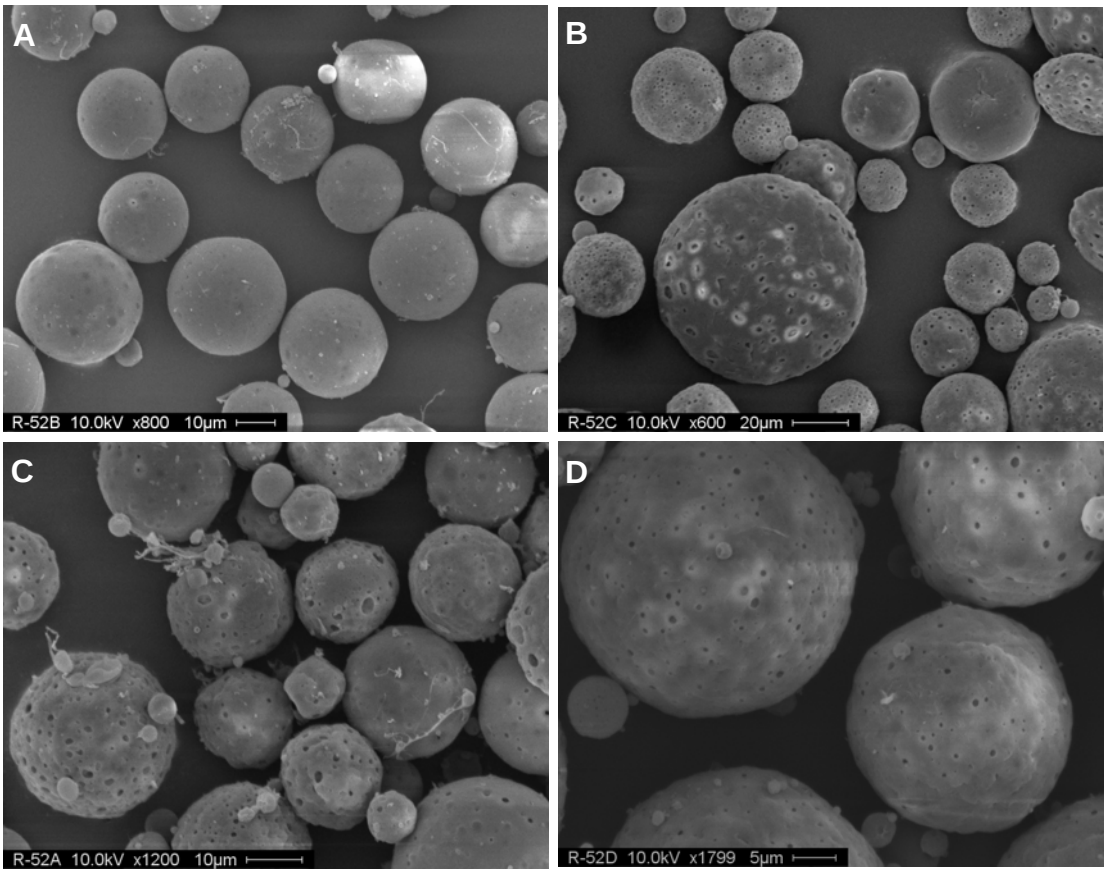

Figure 3.10 Effect of inner water phase volume on SM-microsphere particle porosity. Four formulations were created using differing volumes of inner water phase solution (trehalose in PBS, pH 7.4): A) 25 µl, B) 100 µl, C) 200 µl, and D) 350 µl.

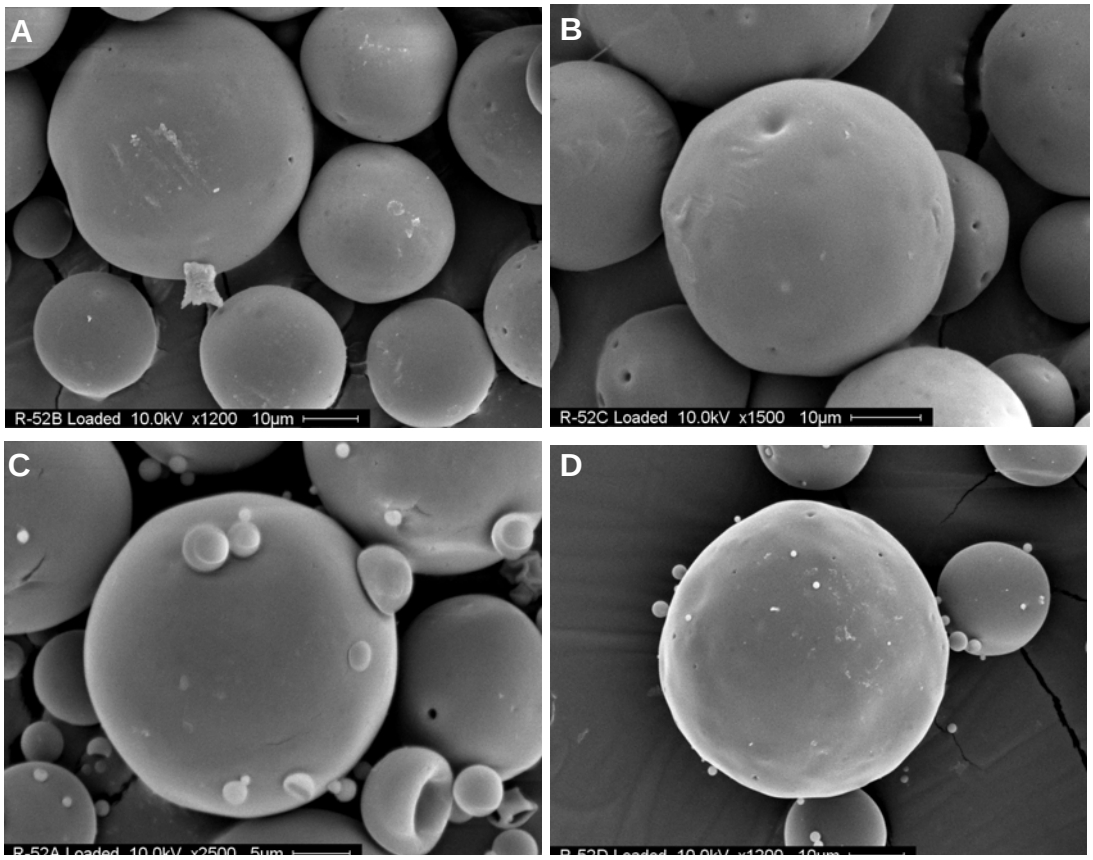

Figure 3.11 Effect of inner water phase volume on lysozyme loaded SM-microsphere morphology. Four formulations were created using differing volumes of inner water phase solution (trehalose in PBS, pH 7.4): A) 25 µl, B) 100 µl, C) 200 µl, and D) 350 µl. Loading/pore closing step in lysozyme solution was 72h at 4°C and 46h at 42°C.

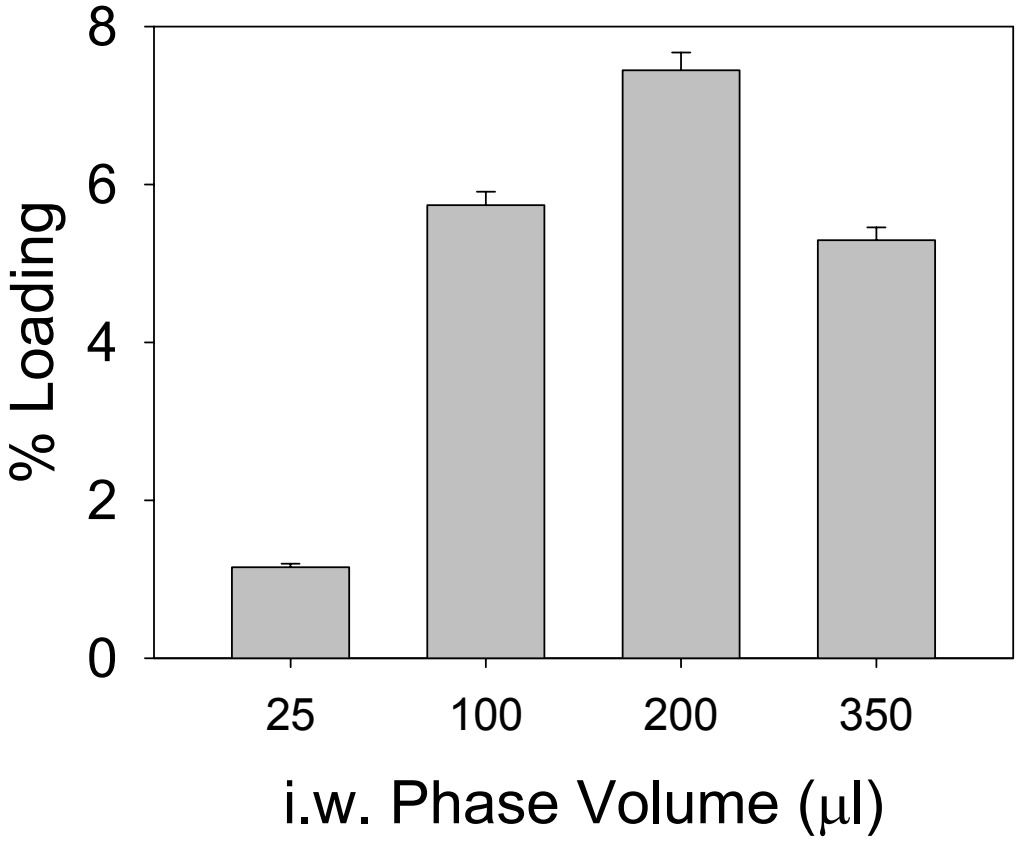

Figure 3.12 Effects of i.w. phase volume in SM-microparticle preparation on lysozyme loading via self-encapsulation. Four SM-formulations were created using differing volumes of inner water phase solution (trehalose in PBS, pH 7.4): 25 µl, 100 µl, 200 µl, and 350 µl.

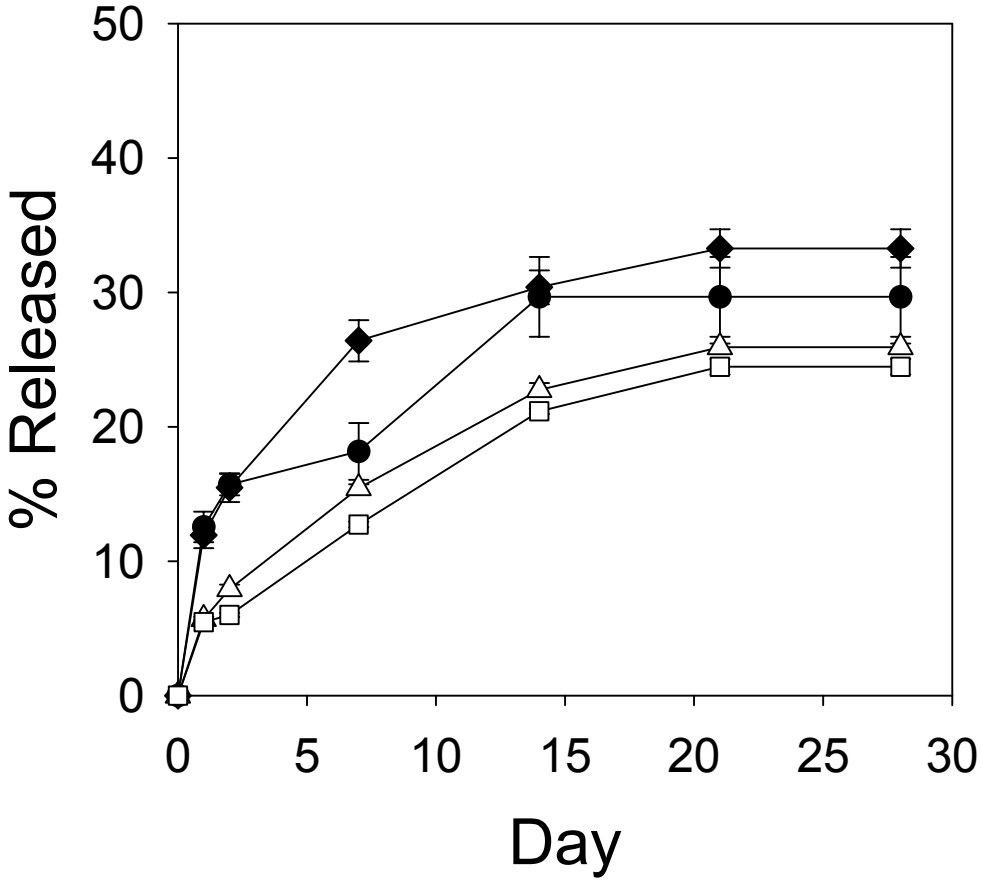

Figure 3.13 Controlled release of lysozyme from microspheres created with various volumes of inner water phase. Four formulations were created using differing volumes of inner water phase solution (trehalose in PBS, pH 7.4): 25 µl (●), 100 µl (△), 200 µl (◆), and 350 µl (□).

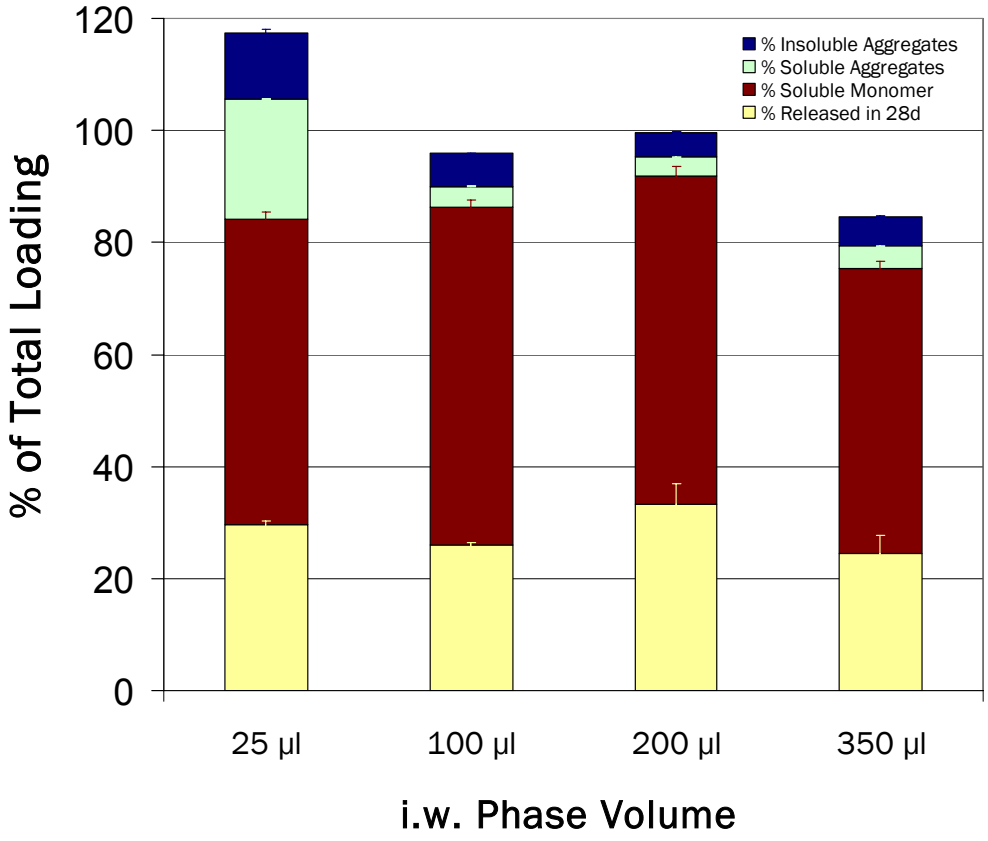

Figure 3.14 Mass balance of lysozyme after 28 d release from SM-microspheres created with differing inner water phase volumes (trehalose in PBS, pH 7.4): 25 µl, 100 µl, 200 µl, and 350 µl.

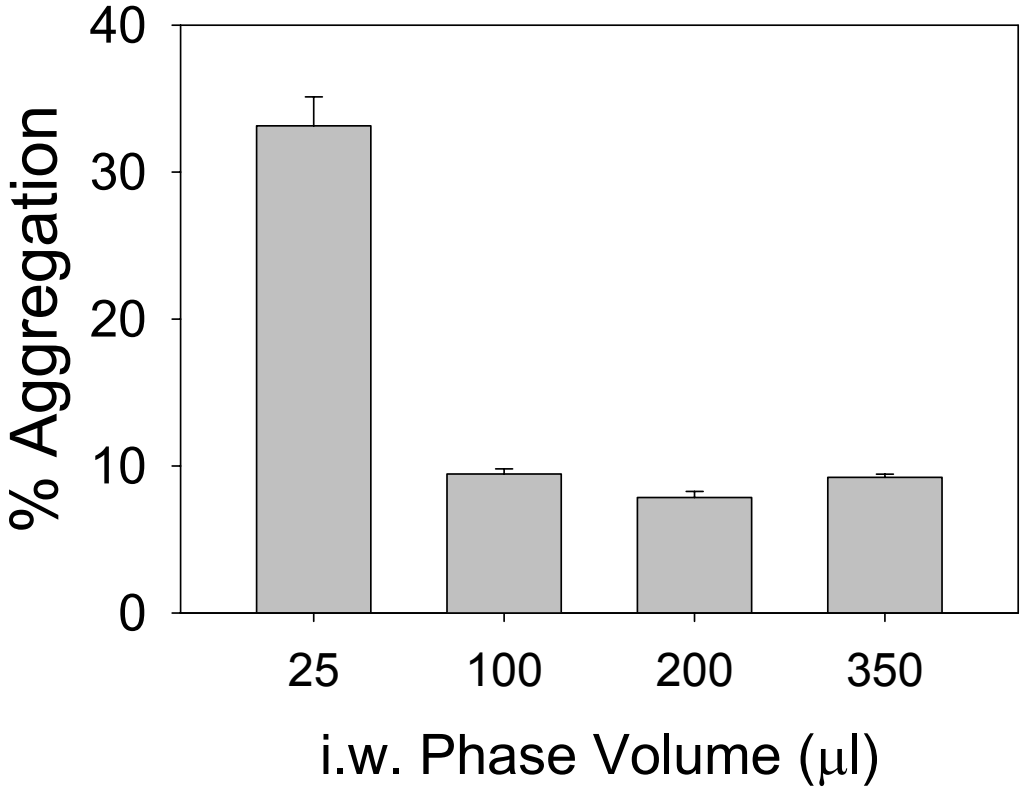

Figure 3.15 Extent of lysozyme aggregation in varying inner water phase formulations after release. Formulations were created with differing volumes of i.w. phase (trehalose in PBS, pH 7.4) in the SM-microparticles. Aggregation was calculated from the solution of loaded lysozyme recovered as soluble and insoluble aggregates after 28 d release. Soluble aggregation was measured by SE-HPLC and insoluble aggregation was measured through Coomassie after dissolving insoluble residual in 6M urea, 1 mM EDTA, 10 mM DTT.

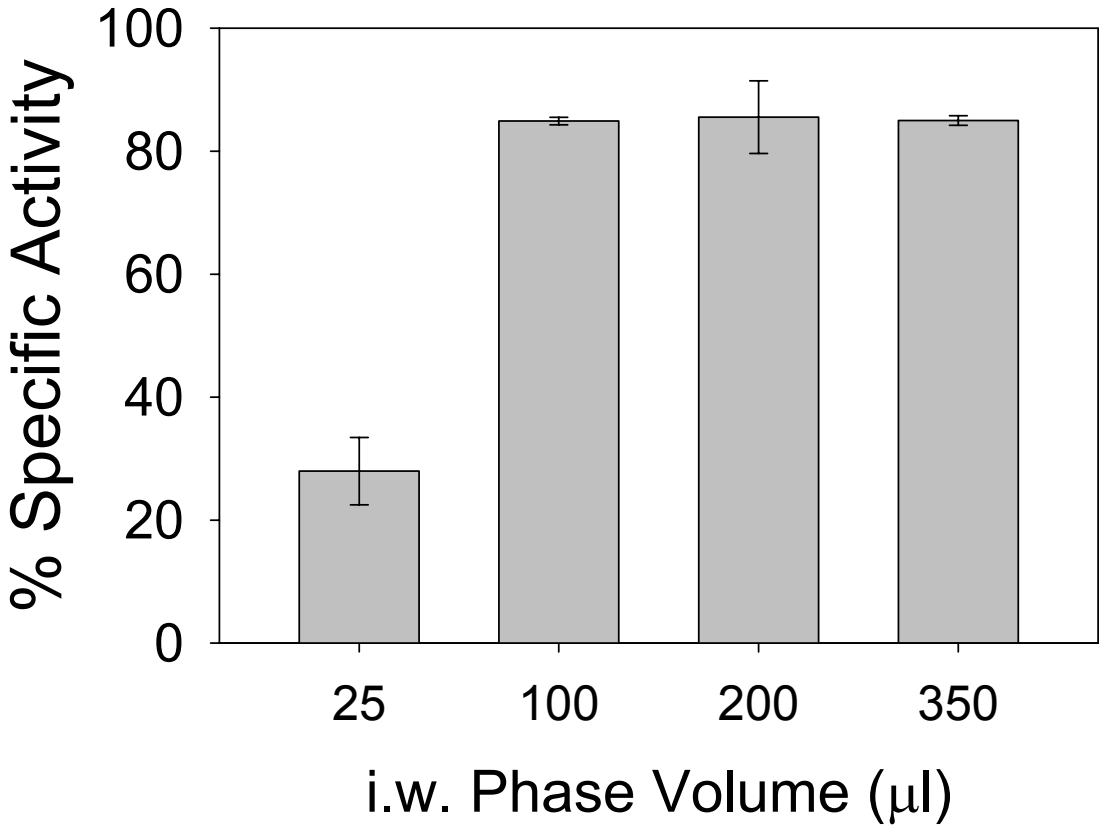

Figure 3.16 Specific activity of lysozyme remaining in varying inner water phase microspheres after 28 d Release. Four formulations were created using differing volumes of inner water phase solution (trehalose in PBS, pH 7.4): 25 µl, 100 µl, 200 µl, and 350 µl.

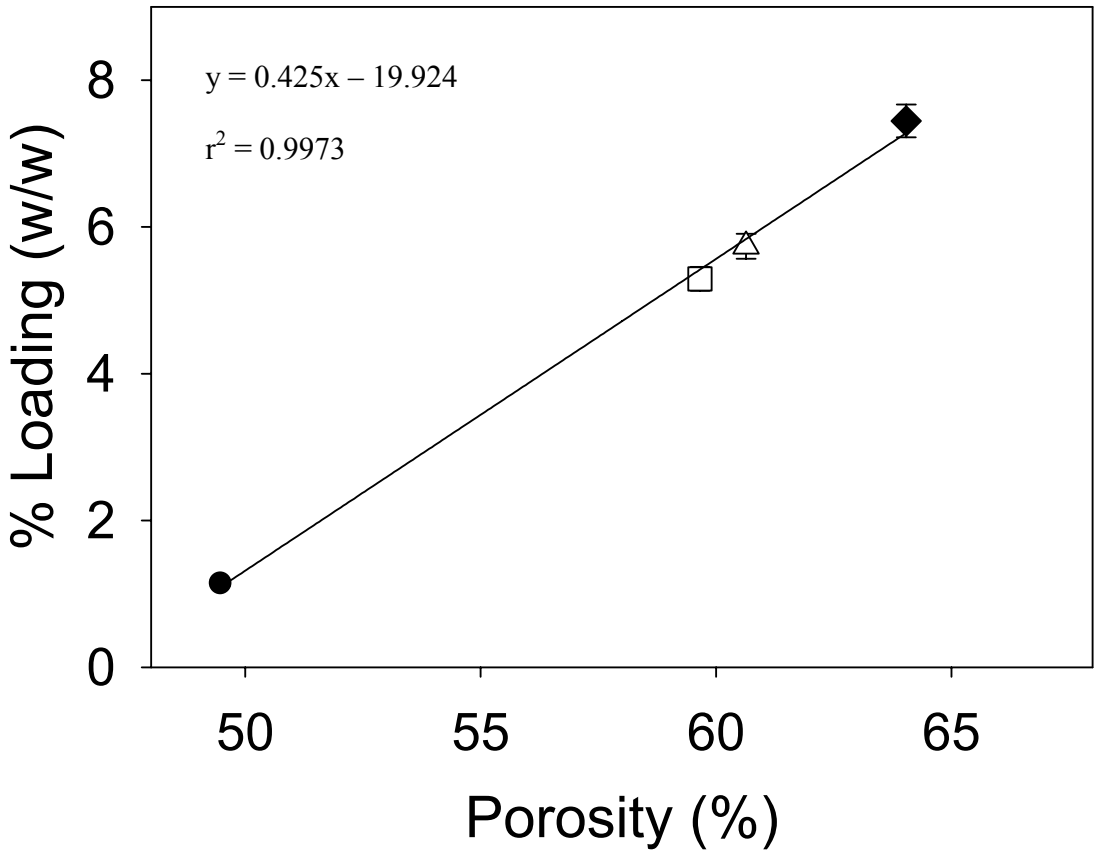

Figure 3.17 Lysozyme loading as a function of porosity from particles created with varying volumes of inner water phase. Four formulations were created using differing volumes of inner water phase solution (trehalose in PBS, pH 7.4): 25 µl (●), 100 µl (△), 200 µl (◆), and 350 µl (□).

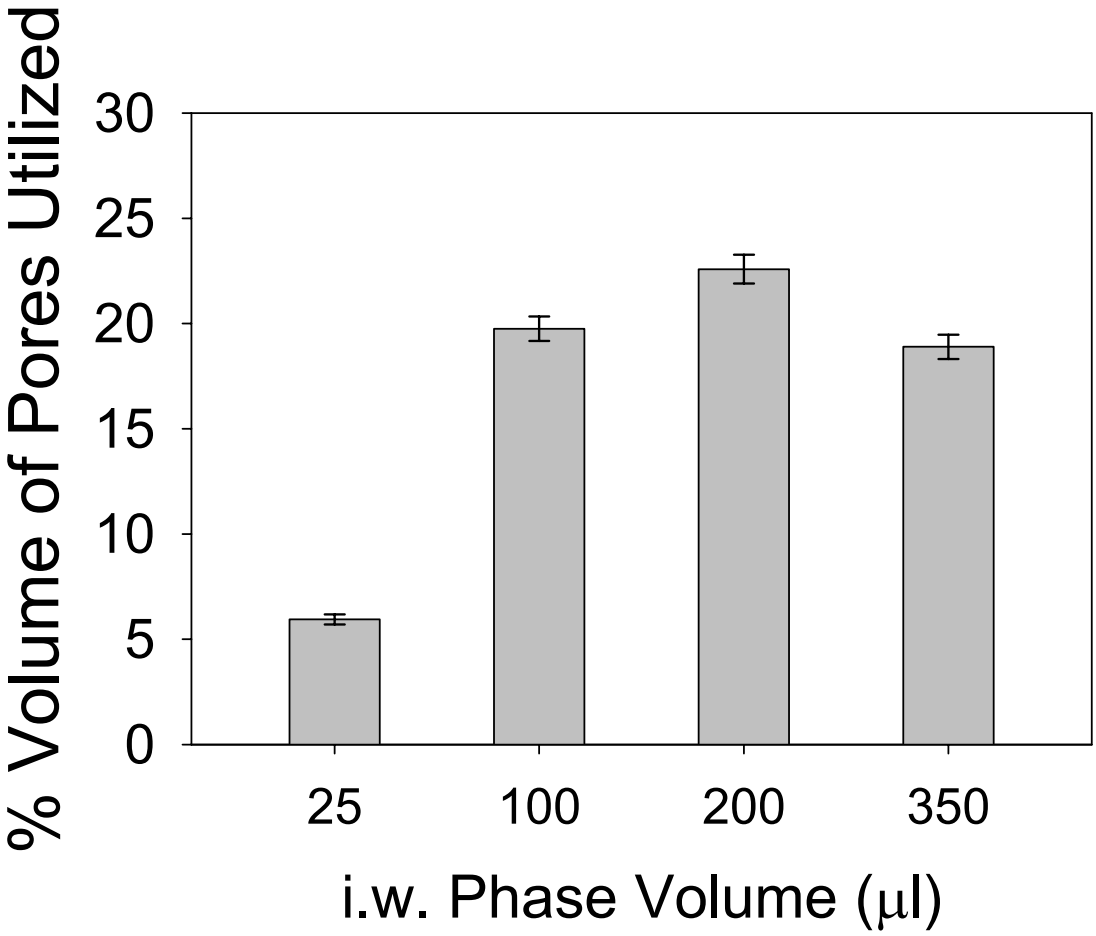

Figure 3.18 Estimate of pore volume utilized for lysozyme loading in varying inner water phase formulations. SM particles were created with differing volumes of i.w. phase solution (trehalose dihydrate in 1X PBS, pH 7.4): 25 µl, 100 µl, 200 µl, and 350 µl. Fraction of pore volume utilized for self-encapsulation was estimated by the SM-microsphere porosity measured by mercury porosimetry and assuming concentration of lysozyme in pores for encapsulation equaled external solution concentration.

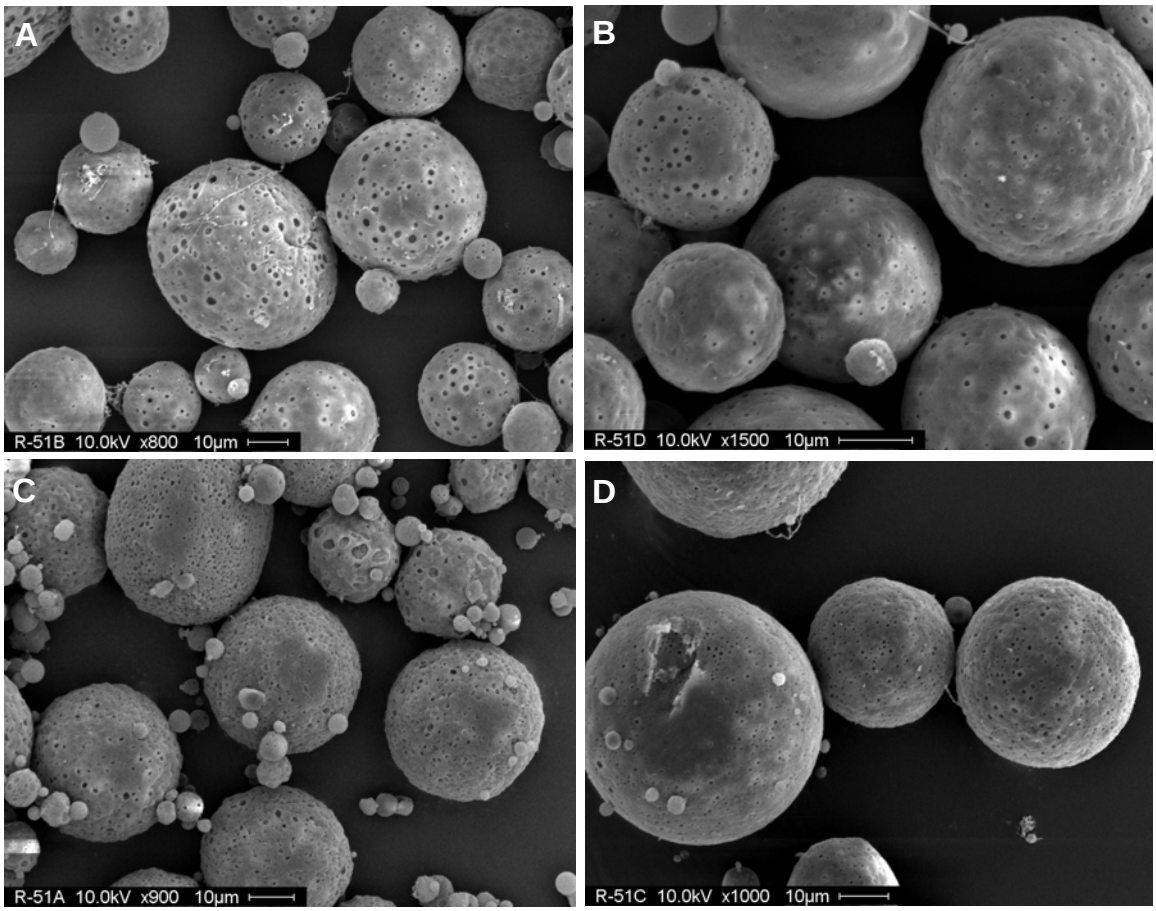

Figure 3.19 Effect of polymer concentration on SM-microparticle porosity by SEM. Four formulations were created using constant base amount (4.8 mg) and different amounts of PLGA (50:50, i.v. = 0.57 dL/g) in 1 ml CH_2Cl_2: A) 200 mg, B) 260 mg, C) 320 mg, and D) 400 mg.

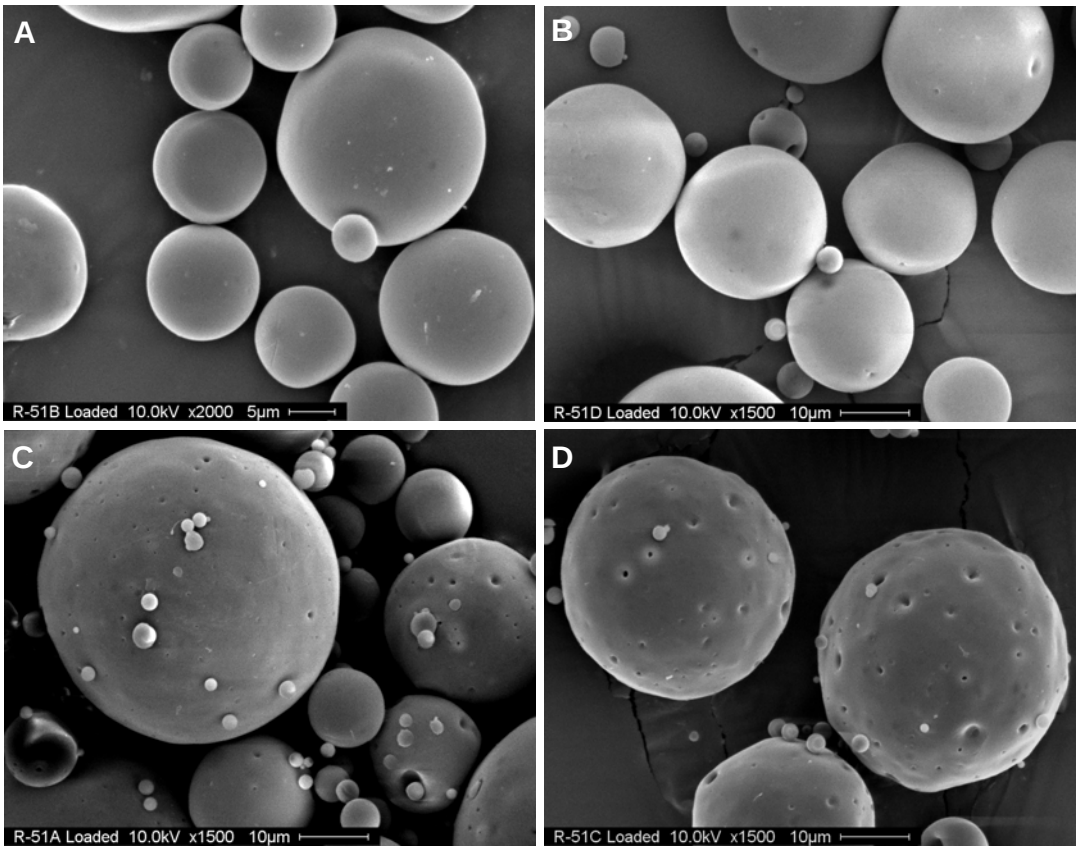

Figure 3.20 Effect of polymer concentration on lysozyme loaded particle morphology by SEM. Four formulations were created using constant base amount (4.8 mg) and different amounts of PLGA (50:50, i.v. = 0.57 dL/g) in 1 ml CH_2Cl_2: A) 200 mg, B) 260 mg, C) 320 mg, and D) 400 mg. Loading/pore closing step in lysozyme solution was 72h at 4°C and 46h at 42°C.

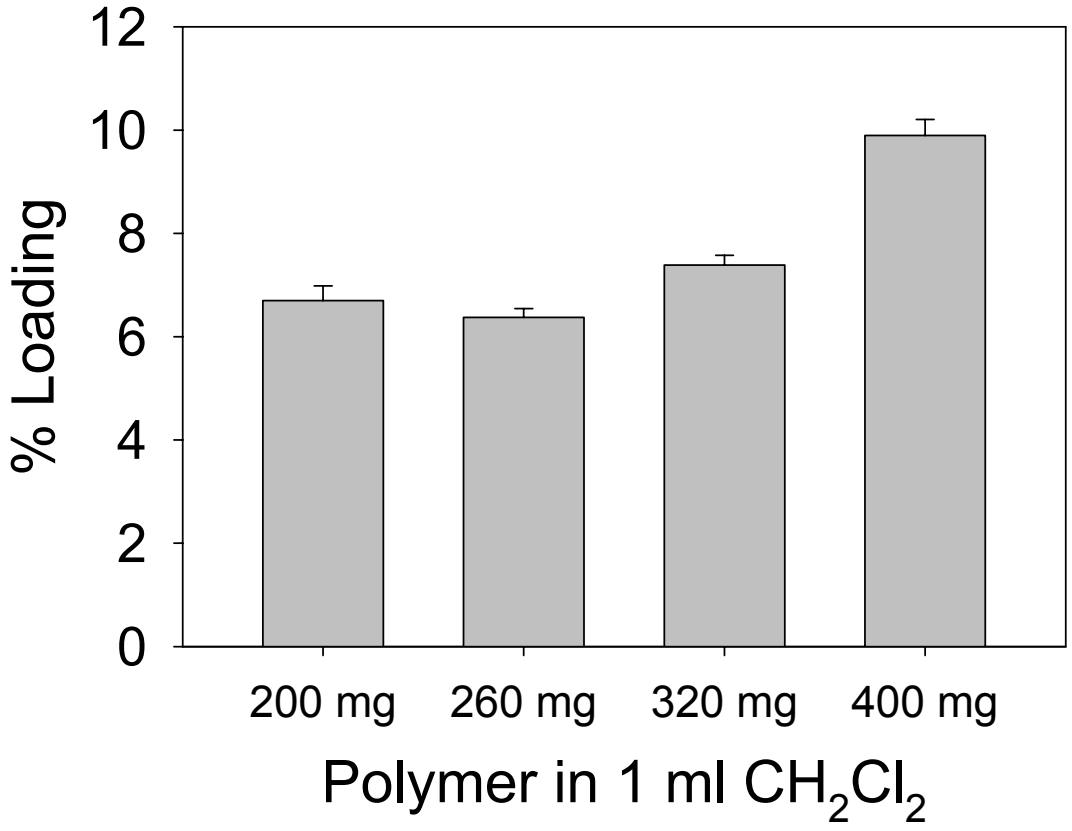

Figure 3.21 Effect of polymer concentration in particle preparation on lysozyme loading via self-encapsulation. Four formulations were created using constant base amount (4.8 mg) and different amounts of PLGA (50:50, i.v. = 0.57 dL/g) in 1 ml CH_2Cl_2: 200 mg, 260 mg, 320 mg, and 400 mg.

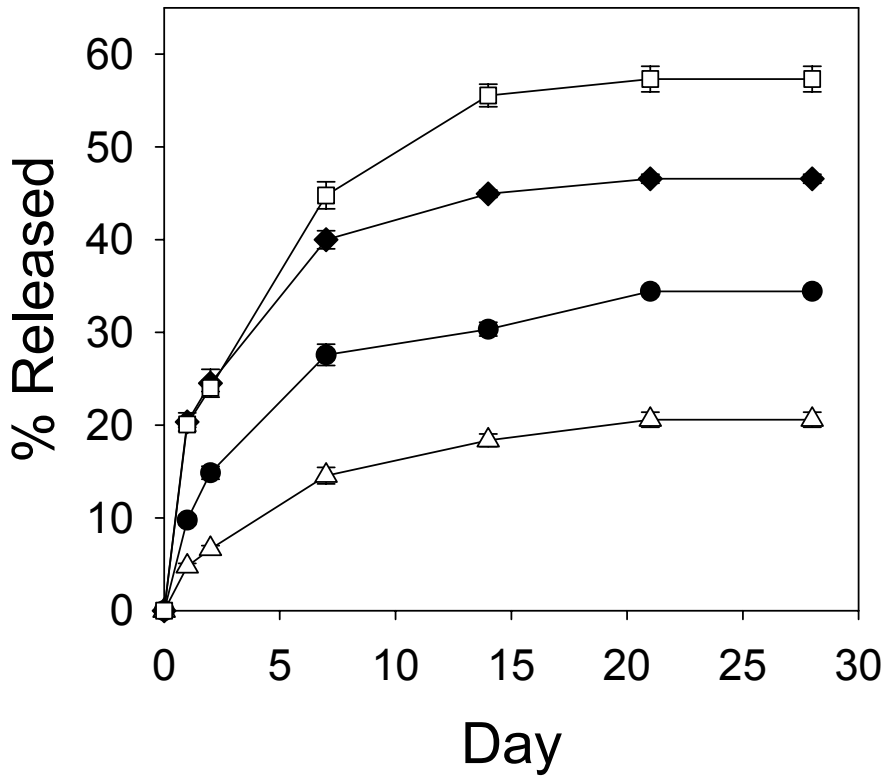

Figure 3.22 Controlled release of lysozyme from SM-microparticles created with varying concentrations of PLGA. Four formulations were created using constant base amount (4.8 mg) and different amounts of PLGA (50:50, i.v. = 0.57 dL/g) in 1 ml CH_2Cl_2: 200 mg (●), 260 mg (△), 320 mg (◆) and 400 mg (□).

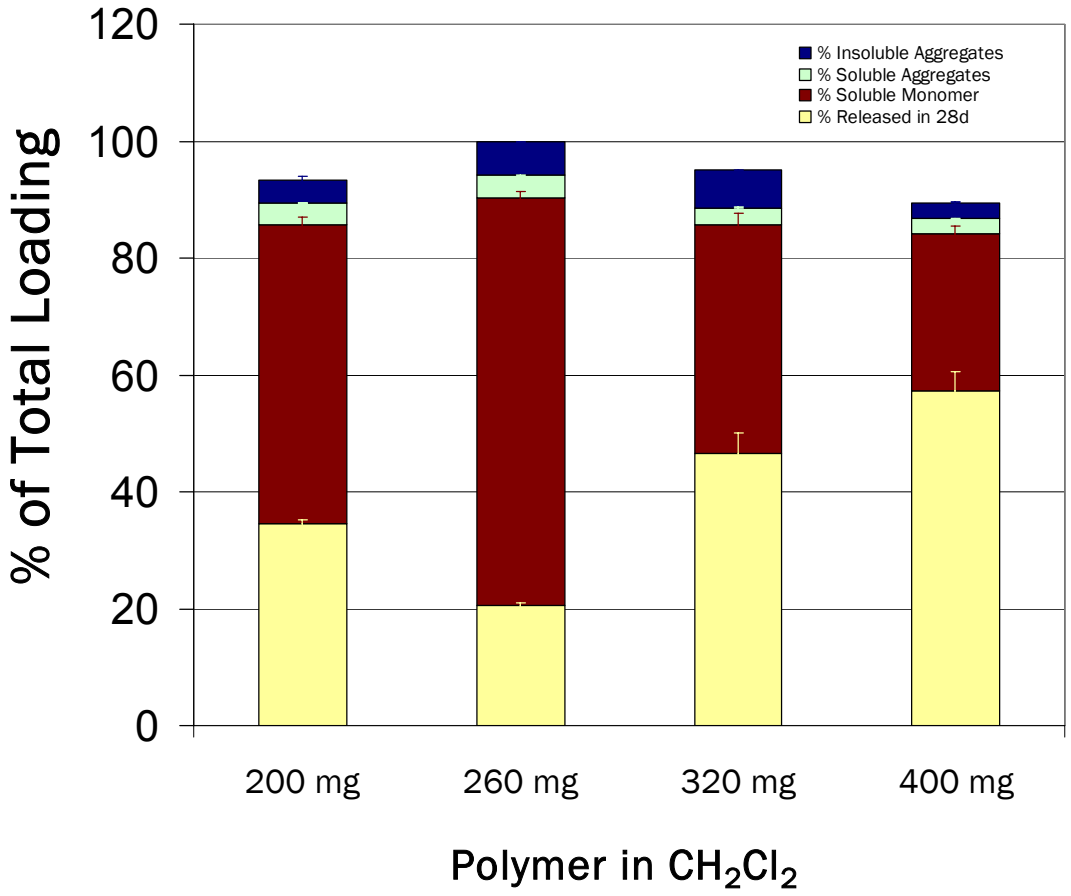

Figure 3.23 Mass balance of lysozyme from particles created with differing polymer concentrations after 28 d Release. Four formulations were created using constant base amount (4.8 mg) and different amounts of PLGA (50:50, i.v. = 0.57 dL/g) in 1 ml CH_2Cl_2: 200 mg, 260 mg, 320 mg, and 400 mg.

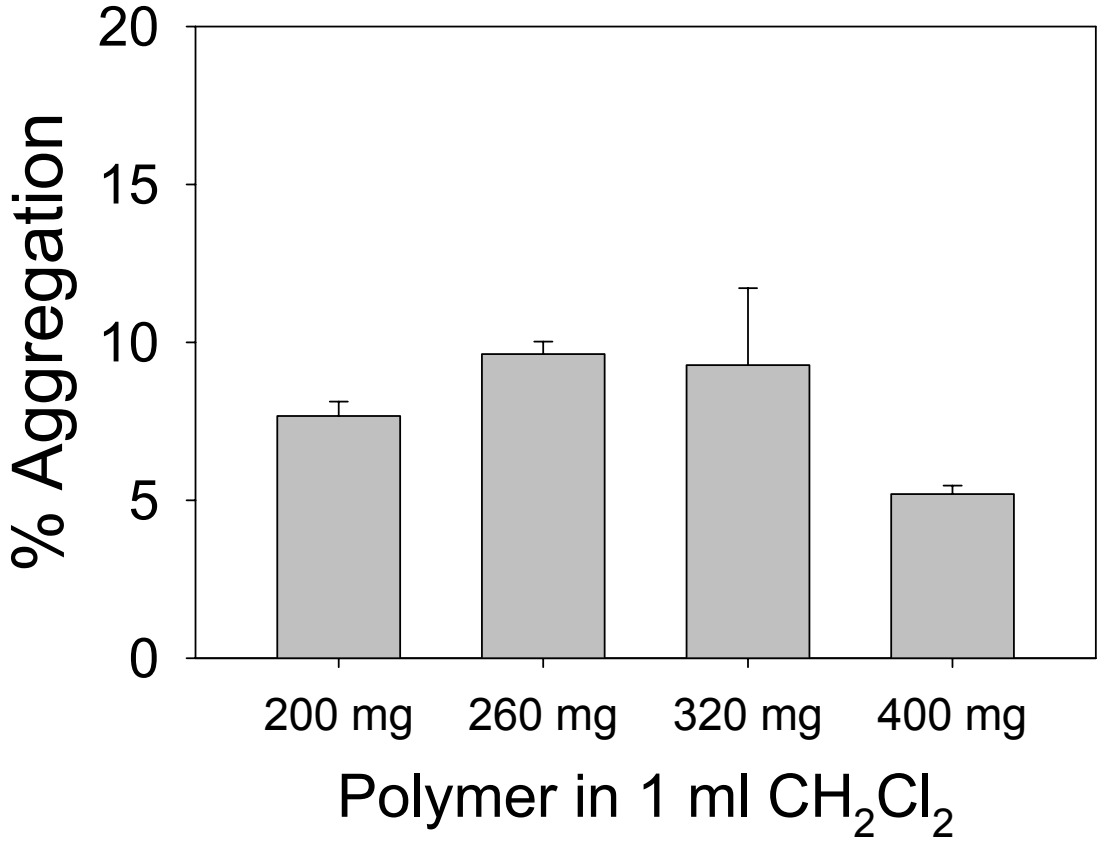

Figure 3.24 Extent of loaded lysozyme aggregation in varying polymer concentration formulations after release. Four formulations were created using constant base amount (4.8 mg) and different amounts of PLGA (50:50, i.v. = 0.57 dL/g) in 1 ml CH_2Cl_2: 200 mg, 260 mg, 320 mg, and 400 mg. Aggregation (%) was calculated from the fraction of loaded lysozyme recovered as soluble and insoluble aggregates after 28 d release. Soluble aggregation was measured through SE-HPLC and insoluble aggregation was measured through Coomassie after dissolving insoluble residual in 6M urea, 1 mM EDTA, 10 mM DTT.

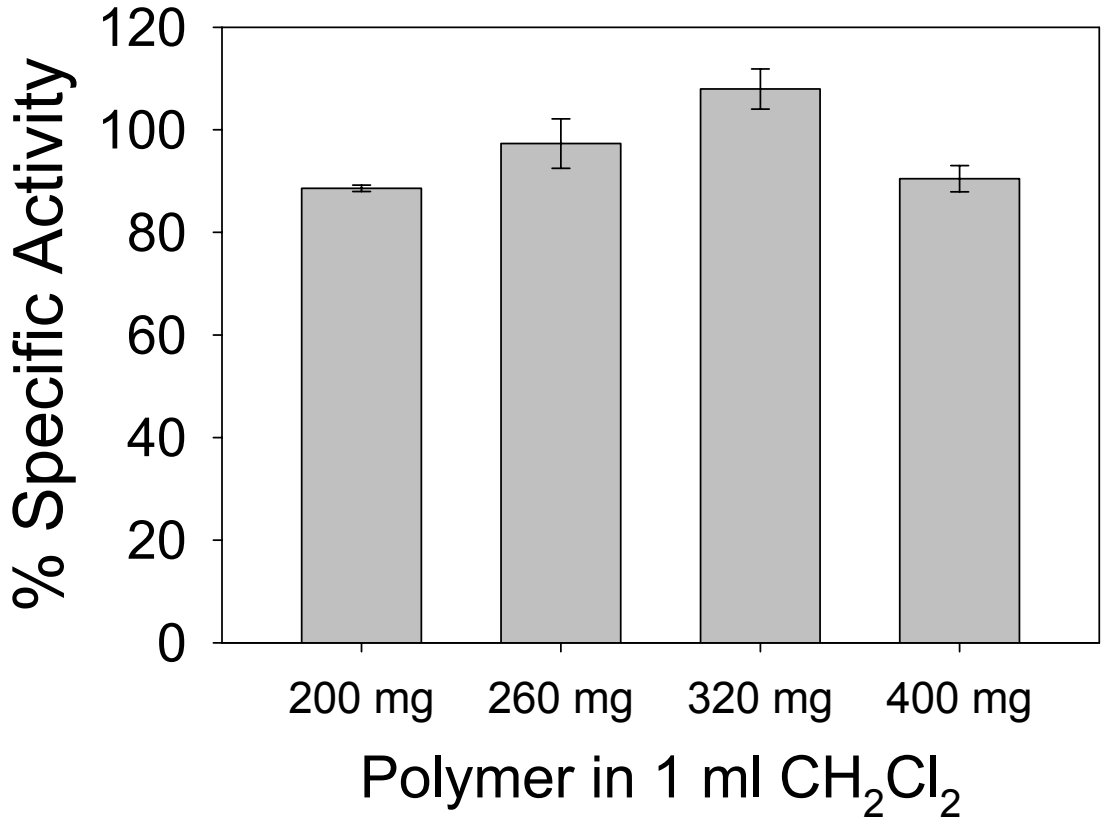

Figure 3.25 Specific activity of lysozyme remaining in varying polymer concentration microspheres after 28 d release. Four formulations of SM-microparticles were created using constant base amount (4.8 mg) and different amounts of PLGA (50:50, i.v. = 0.57 dL/g) in 1 ml CH_2Cl_2: 200 mg, 260 mg, 320 mg, and 400 mg.

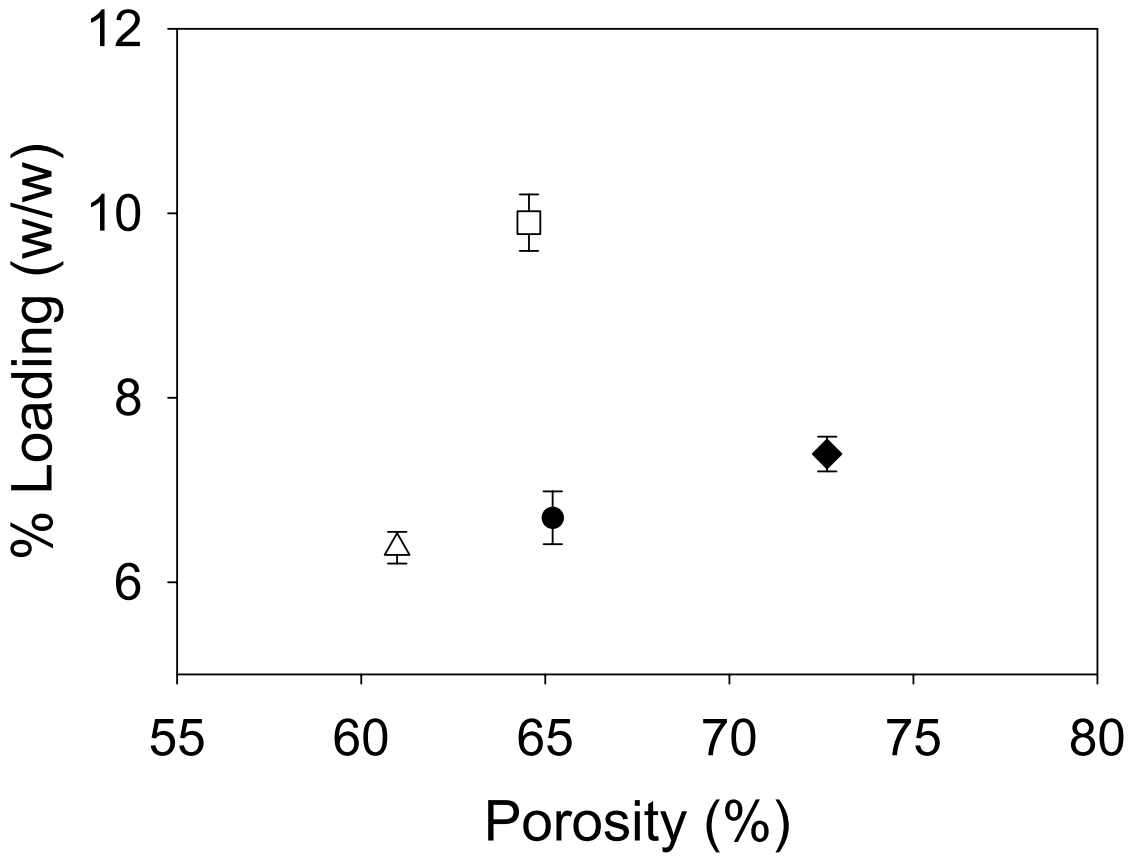

Figure 3.26 Loading as a function of porosity from SM-microparticles created with differing polymer concentrations. Four formulations were created using constant base amount (4.8 mg) and different amounts of PLGA (50:50, i.v. = 0.57 dL/g) in 1 ml CH_2Cl_2: 200 mg (●), 260 mg (△), 320 mg (◆) and 400 mg (□).

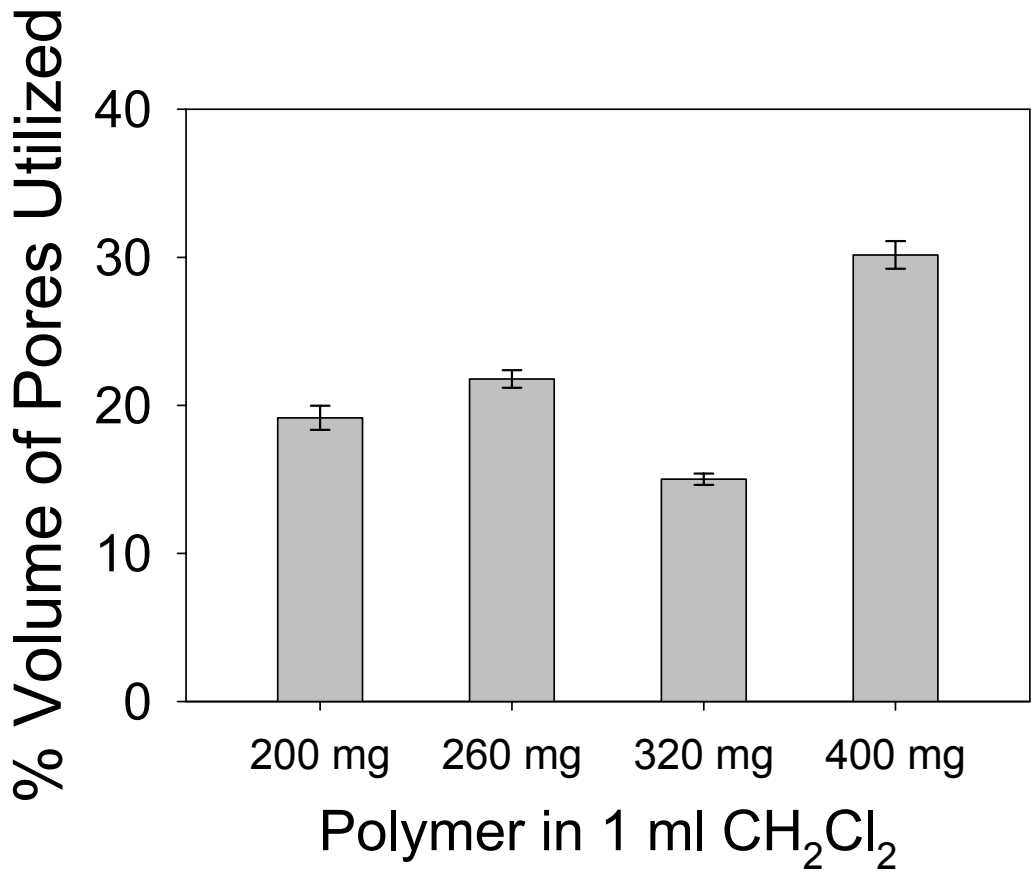

Figure 3.27 Estimate percentage of pore volume utilized for lysozyme loading in varying polymer concentration formulations. Four formulations of SM-microparticles were created using constant base amount (4.8 mg) and different amounts of PLGA (50:50, i.v. = 0.57 dL/g) in 1 ml CH_2Cl_2: 200 mg, 260 mg, 320 mg, and 400 mg. Fraction of pore volume utilized for self-encapsulation was estimated by the SM-microsphere porosity measured by mercury porosimetry and assuming concentration of lysozyme in pores for encapsulation equaled external solution concentration.

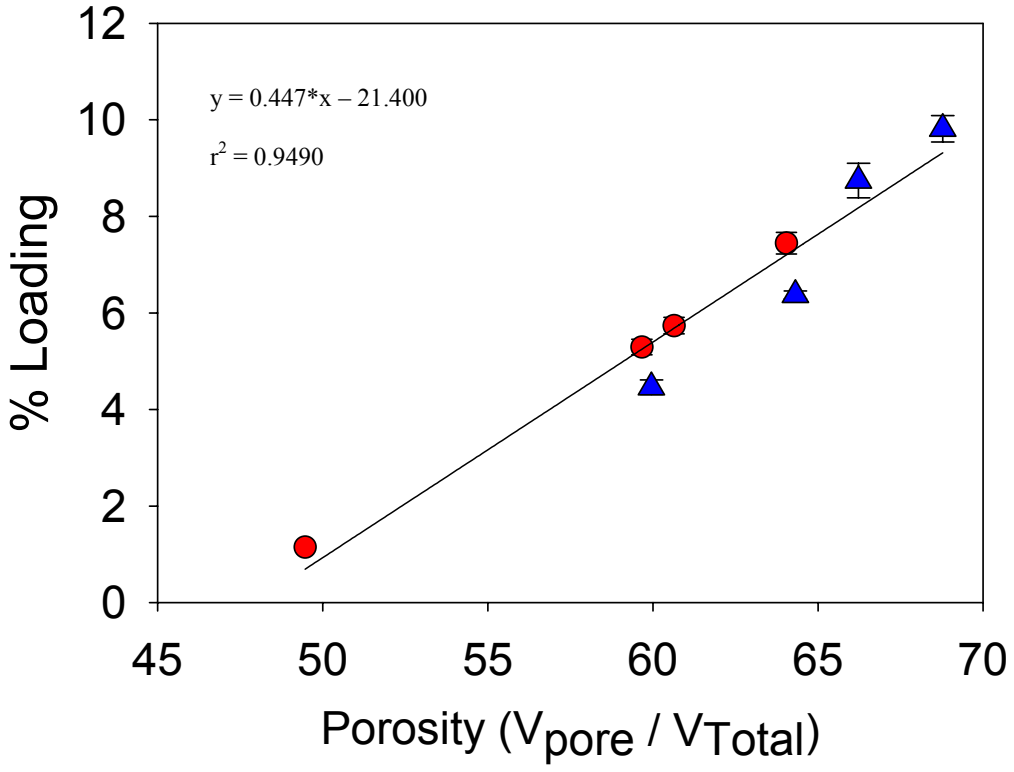

Figure 3.28 Enzyme loading as a function of porosity for varying base and inner water phase microspheres. Triangles represent varying base microparticles and circles represent varying inner water phase microparticles.

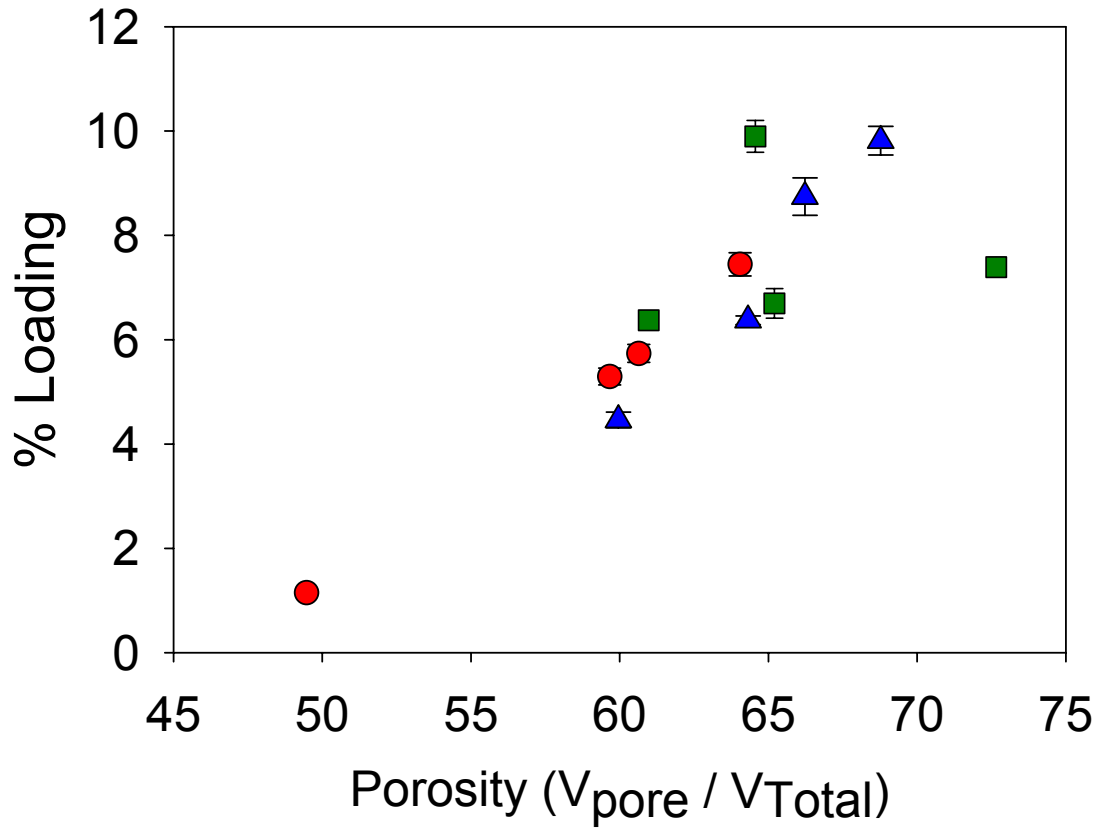

Figure 3.29 Enzyme loading as a function of porosity for varying base, varying inner water phase, and varying polymer concentration microspheres. Triangles represent varying base microparticles circles represent varying inner water phase microparticles, and squares shows varying polymer concentration microparticles.

3.6 References

1. Mehta, R. C.; Thanoo, B. C.; DeLuca, P. P., Peptide containing microspheres from low molecular weight and hydrophilic poly(d,l-lactide-co-glycolide). *Journal of Controlled Release* **1996,** 41, (3), 249-257.
2. Izumikawa, S.; Yoshioka, S.; Aso, Y.; Takeda, Y., Preparation of Poly(L-Lactide) Microspheres of Different Crystalline Morphology and Effect of Crystalline Morphology on Drug Release Rate. *Journal of Controlled Release* **1991,** 15, (2), 133-140.
3. Li, W.-I.; Anderson, K. W.; Mehta, R. C.; Deluca, P. P., Prediction of solvent removal profile and effect on properties for peptide-loaded PLGA microspheres prepared by solvent extraction/ evaporation method. *Journal of Controlled Release* **1995,** 37, (3), 199-214.
4. Herrmann, J.; Bodmeier, R. In *The Effect of Particle Microstructure on the Somatostatin Release from Poly)Lactide) Microspheres Prepared by a W/O/W Solvent Evaporation Method*, 3rd European Symposium on Controlled Drug Delivery, Noordwijk, Netherlands, Apr 04-06, 1994; Elsevier Science Bv: Noordwijk, Netherlands, 1994; pp 63-71.
5. Jeyanthi, R.; Mehta, R. C.; Thanoo, B. C.; DeLuca, P. P., Effect of processing parameters on the properties of peptide-containing PLGA microspheres. *Journal of Microencapsulation* **1997,** 14, (2), 163-174.
6. Zhu, G. Z.; Mallery, S. R.; Schwendeman, S. P., Stabilization of proteins encapsulated in injectable poly (lactide-co-glycolide). *Nature Biotechnology* **2000,** 18, (1), 52-57.
7. Kang, J. C.; Schwendeman, S. P., Comparison of the effects of Mg(OH)(2) and sucrose on the stability of bovine serum albumin encapsulated in injectable poly(D,L-lactide-co-glycolide) implants. *Biomaterials* **2002,** 23, (1), 239-245.
8. De Rosa, G.; Iommelli, R.; La Rotonda, M. I.; Miro, A.; Quaglia, F., Influence of the co-encapsulation of different non-ionic surfactants on the properties of PLGA insulin-loaded microspheres. *Journal of Controlled Release* **2000,** 69, (2), 283-295.
9. Perez-Rodriguez, C.; Montano, N.; Gonzalez, K.; Griebenow, K., Stabilization of alpha-chymotrypsin at the CH2Cl2/water interface and upon water-in-oil-in-water encapsulation in PLGA microspheres. *Journal of Controlled Release* **2003,** 89, (1), 71-85.
10. Ravivarapu, H. B.; Lee, H.; DeLuca, P. P., Enhancing initial release of peptide from poly(d,l-lactide-co-glycolide) (PLGA) microspheres by addition of a porosigen and increasing drug load. *Pharmaceutical Development and Technology* **2000,** 5, (2), 287-296.
11. Zhang, J. X.; Chen, D.; Wang, S. J.; Zhu, K. J., Optimizing double emulsion process to decrease the burst release of protein from biodegradable polymer microspheres. *Journal of Microencapsulation* **2005,** 22, (4), 413-422.

12. Wang, J.; Wang, B. A.; Schwendeman, S. P., Characterization of the initial burst release of a model peptide from poly(D,L-lactide-co-glycolide) microspheres. *Journal of Controlled Release* **2002,** 82, (2-3), 289-307.
13. Wang, X.; Wenk, E.; Hu, X.; Castro, G. R.; Meinel, L.; Li, C.; Merkle, H.; Kaplan, D. L., Silk coatings on PLGA and alginate microspheres for protein delivery. *Biomaterials* **2007,** 28, (28), 4161-4169.
14. Luan, X. S.; Skupin, M.; Siepmann, J.; Bodmeier, R., Key parameters affecting the initial release (burst) and encapsulation efficiency of peptide-containing poly(lactide-co-glycolide) microparticles. *International Journal of Pharmaceutics* **2006,** 324, (2), 168-175.
15. Jiang, G.; Thanoo, B. C.; DeLuca, P. P., Effect of osmotic pressure in the solvent extraction phase on BSA release profile from PLGA microspheres. *Pharmaceutical Development and Technology* **2002,** 7, (4), 391-399.
16. Zhang, J. X.; Zhu, K. J., An improvement of double emulsion technique for preparing bovine serum albumin-loaded PLGA microspheres. *Journal of Microencapsulation* **2004,** 21, (7), 775-785.
17. Schlicher, E. J. A. M.; Postma, N. S.; Zuidema, J.; Talsma, H.; Hennink, W. E., Preparation and characterisation of Poly (lactic-co-glycolic acid) microspheres containing desferrioxamine. *International Journal of Pharmaceutics* **1997,** 153, (2), 235-245.
18. Ghaderi, R.; Sturesson, C.; Carlfors, J., Effect of preparative parameters on the characteristics of poly ,-lactide-co-glycolide)microspheres made by the double emulsion method. *International Journal of Pharmaceutics* **1996,** 141, (1-2), 205-216.
19. Crotts, G.; Park, T. G., Preparation of porous and nonporous biodegradable polymeric hollow microspheres. *Journal of Controlled Release* **1995,** 35, (2-3), 91-105.
20. Ghaderi, R.; Sturesson, C.; Carlfors, J., Effect of preparative parameters on the characteristics of poly(D,L-lactide-co-glycolide) microspheres made by the double emulsion method. *International Journal of Pharmaceutics* **1996,** 141, (1-2), 205-216.
21. Jeyanthi, R.; Thanoo, B. C.; Metha, R. C.; DeLuca, P. P., Effect of solvent removal technique on the matrix characteristics of polylactide/glycolide microspheres for peptide delivery. *Journal of Controlled Release* **1996,** 38, (2-3), 235-244.
22. Ehtezazi, T.; Washington, C., Controlled release of macromolecules from PLA microspheres: using porous structure topology. *Journal of Controlled Release* **2000,** 68, (3), 361-372.
23. Yang, Y. Y.; Chung, T. S.; Ng, N. P., Morphology, drug distribution, and in vitro release profiles of biodegradable polymeric microspheres containing protein fabricated by double-emulsion solvent extraction/evaporation method. *Biomaterials* **2001,** 22, (3), 231-241.
24. Guerin, E.; Tchoreloff, P.; Leclerc, B.; Tanguy, D.; Deleuil, M.; Couarraze, G., Rheological characterization of pharmaceutical powders using tap testing, shear cell and mercury porosimeter. *International Journal of Pharmaceutics* **1999,** 189, (1), 91-103.
25. Perez, C.; De Jesus, P.; Griebenow, K., Preservation of lysozyme structure and function upon encapsulation and release from poly(lactic-co-glycolic) acid

microspheres prepared by the water-in-oil-in-water method. *International Journal of Pharmaceutics* **2002,** 248, (1-2), 193-206.

26. Perez, C.; Griebenow, K., Improved activity and stability of lysozyme at the water/CH2Cl2 interface: enzyme unfolding and aggregation and its prevention by polyols. *Journal of Pharmacy and Pharmacology* **2001,** 53, (9), 1217-1226.
27. Zhu, G. Z.; Schwendeman, S. P., Stabilization of proteins encapsulated in cylindrical poly(lactide-co-glycolide) implants: Mechanism of stabilization by basic additives. *Pharmaceutical Research* **2000,** 17, (3), 351-357.
28. Marinina, J.; Shenderova, A.; Mallery, S. R.; Schwendeman, S. P., Stabilization of vinca alkaloids encapsulated in poly(lactide-co-glycolide) microspheres. *Pharmaceutical Research* **2000,** 17, (6), 677-683.
29. Sah, H., Stabilization of proteins against methylene chloride water interface-induced denaturation and aggregation. *Journal of Controlled Release* **1999,** 58, (2), 143-151.
30. Wang, J. Characterization of Microsphere Drug Delivery Systems During Encapsulation and Initial Drug Release. The Ohio State University, Columbus, OH, 2000.

CHAPTER 4

Release of Peptide and Proteins

4.1 Abstract

Here, the *in vitro* release characteristics of protein and peptide loaded poly(lactic-*co*-glycolic acid) (PLGA) microspheres after self-healing microencapsulation was evaluated. Leuprolide acetate, a peptide currently utilized in commercial injectable depots, was released continuously over a period of 60 days. Formulations using $ZnCO_3$ as the blank particle porosigen provided near zero-order release of the peptide after 7 days. Two proteins, bovine serum albumin and lysozyme, were released over a period of 28 days, although release was closer to first order. By incorporating antacids as the porosigens, the amount of insoluble aggregates after 28 days of release was negligible for BSA (< 2%), indicating the absence of highly acidic pH in the polymer. The amount of PLGA-encapsulated lysozyme aggregation after 28 days of release was also decreased from 8.7 ± 0.6% (0.0% $MgCO_3$ w/w) to 4.7 ± 0.2% (4.3% $MgCO_3$), and 3.4 ± 0.1% (11% $MgCO_3$) relative to the initial enzyme loaded. While some formulations after self-healing microencapsulation experienced little or no initial burst, the incorporation of large amounts of antacids in the blank particle preparation or the incorporation of sugar and lysine in the loading solution predictably increased the initial burst of protein-loaded microparticles after self-healing microencapsulation. Higher amounts of protein in the

loading solution also increased the initial burst. In summary, the feasibility of continued release of protein and peptide from particles loading through self-healing microencapsulation was confirmed, and its rate was dependent on both blank particle preparation parameters as well as loading solution content.

4.2 Introduction

In polymer depot systems, for continual dosing over the course of treatment, a sustained release of drug from the depot is necessary. The desired release rate is usually zero-order, with a constant release rate leading to consistent pharmacological effects and easier dosing. In practice however, zero-order release from polymer systems is not always observed. Obtaining an ideal release profile is an important issue in development of injectable poly(lactic-*co*-glycolic acid) (PLGA) microsphere depots [1].

The release of drug from conventional PLGA microspheres frequently can be broken down into three phases: 1) an initial burst from the drug near the polymer surface and deep in the polymer phase before pore closing [2], 2) a lag period of reduced drug release, when the pore network is isolated from the particle surface and polymer degradation has yet to take place, and 3) a period of increased release due to polymer degradation and erosion [3]. In some instances, the initial burst can be retarded or the lag phase is minimal, but in general these 3 phases predominate.

The first phase, a quick bolus called either the burst release or initial burst, is influenced by a number of formulation parameters, including the molecular weight of the polymer, the ratios of the different phases to one another (i.e. inner water phase, dispersed phase, and continuous phase), the preparation temperature, the concentration of polymer solution, the makeup of the continuous phase, the existence of excipients, and

drug loading, among others [4, 5]. Many of these parameters, including polymer molecular weight and concentration, phase ratios, and preparation temperature – alter the rate of phase separation during the solidification process, ultimately affecting the porosity and morphology of the microparticles. As discussed previously, this porosity can ultimately impact the release of drug from the loaded microparticles, particularly during this initial burst release.

The second phase of release, a lag phase of limited drug release, is generally an undesired release characteristic. The previous initial burst, usually a period of hours or at most several days, may not be sufficient to provide a continued pharmacological response [6], and the consequence is a reduced release and pharmacological activity. In order to overcome the lag phase and have a continuous release, the earlier diffusion dominated phase and the later polymer degradation dominated phase must have some overlap [7]. It is recognized that overcoming this lag phase will thus have to be accomplished by either 1) increasing or extending the diffusion controlled release phase, through modification of protein loading or polymer morphology, namely particle size, surface area, and porosity [6] or 2) accelerating commencement of the third release phase, bulk polymer degradation, namely through reduced polymer molecular weight or lactic acid content [8].

The third and final phase of release, polymer degradation, can be modified by altering polymer composition. Microspheres made up of PLGA undergo bulk degradation, where water penetrates into the entire polymer phase, initiating degradation in the bulk polymer [9]. PLGA undergoes degradation via hydrolysis of its ester bonds into lactic and glycolic acids [10, 11]. This hydrolysis is further catalyzed by both acidic

and alkaline conditions [12], meaning in effect that the PLGA degradation acid products, namely the carboxylic acid end groups, further accelerates bulk polymer degradation. Finally, the polymer undergoes erosion where soluble polymer fragments, sometimes not yet completely degraded, are released from the microspheres [13].

Research has shown that the first phase of initial burst release subsides when the surface pores close, separating the internal pore network from the outside environment [1, 2]. Pore opening in the very early part of the initial burst has also been shown to play a likely role [2]. Furthermore, the opening of pores during normal release conditions can be monitored by uptake of fluorescent-dextran pore markers [1]. Thus, it is clear that the initial porosity and state of the surface pores has an impact on the release rate.

We have previously introduced a new method of microencapsulation, self-healing microencapsulation without organic solvents. The purpose of this study was to examine release characteristics of various formulations prepared via self-healing microencapsulation, in order to determine the feasibility of this microencapsulation method to yield dosage forms suitable for controlled drug delivery. For this purpose, a common peptide, leuprolide acetate, and multiple model proteins, bovine serum albumin (BSA) and lysozyme, were self-microencapsulated in PLGA microspheres. For lysozyme, the initial stability was examined as well.

4.3 Materials and Methods

4.3.1 Materials

Several PLGAs were used. PLGA with an i.v. = 0.19 dL/g (50:50, PLGA DL 2M, methyl ester end group, Alkermes Lot No. 1158-515, 19 kD MW) was purchased from

Lakeshore Biomaterials (Birmingham, AL), formerly Alkermes; PLGA with an i.v. = 0.20 dL/g (50:50, Part #B6017-1G, Lot #A07-044) was from Lactel Absorbable Polymers from DURECT Corporation (Cupertino, CA), formerly Birmingham Polymers; PLGA with an i.v. = 0.57 dL/g (50:50, PLGA DL LOW IV, Lot No. W3066-603, lauryl ester end group, 51 kD) was purchased from Lakeshore Biomaterials (Birmingham, AL), formerly Alkermes. α,α-Trehalose dihydrate was purchased from Pfanstiehl (Waukegon, IL), zinc carbonate ($ZnCO_3$) was purchased from ICN Biomedicals Inc. (Aurora, OH), Germany), poly(vinyl alcohol) or PVA (25 kDa, 88% mol hydrolyzed) was purchased from Polysciences, Inc. (Warrington, PA), and Poly(vinyl alcohol) (9-10 kDa, 80% mol hydrolyzed) was purchased from Sigma Aldrich (St. Louis, MO). Magnesium carbonate ($MgCO_3$), Bovine serum albumin (BSA), fraction V, and lysozyme (from chicken egg white) were purchased from Sigma Aldrich (St. Louis, MO). a-Chymotrypsin, from bovine pancreas, Type II was obtained from Sigma Aldrich (St. Louis, MO). Phthaldialdehyde reagent containing 1 mg σ-phthaldialdehyde (P 0657) per mL solution with 2-mercaptoethanol as the sulfhydryl moiety, was obtained from Sigma Aldrich (P0532, St. Louis, MO). Leuprorelin (leuprolide) acetate (Lot No. 071002) was purchased from Shanghai Shnjn Modern Pharmaceutical Technology Co. (Shanghai, China). 7-methoxycoumarin-3-carbonyl azide was purchased from Molecular Probes (Eugene, OR), now Invitrogen (Carlsbad, CA). Coomassie Plus Protein Reagent was purchased from Pierce (Thermo Fisher Scientific, Rockford, IL). All other common salts, reagents, and solvents were purchased from Sigma Aldrich (St. Louis, MO).

HPLC columns used included an SE-HPLC column from Tosoh Biosciences (TSK gel G3000SWxl column or TSK gel G2000SWxl column), an SE guard column

(Shodex, Protein KW-G), C18 column (4 µm Nova-Pak, 3.9 x 150 mm, Waters, Part #WAT086344, Serial #112837351338), and a C18 guard column (Bonda-Pak, C18 Guard-Pak, Waters, 4 µm).

4.3.2 Methods

4.3.2.1 Leuprolide Acetate

4.3.2.1.1 Preparing Particles for Self-healing Microencapsulation

Two hundred µl of inner water phase solution (either 1X PBS, pH 7.4 or trehalose dehydrate solution (500 mg in 1g 1X PBS, pH 7.4) was added to a 5 ml syringe containing 320 mg PLGA (50:50, i.v. = 0.57 dL/g) or 1100 mg PLGA (50:50, i.v. = 0.20 dL/g) in 1 ml of CH_2Cl_2, with or without 10 mg $ZnCO_3$, and immediately homogenized in an ice water bath at 10,000 rpm for 1 min (i.v. = 0.57 dL/g) or 23,000 rpm for 1.5 min (i.v. = 0.20 dL/g) creating the first emulsion. Two ml of 5% PVA (9-10kDa, 80% hydrolyzed) was added and the mixture vortexed for 15 seconds at medium speed, creating the second emulsion and the resulting solution was injected into 100 ml of 0.5% PVA solution under continuous stirring. Microspheres were stirred 3 h at room temperature, and collected with sieves to separate by size and washed thoroughly with dd H_2O to help remove residual PVA, sugar, salt, and solvent. The particles were immediately freeze dried. The sizes collected were 20-63 µm and 63-90 µm fractions.

4.3.2.1.2 Self-healing Microencapsulation and Release

Two ml of 465 mg/ml for encapsulation in PLGA, i.v. = 0.20 dL/g or 127.5 mg/ml for encapsulation in PLGA, i.v. = 0.57 dL/g leuprolide acetate solution (4°C) was

added to approximately 150-200 mg SM-microparticles (20-63 μm) and the microsphere/peptide suspension were incubated at 4°C for 42 h on a rocking platform, and then transferred to an incubator on a rotary shaker (set at 45% power) at 37°C for 7 h (PLGA i.v. = 0.20 dL/g) or 43°C (PLGA i.v. = 0.57 dL/g) for 48 h. Microspheres were removed and washed thoroughly with dd-H_2O, centrifuged at 3,800 rpm for 5 min to collect microspheres after each of 10 washes, and then freeze dried.

Release of peptide was determined via release in PBST (0.02% Tween), pH 7.4. Remaining peptide content in microspheres was determined at specified time points and a release curve was generated. For both loading assay and release, peptide in microspheres were extracted with 1:1 ratio of methylene chloride and 0.1 M sodium acetate buffer (pH 4.5) followed by another extraction with 1M sodium chloride in 0.1M sodium acetate buffer (pH 4.5).

Analysis of leuprolide acetate was accomplished by HPLC, with a gradient of acetonitrile (Solvent A) and 0.05 sodium phosphate buffer, pH 7.0 (Solvent B) on a Nova-Pak C18 4 μm Waters Column. The gradient method was 0 min (20% A), 6 min (30% A), 9.5 min (37% A), 11.5 min (37% A), 16.5 min (50% A), and 19 min (20% A), followed by a 2 min recovery. UV detection was measured at 215 nm, 280 nm, and fluorescence detection was measured using 278 ex. and 350 em.

4.3.2.2 BSA and Lysozyme

4.3.2.2.3 Preparing Particles for Self-healing Microencapsulation

200 μl of inner water phase solution, 1X PBS, pH 7.4 or trehalose dehydrate solution (500 mg in 1g 1X PBS, pH 7.4) was added to a 5 ml syringe 320 mg PLGA (50:50, 0.57 dL/g) containing 1 ml of CH_2Cl_2, and immediately homogenized in an ice

water bath at 17,000 rpm for 1 min creating the first emulsion. Two ml of 5% PVA was added and the mixture homogenized at 6,000 rpm for 20 to 30 seconds, creating the second emulsion and the resulting solution was injected into 100 ml of 0.5% PVA (9-10kDa, 80% hydrolyzed) solution under continuous stirring. Microspheres were stirred for 3 h at room temperature, and collected with sieves to separate by size and washed thoroughly with dd H_2O to help remove residual PVA, sugar, salt, and solvent. The particles were immediately freeze dried. The sizes collected were 20-63 μm and 63-90 μm fractions.

4.3.2.2.4 Self-healing Microencapsulation and Release

SM-microspheres were suspended in concentrated protein solutions (200 – 300 mg/ml) with or without sucrose (0.45 M) at a ratio of approximately 150 mg microspheres per 1 ml of solution. Particles were immersed in solution at 4°C for 16-48 h, and then removed and incubated at 43°C for 48 h. Loaded particles were then washed thoroughly with dd H_2O and immediately freeze dried.

For release of BSA and lysozyme, protein-loaded particles were dispersed in PBST (0.02% Tween), pH 7.4 at 37°C. Release media was removed and replaced at appropriate intervals, and protein in media was quantified.

For analysis of lysozyme and BSA in the polymer, the proteins were extracted from the polymer by first dissolving the microparticles in acetone and dispersing for 1 h, followed by centrifugation at 13,000 rpm for 25 min and the removal of supernatant. This was repeated twice, and the residual solvent was removed via evaporation. The remaining protein was then dissolved in 1X PBST, pH 7.4 for analysis.

For total lysozyme release and loading, a Coomassie protein assay was run, using Coomassie Plus Protein Reagent and measuring the protein solution absorbance at 595 nm. For determination of soluble lysozyme and BSA monomer, the sample was run using SE-HPLC (Tosoh Biosciences TSKgel G3000SWxl) using a guard column (Shodex Protein KW-G), with a mobile phase of 0.05 M potassium phosphate, 0.2M NaCl, pH 7.0 at a flow rate of 0.9 ml/min. The absorbance at 215 and 280 nm were measured.

Insoluble BSA and lysozyme were detected by preparing fresh samples and standards in 6 M Urea, 1mM EDTA, 10 mM DL-Dithiothreitol (Cleland's Reagent) (DTT) in 1X PBST, and after brief vortexing, measuring the protein using Coomassie Plus Protein Reagent as above.

4.3.2.3 Activity of Lysozyme

The activity of the loaded soluble lysozyme was determined as reported previously [14, 15]**.** Briefly, lysozyme was extracted from the microspheres after 28 day release as discussed above, and dissolved in PBST (0.02% Tween), pH 7.4, at approximately 8.5 ug/ml (± 1 ug/ml). Standard solutions were dissolved in the same buffer at the same approximate concentration at the same time.

For analysis, 0.15 ml of soluble protein solution was combined with the same volume of 1.5 mg/ml *Micrococcus lysodeikticus* in 1X PBS, pH 7.4 and the absorbance at 450 nm was monitored every 30 s for a period of 5 min. The activity was calculated using the decrease in absorbance for the linear portion (between 0.5 and 3.0 minutes) assuming one unit of enzyme activity will reduce the $\triangle A_{450nm}$ by 0.001/min. Specific activity is defined in units of activity per mg of protein and is given as % of the specific activity of

the native, standard lysozyme. The actual amount of soluble monomer lysozyme in the solution was determined via SE-HPLC and was used to determine specific activity.

4.4 Results and Discussion

4.4.1 Loading and Release of Leuprolide Acetate

Blank particles were prepared using trehalose dihydrate in 1X PBS, pH 7.4 as the porosigen with lower MW PLGA (i.v. = 0.20 dL/g, free acid). These particles were loaded in 465 μg/ml leuprolide acetate solution and 7h at 37°C was sufficient to close the surface pores (Figure 4.1). However, the loading was somewhat low at 1.26 ± 0.05% (w/w) with a burst release in first 48h of 17.41 ± 1.07%. Only 30% was released over 28d however (Figure 4.2).

Assaying of the 28-d sample provided evidence of another species in the microspheres. After addition of a concentrated solution of sodium chloride, the separate species slowly merged with the leuprolide acetate peak, indicating ion-pairing with the polymer degradation products as opposed to a degradant (Figure 4.3).

To increase the loading, a higher MW PLGA (i.v. = 0.57 dL/g) was used. SM-microparticles were created using both trehalose in PBS, pH 7.4 as well as PBS, pH 7.4 with $ZnCO_3$ as porosigens. Only 7 h after the loading procedure began at 4°C, using 240 mg/ml leuprolide acetate solution, the congealing of the particles was observed in both formulations, so additional water was added bringing the total concentration of leuprolide acetate to 120 mg/ml. After pore closing at 42°C for 48 h, the surface pores appeared to close (Figure 4.4). The loading using this new polymer was significantly higher, at 3.4 ± 0.2% (trehalose) and 2.7 ± 0.2% ($ZnCO_3$). The release of the two formulations were

significantly different however, with a burst release in the first 24 h of 33 ± 2% for the trehalose formulation compared to only 2 ± 4% for the $ZnCO_3$ formulation. Both did however maintain a continuous release over 7 weeks (Figure 4.5).

This experiment was repeated, except the concentration of leuprolide acetate was kept at 120 mg/ml the entire time through the loading process. The particles appeared similar to the previous experiment (Figure 4.6), and the results of the loading were comparable to the earlier experiment, with a loading of 2.62 ± 0.09% (w/w) in the trehalose formulation, and 2.75 ± 0.01% (w/w) in the $ZnCO_3$ formulation. The release curves for the two formulations were similar to one another (Figure 4.7), with initial burst in the first 72 h of 10.8 ± 2.8% for the trehalose formulation and 12.0 ± 1.8% for the $ZnCO_3$ formulation. An increased initial burst of 19.8 ± 2.2% was seen when the two formulations were combined at 50:50 weight ratio. Although the difference may be attributed to experimental error, it is plausible that the release of the separate formulations influenced one another.

It also should be noted that two release curves utilizing trehalose as the porosigen were starkly different (Figure 4.5 and Figure 4.7). This may be due to simple variance in the loading and the pore closing process, or specifically the difference in the initial loading solution concentration. The initial formulation with the much higher burst did have a higher loading (3.4 ± 0.2% versus 2.6 ± 0.1%) which could possibly explain some of the increased burst, due to the phenomenon of pore opening during initial release. Further support for this notion is that it is expected that any solution encapsulated early on the loading process of the formulation utilizing the higher initial peptide concentration would have more concentrated pockets initially.

4.4.2 Loading and Release of BSA

When a low MW PLGA (50:50, 0.19 dL/g) was used and BSA-Coumarin was self-encapsulated, the release curve over 30 days approached zero order (Figure 4.8), although the release remains low at 0.40 ± 0.2% (SEM) of the loaded microparticles, as was seen in the leuprolide acetate encapsulated inside low MW PLGA.

After self-healing microencapsulation of BSA in blank microspheres prepared with differing amounts of $MgCO_3$ used as a porosigen (3.0 and 4.5% w/w), the release in PBST (PBS + 0.02% Tween), pH 7.4 was conducted (Figure 4.9). The formulations studied used either PBS or trehalose in PBS as the inner water phase, 3.0 or 4.5% $MgCO_3$ (w/w), and some preparations were pore-closed with 0.45 M sucrose in the loading solution. Details for the loading and release of these microspheres can be seen in Table 4.1.

Analysis of the remaining protein in the microspheres after 28 d release provided a mass balance of between 108.54 (± 3.11%) and 120.85 (± 2.06%). However, less than 2% of the recovered BSA after 28 d release had aggregated, as determined through SE-HPLC and Coomassie assay.

4.4.3 Loading and Release of Lysozyme

Lysozyme was loaded in PLGA (50:50, i.v. = 0.57 dL/g) using SM-microparticles that were created with differing concentrations of polymer in original solution, i.e., either 280 or 350 mg in 1 ml CH_2Cl_2, and using trehalose in PBS, pH 7.4 as the inner water phase porosigen. The loading for the two formulations was comparable at 2.52 ± 0.28% (280 mg) and 2.87 ± 0.43% (350 mg). The release rates of lysozyme from

these two formulations were distinctly different however, with initial bursts in the first 48 h of 53.8 ± 0.6% (280 mg) and 28.6 ± 1.2% (350 mg) (Figure 4.10).

As reported previously, the release rate of lysozyme is affected by the amount of excipients encapsulated inside. For instance, as the base content increases, the initial burst of lysozyme also increases. As seen in Figure 3.5, the amount released from the microspheres after 28 days was 30.4 ± 0.7% (0% $MgCO_3$), 41.3 ± 0.5% (1.5% $MgCO_3$), 51.0 ± 3.6% (4.3% $MgCO_3$), and 57.1 ± 3.3% (11.0% $MgCO_3$). Increases in base content resulted in increases in the burst release, specifically the amount of lysozyme released in the first 4 days, while all formulations displayed a similar lag period of the release profile from Day 7 to Day 28. The aggregation of lysozyme decreased with increasing base content as well, with the amount of aggregation after 28d of release was 8.7 ± 0.6% (0.0% $MgCO_3$), 6.0 ± 0.2% (1.5% $MgCO_3$), 4.7 ± 0.2% (4.3% $MgCO_3$), and 3.4 ± 0.1% (11% $MgCO_3$) (Figure 3.7).

Changing the inner water phase volume in blank particle manufacture does not appear to have a significant impact on the release rate however (Figure 3.14), and only those particles prepared with the smallest amount of inner water phase produced significant aggregation after self-healing microencapsulation (Figure 3.16). Changing the polymer concentration does have an impact on the release (Figure 3.23), however not in a clear manner. A PLGA concentration of 260 mg in 1 ml CH_2Cl_2 produced the lowest burst, with both lower and higher concentrations giving a higher burst release. The activity in changing the inner water phase volume, where SM-microparticle formulation utilized no base (Figure 3.17) was lower than both changing the base content (Figure 3.8) and changing the polymer concentration (Figure 3.26).

Clearly, the sustained release of lysozyme from microspheres after self-healing microencapsulation is possible. Self-healing microencapsulation of lysozyme can produce loaded microspheres that have minimal initial burst as well. Furthermore, to ensure its biologic activity is retained, acid-neutralizing base also should be encapsulated inside the microparticles.

It should be noted changing these formulation characteristics can produce release curves with a significant initial diffusion-mediated release phase. This initial release extends from Day 0 to approximately Day 14 during lysozyme release (Figures 3.8, 3.17, and 3.26). However, an apparently extensive subsequent lag release phase appears to follow, lasting from approximately Day 14 to sometime after Day 28. The absence of another more rapid release phase suggests that the microspheres have not hit their diffusion-mediated step yet. In other words, the PLGA (i.v. = 0.57 dL/g) has not begun to rapidly degrade after 28 days of release. Similar results with BSA (Figure 4.9) suggest that self-healing microencapsulation utilizing this particular polymer may result in the degradation phase occurring sometime after Day 28. This delay of the degradation phase may only be a factor with proteins, as a near zero-order release was observed with leuprolide (Figure 4.7).

4.4.4 Porosigens, Excipients, and Protein Concentration Affect Burst

When microspheres are prepared with additional excipients in the loading solution, the initial burst release is altered (Figure 4.11). For instance, while the loading is similar for formulations prepared with BSA (223 mg/ml) 2.25 ± 0.02% (w/w) or BSA (206 mg/ml), trehalose (129 mg/ml), and lysine (34 mg/ml) 1.93 ± 0.02% (w/w) in the loading solution, the burst release was dependent on both the amount of blank particle

porosigen as well as the excipients in the loading solution. Clearly, the presence of $MgCO_3$ and/or the use of lysine and trehalose in the loading solution led to a greater release of loaded protein in the first 3 days of release.

Five formulations of microspheres were prepared with different amounts of $MgCO_3$ used in the CH_2Cl_2/polymer phase: 1%, 2.9%, 4.8%, 9.1%, and 13.0% (w/w). The formulation with the lowest amount of base used displayed both the highest loading and lowest initial burst of BSA in the first 43 h of release, and the formulation with the highest amount of base had the highest burst release (Figure 4.12).

When the protein concentration in the loading solution was increased extensively (from 232 to 316 mg/ml), the loading increased only slightly, but the 48 h burst release increased significantly, from 17% (± 7) to 45% (± 3) (Table 4.2).

4.5 Conclusions

Zero order, sustained release of peptides and proteins from PLGA microparticles continues to be an important issue for controlled release products. Here, we evaluated the release of a synthetic nonapeptide, leuprolide acetate, over an *in vitro* release of 60 days, as well as two proteins, BSA and lysozyme, over a period of 30 days. The leuprolide acetate showed near zero-order release after 7 days, whereas the proteins often exhibited more of a first order release. Further mechanistic studies are needed to help optimize protein release kintecs from SM-microparticles

The incorporation of antacids in the blank particle formulation was found to improve the stability of BSA and lysozyme over 28 days of release, as the amount of aggregation of the remaining protein decreased with increasing base content. Furthermore, the incorporation of excipients in blank particle manufacture, as well as in

the loading solution, was found to substantially increase the initial burst after self-healing microencapsulation. Because the surface pores appeared to be closed after self-healing microencapsulation, this is presumably through a pore opening process during the initial period of release, as has been reported by our group previously. These experiments demonstrate the feasibility of the continued release of proteins and peptides after self-healing microencapsulation, with possibly a new strategy for reducing the initial burst phase.

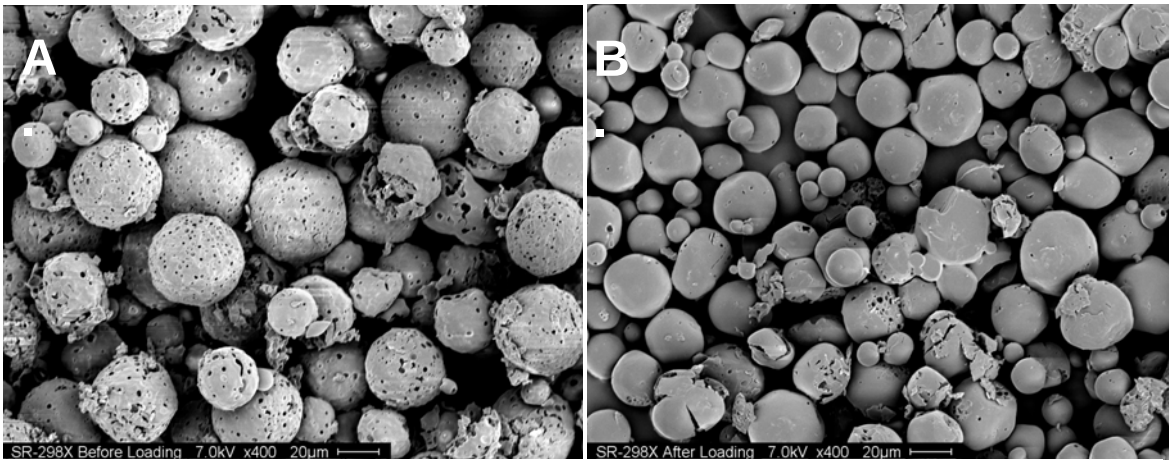

Figure 4.1 Low MW PLGA microspheres before and after self-healing microencapsulation of leuprolide acetate. Blank microspheres (A) of 50:50 PLGA (0.20 dL/g) with free acid end groups were loaded with leuprolide acetate through self-healing encapsulation (B). Loading was at 1.26 ± 0.05% (w/w) with a initial burst of 17.4 ± 1% over the first 48 h of release.

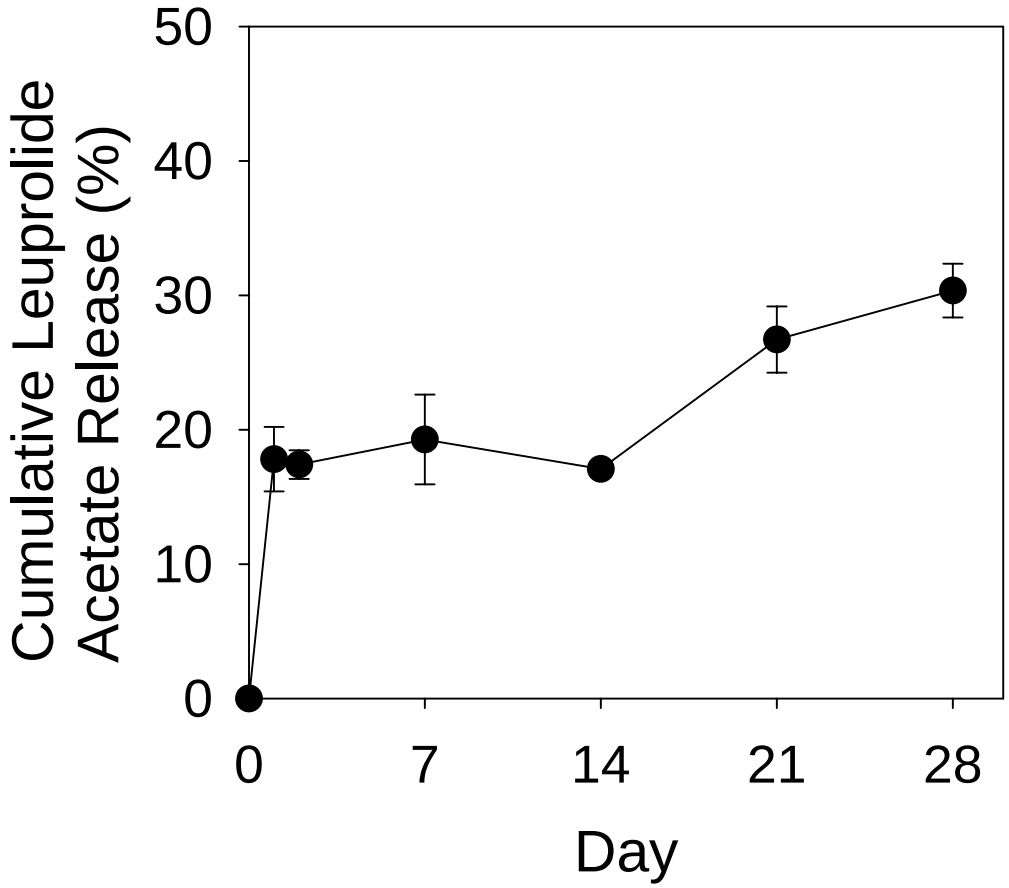

Figure 4.2 Leuprolide acetate release from free acid end group PLGA after self-healing microencapsulation. Leuprolide acetate was loaded via self-healing encapsulation in 0.20 dL/g PLGA at a loading of 1.26 ± 0.05% (w/w).

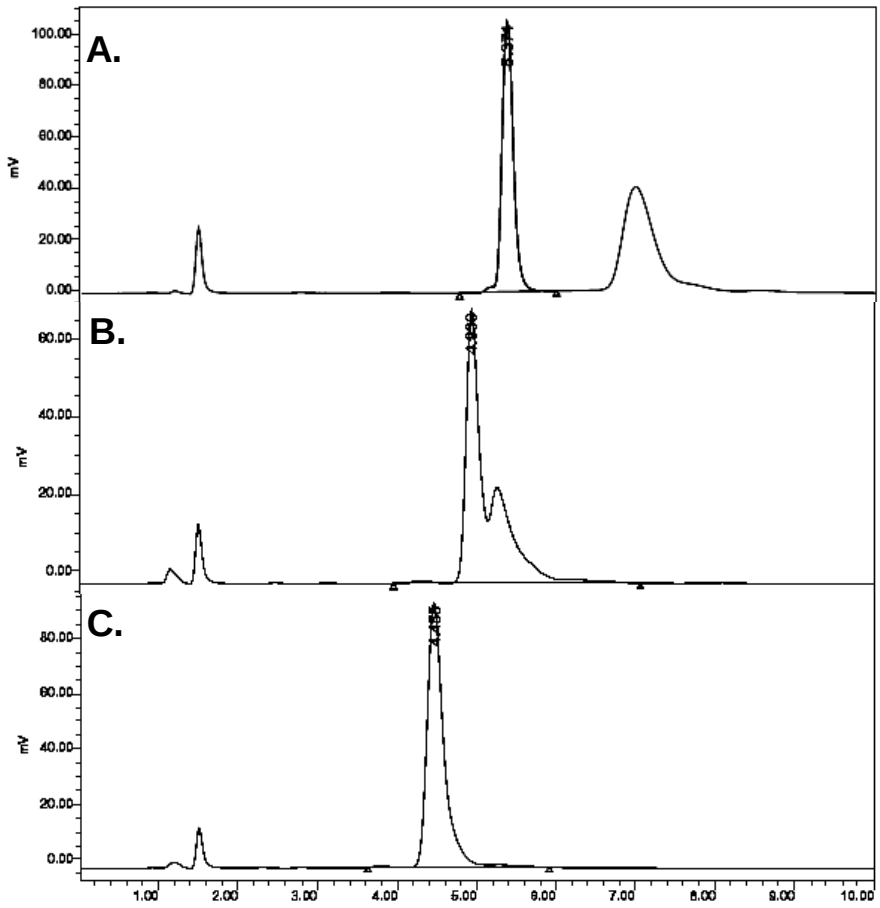

Figure 4.3 Appearance of unidentified peak after 28 d release of leuprolide acetate. Initial extraction of the peptide from the polymer after 28-day release (A) showed two clear peaks that moved closer 10 min after addition of 1M NaCl to the vial (B) and were completely combined 60 minutes after NaCl addition (C).

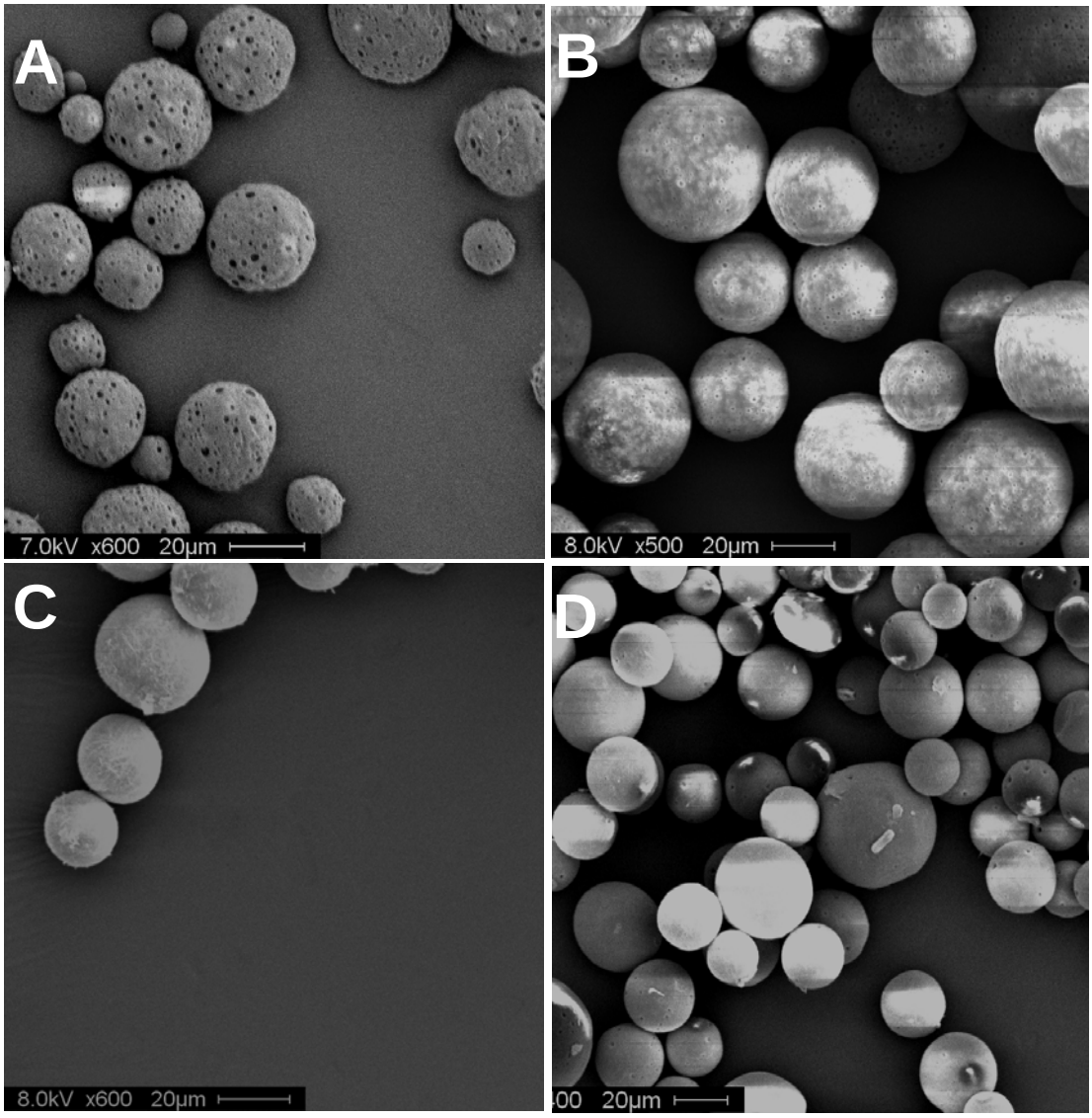

Figure 4.4 Morphology of leuprolide acetate microspheres, before and after encapsulation with additional loading solution to avoid microsphere congealing. PLGA (50:50, 0.57 dL/g) SM-microspheres were made using trehalose (A) or $ZnCO_3$ (B) as the porosigen. Leuprolide acetate solution (240 mg/ml) was loaded and solution dispersed at 4°C for 16 h, before additional water was needed, bringing each concentration to 120 mg/ml. Microspheres were then incubated for an additional 8 h at 4°C, and then pores were closed at 43°C for 48 h for both trehalose (C) and $ZnCO_3$ (D).

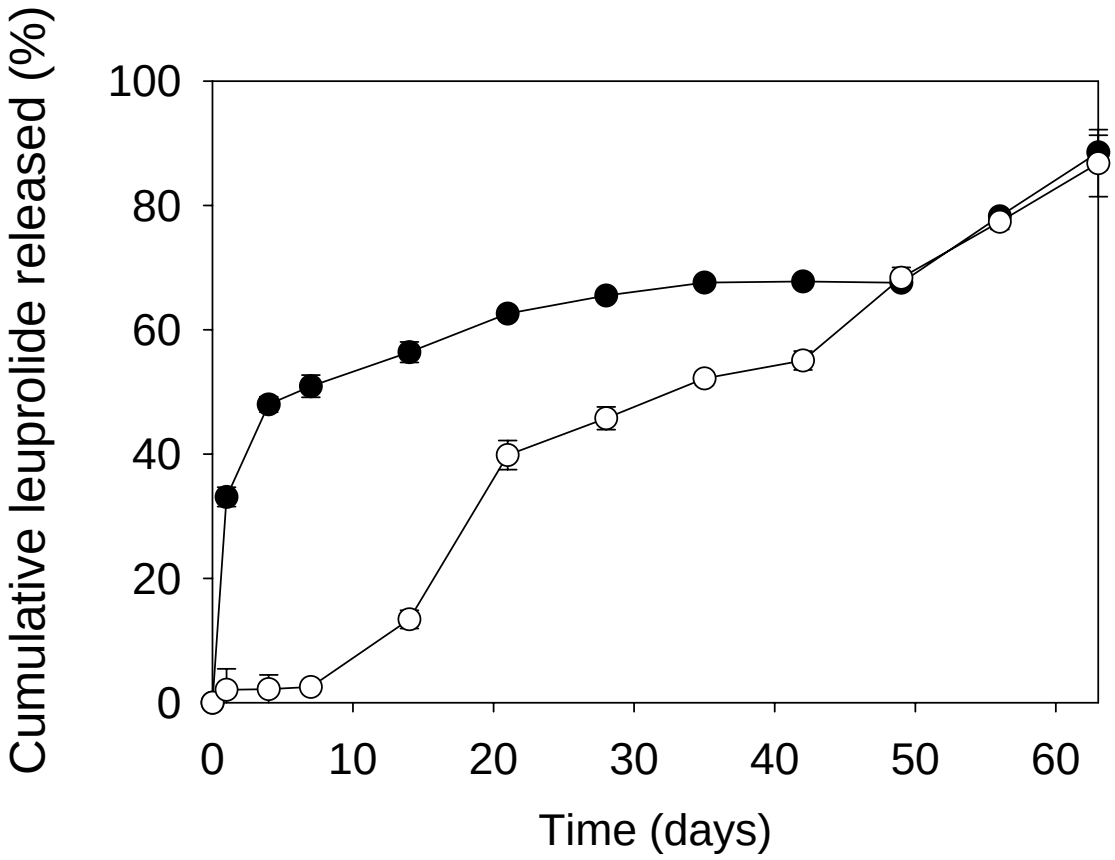

Figure 4.5 Cumulative leuprolide acetate release after self-healing microencapsulation. Leuprolide acetate solution (240 mg/ml) was loaded and solution dispersed at 4°C for 16 h, before additional water was needed, bringing each concentration to 120 mg/ml. Microspheres were then incubated for an additional 8 h at 4°C, and then pores were closed at 43°C for 48 h. Porosigen used for blank porous particles were either trehalose (●, 200 µl of 500 mg trehalose dihydrate in 1g PBS, pH 7.4), or $ZnCO_3$ (○, with 200 µl PBS, pH 7.4).

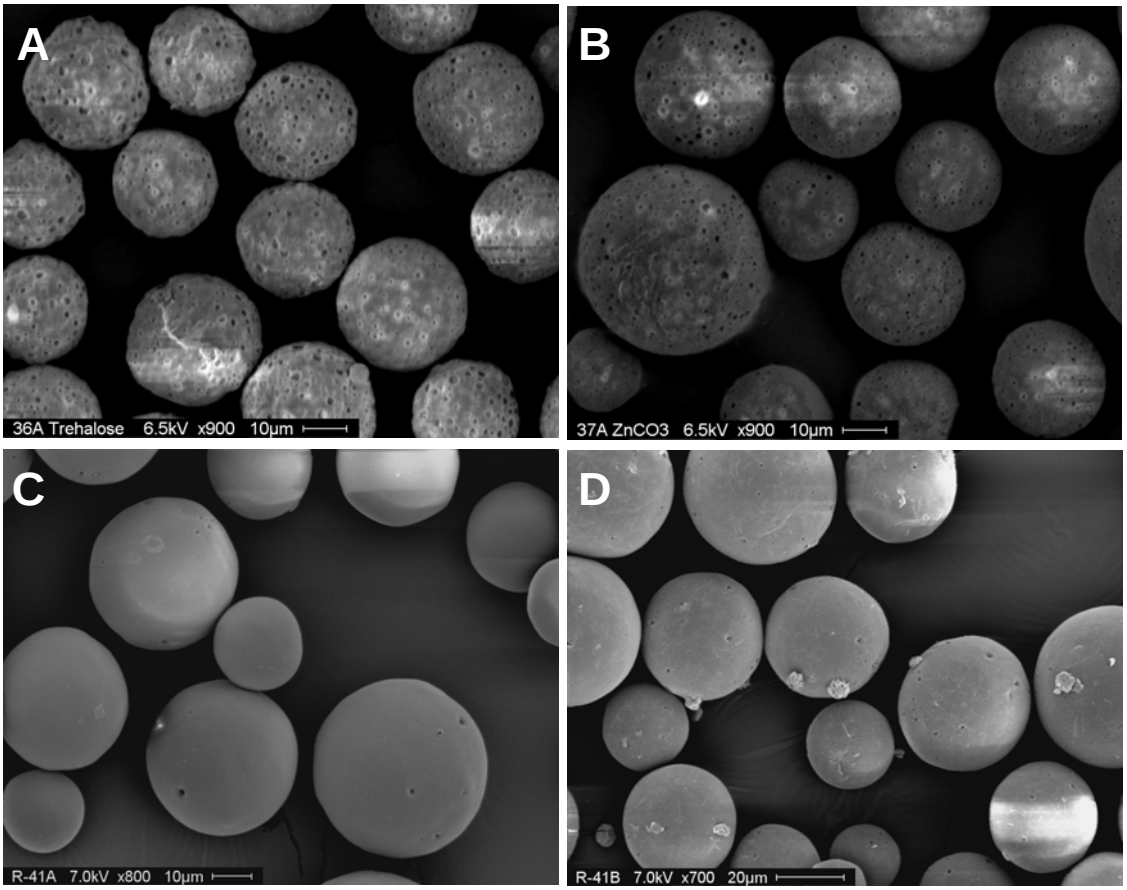

Figure 4.6 Images of leuprolide acetate microspheres, before and after encapsulation. SM-PLGA (50:50, 0.57 dL/g) microspheres were made using trehalose (A) or $ZnCO_3$ (B) as the porosigen. Particles underwent self-healing encapsulation at 4°C for 40 h and 43°C for 48 h for both trehalose (C) and $ZnCO_3$ (D).

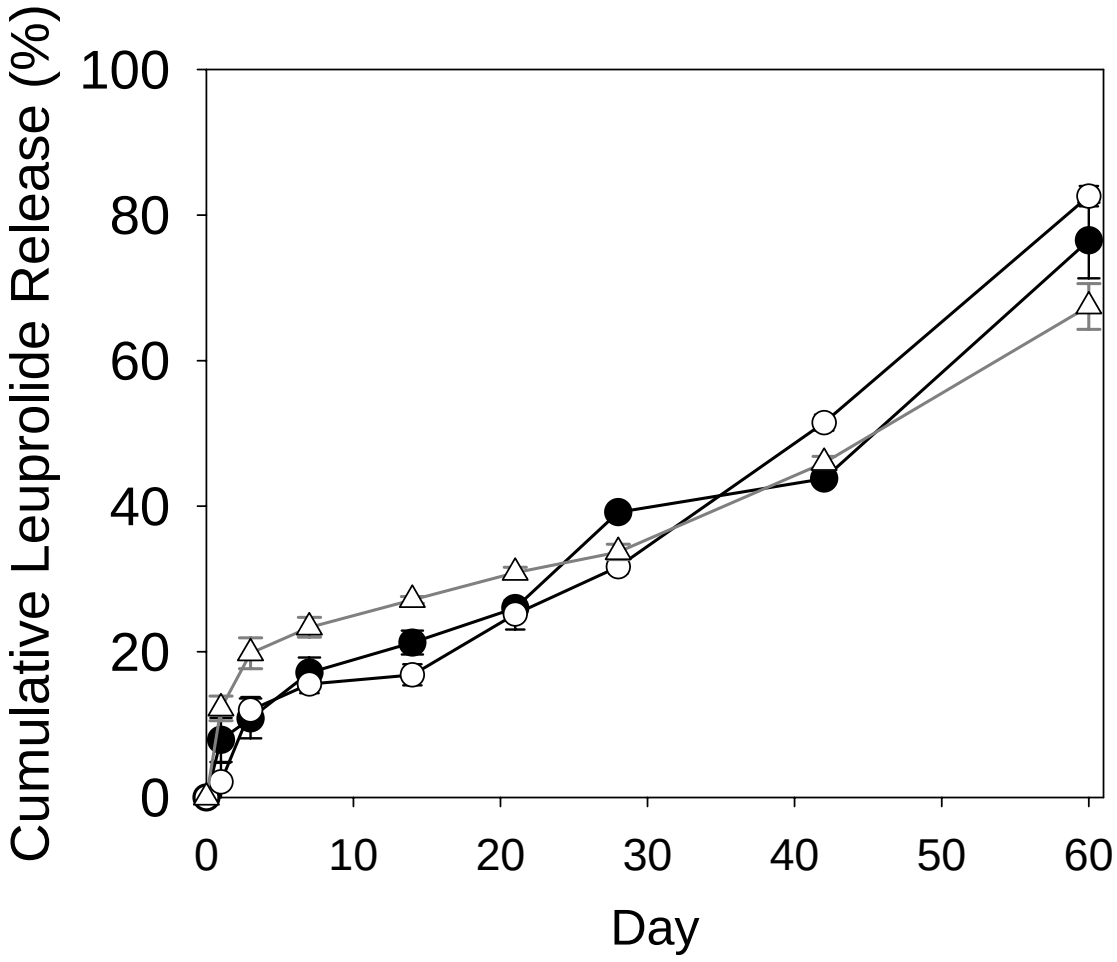

Figure 4.7 Cumulative leuprolide acetate release after self-healing microencapsulation. Leuprolide acetate was loaded from 120 mg/ml peptide 4°C for 40h and 43°C for 48h. Porosigen used for SM-microparticles were either trehalose (●, 200 µl of 500 mg trehalose dihydrate in 1g PBS, pH 7.4), or $ZnCO_3$ (○, with 200 µl PBS, pH 7.4). △: 50:50 weight combination of the other two formulations.

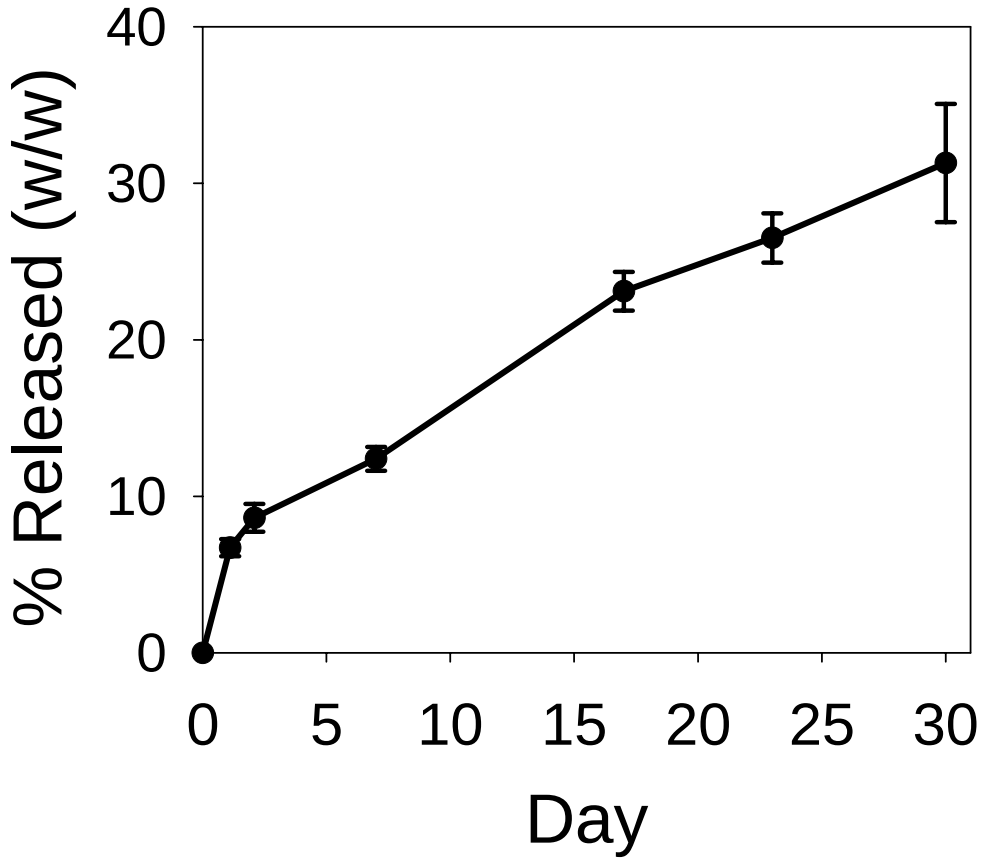

Figure 4.8 30 Day release of BSA-coumarin from 0.19 dL/g microparticles. BSA-coumarin loading was 0.40% (w/w) ± 0.12% (SEM) was released over 30d. Release was in PBST (PBS + 0.02% Tween-80) and was assayed by analyzing release media for monmeric protein by SE-HPLC. N=3.

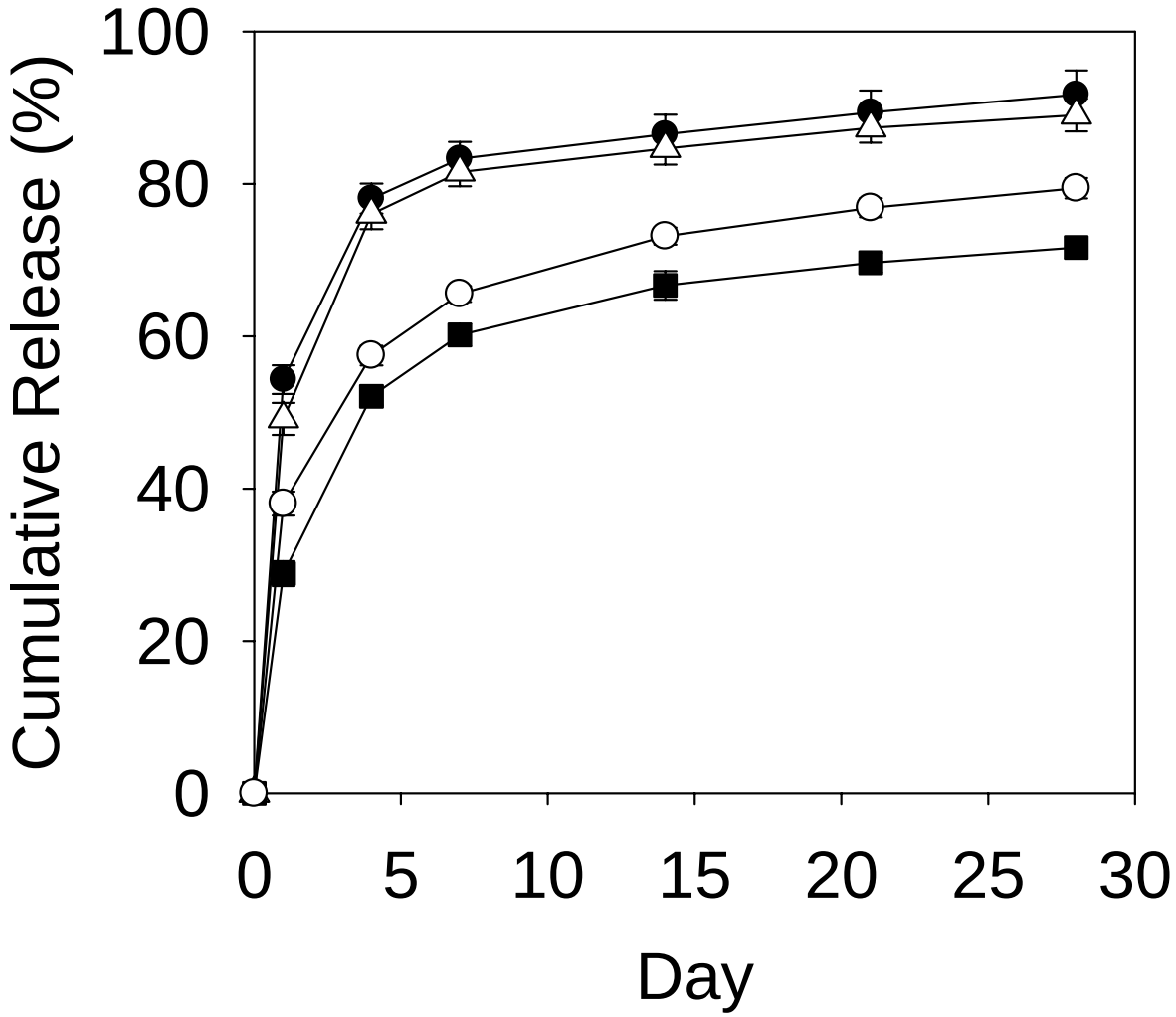

Figure 4.9 Cumulative BSA release after self-healing microencapsulation. BSA was loaded from 250 mg/ml protein solution at 4°C for 16 h and 43°C for 48 h. Porosigen used for SM-microparticles were combinations of PBS, trehalose in PBS, and $MgCO_3$. (●: 200 µl PBS, pH 7.4, 3% $MgCO_3$; △: 200 µl PBS, pH 7.4, 4.5% $MgCO_3$; ■: 200 µl of 500 mg trehalose dihydrate in 1g PBS, pH 7.4, 4.5% $MgCO_3$; ○: 200 µl of 500 mg trehalose dihydrate in 1g PBS, pH 7.4, 4.5% $MgCO_3$ with 0.45 M sucrose in the loading solution). Note burst release dropped when trehalose dihydrate was added to the PBS inner water phase.

Inner Water Phase	$MgCO_3$ (w/w%)	Sucrose in Loading Solution (M)	% Loading (w/w)	Burst Release (24h)
1X PBS (●)	3.0	-	4.25 ± 0.05%	54 ± 2%
1X PBS (△)	4.5	-	5.65 ± 0.06%	49 ± 3%
Trehalose in 1X PBS (■)	4.5	-	7.26 ± 0.09%	29 ± 2%
Trehalose in 1X PBS (○)	4.5	0.45	5.54 ± 0.04%	38 ± 2%

Table 4.1 Results of self-healing microencapsulation of BSA using different parameters. BSA was self-encapsulated in blank PLGA (50:50, 0.57 dL/g) microparticles, and release was conducted in PBST (PBS + 0.02% Tween), pH 7.4.

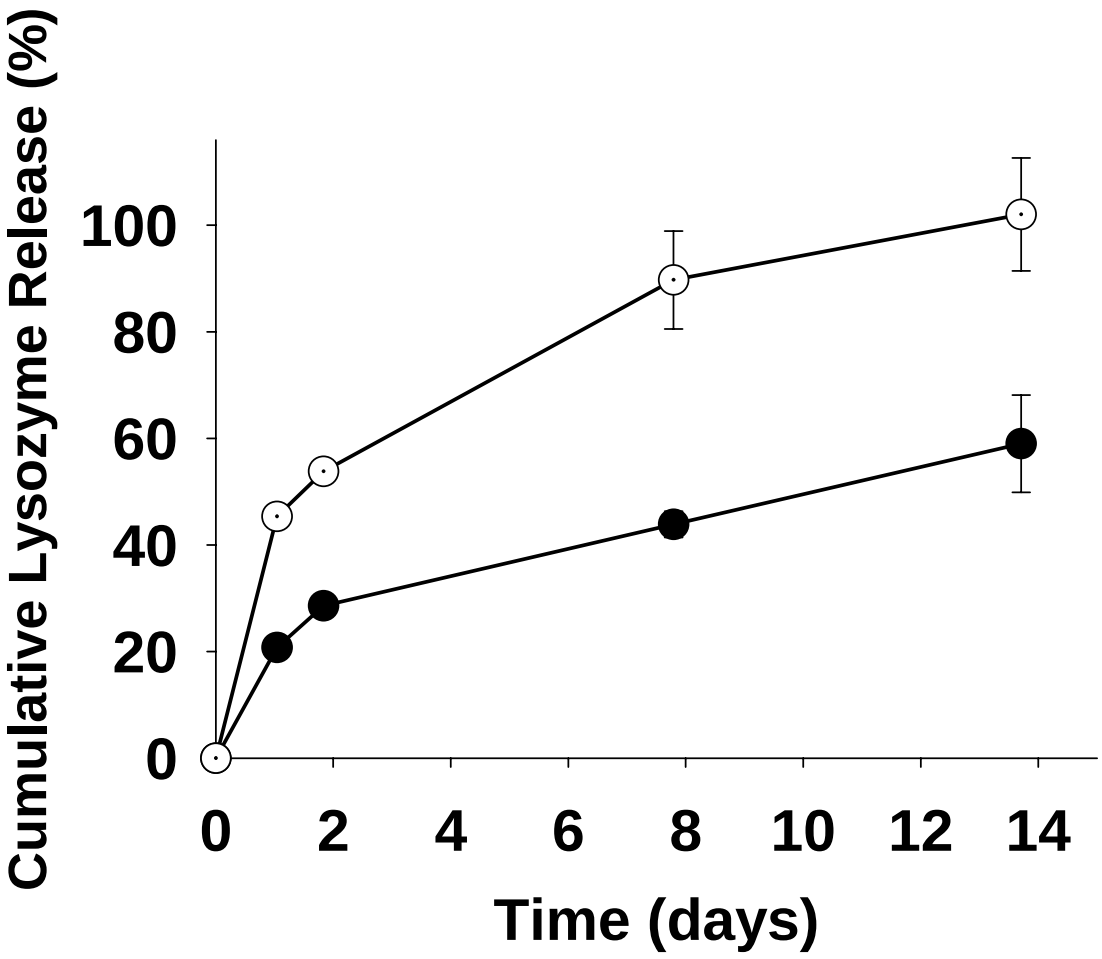

Figure 4.10 Release of lysozyme after self-healing microencapsulation in PLGA over 14 days. Lysozyme was self-encapsulated in PLGA (50:50, 0.57 dL/g), using an initial polymer concentration of 280 mg (○) or 350 mg (●) in 1 ml CH_2Cl_2, with 200 µl of 500 mg trehalose in 1 g PBS, pH 7.4 as the SM-microparticle porosigen. Loading was 2.5 ± 0.3% (280 mg) and 2.9 ± 0.4% (350 mg).

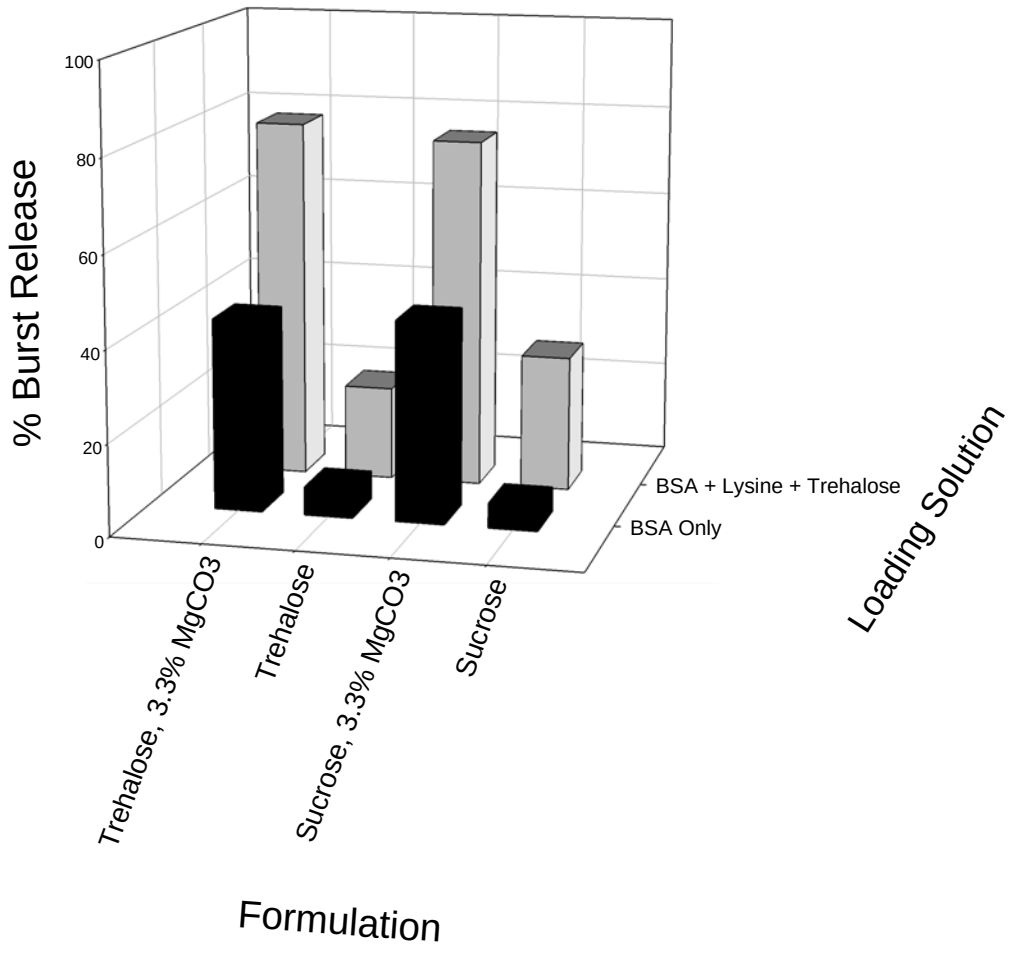

Figure 4.11 Effect of excipients on 48 h initial burst. SM-microparticles were prepared with trehalose or sucrose in the inner water phase (200 µl of 500 mg sugar in 1g 1X PBS, pH 7.4) with or without 3.3% $MgCO_3$ (w/w), and loaded with BSA (223 mg/ml) or BSA (206 mg/ml), trehalose (129 mg/ml), and lysine (34 mg/ml) in solution.

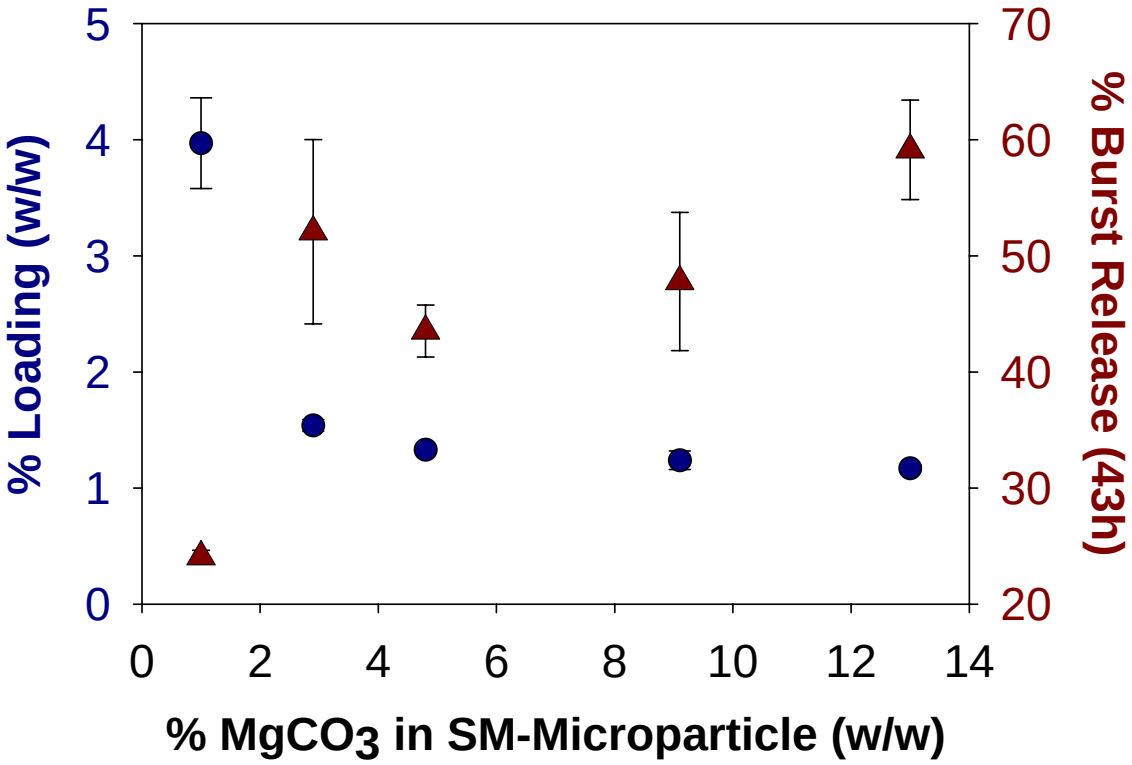

Figure 4.12 Effect of theoretical base content on loading (●) and burst release (▲) in SM-microparticles. Microparticles were prepared using PLGA (50:50, i.v. = 0.57 dL/g) with different amounts of $MgCO_3$ in the organic phase, and the second emulsion was created via vortexing. The lowest amount of base had the highest loading, as well as the lowest burst release.

	Trehalose		Trehalose + 3.0% $MgCO_3$	
	% Loading (w/w)	**% Burst Release**	**% Loading (w/w)**	**% Burst Release**
232 mg/ml BSA Loading Solution	**6.1** (± 0.1)	**16.9** (± 6.7)	**1.8** (± 0.1)	**60.0** (± 0.4)
316 mg/ml BSA Loading Solution	**7.8** (± 0.2)	**45.2** (± 3.0)	**2.7** (± 0.2)	**72.7** (± 3.3)

Table 4.2 Effect of loading solution concentration on loading and burst release for two formulations. When the loading solution concentration is increased from 232 mg/ml BSA to 316 mg/ml BSA for two formulations, A) Trehalose as the lone porosigen and B) trehalose and 3.0% $MgCO_3$ w/w as the porosigens the loading increased from 6.1% w/w to 7.8% w/w, and 1.8% w/w and 2.7% w/w, respectively. Additionally, the burst release (BSA released in the first 48 hours) also substantially increases with the increased loading solution concentrations. Calculated error is standard error of the mean, N=3.

4.6 References

1. Kang, J. C.; Schwendeman, S. P., Pore closing and opening in biodegradable polymers and their effect on the controlled release of proteins. *Molecular Pharmaceutics* **2007,** 4, (1), 104-118.
2. Wang, J.; Wang, B. A.; Schwendeman, S. P., Characterization of the initial burst release of a model peptide from poly(D,L-lactide-co-glycolide) microspheres. *Journal of Controlled Release* **2002,** 82, (2-3), 289-307.
3. Faisant, N.; Siepmann, J.; Benoit, J. P., PLGA-based microparticles: elucidation of mechanisms and a new, simple mathematical model quantifying drug release. *European Journal of Pharmaceutical Sciences* **2002,** 15, (4), 355-366.
4. Yeo, Y.; Park, K. N., Control of encapsulation efficiency and initial burst in polymeric microparticle systems. *Archives of Pharmacal Research* **2004,** 27, (1), 1-12.
5. Freiberg, S.; Zhu, X. X., Polymer microspheres for controlled drug release. *International Journal of Pharmaceutics* **2004,** 282, (1-2), 1-18.
6. Ravivarapu, H. B.; Lee, H.; DeLuca, P. P., Enhancing initial release of peptide from poly(d,l-lactide-co-glycolide) (PLGA) microspheres by addition of a porosigen and increasing drug load. *Pharmaceutical Development and Technology* **2000,** 5, (2), 287-296.
7. Dunne, M.; Corrigan, O. I.; Ramtoola, Z., Influence of particle size and dissolution conditions on the degradation properties of polylactide-co-glycolide particles. *Biomaterials* **2000,** 21, (16), 1659-1668.
8. Ravivarapu, H. B.; Burton, K.; DeLuca, P. P., Polymer and microsphere blending to alter the release of a peptide from PLGA microspheres. *European Journal of Pharmaceutics and Biopharmaceutics* **2000,** 50, (2), 263-270.
9. von Burkersroda, F.; Goepferich, A. M. In *An approach to classify degradable polymers*, Symposium on Biomedical Materials-Drug Delivery, Implants and Tissue Engineering, Boston, Ma, Nov 30-Dec 01, 1998; Neenan, T.; Marcolongo, M.; Valentini, R. F., Eds. Materials Research Society: Boston, Ma, 1998; pp 17-22.
10. Athanasiou, K. A.; Niederauer, G. G.; Agrawal, C. M., Sterilization, toxicity, biocompatibility and clinical applications of polylactic acid polyglycolic acid copolymers. *Biomaterials* **1996,** 17, (2), 93-102.
11. Reed, A. M.; Gilding, D. K., Biodegradable polymers for use in surgery -- poly(glycolic)/poly(Iactic acid) homo and copolymers: 2. In vitro degradation. *Polymer* **1981,** 22, (4), 494-498.
12. Belbella, A.; Vauthier, C.; Fessi, H.; Devissaguet, J.-P.; Puisieux, F., In vitro degradation of nanospheres from poly(D,L-lactides) of different molecular weights and polydispersities. *International Journal of Pharmaceutics* **1996,** 129, (1-2), 95-102.
13. Catiker, E.; Gumusderelioglu, M.; Guner, A., Degradation of PLA, PLGA homo- and copolymers in the presence of serum albumin: a spectroscopic investigation. *Polymer International* **2000,** 49, (7), 728-734.
14. Perez, C.; De Jesus, P.; Griebenow, K., Preservation of lysozyme structure and function upon encapsulation and release from poly(lactic-co-glycolic) acid

microspheres prepared by the water-in-oil-in-water method. *International Journal of Pharmaceutics* **2002,** 248, (1-2), 193-206.

15. Perez, C.; Griebenow, K., Improved activity and stability of lysozyme at the water/CH2Cl2 interface: enzyme unfolding and aggregation and its prevention by polyols. *Journal of Pharmacy and Pharmacology* **2001,** 53, (9), 1217-1226.

CHAPTER 5

Improved Protein Stability

5.1 Abstract

Traditional w/o/w encapsulation techniques to create protein loaded biodegradable microparticles involve a number of manufacturing stresses that can damage the protein. A new method of encapsulation, termed 'self-healing microencapsulation' may circumvent many of these problems by loading the protein after particle manufacture. To test this concept, protein-loaded PLGA microspheres were prepared both via a traditional w/o/w emulsion encapsulation technique and self-healing microencapsulation and examined for stability after encapsulation and controlled release. For self-healing microencapsulation, blank porous microspheres were created and first dispersed in concentrated solutions of lysozyme and α-chymotrypsin (250 mg/ml), with or without 0.45M sucrose as a protein stabilizer, at 4°C, a $T < T_g$ of the polymer, and then the pores were closed by raising the temperature to above the T_g of the polymer, 37 – 42°C, before washing and lyophilization. Protein loading was quantified by amino acid analysis after acid hydrolysis, and soluble and insoluble protein aggregation were determined via both SE-HPLC and amino acid analysis. The specific activity of both loaded enzymes was determined by using established methods. Analysis of loaded

lysozyme in traditional w/o/w (water-in-oil-in-water) microspheres (0.57 dL/g) indicated 12.4 ± 1.1 % (mean ± sem) of loaded protein formed insoluble aggregates, compared to 8.0 ± 2.2 % for self-healing microencapsulation, and < 3% for self-healing microencapsulation formulations utilizing sucrose in the loading solution. Specific activity of loaded α-chymotrypsin was also substantially improved via self-healing microencapsulation compared to w/o/w microspheres, where the self-encapsulated α-chymotrypsin had a specific activity of 54.02 ± 4.51% versus 15.79 ± 2.34% for the traditionally encapsulated protein. Self-encapsulated protein exhibited excellent stability relative to protein loaded by the traditional w/o/w emulsion-based method. Additionally, it was possible to encapsulate large amounts of stabilizers with the protein via the self-healing microencapsulation loading solution.

5.2 Introduction

Proteins can be encapsulated into polymer microparticles numerous ways, including spray drying, emulsion, and coacervation. Perhaps the most popular method is that of an emulsion based technique, in which the protein is dispersed throughout the liquid polymer/organic solvent solution, and after solvent removal, hardened polymer particles with drug encapsulated inside remain. However during the manufacturing process of these microparticles, the protein is exposed to a number of stresses that can damage it. Many of these stresses include an organic solvent/aqueous interface [1], shear forces, an air/liquid interface [2], organic solvent denaturant dissolved in the aqueous protein phase, and elevated temperatures.

The mere presence of an organic solvent can damage a protein [3]. However, its instability with organic solvents is amplified by the subsequent organic/aqueous interface

that is created during the emulsion process, which can further destabilize the protein [1, 4-7]. At this interface, the protein will be in contact with both water and the hydrophobic solvent, increasing its conformational mobility and possibly leading to unfolding and subsequent aggregation [8].

Shear and the existence of the air-liquid interface, particularly in combination with one another, can also be detrimental to proteins [2, 9]. Furthermore, the required addition of energy to create the emulsion, either through homogenization or ultrasonication, can increase local temperatures and harm the integrity of these sensitive molecules [10].

When one such protein, lysozyme, is encapsulated in PLGA microspheres, the result is a substantial loss in activity and an increase in aggregation [11], that has been found to be a direct result of the emulsification step [12] and exposure to the water/organic solvent interface [13]. This aggregation has been described as predominantly non-covalent [13, 14]. As is commonly known for proteins [15], this aggregation and subsequent loss in activity is improved when lysozyme is encapsulated with sugar, particularly lactulose [11], as well as the inclusion of surface-active additives, such as bovine serum albumin and partially hydrolyzed polyvinyl alcohol [14]. The lysozyme encapsulated in the microparticles that remains soluble is usually completely intact and enzymatically active [14, 16].

Another protein that has been studied for stability during microencapsulation is α-chymotrypsin, partly because of its measurable activity and its unfolding is irreversible [17]. The aggregation and activity of α-chymotrypsin during traditional emulsion encapsulation techniques was found to be dependent on inner water phase volume as well

as the type of organic solvent used, with hydrophilic solvents more detrimental to physical instability [18]. Even the mere exposure of some solvents to α-chymotrypsin was enough to lower the enzyme activity of α-chymotrypsin [18], which was particularly sizeable when methylene chloride was used [6], and improved activity was observed with quicker solvent removal from the microparticles [18]. In fact, the formation of as much as 35% non-covalent aggregates was observed after traditional w/o/w encapsulation [6]. This aggregation was found to be mainly caused by the first w/o emulsification step, although subsequent encapsulation steps also played a role [6]. This inactivity and aggregation was also decreased through the inclusion of a sugar, maltose, in the aqueous phase [6].

Thus, both lysozyme and α-chymotrypsin have stability issues during microencapsulation via emulsion methods. We have previously confirmed that it is possible to encapsulate biomacromolecules in self-microencapsulating (SM)-microparticles after particle manufacture, without exposing them to the emulsion process. These biomacromolecules are thus not exposed to any of the normal manufacturing stresses, including organic solvents and shear forces. In order to evaluate any actual improvement over traditional methods, α-chymotrypsin and lysozyme were both encapsulated via self-healing microencapsulation and a traditional w/o/w emulsion method, and the amount of aggregation and activity of the proteins encapsulated via both methods were compared.

5.3 Materials and Methods

5.3.1 Materials

Several PLGAs were used. PLGA with an i.v. = 0.20 dL/g (50:50, Part #B6017-1G, Lot #A07-044) was from Lactel Absorbable Polymers from DURECT Corporation (Cupertino, CA), formerly Birmingham Polymers; PLGA with an i.v. = 0.57 dL/g (50:50, PLGA DL LOW IV, Lot No. W3066-603, lauryl ester end group, 51 kD) was purchased from Lakeshore Biomaterials (Birmingham, AL), formerly Alkermes. α,α-Trehalose dihydrate was purchased from Pfanstiehl (Waukegon, IL), zinc carbonate ($ZnCO_3$) was purchased from ICN Biomedicals Inc. (Aurora, OH), poly(vinyl alcohol) (PVA) (9-10 kDa, 80% mol hydrolyzed) was purchased from Sigma Aldrich (St. Louis, MO). Magnesium carbonate ($MgCO_3$), Bovine serum albumin (BSA), fraction V, and lysozyme (from chicken egg white) were purchased from Sigma Aldrich (St. Louis, MO). a-Chymotrypsin, from bovine pancreas, Type II was obtained from Sigma Aldrich (St. Louis, MO). Phthaldialdehyde reagent containing 1 mg σ-phthaldialdehyde (P 0657) per mL solution with 2-mercaptoethanol as the sulfhydryl moiety, was obtained from Sigma Aldrich (P0532, St. Louis, MO). Coomassie Plus Protein Reagent was purchased from Pierce (Thermo Fisher Scientific, Rockford, IL). All other common salts, reagents, and solvents were purchased from Sigma Aldrich (St. Louis, MO).

HPLC columns used included an SE-HPLC column from Tosoh Biosciences (TSK gel G3000SWxl column or TSK gel G2000SWxl column), an SE guard column (Shodex, Protein KW-G), C18 column (4 μm Nova-Pak, 3.9 x 150 mm, Waters, Part

#WAT086344, Serial #112837351338), and a C18 guard column (Bonda-Pak, C18 Guard-Pak, Waters, 4 μm).

5.3.2 Methods

5.3.2.1 Preparing Traditional w/o/w Formulations

110 μl of 200 mg/ml protein (either α-chymotrypsin or lysozyme) in water was added to 320 mg PLGA (50:50, i.v. = 0.57) in 1 ml CH_2Cl_2 and immediately homogenized in a syringe at 20,000 rpm for 1.5 minutes, creating the first emulsion. 2 ml of 5% PVA was immediately added to the tube and the mixture was then homogenized for 45 seconds at 6,000 rpm and the resultant emulsion was injected into 100 ml of 0.5% PVA under continuous stirring. Microspheres were stirred 3 h at room temperature, and collected with sieves to separate by size and washed thoroughly with dd water to help remove residual PVA, protein, and solvent. The sizes collected were 20-63 μm and 63-90 μm fractions.

5.3.2.2 Preparing SM-Microspheres

5.3.2.2.1 Creating and Loading SM-Microparticles using PLGA (i.v. = 0.20 dL/g)

Trehalose dehydrate solution (175 μl of 500 mg in 1g PBS, pH 7.4) was added to a 10 ml syringe containing 1100 mg PLGA (50:50, 0.20 dL/g) in 1 ml of CH_2Cl_2 and immediately homogenized in an ice water bath at 20,000 rpm for 1.5 min to create the first emulsion. Two ml of 5% PVA was added and the mixture homogenized at 6,000 rpm for 45 s, and the resulting emulsion was injected into 100 ml of 0.5% PVA solution

under continuous stirring. Microspheres were stirred 3 h at room temperature, and collected with sieves to separate by size and washed thoroughly with dd H_2O to help remove residual PVA, sugar, salt, and solvent. The sizes collected were 20-63 μm and 63-90 μm fractions.

To load and microencapsulate the enzymes, 1 ml of 200 mg/ml lysozyme or α-chymotrypsin (with or without 0.45M sucrose) chilled solution (4°C) was added to approximately 200 mg of 20-63 μm blank particles and the microsphere/protein solutions were incubated at 4°C for 24 h on a rocking platform, and then transferred to a 37°C incubator on a rotary shaker (set at 15% speed) for 12 h. Microspheres were removed and washed thoroughly with dd H_2O, centrifuging at 3,000 rpm for 8 min to collect spheres after each of 10 washes, then freeze dried.

5.3.2.2.2 Creating and Loading SM-Microparticles using PLGA (i.v. = 0.57 dL/g)

To prepare SM-microparticles with PLGA (50:50, 0.57 dL/g), the same procedure as in 4.3.2.2.1 was used except that 320 mg PLGA was used instead of 1100 mg of PLGA. To load and microencapsulate the enzymes in SM-PLGA (i.v. = 0.57 dL/g) microparticles, the same procedure was used as in 4.3.2.2.1 except that the following conditions were substituted: a) 1.4 ml of enzyme solution was incubated in 225 mg SM-microparticles and b) microencapsulation was performed at 40.5°C for 40h.

5.3.2.3 Determination of Loading

5.3.2.3.3 Soluble Monomer

For determination of soluble lysozyme and α-chymotrypsin, lysozyme-containing microspheres were dissolved in acetone and α-chymotrypsin-containing microspheres were dissolved in ethyl acetate, both appropriate solvents [19, 20] to separate protein from polymer. Particles were dispersed for 1 h, centrifuged at 13,000 rpm for 25 min and the supernatant removed. This was repeated twice, and the residual solvent was removed via concentrator. The remaining protein was then dissolved in 10 mM potassium phosphate buffer, pH 7.0, with the amount of solution added recorded by weight.

To quantify the protein, the protein was run on an SE column (Tosoh Biosciences TSKgel G3000SWxl) with a guard column (Shodex Protein KW-G). The mobile phase for both proteins was 0.05 M potassium phosphate, 0.2 M NaCl, pH 7.0 at an isocratic flow rate of 0.9 ml/min. The absorbance at 215 and 280 nm was measured, along with the fluorescence (excitation at 278 nm; emission at 350 nm), and all three measurements had strong agreement with each other.

The α-chymotrypsin was unable to be quantified due to its very broad peaks, but the lysozyme, with a retention time of approximately 16 minutes, was quantified via this method.

5.3.2.3.4 Amino Acid Analysis (AAA)

To determine the total content of both α-chymotrypsin and lysozyme in the microparticles as well as the soluble protein in the samples prepared for SE-HPLC, microparticles (approximately 4 mg), soluble protein solutions and standards were weighed into clear glass ampules in a total volume of 1.5 ml 6 N HCl. Ampules were sealed under light vacuum, and incubated at 110°C for 25 h. Following incubation, each vial was completely emptied into microcentrifuge tubes, and the solution was evaporated

under vacuum at room temperature. Approximately 1 ml of 1.0 M sodium bicarbonate buffer, pH 9.5 was weighed into each tube to neutralize the remaining acid.

For individual amino acid analysis, a weighed amount of 350 µl of hydrolyzed protein solution and 350 µl of o-phthaldialdehyde reagent solution (density, ρ, experimentally calculated to be 1.026 mg/ml) were combined in a microcentrifuge tube, vortexed for 15 seconds, and immediately injected onto a C18 column fitted with a guard column (total time from mixing to injection < 1 min), using a previously reported HPLC method for amino acid analysis with o-phthaldialdehyde reagent [21-23]. Each sample had a run time of 50 min, with a mobile phase at 1.4 ml/min of A) methanol-water (65:35) and B) methanol-THF-50 mM phosphoric acid (titrated to pH 7.5 with 10 N NaOH (20:20:960). Conditions for the run were 40% A for 0.5 min, 17 min concave gradient to 50% A, 15 min linear gradient to 100% A, 5 min isocratic elution with 100% A, 7.5 min linear gradient to 40% A, and isocratic 40% A for 5 min. Pressure centered around 3800 psi during the run. The fluorescence was measured (excitation at 350 nm; emission at 455 nm). Protein and standards were quantified using the average of the 3 individual amino acids alanine, phenylalanine, and lysine.

5.3.2.4 Activity of α-Chymotrypsin

The activity of the loaded soluble α-chymotrypsin was determined as reported previously [6, 20, 24]. Briefly, lysozyme was freshly extracted from the microspheres following the procedure used above for soluble protein determination. After extraction, the protein was dissolved in 0.1 M Tris-HCl, 0.01M $CaCl_2$ buffer, pH 7.8. Insoluble protein was separated by spinning tubes at 10,000 rpm for 10 min. (Actual amounts of soluble α-chymotrypsin in the buffer were determined via AAA as above, and were

between 0.84 and 0.97 μg/ml.) The substrate, 0.35 mM of succinyl-Ala-Ala-Pro-Phe-ρ-nitroanilide was dissolved in identical buffer. One hundred fifty ml of substrate solution was added to the same volume of protein solution, and the time-dependent change in absorbance at 405 nm was measured over a period of 10 min. A standard curve of the product of the reaction, ρ-nitroanilide, was also created for determination of the amount of product formed. Specific activity is defined as the rate of substrate converstion (mM/min/mg protein) and is given as a % of the specific activity of the native, standard α-chymotrypsin. For the specific activity determination, the actual amount of soluble α-chymotrypsin in the solution was determined through a separate amino acid analysis.

5.3.2.5 Activity of Lysozyme

The activity of the loaded soluble lysozyme was determined as reported previously [11, 13]. Briefly, lysozyme was freshly extracted from the microspheres following the procedure used above for soluble protein determination. The lysozyme was dissolved in 75 mM potassium phosphate buffer, pH 6.2 at a concentration of approximately 8.5 ± 1 μg/ml. Fresh standard solutions were also dissolved in the same buffer at the same approximate concentration, though actual concentrations were noted.

One hundred fifty ml of soluble protein solution was combined with the same volume of 1.5 mg/ml *Micrococcus lysodeikticus* in identical buffer and the absorbance at 450 nm was monitored every 30 s for a period of 10 min. The activity was calculated using the decrease in absorbance for the linear portion (between 0.5 and 2.5 min) assuming one unit of enzyme activity will reduce the $\triangle A_{450nm}$ by 0.001/min. Specific activity is defined in units of activity per mg of protein and is given as % of the specific activity of the native, standard lysozyme. For the specific activity determination, the

actual amount of soluble lysozyme in the solution was determined through a separate amino acid analysis.

5.4 Results and Discussion

5.4.1 α-Chymotrypsin Loading and Aggregation

In order to determine the difference in integrity and aggregation of the loaded α-chymotrypsin encapsulated via self-healing microencapsulation versus a traditional w/o/w encapsulation technique, soluble α-chymotrypsin extracted from both preparations was examined by SE-HPLC in PBS, pH 7.4. The chromatograms were unquantifiable, probably due to autolysis (Figure 5.1) as has been previously reported [17] and thus measurement of soluble α-chymotrypsin at neutral pH was achieved through amino acid analysis.

Both the soluble and insoluble α-chymotrypsin loading determined by AAA is displayed in Figure 5.2. The highest loadings were achieved through self-healing microencapsulation utilizing PLGA (i.v. = 0.57 dL/g), with or without sucrose at 4.52 ± 0.09% and 7.90 ± 0.30%, respectively. The loading for the traditional w/o/w emulsion techniques were 1.00 ± 0.01% and 3.69 ± 0.06%, with or without sucrose. Self-healing microencapsulation utilizing a lower MW PLGA led to lower loading, with or without sucrose at 1.21 ± 0.06% and 1.50 ± 0.01% respectively. Insoluble protein was less than 20% of the loading for all formulations except for the traditional w/o/w encapsulation that utilized sucrose (Figure 5.3).

Clearly then, the self-healing microencapsulation does not offer a definitive advantage over the traditional w/o/w encapsulation in terms of insoluble aggregation with

α-chymotrypsin. However, when viewing the SE-HPLC chromatograms, the traditional w/o/w encapsulation did indeed affect the integrity of the loaded α-chymotrypsin, as the lower MW fragments (longer retention times) appeared different from protein traditionally encapsulated. In fact, it has been previously reported that α-chymotrypsin is capable of undergoing autocatalysis [25]. Thus, even though there is less insoluble α-chymotrypsin in the traditional w/o/w encapsulation, perhaps the protein that was encapsulated may have been inactivated through autocatalysis, leading to the aforementioned increase in the lower MW fragments on the SE-HPLC chromatograms. The simplest way to determine the effect of the encapsulation methods on the biological activity of the soluble α-chymotrypsin is by enzyme assay.

5.4.2 α-Chymotrypsin Activity

The specific activity of freshly extracted soluble α-chymotrypsin was determined by its ability to convert succinyl-Ala-Ala-Pro-Phe-ρ-nitroanilide into ρ-nitroanilide. The specific activity was determined for α-chymotrypsin that had been self-encapsulated in both low MW PLGA (i.v. = 0.20 dL/g) and medium MW PLGA (i.v. = 0.57 dL/g) with sucrose in the loading solution as well as traditionally encapsulated in PLGA (i.v. = 0.57 dL/g).

As evident in Figure 5.4, the self-encapsulated α-chymotrypsin had a significantly higher specific activity compared to α-chymotrypsin that had been encapsulated via traditional methods. In fact, for the same PLGA (i.v. = 0.57 dL/g), the self-encapsulated α-chymotrypsin had a specific activity of 54 ± 5% for the self-healing microencapsulation versus 16 ± 3% for the traditionally encapsulated protein, where the self-healing microencapsulation of lower MW PLGA (i.v. = 0.19 dL/g) had a specific

activity of 41 ± 7%. Thus, although there was virtually no insoluble α-chymotrypsin in the w/o/w encapsulation, nearly all of the loaded protein was enzymatically inactive, showing that aggregation is not an accurate determinant of α-chymotrypsin stability.

Because of its ability to undergo autolysis, self-healing microencapsulation at less optimal pH for α-chymotrypsin, such as pH 5, may further improve the activity of self-encapsulated α-chymotrypsin.

5.4.3 Lysozyme Loading and Aggregation

As with α-chymotrypsin, the stability of lysozyme encapsulated via self-healing microencapsulation was compared with the enzyme encapsulated via a traditional w/o/w process was investigated. Soluble and insoluble lysozyme was measured via amino acid analysis, with the soluble amounts further investigated through SE-HPLC. The total loading, determined through amino acid analysis after acid hydrolysis, was again higher for those formulations that used the higher MW PLGA (i.v. = 0.57 dL/g). Self-encapsulated microspheres with this PLGA had 3.39 ± 0.03% and 5.17 ± 0.08% protein loading, with or without sucrose respectively, whereas the lower MW PLGA (i.v. = 0.19 dL/g) had 1.01 ± 0.06% and 1.24 ± 0.05% loading, with or without sucrose respectively. The traditional emulsion encapsulation technique resulted in 0.65 ± 0.01% and 4.86 ± 0.04% loading, with or without sucrose respectively. Clearly the addition of sucrose to the inner water phase strongly decreased the encapsulation efficiency and total amount of lysozyme loading, and further analysis showed that over 30% of the loaded protein in that formulation had aggregated (see below).

Loaded lysozyme displayed a single monomer peak when analyzed via SE-HPLC. Furthermore, as seen in both Figure 5.5 and Figure 5.6, the amount of soluble lysozyme

as determined via amino acid analysis and SE-HPLC were in close agreement with each other, indicating that most, if not all of the soluble protein was intact monomer as opposed to soluble aggregates. The percentage of loaded lysozyme that exists as intact soluble monomer is higher in those microparticles that were loaded via self-healing microencapsulation than the traditional w/o/w encapsulation (Figure 5.7). Of the lysozyme loaded via self-healing microencapsulation without sucrose, 92 ± 4% and 90 ± 2% was monomer in the 0.19 dL/g and 0.57 dL/g PLGA respectively, as determined via SE-HPLC and total amino acid analysis. The lysozyme loaded via the traditional encapsulation technique had 85 ± 2% of the protein as intact monomer. Significant improvement was seen however with the addition of sucrose in the loading solution, as the lysozyme loaded this way had 100 ± 6% and 98 ± 2% of the loaded protein as monomer in the 0.19 dL/g and 0.57 dL/g PLGA respectively.

Furthermore, when the fraction of total lysozyme loaded as insoluble is determined for each formulation, it is evident that those formulations that encapsulated lysozyme via a traditional method had a higher amount of protein loaded as insoluble aggregates (Figure 5.8). Lysozyme loaded via traditional encapsulation methods underwent 40 ± 4% and 12 ± 2% insoluble aggregation for the formulations with or without sucrose, respectively. By contrast, those loaded via the new self-healing microencapsulation technique showed marked improvement when sucrose was included in the loading solution, with the loaded lysozyme as 8 ± 5% versus 2 ± 6% insoluble aggregates in lower MW PLGA (i.v. = 0.19 dL/g) without and with sucrose, respectively, and 8 ± 3% versus 1 ± 2% insoluble aggregates in the medium MW PLGA (i.v. = 0.57 dL/g), without and with sucrose, respectively.

Clearly, lysozyme loaded via self-healing microencapsulation had less insoluble aggregates than that which was loaded via a traditional encapsulation technique in all cases. The total soluble protein loading determined via amino acid analysis and SE-HPLC was shown to agree with each other very well (Figure 5.9), validating the amino acid analysis technique as a useful means to measure the protein loading. Earlier research (*data not shown*) had indicated that lysozyme can form soluble aggregates – quantifiable via SE-HPLC – during release, but no such soluble aggregation was detected here immediately after encapsulation.

5.4.4 Lysozyme Activity

The specific activity of freshly extracted soluble lysozyme was determined by its ability to break down the cell walls of *Micrococcus lysodeikticus*. All formulations measured had at or above 100% of the specific activity of non-encapsulated lysozyme standard (Figure 5.10). Activity above the level of the stock solution has been reported before [26] and appears to be a possible artifact of encapsulation. Previous work has indicated that after encapsulation, the amount of intact monomer directly corresponds to the activity of the lysozyme [14, 16]. Activity was reported based upon the amount of soluble lysozyme as measured through SE-HPLC, indicating a strong correlation between the amount of soluble lysozyme and its activity in this instance.

5.5 Conclusions

Both lysozyme and α-chymotrypsin have been confirmed to have stability issues during emulsion encapsulation. By utilizing the self-healing microencapsulation technique, the insoluble aggregation of lysozyme was significantly reduced or eliminated,

with all enzymatic activity retained within experimental error. Additionally, α-chymotrypsin showed improvement in its specific activity compared to a traditional w/o/w emulsion encapsulation method. The addition of high concentrations of sucrose in the loading solution resulted in virtually no aggregation in the self-healing microencapsulation of lysozyme. Encapsulating such high concentrations of sucrose in the microparticles is not normally possible due to the low drug encapsulation efficiency and loading that high sucrose concentrations cause. Thus, the proteins are able to be loaded into a microparticle in a way that reduce the stresses associated with normal emulsion encapsulation, but also that allows additional high amounts of stabilizing excipients to be encapsulated as well.

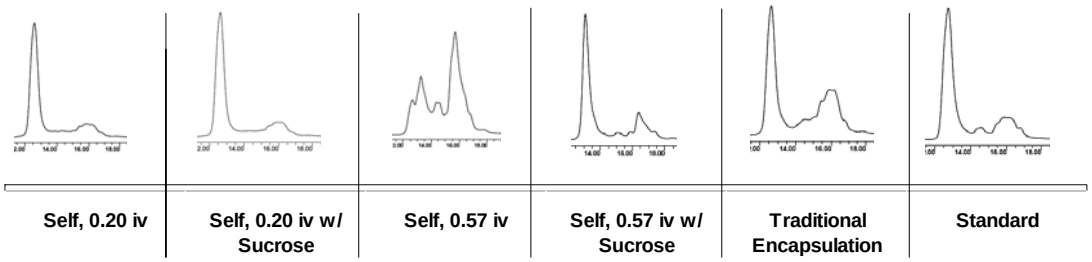

Figure 5.1 SEC chromatograms of α-chymotrypsin. Peaks were broad and unquantifiable.

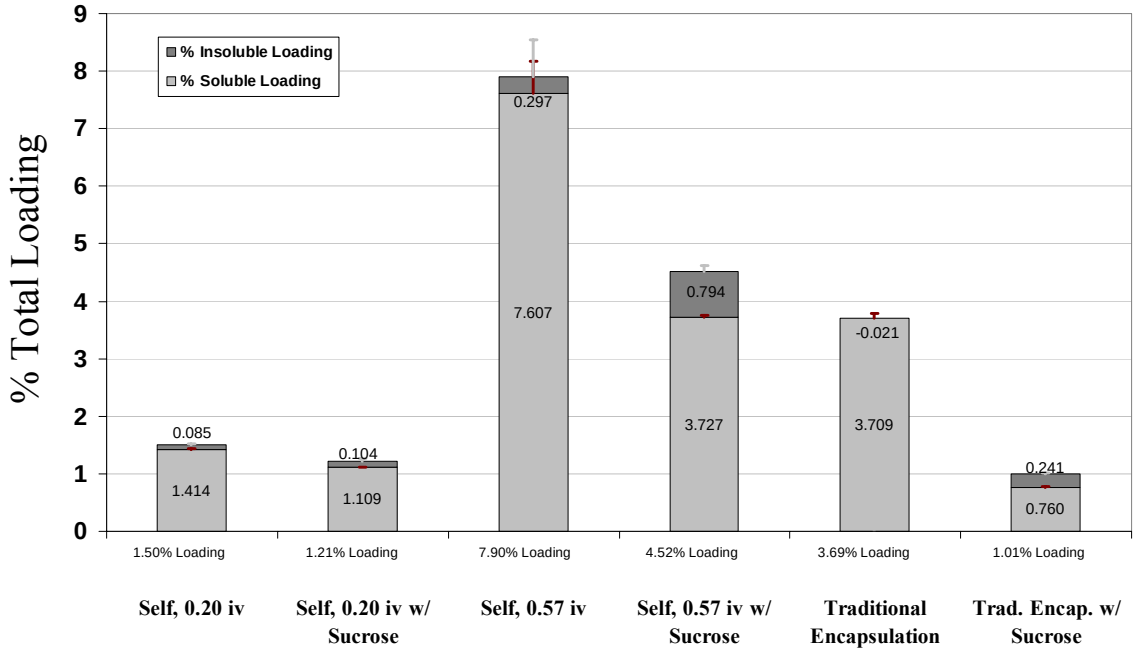

Figure 5.2 Soluble, insoluble, and total loading of α-chymotrypsin in self-microencapsulated and traditional microspheres.

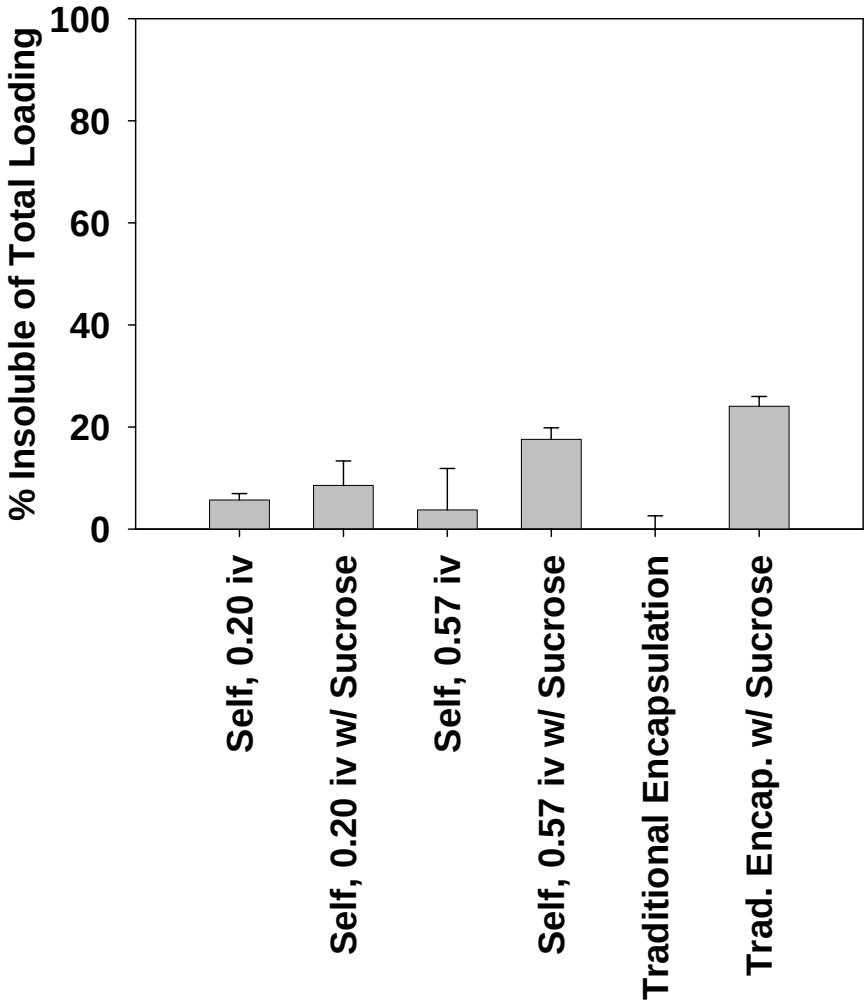

Figure 5.3 Insoluble aggregation of α-chymotrypsin as a percentage of loading. The traditional w/o/w emulsion encapsulation had basically no measurable insoluble α-chymotrypsin.

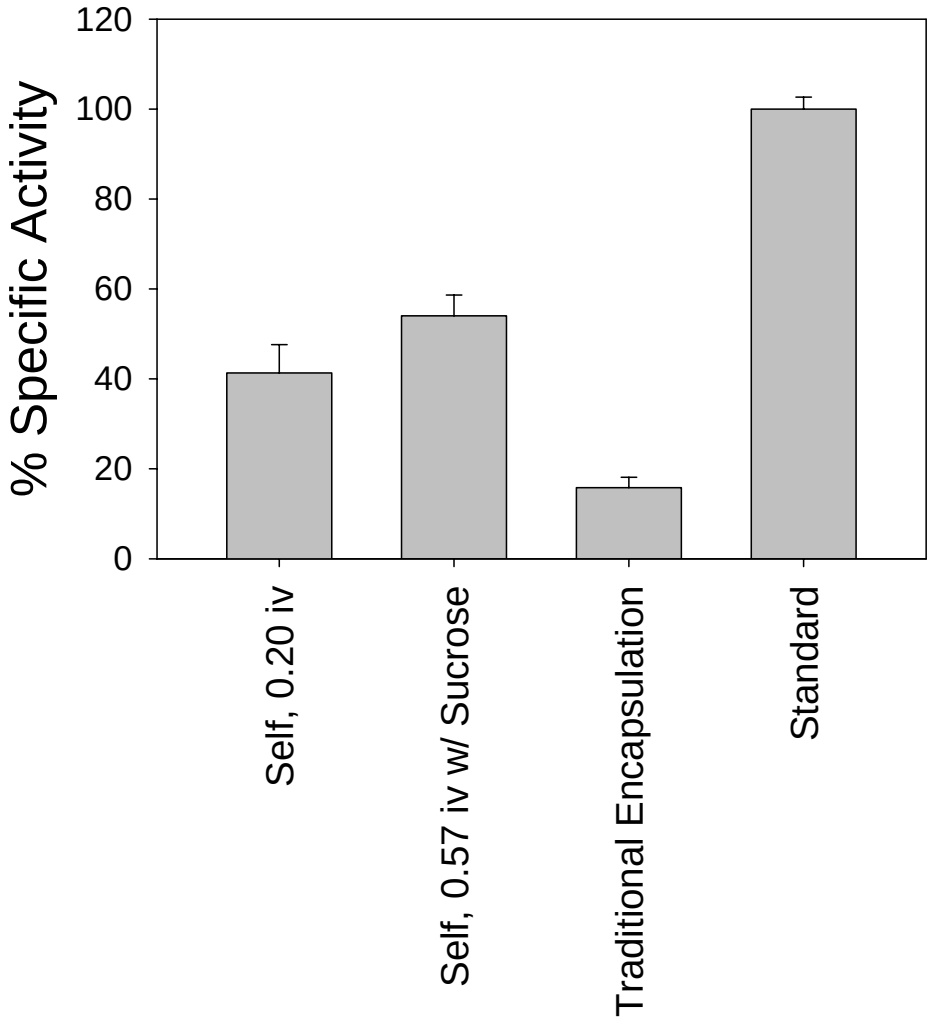

Figure 5.4 Specific activity of soluble α-chymotrypsin. Specific activity is reported as a % of the specific activity of the fresh, standard solution.

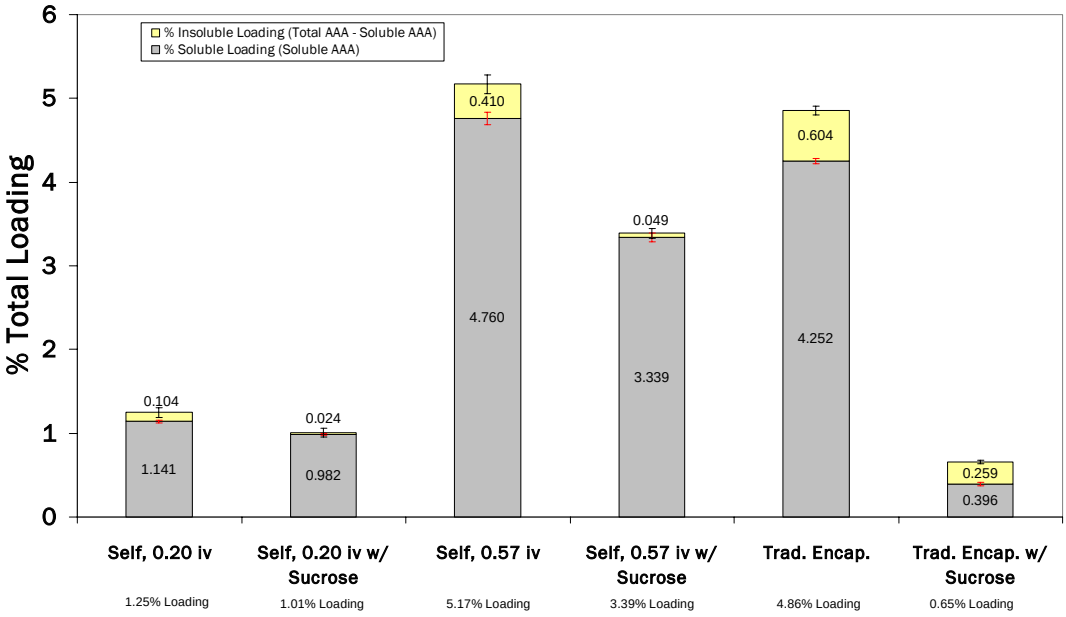

Figure 5.5 Loading of lysozyme via self-healing microencapsulation and traditional w/o/w encapsulation determined via AAA only. Soluble loading was determined via AAA of soluble protein after extraction from loaded microspheres, and insoluble loading is the difference between soluble protein determined via AAA and total protein loaded determined after microsphere hydrolysis via AAA.

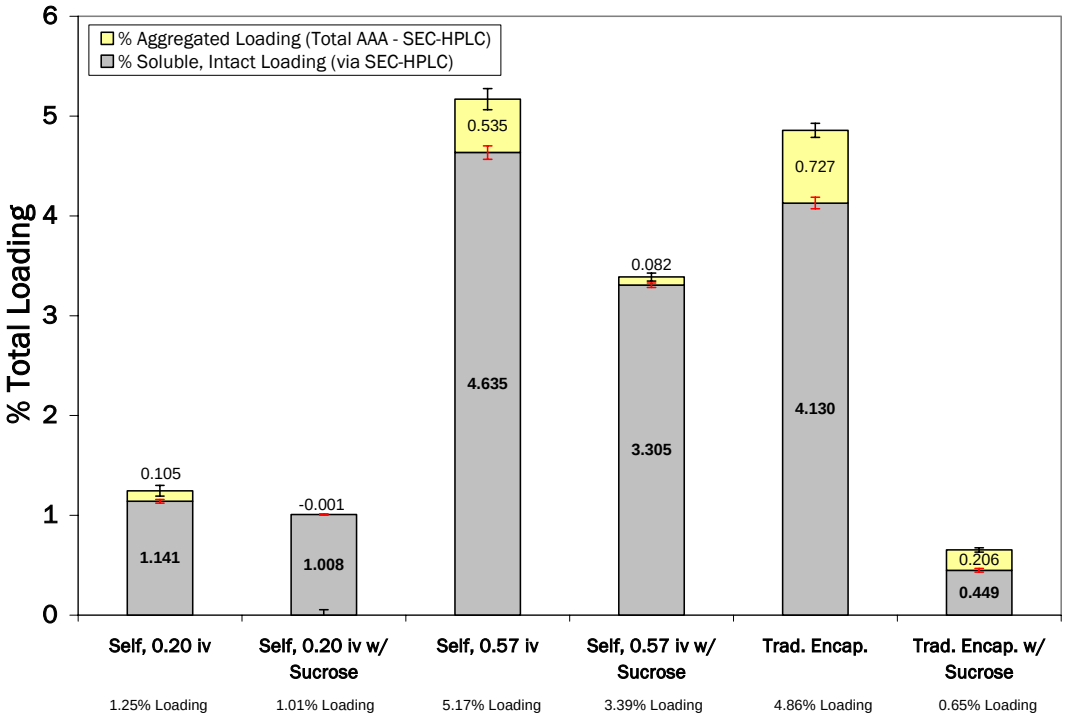

Figure 5.6 Loading of lysozyme via self-healing microencapsulation and traditional w/o/w encapsulation as determined via AAA and SE-HPLC. Soluble loading was determined via SE-HPLC of soluble protein after extraction from loaded microspheres, and insoluble loading is the difference between soluble protein determined via SE-HPLC and total protein loaded determined after microsphere hydrolysis via AAA.

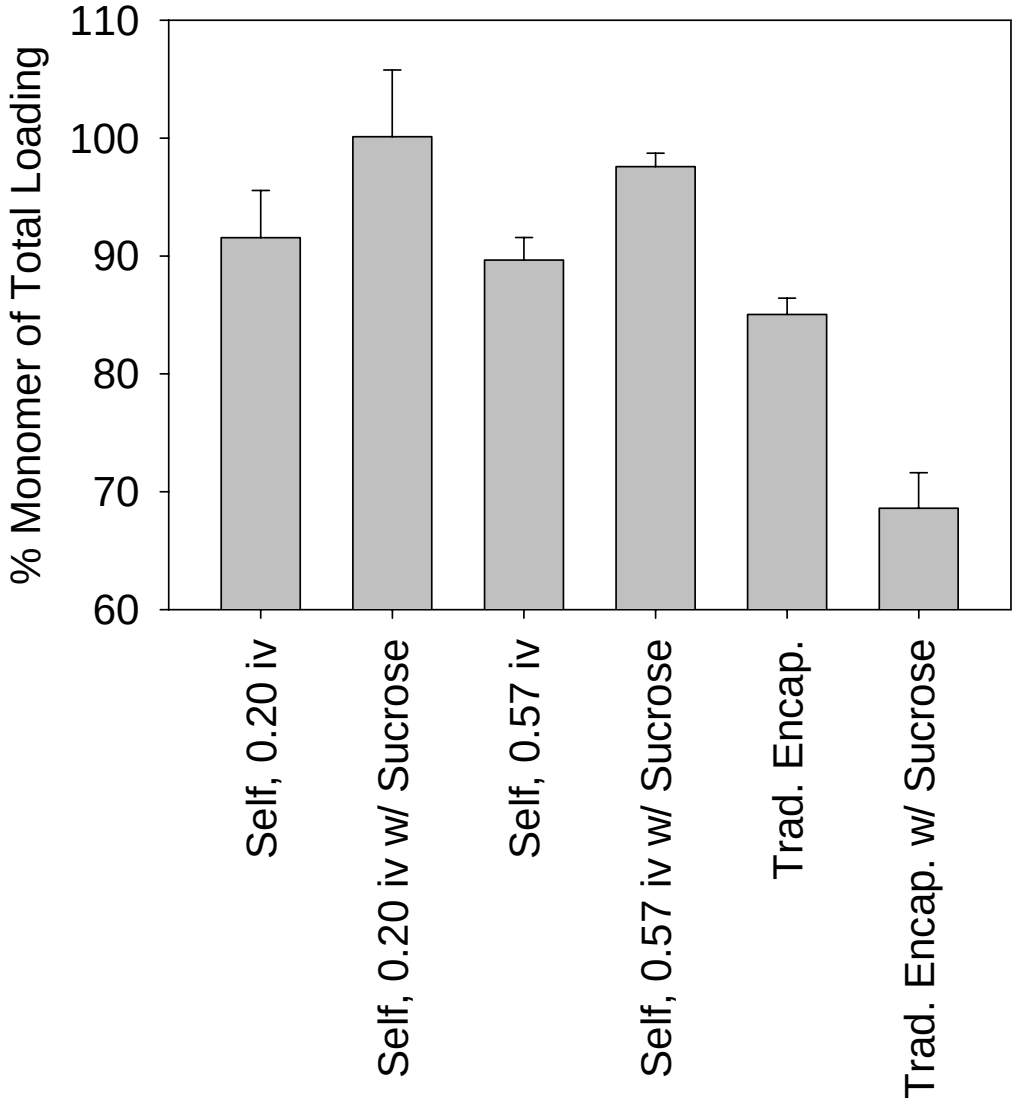

Figure 5.7 Monomer recovery in encapsulated lysozyme measured by SE-HPLC.

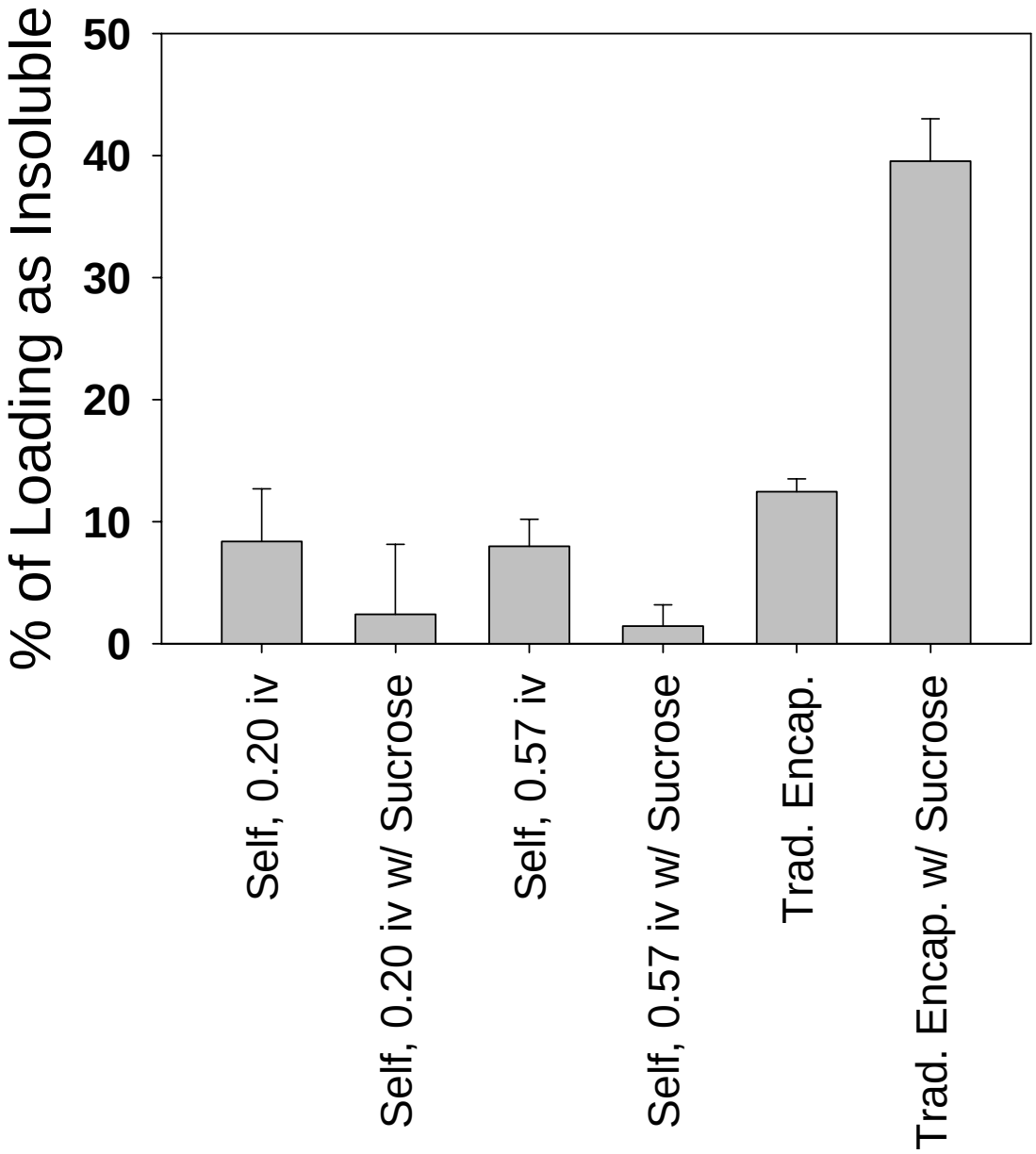

Figure 5.8 Insoluble lysozyme percentage that was determined insoluble via AAA. The amount of total protein encapsulated in microspheres was determined, as well as the amount of total soluble protein. The insoluble protein not present in the soluble fraction was used to determine the amount of lysozyme loaded in each formulation that was insoluble.

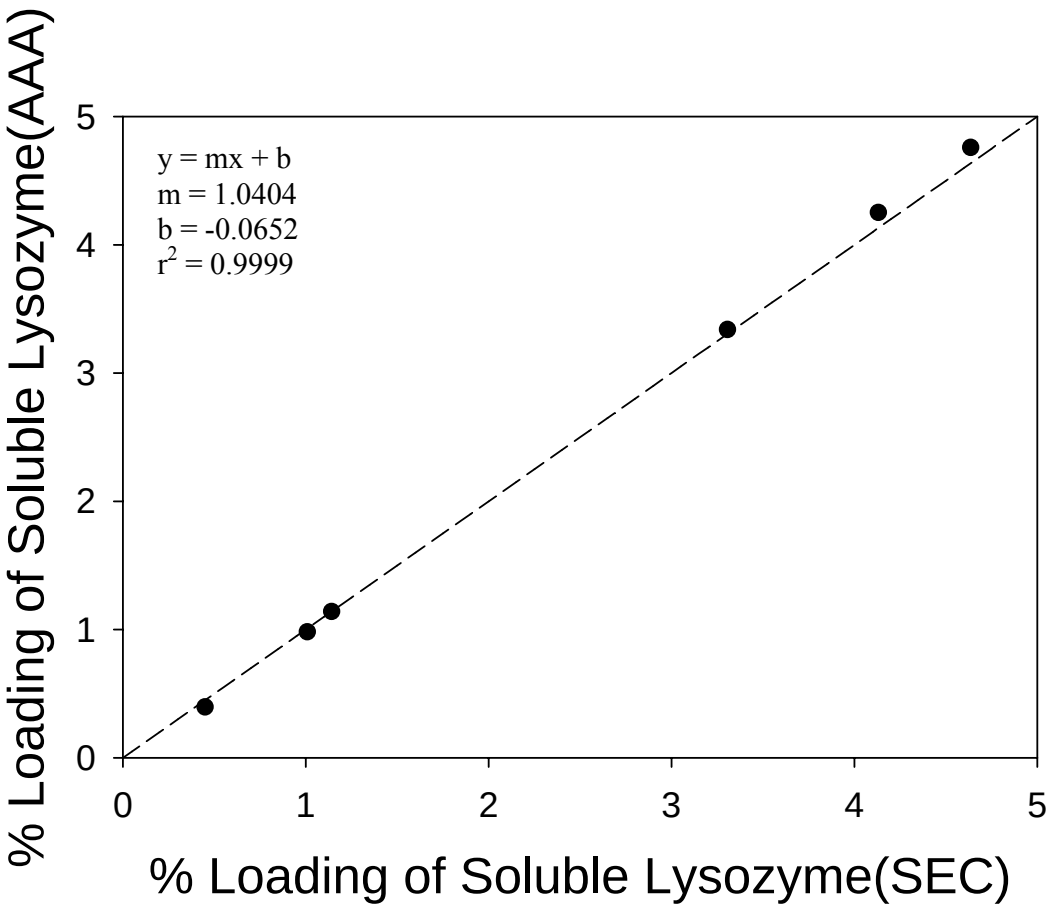

Figure 5.9 Comparison of the loading as determined via AAA versus that determined via SE-HPLC. The loading determined via both methods for the 6 different formulations were in agreement with each other.

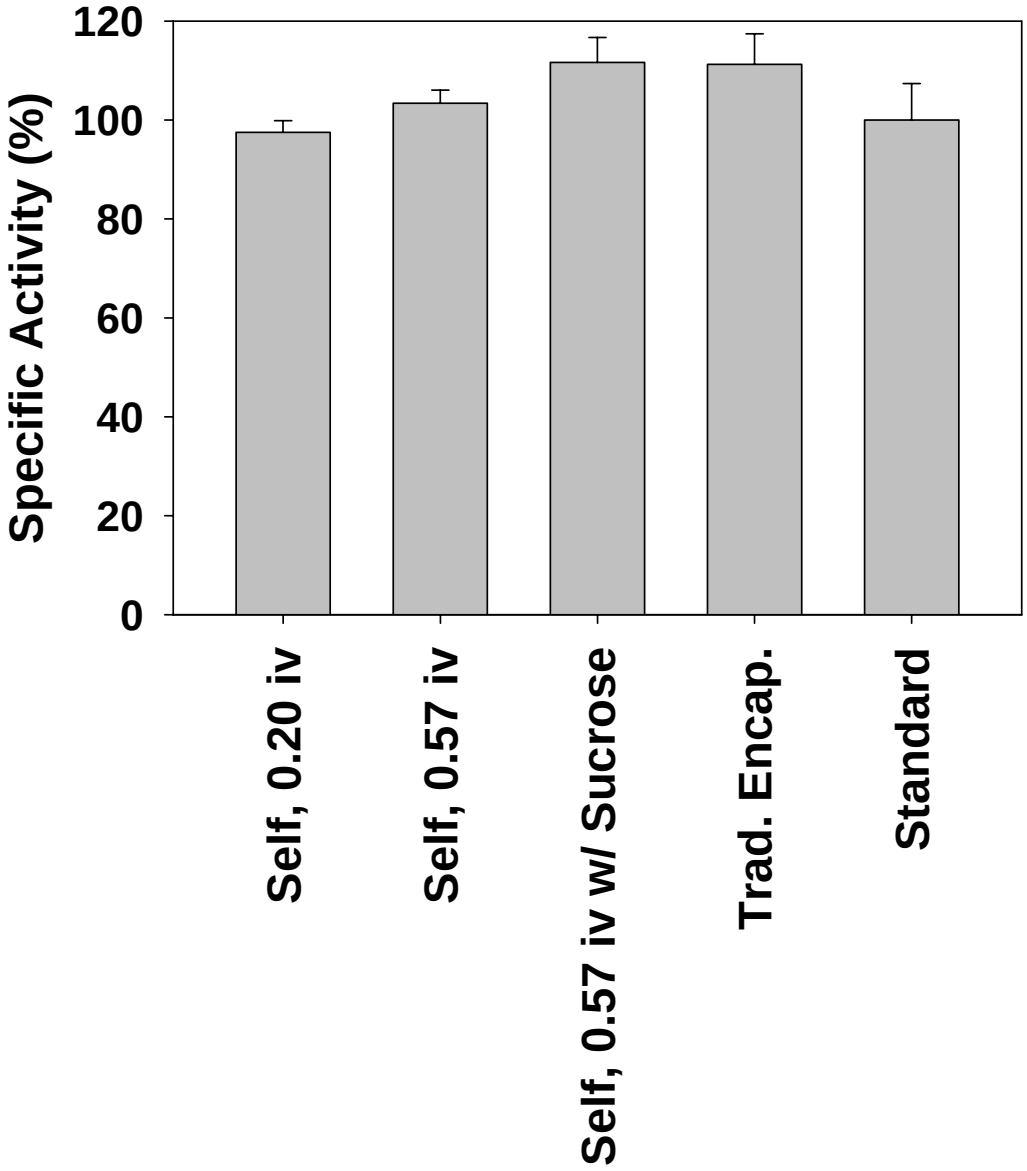

Figure 5.10 Specific activity of loaded lysozyme. Lysozyme was loaded via self-healing microencapsulation and a traditional w/o/w solvent evaporation methods. All samples maintained their activity. Soluble protein was quantified through SE-HPLC and was confirmed via AAA.

5.6 References

1. Sah, H., Protein behavior at the water/methylene chloride interface. *Journal of Pharmaceutical Sciences* **1999,** 88, (12), 1320-1325.
2. Maa, Y. F.; Hsu, C. C., Protein denaturation by combined effect of shear and air-liquid interface. *Biotechnology and Bioengineering* **1997,** 54, (6), 503-512.
3. Desai, U. R.; Klibanov, A. M., Assessing the Structural Integrity of a Lyophilized Protein in Organic Solvents. *Journal of the American Chemical Society* **1995,** 117, (14), 3940-3945.
4. Sah, H., Stabilization of proteins against methylene chloride water interface-induced denaturation and aggregation. *Journal of Controlled Release* **1999,** 58, (2), 143-151.
5. Sah, H.; Bahl, Y., Effects of aqueous phase composition upon protein destabilization at water/organic solvent interface. *Journal of Controlled Release* **2005,** 106, (1-2), 51-61.
6. Perez-Rodriguez, C.; Montano, N.; Gonzalez, K.; Griebenow, K., Stabilization of alpha-chymotrypsin at the CH2Cl2/water interface and upon water-in-oil-in-water encapsulation in PLGA microspheres. *Journal of Controlled Release* **2003,** 89, (1), 71-85.
7. Alonso, M. J.; Gupta, R. K.; Min, C.; Siber, G. R.; Langer, R., Biodegradable Microspheres as Controlled-Release Tetanus Toxoid Delivery Systems. *Vaccine* **1994,** 12, (4), 299-306.
8. Khan, J. A.; Millqvist-Fureby, A.; Vulfson, E. N., Enzymatic Synthesis of Glycosides in Aqueous-Organic Two-Phase Systems and Supersaturated Substrate Solutions. In 1999; Vol. 10, pp 313-322.
9. Oliva, A.; Santovena, A.; Farina, J.; Llabres, M., Effect of high shear rate on stability of proteins: kinetic study. *Journal of Pharmaceutical and Biomedical Analysis* **2003,** 33, (2), 145-155.
10. Wang, J. J.; Chua, K. M.; Wang, C. H., Stabilization and encapsulation of human immunoglobulin G into biodegradable microspheres. *Journal of Colloid and Interface Science* **2004,** 271, (1), 92-101.
11. Perez, C.; De Jesus, P.; Griebenow, K., Preservation of lysozyme structure and function upon encapsulation and release from poly(lactic-co-glycolic) acid microspheres prepared by the water-in-oil-in-water method. *International Journal of Pharmaceutics* **2002,** 248, (1-2), 193-206.
12. Perez, C.; Griebenow, K., Effect of salts on lysozyme stability at the water-oil interface and upon encapsulation in poly(lactic-co-glycolic) acid microspheres. *Biotechnology and Bioengineering* **2003,** 82, (7), 825-832.
13. Perez, C.; Griebenow, K., Improved activity and stability of lysozyme at the water/CH2Cl2 interface: enzyme unfolding and aggregation and its prevention by polyols. *Journal of Pharmacy and Pharmacology* **2001,** 53, (9), 1217-1226.
14. van de Weert, M.; Hoechstetter, J.; Hennink, W. E.; Crommelin, D. J. A., The effect of a water/organic solvent interface on the structural stability of lysozyme. *Journal of Controlled Release* **2000,** 68, (3), 351-359.

15. Arakawa, T.; Timasheff, S. N., Stabilization of Protein-Structure by Sugars. *Biochemistry* **1982,** 21, (25), 6536-6544.
16. Kang, F. R.; Jiang, G.; Hinderliter, A.; DeLuca, P. P.; Singh, J., Lysozyme stability in primary emulsion for PLGA microsphere preparation: Effect of recovery methods and stabilizing excipients. *Pharmaceutical Research* **2002,** 19, (5), 629-633.
17. Castellanos, I. J.; Cruz, G.; Crespo, R.; Griebenow, K., Encapsulation-induced aggregation and loss in activity of [gamma]-chymotrypsin and their prevention. *Journal of Controlled Release* **2002,** 81, (3), 307-319.
18. Castellanos, I. J.; Griebenow, K., Improved alpha-chymotrypsin stability upon encapsulation in PLGA microspheres by solvent replacement. *Pharmaceutical Research* **2003,** 20, (11), 1873-1880.
19. Castellanos, I. J.; Cruz, G.; Crespo, R.; Griebenow, K., Encapsulation-induced aggregation and loss in activity of gamma-chymotrypsin and their prevention. *Journal of Controlled Release* **2002,** 81, (3), 307-319.
20. Castellanos, I. J.; Griebenow, K., Improved α-Chymotrypsin Stability Upon Encapsulation in PLGA Microspheres by Solvent Replacement. *Pharmaceutical Research* **2003,** 20, (11), 1873-1880.
21. Aldrich, S. o-Phtaldialdehyde Reagent Solution Product Number P0532 Datasheet. http://www.sigmaaldrich.com/sigma-aldrich/datasheet/p0532dat.pdf (February 9, 2009),
22. Svedas, V. J. K.; Galaev, I. J.; Borisov, I. L.; Berezin, I. V., Interaction of Amino-Acids with Ortho-Phthaldialdehyde - Kinetic Study and Spectrophotometric Assay of the Reaction Product. *Analytical Biochemistry* **1980,** 101, (1), 188-195.
23. Jones, B. N.; Paabo, S.; Stein, S., Amino-Acid-Analysis and Enzymatic Sequence Determination of Peptides by an Improved Ortho-Phthaldialdehyde Pre-Column Labeling Procedure. *Journal of Liquid Chromatography* **1981,** 4, (4), 565-586.
24. B.F. Erlanger, F. E. a. A. G. C., The action of chymotrypsin on two new chromogenic substrates. *Archs Biochem. Biophys.* **1966,** 115, 206–210.
25. Árpád Bódi, G. K. I. V. L. G., Structural determinants of the half-life and cleavage site preference in the autolytic inactivation of chymotrypsin. *European Journal of Biochemistry* **2001,** 268, (23), 6238-6246.
26. Ding, G. Mechanistic evaluation of acidic microclimate pH development in biodegradable poly(lactic-co-glycolic acid) delivery systems. University of Michigan, Ann Arbor, 2005.

CHAPTER 6

Mechanism of PLGA Self-Healing

6.1 Abstract

Polymer self-healing is a known phenomenon in which a polymer that is damaged undergoes spontaneously rearrangement and repair, and has been shown to occur with porous poly(lactic-co-glycolic) (PLGA) microspheres in aqueous media. To investigate the mechanism behind polymer rearrangement in PLGA microparticles, the rate of pore closing was examined after a number of manufacturing conditions were changed in microsphere preparation, including the hardening time, freezing rate, and the addition of an annealing step prior to initial lyophilization. None of these conditions appeared to have an impact on the rate of surface pore closing. However, the utilization of a series of salts to alter surface and interfacial tension, based on the well-known Hofmeister series, was found to significantly impact the rate of drug entrapment in microspheres. The rate of pore closing through self-healing microencapsulation appeared to act in a manner consistent with an ultimate driving force of minimizing interfacial tension. Ultimately, PLGA pore closing appears to require 1) a temperature above the polymer glass transition temperature, imparting mobility to the polymer chains, and 2) water, to serve as a plasticizer, lowering the glass transition temperature of the PLGA to biological

temperature, as well as serving as a medium for polymer mobility and a possible driving force for minimization of polymer/water interfacial tension.

6.2 Introduction

In some polymers, when a dent or a crack appears in the polymer the damage is repaired through a spontaneously healing process [1]. This healing occurs through diffusion and entanglements of surface polymer chains [2], and a higher number of entanglements lead to increased strength. For this healing to occur, polymer mobility is required; thus, the healing is usually done at a temperature above the glass transition temperature of the polymer.

Poly(lactic-co-glycolic) acid (PLGA) microparticles are used to encapsulate drugs for sustained delivery in the body after injection. During drug release from the spheres, the surface undergoes a similar polymer alteration. Pores that were initially open become closed during incubation in aqueous solutions [3, 4] at temperatures above the hydrated polymer glass transition temperature [5]. This pore closing has been associated with the cessation of the initial burst [3] but its exact mechanism remains unclear. However, understanding its mechanism may help to attenuate the release rate from the microsphere. Furthermore, with the newly introduced encapsulation technique, 'self-healing microencapsulation,' understanding the mechanism behind the polymer rearrangement may allow encapsulation to occur in other conditions more conducive and safe for protein loading.

It is generally accepted that this pore closing is observed after surpassing the glass transition temperature of the polymer, which occurs at biological temperature due to the plasticizing affect of water and large molecular rearrangements [4, 6]. Obviously the

polymer has some mobility given its evolved surface morphology. Yet the exact driving force behind these molecular rearrangements has not been discussed in any detail.

To investigate the driving force, it would be critical to consider three important factors: 1) the impact of the internal enthalpy known to exist in microspheres after manufacture, where the processing creates spheres with excess energy [7] 2) the effect of water, both as a plasticizer and a medium for polymer rearrangement, and 3) the driving force behind the pore closing phenomenon and the spheres assuming a smooth surface.

6.3 Materials and Methods

6.3.1 Materials

PLGA with an i.v. = 0.57 dL/g (50:50, PLGA DL LOW IV, Lot No. W3066-603, lauryl ester end group, 51 kD) was purchased from Lakeshore Biomaterials (Birmingham, AL), formerly Alkermes; PLGA with an i.v. = 0.67 dL/g (50:50, PLGA, Lactel) was purchased from Durect Corporation (Cupertino, CA). α,α-Trehalose dihydrate was purchased from Pfanstiehl (Waukegon, IL), zinc carbonate ($ZnCO_3$) was purchased from ICN Biomedicals Inc. (Aurora, OH), poly(vinyl alcohol) or PVA (25 kDa, 88% mol hydrolyzed) was purchased from Polysciences, Inc. (Warrington, PA), and Poly(vinyl alcohol) (9-10 kDa, 80% mol hydrolyzed) was purchased from Sigma Aldrich (St. Louis, MO). Magnesium carbonate ($MgCO_3$) was purchased from Sigma Aldrich (St. Louis, MO). All other salts, reagents, and solvents were purchased from Sigma Aldrich (St. Louis, MO).

HPLC columns used included an SE-HPLC column from Tosoh Biosciences (TSK gel G3000SWxl column or TSK gel G2000SWxl column), an SE guard column (Shodex, Protein KW-G), C18 column (4 μm Nova-Pak, 3.9 x 150 mm, Waters, Part

#WAT086344, Serial #112837351338), and a C18 guard column (Bonda-Pak, C18 Guard-Pak, Waters, 4 μm).

6.3.2 Methods

6.3.2.1 Preparing Blank Particles

Two hundred μl of inner water phase (500 mg Trehalose in 1g 1X PBS, pH 7.4 or 1X PBS, pH 7.4) was added to 320 mg PLGA (50:50, 0.57 dL/g, lauryl ester end-capped or 50:50, 0.67 dL/g, free acid end group) with 0%, 1% or 3% w/w $ZnCO_3$ (0, 3.2, and 10.0 mg respectively), in 1 ml of CH_2Cl_2 in a test tube immediately homogenized in an ice water bath at 10,000 rpm for 1 min creating the first emulsion. Two ml of 5% PVA (9-10 kDa, 80% hydrolyzed) was added and the mixture vortexed for 15 seconds, creating the second emulsion and the resulting solution was poured into 100 ml of 0.5% PVA solution under continuous stirring. Microspheres were stirred 3 h at room temperature, and collected with sieves to separate by size and washed thoroughly with dd H_2O to help remove residual PVA, sugar, salt, and solvent. The particles were immediately freeze dried. The sizes collected were 20-45 μm and 45-90 μm fractions.

6.3.2.2 Determining Solution/Polymer Contact Angle

Solutions of PLGA (50:50, 0.57 dL/g) at 20% (w/w) using a SCS G3p-8 spin coater. 320 μl was dropped onto a glass round slide and spun at 850 rpm for 20 s with a 5 s deceleration time and left to air dry overnight.

A goniometer was used to measure the contact angle of various salt and control solution on the polymer film (Figure 6.1). Approximately 5-8 samples were run for each solution, and the angles were averaged and a standard error of the mean calculated.

6.3.2.3 Pore Closing with Various Salt Solutions

Approximately 50 mg were placed into separate tubes of salt solutions (3.5 or 4.0 M) known to affect the surface tension of water (NH_4F, NH_4Cl, NH_4Br, NH_4SCN, $(NH_4)_2SO_4$, NH_4I, NaCl, NaBr, NaSCN, Na_2SO_4, $(CH_3)_4NCl$, and Guanidine HCl) or methylcellulose (45 ng/ml, 180 ng/ml, 3.6 μg/ml, and 3.6 mg/ml) along with dextran-FITC (4,000 or 10,000 MW). Microspheres were incubated for 24-48 h at 4°C, and then transferred to 42.5°C for 48-72 h, with approximately 10% of microspheres removed at specified time points (fresh salt + dextran-FITC solutions were added to replace lost solution where possible). Sample microspheres were washed 10-fold with dd H_2O, with centrifugation at 3200 rpm for 10 min to collect the spheres after each wash. Microsphere morphology was determined via scanning electron microscopy (SEM), and the dextran-FITC was extracted using acetone to dissolve the PLGA and concentrating the insoluble dextran-FITC using centrifugation (10,000 rpm at 10 min), and repeating 3-fold. Dextran-FITC was dissolved in 1X PBS, pH 7.4, and loading was determined through HPLC fluorescence (absent of a column) using 20 or 40 μl injection volume and a 1 ml/min 1X PBS, pH 7.4 mobile phase. The fluorescence of the dextran-FITC was measured (490nm ex, 520nm em.) using unencapsulated dextran-FITC for a standard curve of the appropriate molecule.

One study utilized a higher temperature prehydration step of dextran-FITC at 42.5°C for 2 h after 4°C incubation, after which the spheres were split up and the dextran-FITC solution was replaced with dextran-FITC + salt solutions at the higher temperature.

6.3.2.4 Scanning Electron Microscopy

Surface images of microspheres were taken after a brief gold coating (60 s) using a Hitachi S3200N Scanning Electron Microscope at voltages ranging from 5 to 10 kV.

6.3.2.5 Changing Hardening and Annealing Conditions

For varying hardening times, 200 µl of inner water phase (500 mg Trehalose in 1g 1X PBS, pH 7.4) was added to a 6 ml syringe containing 320 mg PLGA (50:50, 0.57 dL/g, lauryl ester end-capped) with 1.75% w/w $MgCO_3$ (5.6 mg respectively) in 1 ml of CH_2Cl_2 in a 6ml syringe and immediately homogenized in an ice water bath at 20,000 rpm for 1.5 m to create the first emulsion. Two ml of 5% PVA (9-10kDa, 80% hydrolyzed) was added and the mixture homogenized at 6,000 rpm for 30 s, creating the second emulsion and the resulting solution was injected into 100 ml of 0.5% PVA (9-10 kDa, 80% hydrolyzed) solution under continuous stirring. Microspheres were stirred 1.5, 3, and 5 h at room temperature. For annealing step, microspheres were then incubated at 60°C for 1 h in 0.5% PVA continuous phase. All microspheres were collected with sieves to separate by size and washed thoroughly with dd H_2O to help remove residual PVA and solvent, collecting the 20-63 µm fraction. The particles were immediately flash frozen with liquid N_2 and freeze dried.

6.4 Results and Discussion

6.4.1 Microspheres Start With a Higher Internal Enthalpy

During the hardening process of PLGA microsphere preparation, otherwise known as solvent evaporation or phase separation, polymer mobility observed is first slowed by polymer chain friction [8, 9] and later by the formation of chain entanglements

[6, 10, 11]. When microspheres are subsequently freeze dried after manufacture, the polymer chains can be 'trapped' in unfavorable energy states [7]. During subsequent storage of the polymer at a temperature below its T_g, the polymer can slowly 'relax' to a lower energy state, a process known as polymer ageing. Physical ageing of the polymer can be observed through comparison of two heating curves of the same sample using differential scanning calorimetry. The difference in area between the curves, an endothermic peak, is due to 'enthalpy relaxation' [12] between the samples, and corresponds to the original amount of excess internal enthalpy inside the microparticles. This relaxation, occurring at a temperature less than the T_g of the polymer, is usually thought to involve side chain (β-relaxations) and not backbone motions (α-relaxations) in different types of polymers, even in PLGA [7]. However, a more accurate explanation is likely that the relaxation is from the low amplitude twisting motions of the backbone itself [6, 13]. This physical ageing is not observed at 10°C for 50:50 high and low MW PLGA microspheres with glass transition temperatures of 47°C and 32°C, respectively [7].

The amount of internal energy 'stored' in this backbone motion is directly related to its quench rate, and fast quenching from the molten state produces a glassy polymer with a higher amount of excess energy [6]. Manipulating the rate of freezing of PLGA in dioxane solution showed that quick flash freezing in liquid nitrogen resulted in lower, broader, glass transition temperature compare to slow freezing or high polymer concentrations. It is believed that the lower T_g for the flash frozen polymer resulted from a lower density polymer with higher free volume with little resistance to mobility. Furthermore, the drying temperatures impacted the final T_g of the PLGA as well,

suggesting that this step also played a role in polymer mobility [8], along with the microsphere hardening process itself.

Accordingly, the influence of this excess internal energy was investigated briefly. After microsphere hardening, the microspheres were annealed in the aqueous hardening bath for 1 h at 60°C. Microspheres that had been annealed showed a surface very similar to those that had not gone through this step (Figure 6.2). However, after these microspheres were incubated in pore closing conditions, the annealed microspheres had a rough, uneven surface compared to those without previous annealing (Figure 6.2). The pore closing was monitored over a period of 48h, and the rate of pore closing was not different for these annealed microspheres. Obviously from the pore closed morphology images, the annealing step had altered the polymer, presumably in lowering the internal enthalpy, yet the pore closing still took place at roughly the same rate. Indeed, when microspheres were allowed to slowly freeze at a temperature of -10°C instead of flash frozen in liquid nitrogen, the pores were still present and were able to subsequently close in aqueous conditions (data not shown). Even further indications that changes in microsphere structure do not alter the rate of pore closing were seen when the hardening time was altered from 1.5 to 3 to 4.5 hours, all at room temperature. The morphology after immediate freeze drying was slightly different, with more pores visible at 3 hours than either 1.5 or 4.5 hours (Figure 6.3), but all surface pores appeared to close at the same rate (*data not shown*).

PLGA microspheres that start with a higher internal enthalpy may undergo an ageing process that lessens this stored energy. Over time, even storage of such particles at temperatures less than the T_g of the microspheres can allow these particles to 'relax,'

reducing both enthalpy and free volume [6] which can subsequently influence their release characteristics. In some experiments, structural changes (e.g. polymer relaxation) of porous microspheres that did not appear to correlate with any morphological changes, surface or otherwise (e.g. pore closing), still lowered the burst release [4]. This change in polymer structure that was undetected by the electron microscope and pore closing steps agrees with the previous annealing experiment. Importantly, this indicates 1) polymer relaxation may occur even without a visual cue and 2) polymer relaxation and pore closing are not necessarily strongly related to each other. Polymer relaxation may lower the internal enthalpy of the microspheres and affect their T_g, but may not influence the pore closing process. However, there are two conditions that appear to be necessary for normal pore closing: water and a temperature greater than the T_g.

6.4.2 Water a Critical Component

It has been firmly established that water can serve as a plasticizer of PLGA, lowering its glass transition temperature (a typical unwet T_g is around 40-50°C) by as much as 15°C when hydrated [5]. PLGA will take on as much as 2-3% water (w/w) in the polymer phase during incubation at high humidity and in solution [5]. Thus, incubation of polymer at biological temperature (i.e. 37°C) will typically be below its T_g unless the polymer is plasticized, for instance by water. Again, while below the T_g the polymer will still have some mobility (the aforementioned low amplitude twisting motions of the backbone), its mobility above the T_g will be much greater with the increased flexibility of the polymer backbone (α-relaxations). Thus, the mobility of the polymer will be significantly higher in water due to its plasticizing affects. Indeed, porous microspheres incubated in different amounts of relative humidity showed a higher

pore modification as the humidity was increased from 55 to 75% [4]. The authors theorized that this was due to increasing plasticizing effect of water, providing the polymer chains with mobility. While 75% relative humidity resulted in major surface structural pore changes, it did not completely eliminate the visible pores. However, experiments with porous microspheres in solution have shown that complete surface pore closure is possible [3] when the temperature is raised above the polymer glass transition temperature [14]. Similarly, pore closure is much slower or non-existent in dry environments [4]. The authors conclude that this indicated that the water serves as a plasticizer, as well as enabling large polymer molecular rearrangements [4], which others have attributed this to behavior similar to viscous flow that can dramatically reduce micron-scale porosity [6]. However, these discussions do not entertain the possibility of any interfacial driving force behind the pore closing phenomenon.

Plasticizers, often reducing the T_g, can result increase PLGA mobility from segmental motion to normal mode mobility similar to viscous flow [6]. The plasticizer Triton X100 was observed to allow PLGA microsphere surface pores to close at ambient temperature. While water and Triton X100 are PLGA plasticizers, it should be noted the surfactant used in these experiments, poly(vinyl alcohol) (PVA), has been determined to be a mild antiplasticizing agent [7], though its effects are much less than that of water. All of these parameters need to be accounted for, however, as the T_g is a critical determinant of polymer relaxation, pore closing, as well as appearing to be one of the most important parameters in determining release rates at later release times [15]

As mentioned previously, it is important to note that although the PLGA glass transition temperature is commonly referred to as one value, actually the polymer and

microsphere may have a range of glass transition temperatures from its surface to the bulk. A reduced glass transition temperature near the surface has been seen at the surface, with a steady increase in T_g towards the bulk [16-18]. This has been observed for polystyrene [19-24] as well as poly(methyl methacrylate) [22]. This reduced T_g, due to the surface free volume increase and reduced intermolecular coupling from the presence of the surface itself [21], provides a greater polymer surface mobility than found in the bulk polymer [25].

6.4.3 Interfacial Effects

6.4.3.1 Background on the Hofmeister Series

First reported in 1888 [26], the Hofmeister series is a ranking of ions that are known to affect the solubility of proteins [27]. Some are known to increase the solubility of proteins, while some decrease the solubility. While both anions and cations influence solubility, anions are clearly much more important [28]. This series has an effect on the surface tension of the solution, and in turn any interfacial tension, which is defined as the surface tension between two immiscible liquids. Research indicates that these dissolved salts have no effect on the bulk structure of water [29-31], and instead only have an effect on the molecules immediately surrounding the ions.

Up until very recently, the Hofmeister series was thought affect the water's ability to solvate proteins by making and breaking the structure of water at the interface [28, 32]. Dissolved solutes that increase the surface tension were thought to do so by disrupting the geometry at the water interface and preventing water molecules from maximizing interactions at the interface, thus causing the water molecules to prefer to be not at the

interface and subsequently creating a force for minimizing the interface [32]. The thought behind this is that some strongly hydrated ions (kosmotropes) 'steal' water from the surface, and from protein hydration, whereas other ions (chaotropes) in fact do the opposite, allowing water to 'lend' itself to protein hydration (Figure 6.4). Such traditional views perceive the surface of water as ion-free [33, 34].

Only in the last few years, beginning in 2006, has the consensus switched completely the other direction. Now, evidence supports the notion that the ions affect the hydration of proteins through their direct presence at the surface and even through subsequent interactions with the interface of interest [34-39]. Although these ions may not exist at the open water surface, they all seem to show some affinity for water/protein interfaces [40]. Thus, it may not be their affect on the water structure that gives rise to the different properties of Hofmeister salt solutions, but their direct presence on the surface and interaction with the interface. The Hofmeister series has shown agreement with the ability of ions to 'salt-out' the surfactant octadecylamine [41], which the authors proposed is through the ions' differing ability at the surface to penetrate the surfactant head groups. This is very relevant considering the blank particles prepared herein have a surfactant, PVA, on their surface.

It is generally recognized that there remains an inability to explain the Hofmeister series, and its specific ion effects [42, 43]. There may be many ways an ion interacts with an interface (Figure 6.5), and separating them experimentally is not trivial. Whatever their method of action, the ability of ions to 'salt-out,' generally increases as ionic charge density increases, in agreement with the Hofmeister series [44, 45]. These increases in ionic charge density with the Hofmeister series have been reported to show

stronger hydrophobic interactions in aqueous solutions between hydrophobic particles and a tendency of the hydrophobic particles to aggregate [46]. Experiments with another polymer, hydroxypropylmethylcellulose, has shown that the anions of the Hofmeister series can disrupt the structure of water at the surface, altering the strength of the 'water cages' and consequently altering hydrophobic association [47]. Thus, using kosmotropic ions over chaotropic ions from the Hofmeister series increases the hydrophobic effect. If the pore closing is dominated by surface effects with underlying hydrophobic effect components, changing these ions should alter the rate of pore closing.

6.4.3.2 Investigating Hofmeister Series Effects on Pore Closing

The Hofmeister salts in this study were selected for their high water solubility. Dextran-FITC (4 kDa) was chosen as the marker with which to monitor pore closing. The contact angles for the different salt solutions were measured using a goniometer and were found to agree with the Hofmeister series, with the plain dextran-FITC solution lying somewhere in the middle (Table 6.1). Thus, according to earlier discussion and this result, the interfacial tension between PLGA and salt solutions was assumed to agree with the Hofmeister series.

It was expected that if the pore closing was due to interfacial energy driving forces, increasing the interfacial energy by selecting kosmotropic Hofmeister salts would increase the rate of pore closing. However, this was at first shown to be not the case (Figure 6.6). In this preliminary experiment, the salts that have a tendency to 'salt-out' through raising surface tension (for ranking see Figure 6.4), actually decreased the amount of loaded molecule over the duration of the experiment, especially at the

beginning. Scanning electron microscopy indicated that once the curves approached a horizontal orientation (e.g., NH_4F at 4h), the visible surface pores closed (data not shown), presumably preventing further uptake up the dextran, and at which point the microspheres were at their maximum loading.

Additionally, this experiment indicated three things. First, virtually no loading was seen at 4°C for all salts, further confirming that the temperature for pore closing needs to above the polymer glass transition temperature. Second, those microsphere/salt solution suspensions for the most kosmotropic salts (i.e. NH_4F and $(NH_4)_2SO_4$) had a significant amount of microspheres were found floating during incubation. This suggests that the solution had not fully wetted these spheres [48], albeit there are also unknown differences in solution density among these solutions. Third, aggregation was seen in particles at both extremes of the Hofmeister series. The first spheres to aggregate during the incubation were the kosmotropic salts (NH_4F and $(NH_4)_2SO_4$) and the most chaotropic salts (NH_4SCN and NaSCN, data not shown). Nonetheless, it is hypothesized that the floating particles were a result of the extremely high surface tension and a lack of proper hydration of the particles, and similarly the particles that aggregated first were the most hydrated. This would obviously subsequently lower the loading, and thus the loading may not be a proper indicator of pore closing. Hence, a pre-hydration step was deemed necessary.

The pore closing was again monitored through the loading of dextran-FITC in a series of Hofmeister salt solutions, except this time a hydration step was added. All microspheres were incubated at 4°C for 24 h followed by 2 h at 37°C in a dextran-FITC

only solution, in an attempt to start the experiment with all microspheres properly hydrated.

The results (Figure 6.7) are in stark contrast to the earlier experiment without the pre-hydration step. With all microspheres hydrated properly before exposure to the Hofmeister salts, the highest loading was now the most kosmotropic salt, the $(NH_4)_2SO_4$. In fact, the overall trend appeared to agree with the Hofmeister series (highest surface tension salts loaded the quickest), with the lone exception being those utilizing the chloride salts (NH_4Cl and NaCl). Clearly though, there was another factor in the calculated loading than simply pore closing. The results show an actual decrease in loading after the pre-hydration step for some salts, and especially for the chloride solutions. This suggests some sort of pore opening or microsphere rupturing ongoing during this time, presumably driven by osmotic related events [14]. Similar decreases in loading were observed at later time points for nearly all salts as well. Hence, using the dextran loading determination as a determinant of the speed of polymer rearrangement may be incorrect for these solutions. Hence, except for the chloride salts, the rate of pore closing/drug entrapment was consistent with the notion that hydrophobic association and interfacial tension are the driving forces behind rearrangement.

It should be noted that no significant difference was seen with any of the solutions of methylcellulose used for either the contact angles or the rate of pore closing. These solutions mirrored the dextran-FITC controls, and as the contact angles were not different from one another, it was deemed that the methylcellulose did not significantly alter the interfacial tension.

6.4.4 Altering End Groups

Nearly all formulations that utilized self-healing microencapsulation contained lauryl (C12) ester end groups at the end of each polymer chain. To confirm this long hydrophobic chain was not the key parameter necessary for hydrophobic rearrangement to take place, pore closing was attempted utilizing microspheres prepared with PLGA (50:50, i.v. = 0.67 dL/g) without this end group. Instead, this polymer utilized a free carboxylic acid end group and as such is not considered 'end-capped.' In addition, microspheres were created from both polymers using two different molecular weight surfactants: 9-10 kD PVA and 25 kD PVA. All four formulations started with very similar porous surface morphologies and had no distinguishable difference in the observed surface pore morphology during 48 hours of pore closing incubation, and all surface pores appeared to close at the same rate.

6.4.5 Self-Healing

Thus it has been established that the chain mobility of a polymer is higher at the surface than the bulk. This increased flexibility is evident in the decreased T_g at the polymer surface. Further evidence of polymer surface mobility can be seen through the phenomenon known as 'self-healing,' where two separate interfaces join when brought into close proximity to each other. Such healing is only possible once the polymer coils from each side are at least capable of spanning half the distance during their random motion, meeting one another in the middle [49]. Wool and O'Connor have established five critical steps of this polymer healing [1, 2]: 1) surface rearrangement, including post-crack chain-end distribution changes at the surface and surface chemical reactions, 2)

surface approach, or the time, space, and force required to bring the two surfaces in contact with each another, 3) wetting, specifically the initial formation of an interface between the two surfaces, 4) diffusion, the migration and diffusion of the polymer chains with one another, and 5) randomization, the further random crossing of the interface, forming new polymer entanglements [50-52], which are thought to occur through Brownian motion [49]. These last two steps, diffusion and randomization of the polymer chain segments, are what gives the healed polymer segment its strength.

Self-healing has been observed via the spontaneous formation of latex films from a spread of latex particles, in a dry open air state above the Tg of the polymer [53, 54]. In the self-healing of polymer 'dents,' it is believed that the driving force behind the healing of the polymer is surface tension, in an attempt to keep the polymer surface as small as possible [55]. The time scale of such rearrangement depends ultimately on the mobility of the polymer chains, i.e., the glass transition temperature of the polymer [55]. It is hypothesized that the unknown pore closing mechanism may be a form of polymer self-healing, in which surface entanglements, facilitated by a temperature above the T_g, entangled and strengthened through random motion, and further driven by an attempt to minimize interfacial tension, allow polymer rearrangement and pore closing to take place.

It should also be noted that the polymer surface rearrangement is not limited to pore closing. In fact, pore closing appears because the aforementioned two interfaces are in constant vicinity of one another. However, the particles during loading are in constant mixing, preventing self-healing among different spheres. If this mixing process is not sufficient, microspheres will begin to self-heal with one another (Figure 6.8). This may

be another way to properly quantify the rate of polymer rearrangement in future experiments.

6.5 Conclusions

The observed pore closing phenomenon is believed to occur in much the same manner as traditional self-healing systems. As the temperature is increased above the glass transition temperature, which is lowered by the plasticization effect of water, the polymer chains are given the freedom to reorient themselves. While relaxation can occur at temperatures less than the T_g of the polymer, it appears that increased polymer backbone mobility is required (i.e. temperatures above the T_g). This surface rearrangement does not appear to be necessarily coupled to polymer relaxation, as annealed particles and those with lower internal enthalpies still closed at roughly the same rate. Instead, the surface rearrangement appears to act through polymer entanglement, and may be driven by an attempt to minimize interfacial tension. The attempt to change these forces through the use of Hofmeister series generated data consistent with this theory, though evidence exists that another phenomenon, osmotic pressure mediated pore rupturing, was also taking place, complicating interpretation of these results.

One result of self-healing microencapsulation may be a reduced internal free volume due to the polymer reaching a lower energy state during the pore closing at a temperature above the T_g, similar to observed in ageing. However, such lower internal energy states in PLA microparticles have produced spheres with the ability to lessen the rate from enzymatic degradation [56]; similarly, an increased rate of degradation was seen with lower density particles from hydrolysis [57] and the inverse could be expected

for higher density particles with less free volume. Thus, by harnessing this pore closing process, self-healing microencapsulation may create microspheres with less free volume and a subsequent attenuated release (e.g. extended lag phase). Additional formulation considerations (e.g. additives) may have to be added to counteract this.

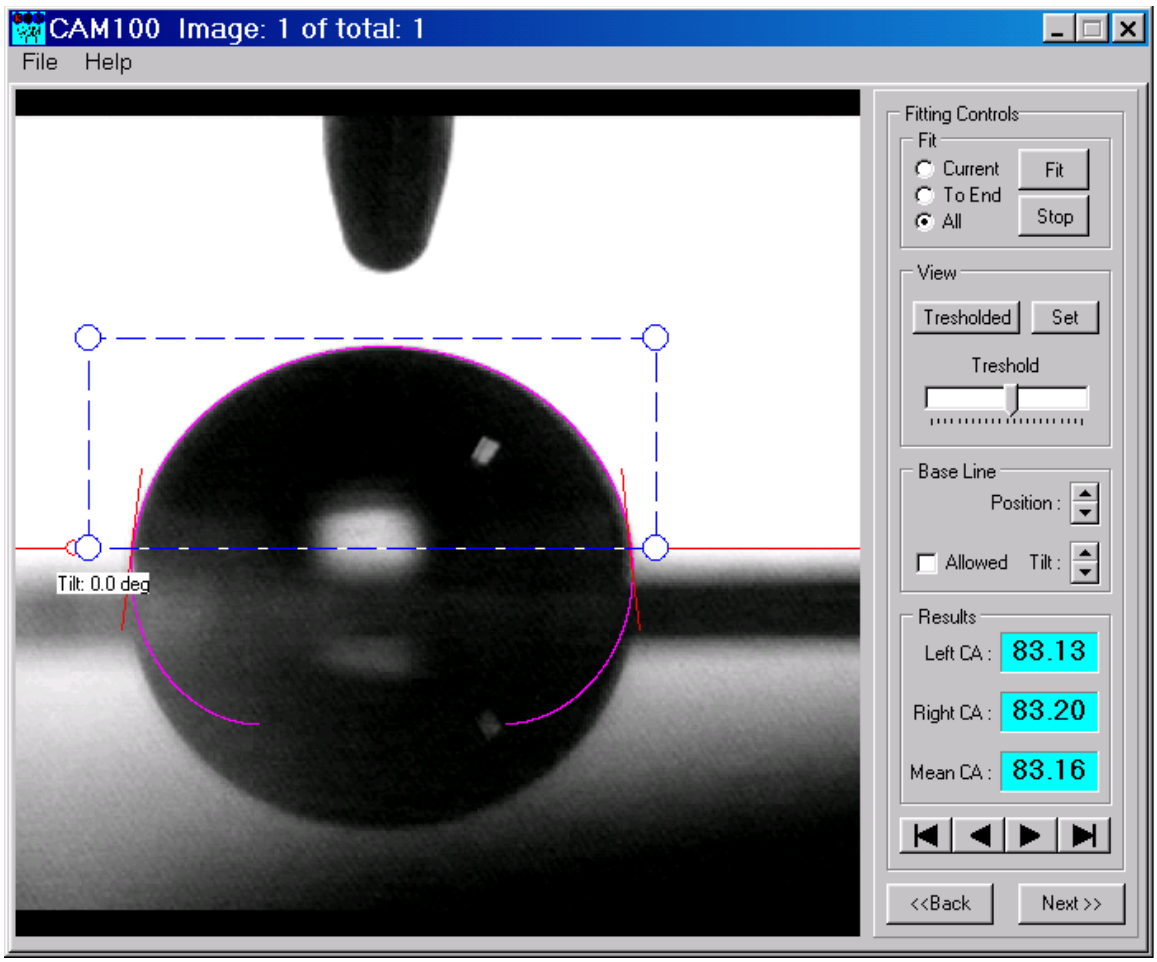

Figure 6.1 Measurement of contact angle on polymer films using goniometer. A goniometer was used to measure the contact angle of various salt solutions on a prepared PLGA (50:50, 0.57 dL/g) film.

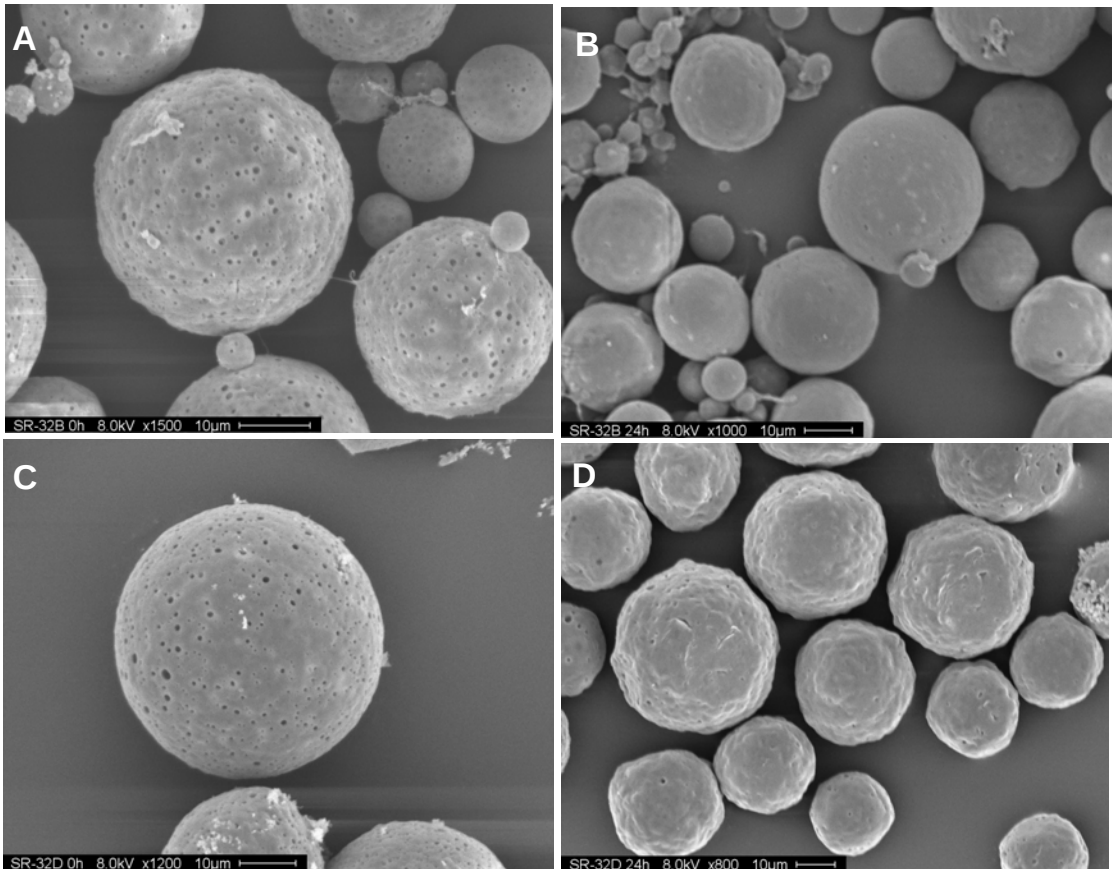

Figure 6.2 The effect of aqueous annealing on pore closing. SM-microspheres were prepared with PLGA (50:50, i.v. = 0.57 dL/g) and immediately freeze dried (A) or annealed in the hardening bath for 1 h at 60°C (B) before freeze drying. Both formulations were then incubated in pore closing conditions for 24 h. Those that were immediately freeze dried (C) showed a smoother surface compared to those that had been annealed (D).

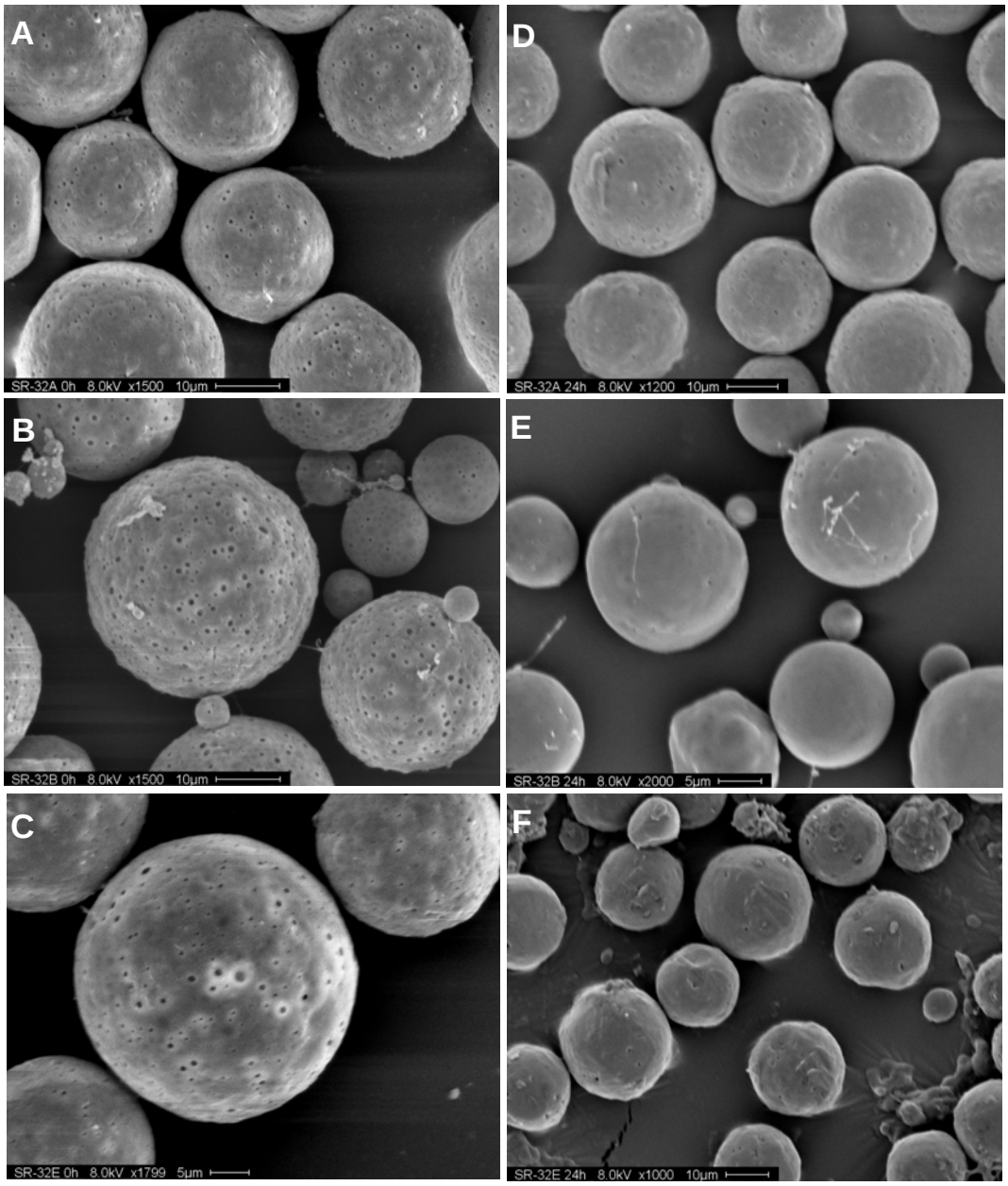

Figure 6.3 The effect of hardening time on pore closing. Blank microspheres were prepared with PLGA (50:50, i.v. = 0.57 dL/g) and hardened for different times in 0.5% PVA solution for 1.5 h (A), 3 h (B), or 4.5 h (C), immediately freeze dried (A,B,C), and later incubated in pore closing conditions for 24 h (D,E,F). Hardening times were 1.5 h (A,D), 3 h (B,E), and 4.5 h (C,F).

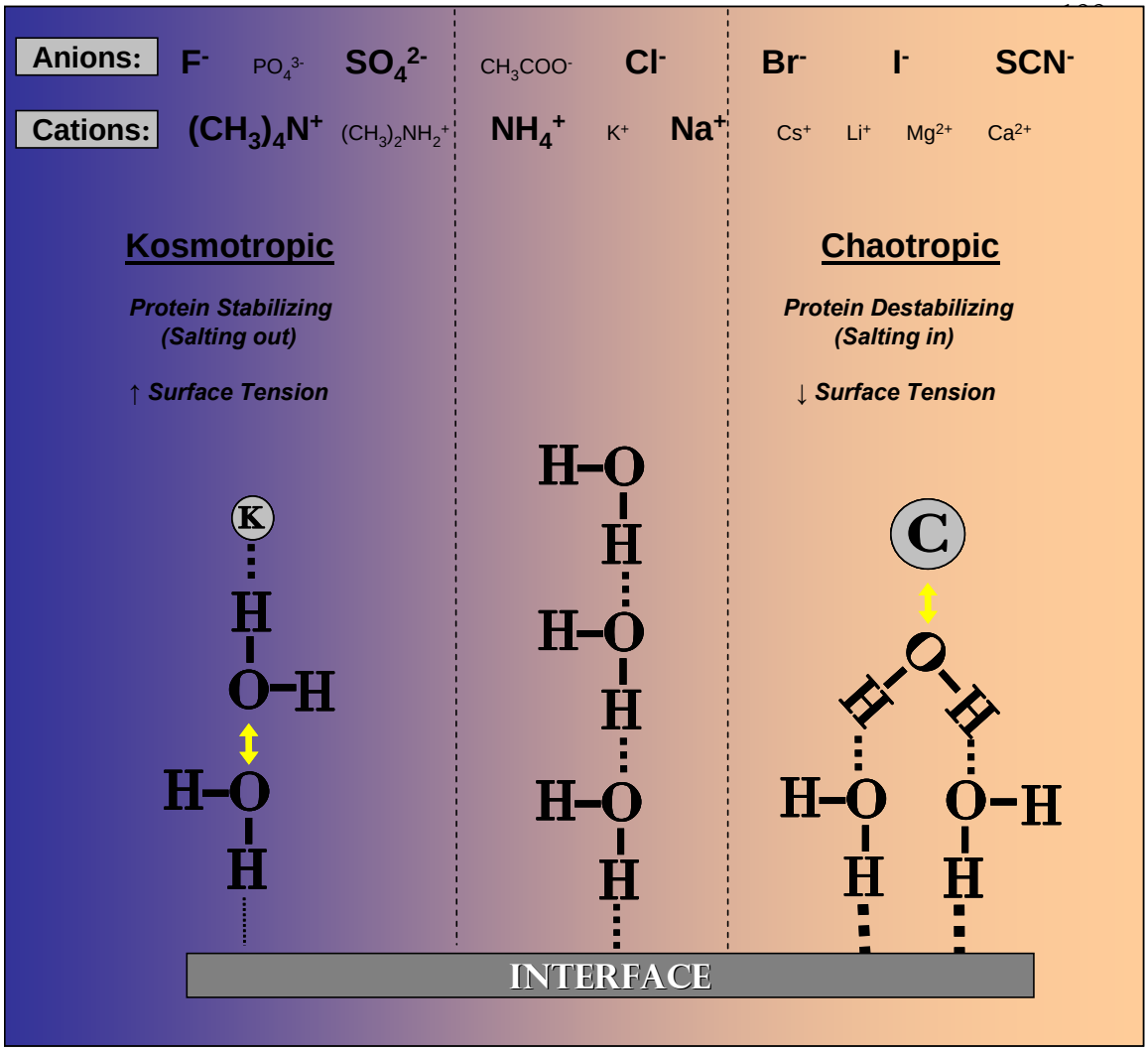

Figure 6.4 Hofmeister series and its effects. For over 20 years, the Hofmeister series has been thought to affect protein solubility and surface tension through its presence near, but not at, the interface. Neutral ions (middle column) have a normal amount of interaction at the interface. In solutions with chaotropic ions (right column), the oxygen at the water layer at the surface has more hydrogen bonding available to it, 'freeing up' some of its own hydrogen for solvating the solute. Kosmotropic ions (left column), 'borrow' a hydrogen bond from water molecules near the interface, thus causing the molecule at the interface to bind tighter to its hydrogen atoms, and decreasing its ability to solvate at the interface. Recent research has suggested that this model is not completely correct, however, and the ions are present on the water surface and subsequently interact with the interface themselves. (Bold ions above were used in these series of experiments.) Adapted from Collins, Zhang and Cremer, and Cacace et al.

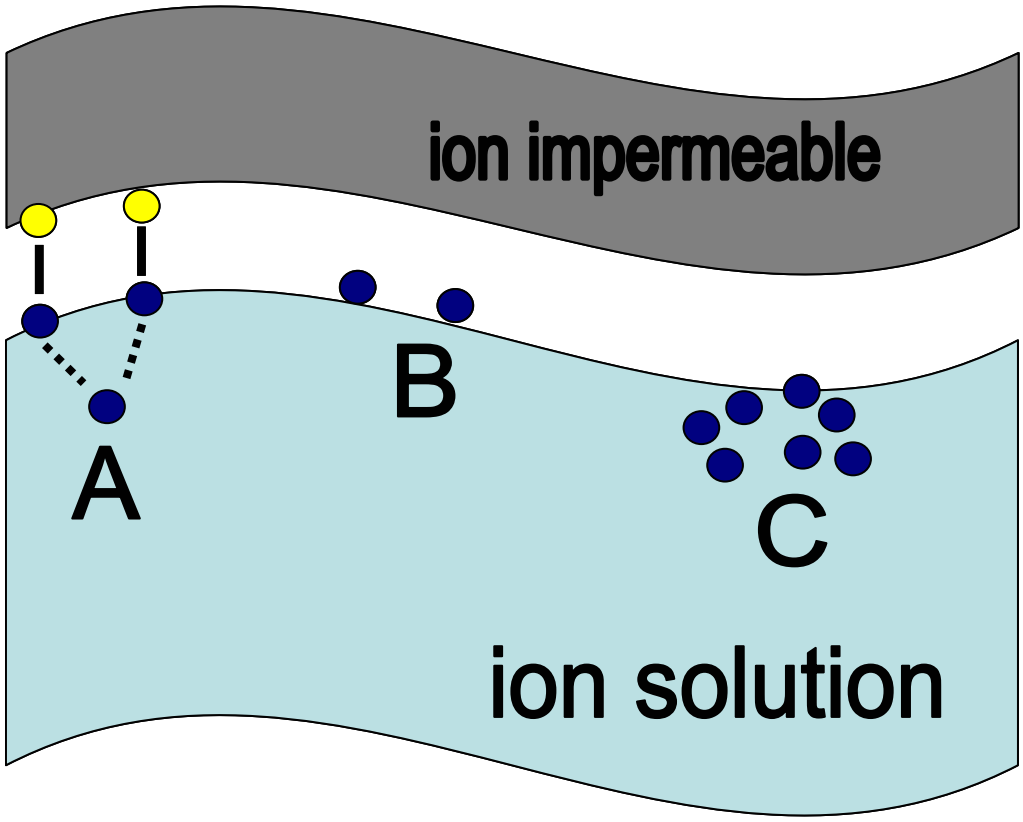

Figure 6.5 Possible ion interactions at the boundary layer between two phases. An ion (dark circles) in water solutions can interact with a hydrophobic phase through A) local binding to atoms in the other phase (light circles) at certain locations along the ion impermeable phase, B) partitioning into the interfacial area, giving rise to different solvent properties of the solution, and C) uneven ion distribution due to the interfacial field. Adapted from Leontidis et al.

Salt (3.5M)	Contact Angle
NH_4SCN	62.5 (± 0.7)
NH_4I	69.0 (± 0.6)
NH_4Cl	76.4 (± 0.9)
$(NH_4)_2SO_4$	83.0 (± 0.7)
NaSCN	66.9 (± 0.7)
NaCl	78.2 (± 1.2)
Dex-FITC	70.4 (± 0.4)

Table 6.1 Contact angles of Hofmeister series salt solutions on PLGA Films. Salt solutions (3.5 M) wwith 35 mg/ml dextran-FITC (4,000 MW Avg) and their contact angle on a PLGA (50:50, 0.57 dL/g, lauryl ester end group) was measured by a goniometer. Dex-FITC is the dextran-FITC dye in dd H_2O without salt. Values are mean ± SEM (n=5).

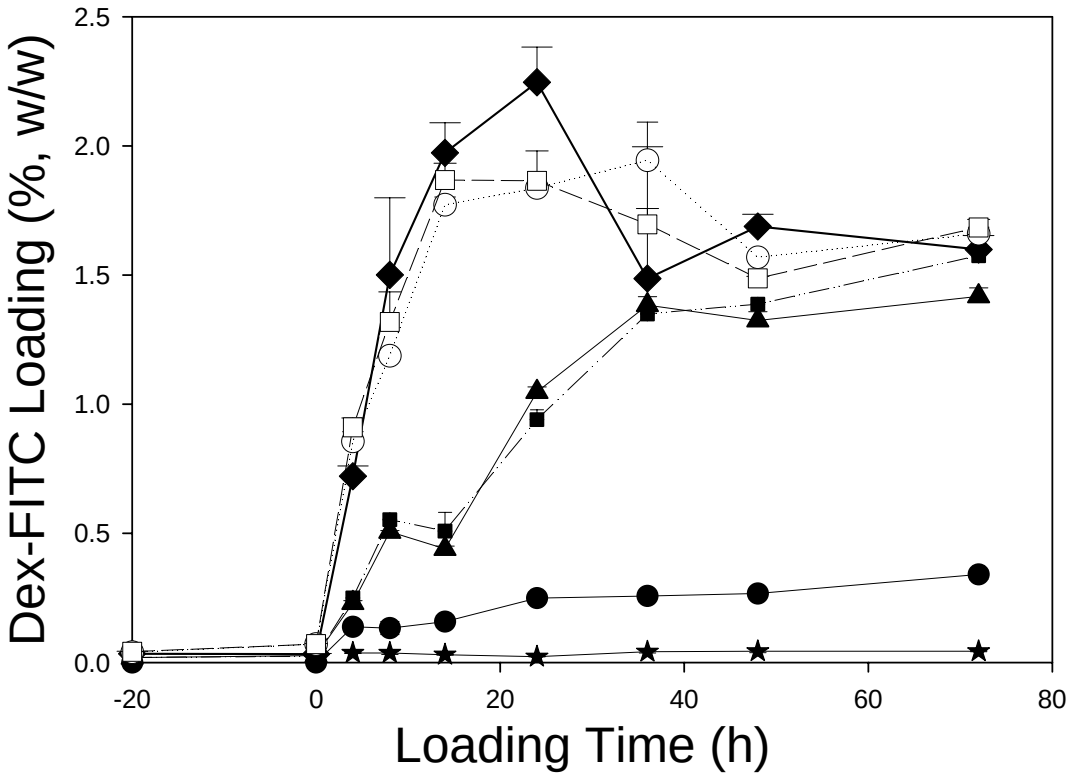

Figure 6.6 Dextran-FITC loading as a function of loading time in Hofmeister Salt Solutions. Hofmeister salt solutions (3.5M) were made with dextran-FITC (10 kDa) in solution (65 mg/ml). Shown in increasing order of availability to 'salt-in': ●:NH_4F, ★:NH_4SO_4 , ■:NH_4Cl, ▲:NH_4Br, and ◆:NH_4SCN. The open circle and square represent the control solutions (dextran-FITC only). Time 20h: incubation at 4°C; Time 0: incubation began at 42°C.

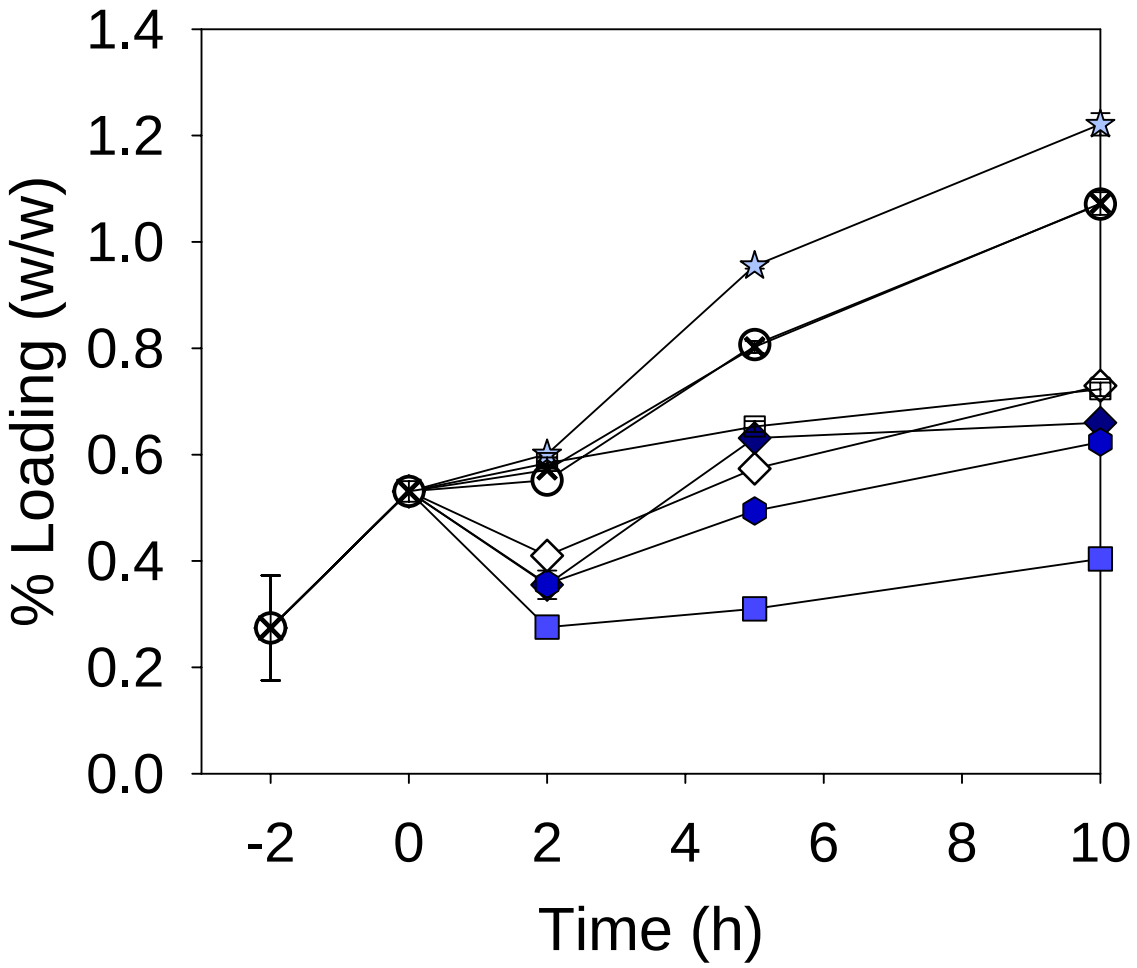

Figure 6.7 Dextran-FITC loading as a function of loading time in Hofmeister salt solutions after pre-hydration. Hofmeister salt solutions (3.5M) were made with dextran-FITC (4 kDa) in solution (35 mg/ml). Listed in increasing order of availability to 'salt-in' ammonium salts were: ★:NH_4SO_4 , ■:NH_4Cl, ⬢:NH_4I, ◆:NH_4SCN. Listed in increasing order of availability to 'salt-in' of sodium salts were: □:NH_4Cl, ◇:NH_4SCN. The open circle and x represent the control solutions (dextran-FITC only). Time -2h: incubation began at 37°C in dextran-FITC only solution; Time 0h: incubation began at 37°C in Hofmeister salt solutions.

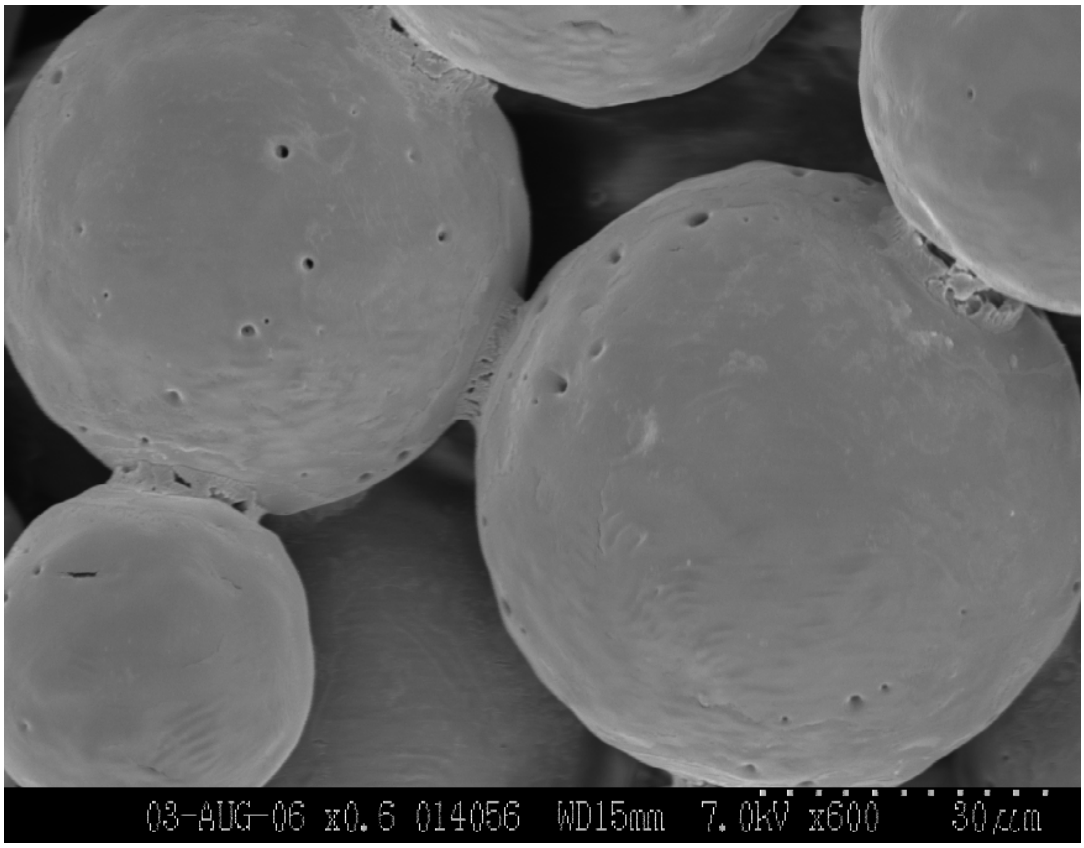

Figure 6.8 Interparticle self-healing in PLGA microspheres. If microspheres are not properly dispersed, self-healing between particles takes place as well.

6.6 References

1. Wool, R. P.; Oconnor, K. M., A Theory of Crack Healing in Polymers. *Journal of Applied Physics* **1981,** 52, (10), 5953-5963.
2. Wool, R. P., Self-healing materials: a review. *Soft Matter* **2008,** 4, (3), 400-418.
3. Wang, J.; Wang, B. A.; Schwendeman, S. P., Characterization of the initial burst release of a model peptide from poly(D,L-lactide-co-glycolide) microspheres. *Journal of Controlled Release* **2002,** 82, (2-3), 289-307.
4. Bouissou, C.; Rouse, J. J.; Price, R.; van der Walle, C. F., The influence of surfactant on PLGA microsphere glass transition and water sorption: Remodeling the surface morphology to attenuate the burst release. *Pharmaceutical Research* **2006,** 23, (6), 1295-1305.
5. Blasi, P.; D'Souza, S. S.; Selmin, F.; DeLuca, P. P., Plasticizing effect of water on poly(lactide-co-glycolide). *Journal of Controlled Release* **2005,** 108, (1), 1-9.
6. Allison, S. D., Effect of structural relaxation on the preparation and drug release behavior of poly(lactic-co-glycolic)acid microparticle drug delivery systems. *Journal of Pharmaceutical Sciences* **2008,** 97, (6), 2022-2035.
7. Rouse, J. J.; Mohamed, F.; van der Walle, C. F., Physical ageing and thermal analysis of PLGA microspheres encapsulating protein or DNA. *International Journal of Pharmaceutics* **2007,** 339, (1-2), 112-120.
8. Sasaki, T.; Yamauchi, N.; Irie, S.; Sakurai, K., Differential scanning calorimetry study on thermal behaviors of freeze-dried poly(L-lactide) from dilute solutions. *Journal of Polymer Science Part B-Polymer Physics* **2005,** 43, (2), 115-124.
9. Ren, J. D.; Urakawa, O.; Adachi, K., Dielectric study on dynamics and conformation of poly(D,L-lactic acid) in dilute and semi-dilute solutions. *Polymer* **2003,** 44, (3), 847-855.
10. Ren, J. D.; Urakawa, O.; Adachi, K., Dielectric and viscoelastic studies of segmental and normal mode relaxations in undiluted poly(d,l-lactic acid). *Macromolecules* **2003,** 36, (1), 210-219.
11. Steendam, R.; van Steenbergen, M. J.; Hennink, W. E.; Frijlink, H. W.; Lerk, C. F., Effect of molecular weight and glass transition on relaxation and release behaviour of poly(DL-lactic acid) tablets. *Journal of Controlled Release* **2001,** 70, (1-2), 71-82.
12. Chartoff, R. P., Thermoplastic polymers. In *Thermal Characterization of Polymeric Materials*, Turi, E. A., Ed. Academic Press: San Diego, 1997; pp 551–554.
13. Dastbaz, N.; Middleton, D. A.; George, A.; Reid, D. G., Molecular Dynamics of Poly(Lactide-Co-Glycolide) Controlled Pharmaceutical Release Polymers: Preliminary Solid State NMR. *Molecular Simulation* **1999,** 22, (1), 51 - 55.
14. Kang, J.; Schwendeman, S. P., Pore Closing and Opening in Biodegradable Polymers and Their Effect on the Controlled Release of Proteins. *Molecular Pharmaceutics* **2007,** 4, (1), 104-118.
15. Reich, G., Use of DSC to study the degradation behavior of PLA and PLGA microparticles. *Drug Development and Industrial Pharmacy* **1997,** 23, (12), 1177-1189.

16. Hsu, D. T.; Shi, F. G.; Zhao, B.; Brongo, M. In *Theory for the thickness dependent glass transition temperature of amorphous polymer thin films*, 4th International Symposium on Low and High Dielectric Constant Materials/2nd International Symposium on Thin Film Materials for Advanced Packaging Technologies, Seattle, Wa, May 02-07, 1999; Singh, R.; Rathore, H. S.; Thakur, R. P. S.; Ang, S. S.; Laboda, M. J.; Ulrich, R. K., Eds. Electrochemical Society Inc: Seattle, Wa, 1999; pp 53-61.
17. Keddie, J. L.; Jones, R. A. L.; Cory, R. A., Size-Dependent Depression of the Glass-Transition Temperature in Polymer-Films. *Europhysics Letters* **1994,** 27, (1), 59-64.
18. Mayes, A. M., Glass Transition of Amorphous Polymer Surfaces. *Macromolecules* **1994,** 27, (11), 3114-3115.
19. Meyers, G. F.; DeKoven, B. M.; Seitz, J. T., Is the molecular surface of polystyrene really glassy? *Langmuir* **1992,** 8, (9), 2330-2335.
20. Satomi, N.; Takahara, A.; Kajiyama, T., Determination of Surface Glass Transition Temperature of Monodisperse Polystyrene Based on Temperature-Dependent Scanning Viscoelasticity Microscopy. *Macromolecules* **1999,** 32, (13), 4474-4476.
21. Tanaka, K.; Takahara, A.; Kajiyama, T., Rheological Analysis of Surface Relaxation Process of Monodisperse Polystyrene Films. *Macromolecules* **2000,** 33, (20), 7588-7593.
22. Fryer, D. S.; Nealey, P. F.; de Pablo, J. J., Thermal Probe Measurements of the Glass Transition Temperature for Ultrathin Polymer Films as a Function of Thickness. *Macromolecules* **2000,** 33, (17), 6439-6447.
23. Forrest, J. A.; Dalnoki-Veress, K.; Stevens, J. R.; Dutcher, J. R., Effect of Free Surfaces on the Glass Transition Temperature of Thin Polymer Films. *Physical Review Letters* **1996,** 77, (10), 2002.
24. DeMaggio, G. B.; Frieze, W. E.; Gidley, D. W.; Zhu, M.; Hristov, H. A.; Yee, A. F., Interface and Surface Effects on the Glass Transition in Thin Polystyrene Films. *Physical Review Letters* **1997,** 78, (8), 1524.
25. Kawaguchi, D.; Tanaka, K.; Takahara, A.; Kajiyama, T., Surface mobile layer of polystyrene film below bulk glass transition temperature. *Macromolecules* **2001,** 34, (18), 6164-6166.
26. Hofmeister, F., Zur Lehre von der Wirkung der Salze. *Arch Exp Pathol Pharmakol* **1888,** 24, 247-260.
27. Cacace, M. G.; Landau, E. M.; Ramsden, J. J., The Hofmeister series: salt and solvent effects on interfacial phenomena. *Quarterly Reviews of Biophysics* **1997,** 30, (3), 241-277.
28. Collins, K. D.; Washabaugh, M. W., The Hofmeister Effect and the Behavior of Water at Interfaces. *Quarterly Reviews of Biophysics* **1985,** 18, (4), 323-422.
29. Omta, A. W.; Kropman, M. F.; Woutersen, S.; Bakker, H. J., Negligible effect of ions on the hydrogen-bond structure in liquid water. *Science* **2003,** 301, (5631), 347-349.
30. Batchelor, J. D.; Olteanu, A.; Tripathy, A.; Pielak, G. J., Impact of protein denaturants and stabilizers on water structure. *Journal of the American Chemical Society* **2004,** 126, (7), 1958-1961.

31. Naslund, L. A.; Edwards, D. C.; Wernet, P.; Bergmann, U.; Ogasawara, H.; Pettersson, L. G. M.; Myneni, S.; Nilsson, A., X-ray absorption spectroscopy study of the hydrogen bond network in the bulk water of aqueous solutions. *Journal of Physical Chemistry A* **2005,** 109, (27), 5995-6002.
32. Collins, K. D., Ions from the Hofmeister series and osmolytes: effects on proteins in solution and in the crystallization process. *Methods* **2004,** 34, (3), 300-311.
33. Randles, J. E. B., Ionic Hydration and the Surface Potential of Aqueous Electrolytes. *Discussions of the Faraday Society* **1957**, (24), 194-199.
34. Jungwirth, P.; Winter, B., Ions at aqueous interfaces: From water surface to hydrated proteins. *Annual Review of Physical Chemistry* **2008,** 59, 343-366.
35. Zhang, Y. J.; Cremer, P. S., Interactions between macromolecules and ions: the Hofmeister series. *Current Opinion in Chemical Biology* **2006,** 10, (6), 658-663.
36. Gopalakrishnan, S.; Liu, D. F.; Allen, H. C.; Kuo, M.; Shultz, M. J., Vibrational spectroscopic studies of aqueous interfaces: Salts, acids, bases, and nanodrops. *Chemical Reviews* **2006,** 106, (4), 1155-1175.
37. Winter, B.; Faubel, M., Photoemission from liquid aqueous solutions. *Chemical Reviews* **2006,** 106, (4), 1176-1211.
38. Chang, T. M.; Dang, L. X., Recent advances in molecular simulations of ion solvation at liquid interfaces. *Chemical Reviews* **2006,** 106, (4), 1305-1322.
39. Jungwirth, P.; Tobias, D. J., Specific ion effects at the air/water interface. *Chemical Reviews* **2006,** 106, (4), 1259-1281.
40. Hrobarik, T.; Vrbka, L.; Jungwirth, P. In *Selected biologically relevant ions at the air/water interface: A comparative molecular dynamics study*, 230th National Meeting of the American-Chemical-Society, Washington, DC, Aug 28-Sep 01, 2005; Elsevier Science Bv: Washington, DC, 2005; pp 238-242.
41. Gurau, M. C.; Lim, S. M.; Castellana, E. T.; Albertorio, F.; Kataoka, S.; Cremer, P. S., On the mechanism of the Hofmeister effect. *Journal of the American Chemical Society* **2004,** 126, (34), 10522-10523.
42. Ninham, B., The Present State of Molecular Forces. In *Smart Colloidal Materials*, 2006; pp 65-73.
43. Leontidis, E.; Aroti, A.; Belloni, L., Liquid Expanded Monolayers of Lipids As Model Systems to Understand the Anionic Hofmeister Series: 1. A Tale of Models. *The Journal of Physical Chemistry B* **2009,** 113, (5), 1447-1459.
44. McDevit, W. F.; Long, F. A., The Activity Coefficient of Benzene in Aqueous Salt Solutions. *Journal of the American Chemical Society* **1952,** 74, (7), 1773-1777.
45. Albright, P. S., Experimental Tests of Recent Theories Descriptive of the Salting-out Effect. *Journal of the American Chemical Society* **1937,** 59, (11), 2098-2104.
46. Zangi, R.; Berne, B. J., Aggregation and Dispersion of Small Hydrophobic Particles in Aqueous Electrolyte Solutions. *The Journal of Physical Chemistry B* **2006,** 110, (45), 22736-22741.
47. S. Q. Liu, S. C. J. Y. C. L., Effects of salts in the Hofmeister series and solvent isotopes on the gelation mechanisms for hydroxypropylmethylcellulose hydrogels. *Journal of Applied Polymer Science* **2008,** 109, (1), 363-372.
48. Burgess, D.; Hickey, A., Microspheres: Design and Manufacuturing. In *Injectable dispersed systems*, Burgess, D., Ed. Taylor & Francis: Boca Raton, 2005; pp 319-320.

49. Kara, S.; Pekcan, O.; Sarac, A.; Arda, E., Film formation stages for poly(vinyl acetate) latex particles: a photon transmission study. *Colloid and Polymer Science* **2006,** 284, (10), 1097-1105.
50. Zeinolebadi, A.; Mohammadi, N.; Sangari, H. H., The Role of Polymer/Polymer Miscibility in Interfacial Healing Kinetics and Equilibrium Adhesion Energy: A Universal Approach. *Journal of Adhesion Science and Technology* **2008,** 22, (12), 1301-1311.
51. Farinha, J. P. S.; Wu, J.; Winnik, M. A.; Farwaha, R.; Rademacher, J., Polymer diffusion in gel-containing poly(vinyl acetate-co-dibutyl maleate) latex films. *Macromolecules* **2005,** 38, (10), 4393-4402.
52. Arda, E.; Pekcan, O., Time and temperature dependence of void closure, healing and interdiffusion during latex film formation. *Polymer* **2001,** 42, (17), 7419-7428.
53. Ertan Arda, S. K. Ö. P., A photon transmission study for film formation from poly(vinyl acetate) latex particles with different molecular weights. *Journal of Polymer Science Part B: Polymer Physics* **2007,** 45, (20), 2918-2925.
54. Canpolat, M.; Pekcan, Ö., Healing and interdiffusion processes at particle--particle junction during film formation from high-T latex particles. *Polymer* **1995,** 36, (10), 2025-2031.
55. Benthem, R.; Ming, W.; With, G., Self Healing Polymer Coatings. In *Self Healing Materials*, 2007; pp 139-159.
56. Cai, H.; Dave, V.; Gross, R. A.; McCarthy, S. P., Effects of physical aging, crystallinity, and orientation on the enzymatic degradation of poly(lactic acid). *Journal of Polymer Science Part B-Polymer Physics* **1996,** 34, (16), 2701-2708.
57. Mehta, R. C.; Jeyanthi, R.; Calis, S.; Thanoo, B. C.; Burton, K. W.; Deluca, P. P. In *Biodegradable Microspheres as Depot System for Parenteral Delivery of Peptide Drugs*, 4th International Symposium on Disposition and Delivery of Peptide Drugs, Leiden, Netherlands, Apr 23-25, 1993; Elsevier Science Bv: Leiden, Netherlands, 1993; pp 375-384.

CHAPTER 7

Significance and Future Directions

7.1 Significance

Self-healing microencapsulation is a new technique that offers significant advantages over traditional encapsulation techniques. First, this new encapsulation technique has been demonstrated to offer improved protein stability over a traditional emulsion-based encapsulation technique. Additionally, high amounts of excipients can be encapsulated through this new method as well, providing the opportunity to further stabilize any loaded protein during subsequent release. Thus, self-healing microencapsulation may hold a significant advantage in delivering proteins that are known to be highly unstable.

In addition to the stability improvements offered via this new technique, self-healing microencapsulation also provides a means to terminally sterilize microspheres after manufacture. Traditional encapsulation techniques encapsulate the protein during manufacture, and as such the loaded protein would also be subjected to any sterilization procedures (e.g. γ-irradiation). Consequently, due to the detrimental effects of γ-irradiation on protein integrity, the manufacturing of protein-loaded microparticles has to be undertaken in aseptic conditions, without a final sterilization step. However, self-

healing microencapsulation allows blank porous microparticles to be produced under normal manufacturing conditions, and since there is no protein encapsulated inside. Only the final loading step has to be conducted in aseptic conditions, a much easier task than the entire manufacturing process.

7.2 Issues and Future Directions

Although self-healing microencapsulation offers some significant advantages over traditional microencapsulation techniques, there are a number of issues that will have to be improved before this new method is put into widespread use. First, there is a current issue with the encapsulation efficiency through self-healing microencapsulation. While the amount of loading (w/w) in each sphere is relevant to practical use, the amount of unencapsulated protein solution following self-microencapsulation is not trivial. In this interpretation then, self-healing microencapsulation results in low encapsulation efficiencies. Traditional encapsulation techniques also can have low encapsulation efficiencies, though the unloaded molecule has been exposed to a number of destabilizing stresses during the encapsulation process. Because the protein encapsulated via self-healing microencapsulation shows, in some instances, virtually no aggregation or decrease in activity, it is believed that this protein could be recycled for additional loading attempts utilizing self-healing microencapsulation. Additional filtering steps and/or quality control checks may be required in between these two separate loading procedures.

A related issue to the low encapsulation efficiency of self-healing microencapsulation is the current dependence of loading on the drug solution concentration (e.g. a high concentration of drug solution is required for high loadings).

With some proteins, high concentrations are feasible and the protein appears to remain stable during the self-healing microencapsulation loading procedure. However, for proteins with solubility issues at an appropriate loading solution pH (e.g. insulin) or have stability concerns at high concentrations (e.g. α-chymotrypsin), this requirement of high drug concentration is a significant problem. A possible solution to overcome this problem is through the use of an active loading procedure that allows for the drug to preferentially exist inside the microparticles as compared to the loading solution. Such a loading method will also provide improved encapsulation efficiencies.

Another issue that will need to be addressed with self-healing microencapsulation is the optimization of the release profile. Currently, loaded microparticles prepared via self-healing microencapsulation appear to have a distinct lag phase after the diffusion mediated step passes. Further research may produce formulations with close to zero-order release profiles.

Other unknown questions about this process include the unknown stability of the unloaded protein after self-healing microencapsulation. If recycling of this solution is to be accomplished, the unencapsulated protein, which had been exposed to interfaces longer than that protein which had been encapsulated quickly, must be investigated. Also, while excipients are used to create porous blank microparticles, their remaining quantity during and after self-healing microencapsulation, as well as during release, are unknown. It is expected that much of these excipients are washed out from the microsphere during the loading procedure, but additional retention of certain protein stabilizing excipients (e.g. sugars and acid-neutralizing base) would be beneficial.

Obviously, questions remain about the cause of the polymer rearrangement that is so crucial for self-healing microencapsulation. Further experiments examining the role of internal enthalpy as well as interfacial tension need to undertaken. Investigating the pore closing in microspheres that have been annealed in the dry state after lyophilization is crucial. In conjunction, the actual decrease in internal enthalpy should be examined by DSC. Accordingly, the presumed decrease in internal enthalpy of microparticles annealed after phase separation and before lyophilization should also be confirmed by DSC. In order to determine the affects of interfacial tension on the rate of pore closing, agents that alter the surface tension that do not come with the same problems as the Hofmeister series (e.g. altering water activity, possibly instigating pore opening) should be used. Such water soluble agents are not numerous, and the affects on interfacial tension should be investigated before the pore closing rate experiment is run.

In such mechanism elucidation experiments, it may be easier to investigate the rate of polymer healing through films and not microspheres. The rate of film healing offers numerous advantages over the rate of microsphere pore closing. For one, the rate of polymer rearrangement can be observed through SEM as well as film strength analytical techniques, whereas with microsphere pore closing the rate of pore closing can only properly be investigated by the loading of a model drug. Consequently, other factors can mask the true polymer rearrangement rate, such as the known phenomenon of pore opening, as well as the possibility of incomplete penetration into the microsphere pore network of the model drug solution in different interfacial tension solutions.